Molecular Genetic Studies on Retinal Dystrophies

THESIS

Submitted in partial fulfilment

of the requirements for the degree of

DOCTOR OF PHILOSOPHY

by

HARDEEP PAL SINGH

Under the Supervision of

Dr. Chitra Kannabiran

BIRLA INSTITUTE OF TECHNOLOGY AND SCIENCE

PILANI (RAJASTHAN) INDIA

2009

BIRLA INSTITUTE OF TECHNOLOGY & SCIENCE
PILANI (RAJASTHAN)

CERTIFICATE

This is to certify that the thesis entitled **"Molecular Genetic Studies on Retinal Dystrophies"** which is submitted by **Hardeep Pal Singh**, ID No. **2005PHXF436**, for award of Ph.D. degree of the institute, embodies original work done by him under my supervision.

Date:

DR. CHITRA KANNABIRAN
Scientist
Kallam Anji Reddy Molecular Genetics Laboratory
L V Prasad Eye Institute
Hyderabad. 500034

BIRLA INSTITUTE OF TECHNOLOGY & SCIENCE
PILANI (RAJASTHAN)

CERTIFICATE

This is to certify that the thesis entitled **"Molecular Genetic Studies on Retinal Dystrophies"** which is submitted by **Hardeep Pal Singh**, ID No. **2005PHXF436**, for award of Ph.D. degree of the institute, embodies my original work.

Date:

HARDEEP PAL SINGH
ID No.2005PHXF436
Kallam Anji Reddy Molecular Genetics Laboratory
L V Prasad Eye Institute
Hyderabad. 500034

Dedicated to

My Parents and Brother Raja

ACKNOWLEDGEMENTS

I am grateful to my advisor for providing me a healthy/educative working environment. Under her guidance it was a great opportunity to learn right from the very basic things of research, such as to plan ahead of time, making proper lab notes, critically analyzing the results, making crisp presentations, write ups as simple as possible so that the message is clear and understandable. I am indebt of my adviser for bringing a significant difference in myself.

I am thankful to Dr Subhadra for clinically evaluating all the study patients, without her support and enthusiasm; it would not have been possible to collect samples from a large number of patients.

I acknowledge the financial support from HERF and CSIR for my fellowship.

I am thankful to Prof Balu for his efforts in registering me at BITS Pilani, arranging classes for me at BLSO Kismatpur so as to avail semester fee waiver and letting us chat with some of the eminent scientists including noble laureates.

I am grateful to Dr GN Rao for making a great place like the LV Prasad Eye Institute. I am honored to be a part of LVPEI.

Thanks to my M.Sc teacher Dr Inderjeet kaur for introducing me to LVPEI, and for her support in all times.

I appreciate the support from the research and consultancy division of BITS Pilani for taking care of my PhD related matters. It was very kind of Prof Ravi Prakash for helping me and clarifying my doubts whenever I was in need. I would also like to thank Mr Dinesh and Mr Sharad Srivastava for taking care of my PhD related matters.

I would like to acknowledge Dr Subho, Dr Indu, Dr Geeta, Dr Savitri, Dr Usha, Dr Nishant, Dr Indumathi, Dr Ramya and Dr Yashoda for their valuable suggestion and encouragement during my stay at LVPEI.

I appreciate the clinical inputs from the clinical faculty and fellows during my morning class presentations. Thanks to our general physicians for taking care of my health whenever I was sick.

I am thankful to my colleagues Sagar, Surya, Saritha, Vidya, Nageshwer, Subhash, Afia, Anees, Kalyan, Naresh, Purush, Guru, Joveeta, Aparna, Kiranpreet, Ganesh, Priya, Roby, Sreelatha, Rajeshwari, Venu, Pulla, Neerja, Rachna, Maithili, Shubha, Gayathri, Pavani and Soumya for maintaining a friendly environment and helping me in the time of need.

Members of ww3.CCMB yahoo group, Nishant, Sandeepa, Pawandeep, Rajeshwari, Banu, Venkat and Preeji did a great help for me by providing full texts of research articles for my independent studies and thesis, I am grateful for their support.

LVPEI is great because the people who work for it are sincere and dedicated to their work. I would like to thank members of the departments of clinical biochemistry, library, house keeping, stores, purchase, maintenance, biomedical, ISD, communications, graphics, reception, cafeteria and security for their help at the time of need.

I am grateful to my parents and brother Raja for their constant support and allowing me to give first preference to my PhD even during bad times at home.

I am thankful to Indu ma'am, Subho sir and Sagar for their excellent company and taking care of me most of the times especially when I was alone.

Thanks to Balaji food joint for taking care of my dinner for 5 years, without which I would not have survived till this point.

Finally I am thankful to the study patients for providing their valuable samples and responding to our calls for the follow-ups.

Hardeep Pal Singh

ABSTRACT

Retinal dystrophies are a clinically and genetically heterogeneous group of progressive disorders in which retinal cells undergo degeneration and death, leading to either partial or complete blindness. Retinitis Pigmentosa (RP) is the most common type of retinal dystrophy with a worldwide prevalence ranging from 1: 1000–8000. Most forms of retinitis pigmentosa are monogenic and have classical inheritance patterns of autosomal dominant, autosomal recessive, X-linked or mitochondrial (maternally inherited). However, they show extensive genetic and clinical heterogeneity, with over 40 genes identified till date and possibly, more to be identified. Identification of mutations in families with retinal dystrophy is possible by various approaches ranging from whole genome mapping, linkage and/or haplotyping of candidate gene loci, to direct screening of candidate genes for mutations.

The aims of this study were- (1) to identify the disease genes in families with autosomal recessive retinitis pigmentosa by homozygosity screening. (2) to map the disease locus in a family with autosomal dominant retinitis pigmentosa. (3) to determine the role of the *RD3* gene in human retinal dystrophy by mutational screening of 100 unrelated patients.

The study protocol was approved by the Institutional Review Board and adhered to the guidelines of the Declaration of Helsinki. Eligible patients with retinal dystrophy seen at the outpatient clinic of the retina service of LVPEI were recruited for the study. A

total of 34 families with ARRP were included for homozygosity screening as per specific aim 1. For Aim 2, one family with ADRP having affected individuals in 3 generations was included. For Aim 3, 103 probands with RP and LCA were included for screening of the *RD3* gene.

Specific Aim 1: Twenty-three candidate genes were selected for homozygosity screening. The presence of homozygosity was assessed by genotyping flanking microsatellite markers at each locus in affected individuals. Mutations were identified by sequencing of coding regions of genes.

Homozygosity was identified in 14/44 families (34 families from the present study, 10 from a previous study in our group). Mutational screening in 14 families resulted in the identification of mutations in 7/14 families. Five mutations are novel and are previously not reported, while all 7 mutations c.1060delA (*RPE65*), c.2847delT (*RP1*), c.1199G>A (*TULP1*), c.451C>T (*RLBP1*), c.1995C>A (*ABCA4*), c.6088C>T (*ABCA4*), c.1225delA (ABCA4) are being reported for the first time in Indian patients. These mutations belong to different categories such as frameshift (n=3), missense (n=2) and nonsense (n=2).

Specific Aim 2: Genotyping of 28 microsatellite markers selected on the basis of proximity to loci for retinal dystrophy was carried out on 23 individuals of family RP161, with ADRP. Linkage analysis with these markers showed significant linkage of disease to chromosome 6q23 with a two-point LOD score of 3.2 for marker D6S262. This was

confirmed with multipoint linkage, which gave a maximum LOD score of 1.8 for marker D6S262.

Specific Aim 3: *RD3* gene screening in 103 unrelated patients with RP and LCA resulted in the identification of a pathogenic mutation in one patient with autosomal recessive LCA. The mutation co-segregated with disease in the family, was absent in 100 normal controls and involved the conserved splice donor site (c.296+1G>A) of the 2nd intron of *RD3* gene.

In conclusion this study revealed novel causes of retinal dystrophy in a subset of families of Indian origin. The genes evaluated were found to be responsible for a small proportion of total cases suggesting that additional loci are involved in the remaining families.

TABLE OF CONTENTS

		Page number
Chapter: 1 Introduction and Review of Literature		1
1.1	Retina	1
1.1.1	Major types of cells of the retina	1
1.1.2	Topography of retina	5
1.1.3	Distribution of photoreceptors	6
1.1.4	Structure of the photoreceptors	7
1.2	Embryology	9
1.2.1	Retinal differentiation	11
1.2.2	Retinal maturation	12
1.3	Phototransduction	13
1.4	Visual cycle	16
1.4.1	Visual cycle in rods	17
1.4.2	Visual cycle in cones	18
1.5	Retinal dystrophies	20
1.5.1	Classification	20
	1.5.1a Rod & rod-cone dystrophies	20
	1.5.1b Cone dystrophies	24
	1.5.1c Macular dystrophies	25
	1.5.1d Leber Congenital Amaurosis	26
1.6	Genetics of RP	27
1.6.1	Overview of genes causing RP	27
1.6.2	Genes involved in ARRP	32
1.6.3	Genotype-phenotype correlations	48
1.7	Animal models of retinal dystrophy	54
1.8	Therapeutic approaches in retinal dystrophies	64
1.8.1	Gene therapy	64
1.8.2.	Non-genetic therapeutic approaches	76
	1.8. 2a Growth factors	77
	1.8.2b Ca-channel blockers	80
	1.8.2c Anti-oxidant/nutrient supplementation	80
	1.8.2d Cell/tissue transplantation	82
	1.8.2e Retinal prosthesis	84
1.9	Approaches and potential uses of molecular diagnostic testing	85

Page number

1.10 Objectives of the study 87

Chapter 2: Materials and Methods 88

2.1 Recruitment of patients and sample collection 88

2.1.1 Inclusion criteria 88
2.1.1a. Inclusion criteria for RP 88
2.1.1b. Inclusion criteria for LCA 89

2.1.2 Exclusion criteria 90
2.1.2a Exclusion criteria for RP 90
2.1.2b Exclusion criteria for LCA 90

2.1.3 Sample collection 91

2.1.4 Details of patients and families 91

2.1.5 Controls 92

2.2 Molecular genetic analysis 92

2.2.1 Extraction of genomic DNA from blood leukocytes 92
2.2.2 Quantitation of DNA 93
2.2.3 Polymerase chain reaction (PCR) 93
2.2.4 Genotyping and linkage analysis 95
2.2.5 Gel electrophoresis 101
2.2.5a. Agarose 101
2.2.5b. Polyacrylamide 102
2.2.6 DNA sequencing 103
2.2.7 PCR-RFLP 104
2.2.8 Gene sequences and nomenclature 105
2.2.9 Multiple sequence alignment 106
2.2.10. SIFT 106

Chapter 3: Identification of Genes in Families with ARRP by Homozygosity Screening 107

3.1 Introduction 107
3.2 Results 108
3.2.1 Homozygosity screening 108
3.2.2 Screening of candidate genes 126
3.3 Discussion 150

Page number

Chapter 4: Mapping of the Disease Locus in a Family with ADRP 155

4.1 Introduction 155
4.2 Results 155
4.2.1 Genotyping and linkage analysis 155
4.3 Discussion 163

Chapter 5: Candidate Gene Screening 164

5.1 Introduction 164
5.2 Results 164
5.2.1 Screening of the *RD3* gene 164
5.3 Discussion 169

Chapter 6: Discussion and Conclusions 171

Specific Contributions of the Study 175

Limitations of the Study 176

Future Scope of the Study 177

References 178

Appendix 209

List of Publications 224

List of Presentations 225

List of Awards 226

Brief Biography of Candidate 227

Brief Biography of Supervisor 229

Full text of Publications 232

LIST OF TABLES

		Page number
1.1	Genes involved in ADRP	27
1.2	Genes involved in ARRP	29
1.3	Genes involved in XLRP	30
1.4	Mitochondrial genes associated with RP	30
1.5	Genes involved in autosomal dominant LCA	31
1.6	Genes involved in autosomal recessive LCA	31
2.1	Genes selected for homozygosity screening	96
2.2	Microsatellite markers used in multiplex PCR	96
2.3	Shortlisted markers corresponding to ADRP loci from the ABI linkage panels	99
2.4	Transcript IDs of the genes selected for mutation screening	105
3.1	Number of individuals screened in the 34 families	109
3.2	Genotyping results at *ABCA4* locus in family RP213	111
3.3	Genotyping results in family RP119	113
3.4	Genotyping results in family RP169	115
3.5	Genotyping results in family RP205	117
3.6	Genotyping results in family RP126	118
3.7	Genotyping results in family RP153	119
3.8	Genotyping results in family RP200	120
3.9	Genotyping results in family RP160	121
3.10	Genotyping results in family RP126	122
3.11	Genotyping results in family RP184	123
3.12	Genotyping results in family RP160	123
3.13	Genotyping results in family RP170	125
3.14	Families with autosomal recessive RP and loci showing homozygosity	126
3.15	Sequence changes identified in the ABCA4 gene in families RP109, RP111 and RP213	132

Page number

3.16	Putative pathogenic changes found in autosomal recessive RP families	146
3.17	Non-pathogenic/changes of uncertain significance identified in the 14 families	147
3.18	Clinical features of the affected individuals with mutations identified	148
4.1	Linkage analysis in family RP161	159
4.2	Linkage analysis of markers on chromosome 6q23 in family RP161	160
5.1	Sequence changes identified in *RD3* gene in families with retinal dystrophy	166

Appendix Tables

1	Microsatellite markers genotyped in ARRP families	209
2A	Primers for amplification of coding regions of *PDE6B* gene	215
2B	Primers for amplification of coding regions of *CNCG1* gene	216
2C	Primers for amplification of coding regions of *CRB1* gene	216
2D	Primers for amplification of coding regions of *TULP1* gene	217
2E	Primers for amplification of coding regions of *RLBP1* gene	218
2F	Primers for amplification of coding regions of *RP1* gene	218
2G	Primers for amplification of coding regions of *RGR* gene	219
2H	Primers for amplification of coding regions of *NRL* gene	219
2I	Primers for amplification of coding regions of *ABCA4* gene	219
2J	Primers for amplification of coding regions of *RPE65* gene	222
2K	Primers for amplification of coding regions of *RDS* gene	222
2L	Primers for amplification of coding regions of *RD3* gene	223

LIST OF FIGURES

		Page number
1.1	Section of the human retina showing the different layers	4
1.2	Schematic representation of the structure of the rod and cone cells	8
1.3	Development of the retina	10
1.4	The phototransduction cascade in the rods	16
1.5	Schematic of visual cycle in rods and cones	18
3.1	Pedigrees of families in which homozygosity was observed	139
3.2	Sequence electropherograms showing pathogenic sequence changes in ARRP families	141
3.3	Representative fundus pictures	143
3.4	Multiple sequence alignment of TULP1 proteins from different species	145
3.5	Multiple sequence alignment of the RLBP1 protein sequence in different species	145
4.1	Pedigree of family RP161	158
4.2	Representative fundus pictures of family RP161	158
4.3	Two-point LOD scores with 9 markers	161
4.4	Multipoint linkage analysis	162
5.1	Details of family RP146	168

LIST OF ABBREVIATIONS

ADRP	Autosomal Dominant Retinitis Pigmentosa
ARRP	Autosomal Recessive Retinitis Pigmentosa
bp	Base Pair
c.DNA	Complementary DNA
cm	Centimeter
CRD	Cone-Rod Dystrophy
del	Deletion
DNA	Deoxyribonucleic Acid
dNTP	Deoxynucleotide Triphosphate
ERG	Electroretinogram
ETDRS	Early Treatment Diabetic Retinopathy Study
IU	International Unit
kDa	Kilodaltons
LCA	Leber's Congenital Amaurosis
mg	Milligram
ml	Millilitre
mM	Millimolar
mm	Millimeter
nm	Nanometer
^{o}C	Degree Centigrade
OD	Right Eye
OS	Left Eye
OU	Both Eyes
PBS	Phosphate Buffered Saline
PCR	Polymerase Chain Reaction
RP	Retinitis Pigmentosa
RPM	Revolutions Per Minute
RFLP	Restriction Fragment Length Polymorphism
SDS	Sodium Dodecyl Sulfate

SNP	Single Nucleotide Polymorphism
VA	Visual Acuity
µg	Microgram
µl	Microlitre

Chapter-1

Introduction and Review of Literature

CHAPTER 1: INTRODUCTION AND REVIEW OF LITERATURE

1.1 Retina

The retina is the innermost layer of the eye occupying the posterior two-third of the eye. It is a layer of photosensitive cells concerned with initial processing of visual information. The sensation of sight is based on a step-wise process in which light is focused on the retina, converted to electrical impulses that are conveyed through the visual pathways to the visual cortex of the brain where it is interpreted as a visual signal.

The neurons in the retina are broadly of three types. (1) the photoreceptors, which are located the most externally, (2) the intermediate neurons (3) the ganglion cells.

1.1.1 Major types of cells of the retina

1. Photoreceptors

Rods and cones are the two types of photoreceptor cells present in the retina. Rods mediate dim light vision, whereas cones function in bright light. Rods provide sensitivity to scotopic (dim light) vision whereas cones provide visual acuity for pattern detection

and color vision. All the photoreceptors have an outer segment that contains the visual pigment and an inner segment which contains the nucleus.

2. Interneurons

The bipolar, the horizontal and the amacrine cells are called as interneurons and their cell bodies make up the inner nuclear layer.

3. Bipolar cells

Bipolar cells are a class of retinal interneurons that selectively contact either rods or cones and send the signal to the ganglion cells.

4. Horizontal cells

Horizontal cells are the local circuit neurons, which interconnect the photoreceptors laterally across the plane of the outer plexiform layer of retina. The processes of horizontal cells modulate and transform the visual information that is conveyed to brain.

5. Amacrine cells

Amacrine cells are a class of neurons, which forms synaptic contacts with the axons of bipolar cells, the dendrites of interplexiform, ganglion cells as well as with other amacrine cell processes.

6. Ganglion cells

Ganglion cells are the retinal neurons whose cell bodies lie internal to the inner plexiform layer; their dendrites branch in the inner plexiform layer, where they receive synapses from bipolar and amacrine cells. The axons of the ganglion cells form the optic nerve.

7. Muller cells

Muller cells are the glial cells of retina and gives the basic architectural support to retina and extends radially across the entire thickness of retina to from outer and inner limiting membranes.

In histologic sections, the retina is seen to consist of ten layers (shown in Fig 1.1). The outermost layer is the retinal pigment epithelium (RPE), consisting of melanin granules which help in the absorption of scattered light and increase the efficiency of photoreceptors. The RPE also acts as blood retinal barrier, helps in transport of nutrients, is essential for metabolism of vitamin A derivatives, and performs phagocytosis of outer segments of rods and cones. Inner to the RPE is the layer of rods and cones, which consists of the photoreceptor outer and inner segments. The outer segments contain visual

pigment and function in phototransduction, while the inner segment contains their metabolic machinery i.e the nucleus and dense aggregation of mitochondria. The external limiting membrane is adjacent to the photoreceptor inner segments and is formed by the Muller cell tight junction connections with the photoreceptors. The next layer consists of the outer nuclear layer, which is formed by the nuclei of rods and cones. Inner to the outer nuclear layer is the outer plexiform layer, containing synapses between the photoreceptors and horizontal and bipolar cells. Interior to this is the inner nuclear layer, containing the nuclei and cell bodies of bipolar cells, horizontal cells and muller cells, followed by the inner plexiform layer, which is made up of synapses between bipolar, amacrine and ganglion cells. The innermost cell layer is the ganglion cell layer, which consists of cell bodies of ganglion cells. Inner to this is the nerve fiber layer, which consists of the axons of ganglion cells. The innermost layer of retina is the internal limiting membrane, formed by the projections of the Muller cells (Blanks *et al*., 1994).

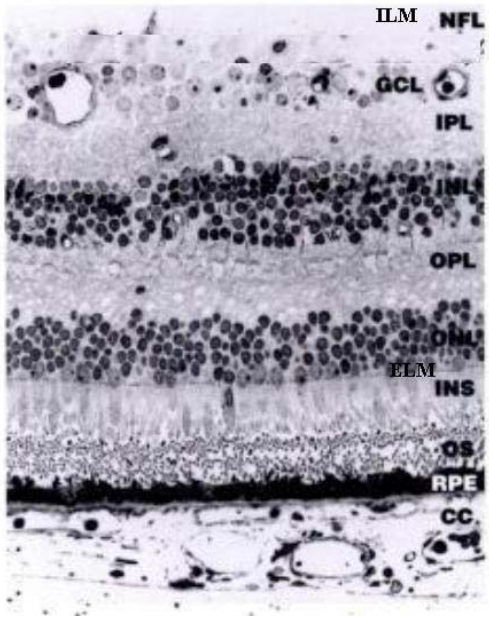

Figure 1.1: Section of the human retina showing the different layers. From the inner to the outer retina, these are- internal limiting membrane (ILM), nerve fiber layer (NFL), ganglion cell layer (GCL), inner plexiform layer (IPL), inner nuclear layer (INL), outer plexiform layer (OPL), outer nuclear layer (ONL), external limiting membrane (ELM), inner segments (INS) and outer segments (OS) of the photoreceptors, retinal pigment epithelium (RPE), chorio capillaris (CC) (Picture taken from Forrester *et al*., 2001).

1.1.2 Topography of the retina

The retina varies in thickness in different regions from about 0.1 mm to 0.5 mm (Reh *et al*., 2001). It has regional specializations that are of functional importance.

1. Fovea

Fovea is on the optic axis of the globe. A beam of light perpendicular to the center of the compound lens system of the eye will fall on the fovea. The fovea is 1.5 mm in diameter and in its center lies the foveal pit, which is 0.1 mm in diameter. This foveal pit is free of cells, except for the outer segments of red and green cones. The central most region subtending about 2 degrees of visual angle, is thought to be free of blue cones. The cones of the fovea are specialized with an extremely high packing density (Blanks *et al*., 1994).

2. Area centralis–Macula

The area centralis surrounds the fovea. It is more than one cell thick. It is about 6 mm in diameter and extends nasally from the fovea, almost reaching the nerve head margin. The macula lutea or the yellow spot extends about 1 mm laterally and 0.8 mm above and below the fovea. The fovea is surrounded by parafoveal ridge, a region of retina thickened by layers of ganglion cells and cells of inner nuclear layer displaced from the fovea (Blanks *et al*., 1994). Macula is a region of highest visual acuity and the best color vision. This is due to the presence of highest density of cones in the central foveal region of macula. However this density decreases as we move away from the fovea.

1.1.3 Distribution of photoreceptors

The density of cones is maximal at the fovea, with an average of 199,000 cones/mm^2, but the number of cones is highly variable and ranges from 100,000 to 324,000 cones/mm^2. With increasing distance away from the center of the fovea, the density of cones decreases rapidly. This density is 40-45 % greater on the nasal than on the temporal retina, and slightly lower in the superior than in the inferior retina at the mid periphery. The distribution of rods and cones is heterogeneous. The regional heterogeneity of photoreceptors provides a mean for a visual image to differ across the visual field. Rods are also distributed unevenly across the retina. There is no rod photoreceptor with in approximately the central 0.35 mm of the fovea. The highest concentration of the rods occurs along a contour that describes a broad, horizontally oriented ellipse with the same eccentricity as the center of optic disc and extending towards the nasal and superior

retina. The density of rods slowly decreases from this area to the far periphery. The nasal retina has 20-25% more rods than temporal retina and superior retina has 2% more rods than the inferior retina (Bron *et al*., 1997).

1.1.4 Structure of photoreceptors

Photoreceptors can be divided into three compartments, namely the outer segment, the inner segment and the synapse (Figure 1.2). The outer segments contain photosensitive visual pigment rhodopsin in rods and cone opsin in cones. Outer segments have the highly specialized function of converting the light energy into the nerve impulses. The inner segment contains the cells protein synthesis (golgi body and endoplasmic reticulum) and the metabolic machinery (nucleus and mitochondria). The synaptic connections are made by second order retinal neuron (bipolar and horizontal cells) utilizing an inhibitory neurotransmitter, glutamate. The nerve impulse generated in the outer segments during the phototransduction cascade flows rapidly from the outer segment to the inner segment and to the synaptic terminal leading to the release of neurotransmitter (Bron *et al*., 1997).

The outer segment of rods is cylindrical in shape and contains stacks of flattened double lamellae in the form of discs (shown in Figure 1.2). The number of discs varies from 600 to 1000 per rod and each disc has a thickness of 22.5–24.5 nm (Bron *et al*., 1997). No attachments are seen between the discs or between the discs and the enclosing

plasma membrane. The discs contain 90% of the visual pigment in the rod while the remaining visual pigment is scattered on the surface of plasma membrane (Bron *et al*., 1997). The outer segment of cones has a morphology that differs depending on the location of cones in the retina. At the ora serrata and at the periphery the cone outer segments are short and conical, while at the fovea centralis cone outer segments are long and resemble the rods. The cone outer segments have more discs (1000-1200 per cone cell) than the rod outer segments. Unlike the rod discs the cone discs are attached to each other as well as to the surface of plasma membrane (Bron *et al*., 1997)

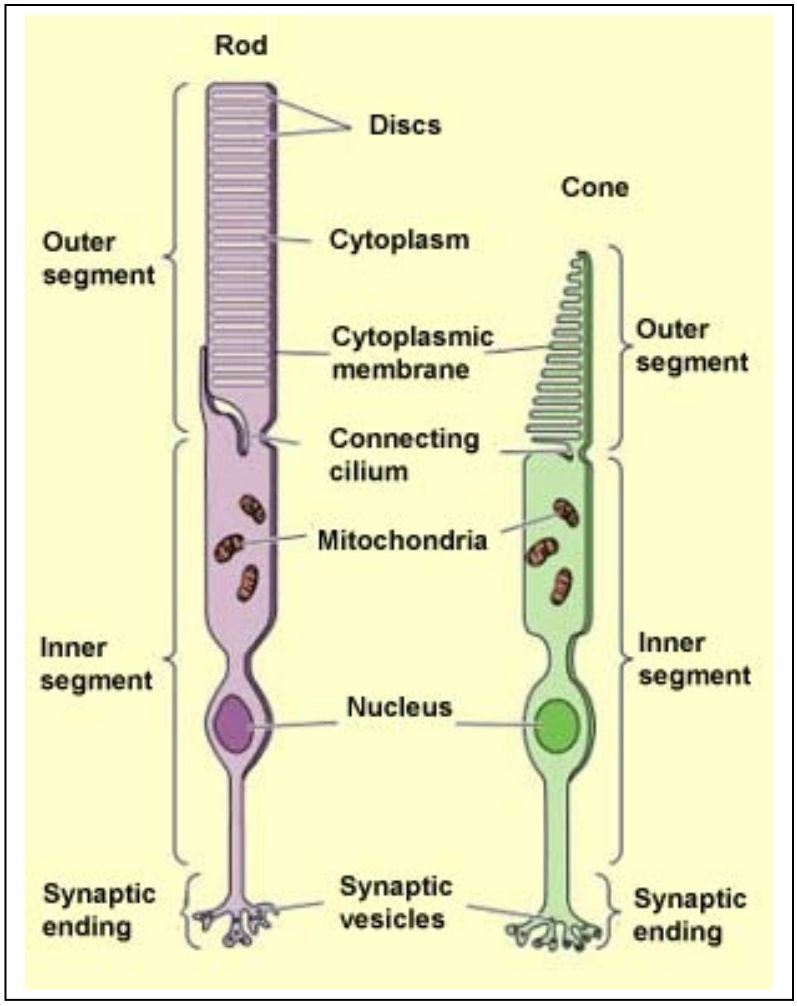

Figure 1.2. Schematic representation of the structure of the rod and cone cells. (Taken from http://thebrain.mcgill.ca)

1.2 Embryology

Experimental embryology of developing eye has been carried out in various organisms like zebrafish, frog, chick, drosophila, etc and the process of eye development is largely conserved (Gehring *et al*., 1999, Neumann *et al.*, 2000). The eye is formed almost entirely from the ectoderm, however the mesodermal layer contributes to the vascular endothelial cells and extraocular (striated) muscles.

Within the eye, the retina is a highly conserved part of the central nervous system, with similar cell types and gene activity from drosophila to humans (Zaghloul *et al*., 2005). The specification of retinal cell fate begins early in embryogenesis, even before gastrulation and the establishment of the neural plate (Figure 1.3). First, a subset of pluripotent embryonic cells during cleavage stage acquire the competence to contribute to the retina. From this competent pool, a smaller subset is biased to become the definitive embryonic retina producing precursors. Later a specified retinal stem cell population emerges from the lineage to form the eye field in the anterior neural plate, which gives rise to all the structures of the mature retina. Further interactions during neural tube morphogenesis segregate this population into three major compartments: optic stalk, retinal pigment epithelium (RPE) and neural retina (Figure 1.3). Each of these compartments goes in to produce different subset of retinal progenitor cells that

ultimately produce several classes of specialized cells: cone and rod photoreceptors in the outer nuclear layer, horizontal, bipolar, amacrine and muller glial cells in the inner nuclear layer and ganglion cells in the ganglion cell layer (Zaghloul *et al*., 2005).

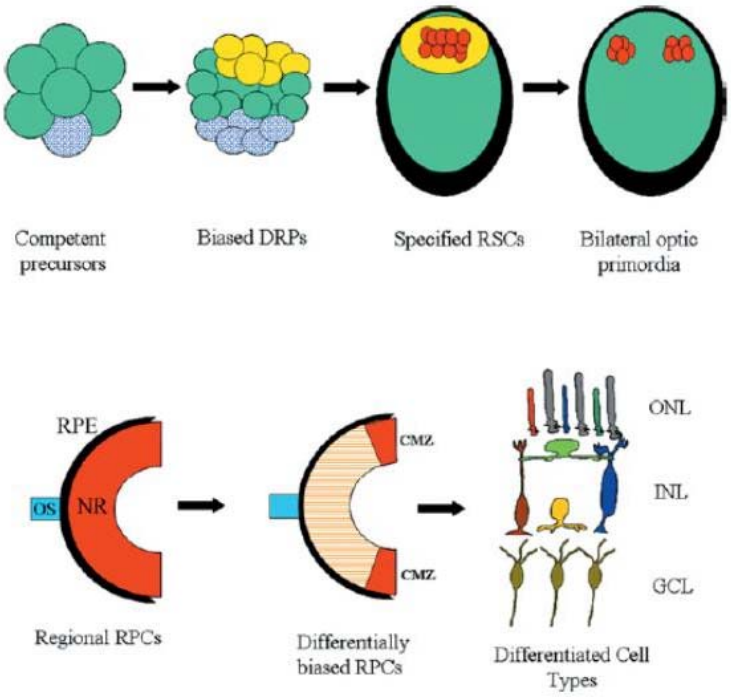

Figure 1.3. Development of the retina. Shown are the different steps of retinal development. At first a subset of embryonic cells acquires competence to become the retina. In response to retinogenic signals some of the cells become DRPs (definitive embryonic retina producing precursors) which eventually forms RSCs (retinal stem cells). Next the RSCs separate into right and left optic primordia which give rise to optic vesicle and eventually to optic cup. Optic cup separates into 3 domains (optic stalk (OS), RPE and neural retina (NR)) each of which contains region specific RPCs (retinal progenitor cells), which give rise to differentiated cell types of retina (This figure is taken from Zaghloul *et al*., 2005).

These various classes of retinal cells are not produced at a time, by the progenitor cells, rather one cell class induces the progenitor cells to make next cell type in a sequential process (Reh *et al*., 2001). Based on the studies done on rat and mouse models, it has been suggested that the retinal progenitor cells change over development in the cell

types they are competent to give rise to. Firstly the default state is the retinal ganglion cells. Next, the progenitor cells shift their competence so that they are more likely to produce horizontal cells, and then cone photoreceptor, followed by amacrine cells, rod photoreceptor, bipolar cells, and Muller glia cells (Rapaport *et al*., 2004).

The appropriate development of the structures like neural retina and pigment epithelium requires the interaction with the adjacent tissues. This is evident from an experiment (Pittack *et al*., 1997) which showed that if the optic vesicle is isolated from the surrounding epidermis and mesenchyme, then the differentiation is arrested at the optic vesicle stage and the eye does not forms. It has been found that the lens ectoderm immediately adjacent to the presumptive neural retina of the optic vesicle expresses a fibroblast growth factor (Moshiri *et al*., 2004) and treatment of the developing chick optic vesicle with exogenous fibroblast growth factor or with the antibodies against this factor causes perturbation in the development of retina (Pittack *et al*., 1997). There is evidence showing that fibroblast growth factor controls eye development through its action on a class of transcription factors that bind to DNA and selectively activate the genes important for eye development (Moshiri *et al*., 2004).

1.2.1 Retinal differentiation

Differentiation of photoreceptors in the retina of various species has been studied and it has been found that in all the vertebrates the cone photoreceptors are generated before the

rod photoreceptors (Levine *et al*., 2000). *In vitro* experiments with chick embryo tissue destined to form retinal progenitor cells have suggested that cones are not dependent on the surrounding cells for differentiation, while the differentiation of rods *in vitro* requires a critical cell density suggesting a requirement of signaling molecules from surrounding cells. Some of the factors that promote rod photoreceptor differentiation are hedgehog factors, activin, retinoic acid, ciliary neurotrophic factor and fibroblast growth factor (Levine *et al*., 2000).

Differentiation of the inner retina starts immediately after the final mitotic division at their ventricular surface. Retinal cells then migrate to their appropriate lamina. As they migrate, the different types of neuron begin to take on some morphological features of their characteristic cell type. For example, ganglion cells begin to elongate their axon before the point when their lamina reaches the ganglion cell layer. The next phase in the differentiation of retinal neurons is the growth of dendritic processes. In the last stages of differentiation the retinal neurons make morphologically identifiable synapses with one another and express their transmitters and receptors. The time course of these events overlaps considerably (Reh *et al*., 2001).

1.2.2 Retinal maturation

As the retina matures, nearly all the events continue to proceed in a central to peripheral direction. Once the process of retinal histogenesis is complete, remodeling continues

primarily in the form of retinal stretch, owning to steadily increasing intraocular pressure. The development of the fovea in primates is another aspect of later retinal development (Reh *et al*., 2001).

1.3. Phototransduction

Phototransduction is the process by which a photon of light captured by a visual pigment generates an electrical response in a photoreceptor cell. The phototransduction cascade can be divided into three phases (Pugh *et al*., 1993, Dizhoor *et al*., 1994**,** Chen *et al*., 1995, Calvert *et al*., 1995, Burns *et al*., 2005) (depicted in Figure 1.4)

1. Activation and signal amplification
2. Recovery of photoresponse
3. cGMP restoration

1. <u>Activation of the phototransduction cascade and signal amplification</u>

Opsin proteins which are integral membrane proteins, bound to a 11-*cis* retinal chromophore form the vertebrate visual pigments. 11-*cis* retinal is a light sensitive chromophore attached to the opsin protein molecule. Rhodopsin is a protein consisting of rod opsin bound to 11-*cis* retinal chromophore. Capture of a single photon results in the isomerization of the chromophore 11-*cis* retinal to all-*trans* retinal. The

photoisomerization reaction converts the rhodopsin molecule into another species termed metarhodopsin II (R*). This activated molecule activates a heterotrimeric (three non-identical subunits) GTP-binding protein, transducin, by exchanging the GDP bound to the α subunit of transducin with GTP. This results in the formation of transducin-GTP complex (Gαt-GTP). At this stage of phototransduction cascade the signal amplification is achieved by the activation of multiple transducin molecules by a single R*. Studies on the toad (*Bufo marinus*) have shown that 120-150 transducins per second are activated by a single R* (Leskov *et al*., 2000). Further, Gαt-GTP activates phosphodiesterase (PDE), which is complexed with cGMP, by binding to the γ subunit of PDE. Activated PDE hydrolyses cGMP to 5' GMP. The cGMP is involved in the activity of cationic channels. cGMP binds to the cationic channels in the dark thereby opening them (Figure 1.4), so that there is an influx of Ca^{2+} and Na^{+} ions into the cell. Hydrolysis of cGMP by activated PDE leads to the closing of channels, in turn interrupting the steady inward current of Na^{+} and Ca^{2+}, thus hyperpolarizing the cell and decreasing the neurotransmitter release at the synaptic terminal (Figure 1.4) (Pugh *et al*., 1993, Jindrova *et al*., 1998, Thompson *et al*., 2003).

2. Recovery of photoresponse

Recovery is essential for the photoreceptors to respond to subsequently absorbed photons. Recovery to the dark states requires efficient termination of the each of the steps of the phototransduction cascade. Inactivation of R* is achieved by the phosphorylation of R* by rhodopsin kinase. A calcium-binding protein recoverin regulates the activity of

rhodopsin kinase in a calcium-dependent manner. Recoverin contains a covalently attached N-terminal myristoyl group. Ca^{2+} binding to recoverin extrudes this myristoyl group of the protein and enables it to interact with disc membranes and this membrane-binding inhibits the activity of rhodopsin kinase (Calvert *et al*., 1995). Rhodopsin kinase is inhibited in the dark when intracellular calcium is high. The next step in R* inactivation is the binding of arrestin to phosphorylated rhodopsin, preventing further activation of of transducin by steric hindrance. The termination of transducin activity is achieved by the hydrolysis of transducin (Tα) bound GTP to GDP, in the presence of regulator of G protein signaling (RGS9) (Burns *et al*., 2005, Jindrova *et al*., 1998).

3. cGMP restoration

In the presence of light, the cGMP-gated channels are closed due to which entry of Ca^{2+} through the cGMP gated channels is stopped while Ca^{2+} continues to be extruded through the $Ca^{2+}K^{+}/Na^{+}$ exchanger (Figure 1.4) This leads to a decline in the Ca^{2+} concentration of the photoreceptor cell. This fall in Ca^{2+} is detected by a Ca^{2+} binding protein called guanylate cyclase activating protein (GCAP) which rapidly stimulates cGMP synthesis by guanylate cyclase (Dizhoor *et al*., 1994, Burns *et al*., 2005). Once the cGMP levels are restored the cationic channels open again.

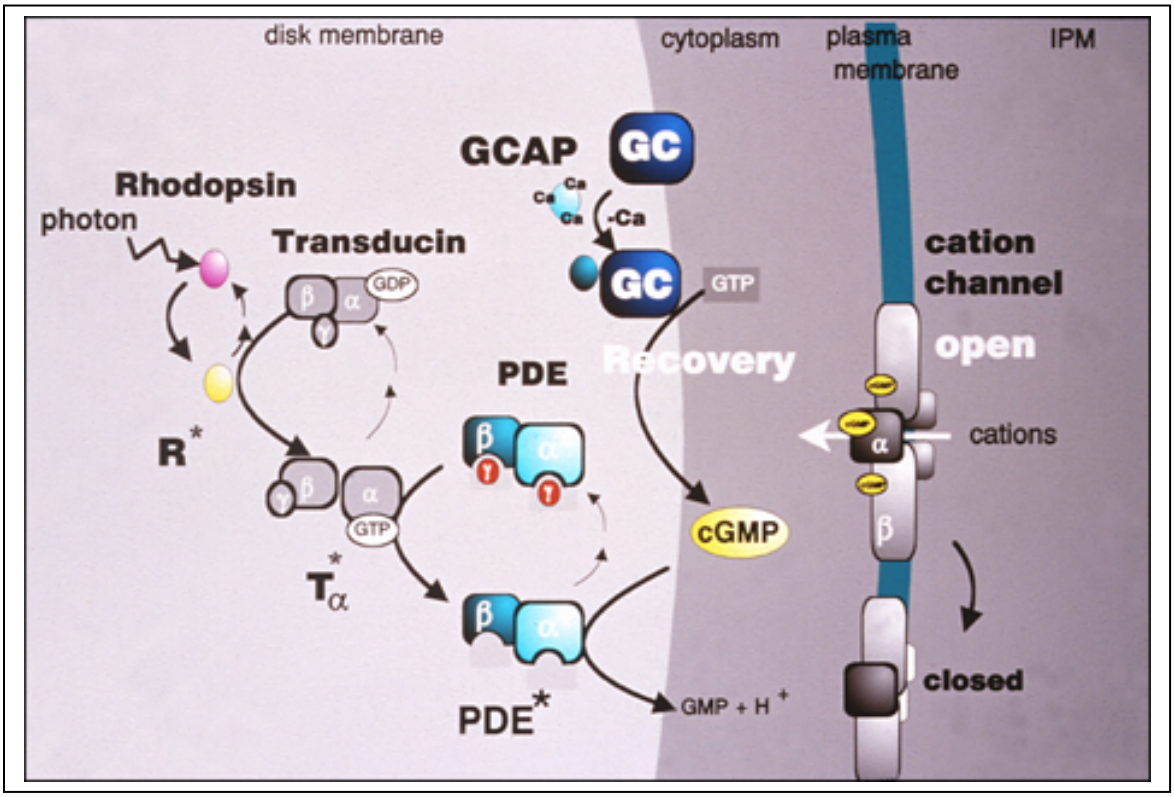

Figure 1.4. The phototransduction cascade in the rods. Abbreviations used: R (Rhodopsin), R* (activated rhodopsin), T (Transducin), GCAP (guanylate cyclase activating protein), PDE* (activated phosphodiesterase), GMP (guanosine monophosphate), GTP (guanosine triphosphate), IPM (inter photoreceptor matririces), GC (guanylate cyclase). (Taken from http://depts.washington.edu/ophthweb/KPgraphpic.html).

1.4 Visual cycle

The visual cycle comprises a series of enzymatic reactions that help in the regeneration of 11-*cis* retinal from all-*trans* retinal. The process of vision begins with the

photoisomerization of visual pigment chromophore 11-*cis* retinal to all-*trans* retinal. For opsin to function in vision, it must reunite with another 11-*cis* retinal molecule to produce rhodopsin or cone opsins. But neither rods nor cones can regenerate 11-*cis* retinal without the involvement of other ocular cells (Mata *et al*., 2002). The regeneration of 11-*cis* retinal is accomplished by the cycling of vitamin A analogs between the photoreceptors and retinal pigment epithelium, in case of rods (Rando *et al*., 2001) which is well accepted, and recently it has been proposed (Calvert *et al*., 1995) that in case of cones the Muller cells are involved in the regeneration of 11-*cis* retinal (Figure 1.5).

1.4.1 Visual cycle in rods

On absorption of light by rhodopsin, the chromophore of rhodopsin, 11-*cis* retinal, gets isomerised to all-*trans* retinal. All-*trans* retinal formed after photoisomerization eventually gets detached from opsin, as a result photochemically inactive opsin and all-*trans* retinal are formed. For opsin to function again in vision, it must reunite with a molecule of 11-*cis* retinal, to form a rhodopsin molecule. The all-*trans* retinal is short lived in photoreceptors, as it is chemically highly reactive (Lamb *et al*., 2004), and is rapidly reduced to all-*trans* retinol by alcohol dehydrogenase enzyme (RDH12) in the photoreceptor outer segments. All-*trans* retinol (vitamin A) thus formed leaves the photoreceptor outer segment and is transported to retinal pigment epithelium (RPE) by interphotoreceptor retinoid-binding protein (*IRBP*), which is found in the interphotoreceptor space. On entry to the RPE all-*trans* retinol is recognized by cellular

retinol binding protein (*CRBP*), which is highly specific for binding to all-*trans* retinol in comparison to other isomers including 11-*cis* retinol (Lamb *et al*., 2004). Next the all-*trans* retinol is esterified to all-*trans* retinyl esters in the presence of lecithin retinol acyl transferase (*LRAT*) enzyme by transferring the acyl group of lecithin to all-*trans* retinol. All-*trans* retinyl esters formed are then isomerized and hydrolyzed to 11-*cis* retinol by as single enzyme called isomerohydrolase/RPE65 (Moiseyev *et al*., 2005). The final step in the generation of chromophore is the oxidation of 11-*cis* retinol to 11-*cis* retinal by 11-*cis* retinol dehydrogenase enzyme (RDH5) (Simon *et al*.,1999). The 11-*cis* retinal regenerated in the RPE is transported to the outer segments of the photoreceptor through *IRBP* and the bleached opsin is regenerated and the rod visual cycle is completed (Figure 1.5) (Carlson *et al*., 1992, Rando *et al*., 2001).

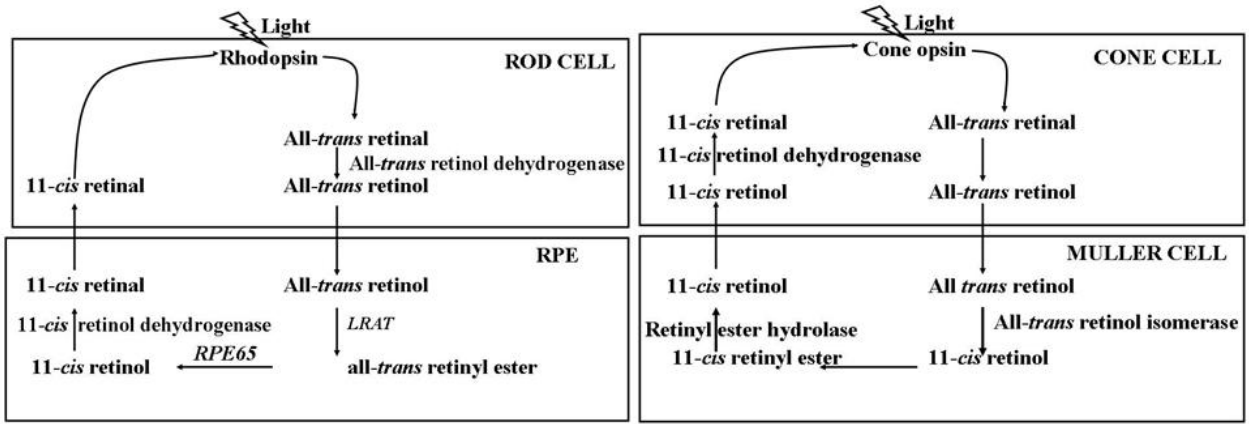

Figure 1.5. Schematic of visual cycle in rods (left) and cones (right). (Schematic drawn by taking the concept form Rando *et al*., 2001, Mata *et al*., 2002)

1.4.2 Visual cycle in cones

Through experiments on the retinas of cone-dominated animals (chicken and ground squirrel) Mata and coworkers (2002), have proposed that the cones regenerate their visual pigment by using Muller cells. Apart from similarities with the rod visual cycle, visual pigment regeneration in cones shows three catalytic activities, as shown in Figure 1.5 (Mata *et al*., 2002).

The all-*trans* retinol generated in the cones is transported to the Muller cells, where all-*trans* retinol is isomerized to 11-*cis* retinol by all-*trans* retinol isomerase in the presence of palmitoyl coenzyme A. The 11-*cis* retinol formed is converted to 11-*cis* retinyl ester by a second enzyme called 11-*cis* retinyl ester synthase which is distinct from lecithin retinol acyltransferase (*LRAT*) (Mata *et al*., 2002). This enzyme catalyses the formation of 11-*cis* retinyl esters but not the all-*trans* retinyl esters. The11-*cis* retinyl ester is then converted to 11-*cis* retinol by retinyl ester hydrolase enzyme, and is transported to the cones by interphotoreceptor retinoid-binding protein (IRBP). In the cones 11-*cis* retinol is converted to 11-*cis* retinal by 11-*cis* retinol dehydrogenase. This dehydrogenase is different from the enzyme of the rod visual cycle in that it uses NADP+ as cofactor (Mata *et al*., 2002), while 11-*cis* retinol dehydrogenase of the rod visual cycle uses NAD+ as cofactor (Jang *et al*., 2000). The 11-*cis* retinal is used to regenerate the cone opsins, and the cone visual cycle is completed.

1.5 Retinal dystrophies

Retinal dystrophies are a group of disorders characterized by inherited, progressive dysfunction, cell loss and eventual atrophy of retinal tissue. Retinal dystrophies are heterogeneous both genetically and clinically and involve primarily the degeneration of photoreceptors. They are classified according to the type of photoreceptor (rod or cone) primarily involved and on the mode of inheritance. Further, in certain forms, there are manifestations of disease that are restricted to the retina (non-syndromic) or involve dysfunction of other organs apart from the eye (syndromic). The involvement of both rods and cones in advanced stages of disease in several of these disorders may make them clinically indistinguishable.

1.5.1 Classification

Retinal dystrophies can be broadly classified into following types:

1. Rod and rod-cone dystrophies
2. Cone dystrophies
3. Macular dystrophies
4. Leber congenital amaurosis

1.5.1a. Rod and rod-cone dystrophies

Rod and rod-cone dystrophies include those retinal dystrophies which primarily involve the degeneration of rod photoreceptors. Loss of rod photoreceptors can be progressive or non-progressive. The progressive forms are termed rod-cone types as loss of rod cells eventually lead to loss of cone photoreceptors, while in the non-progressive forms, only rod cells are lost.

A. Progressive forms of rod and rod-cone dystrophies

i. Retinitis pigmentosa

Retinitis pigmentosa is a major form of rod-cone type of retinal dystrophy, which arises due to the primary degeneration of rod photoreceptors. As a consequence of this, visual impairment manifests initially in the form of night blindness and peripheral visual field loss. The visual field loss may be restricted to a small area, unnoticed by the patient, or it may be so severe as to result in profound loss of peripheral visual field, also known as tunnel vision. Degeneration of cones occurs in later stages, resulting in loss of central vision and may eventually lead to total blindness (Berson, 1993). Retinitis pigmentosa (RP) is extremely genetically heterogeneous being inherited in autosomal, sex-linked and mitochondrial modes. One of the characteristic features associated with RP is the formation of pigmentary deposits which arise from the RPE cells that detach and migrate through the Bruchs membrane as photoreceptor loss progresses and deposit around blood vessels as perivascular clusters in the form of bone spicules. Other clinical signs include

attenuation of retinal vessels as a result of degeneration of the retina, diminished or extinguished electroretinogram (ERG) reflecting the loss of photoreceptor activity, and pallor of the optic disc (Berson, 1993).

The term *retinitis pigmentosa* was first described by Donders in 1855 and 1857 (Richard *et al*., 1994). *Retinitis* means inflammation of retina, but as inflammation is not a prominent part of the pathophysiology of the condition, the term is inaccurate. World-wide prevalence of RP varies from 1 in 3000-5000 (Haim *et al*., 1992, Bundey *et al*., 1984, Bunker *et al*., 1984) to 1 in 1000 (Xu *et al*., 2006). According to the Andhra Pradesh Eye Disease Study (APEDS) the prevalence of blindness due to RP in Andhra Pradesh is 1 in 1000 (Dandona *et al*., 2001).

RP is sometimes associated with involvement of other tissues in addition to the retina. Usher syndrome is the most common forms of syndromic RP. It is defined as an autosomal recessive congenital deafness with retinopathy, which is indistinguishable from typical RP. It is the most common syndrome associated with RP (Boughman *et al*., 1983, Hope *et al*., 1997). Bardet-Biedl Syndrome (BBS) is another major type of syndromic RP. It is characterized by five main features, retinopathy, polydactyly, congenital obesity, mental retardation and hypogenitalism (Steiner, 1990). If paraplegia (paralysis of lower half of body) is present along with mental retardation and retinopathy then this is referred to as Laurence-Moon-Bardet-Biedl syndrome (Clay, 1933). The fundus in BBS shows very little pigmentary dispersion in the early stages. Macular

abnormalities are seen in the form of macular wrinkling, preretinal membrane formation and leakage on fluorescein angiogram from paramacular capillaries (Steiner, 1990).

Sectoral retintis pigmentosa is an atypical variant of RP which is characterized by late onset, regionalized areas of bone spicule pigmentation, which is usually found in inferior quadrant of retina, subnormal electroretinograms, visual field defects corresponding to the sector areas involved and slow to no progression (Richard *et al*., 1994).

B. Non-progressive forms of rod dystrophy

Congenital stationary night blindness (CSNB) is a non-progressive type of retinal dystrophy which involves the impairment of only rod photoreceptors. Rod electroretinograms are severely impaired while the fundus appears normal and cone function is normal (Carr, 1974).

Fundus albipunctatus is a type of congenital stationary night blindness which is inherited in an autosomal recessive form, characterized by multiple white yellow spots located in the RPE and by a delayed course of dark adaptation. These patients show severely depressed rod function during dark adaptation, however after 2-3 hours of dark adaptation rod sensitivity improves to the normal level. The cone electroretinograms are also abnormal (Lamb *et al*., 2004). Newfoundland rod–cone dystrophy is similar to fundus albipunctatus but with a lower age of onset (1st decade) and more rapid

progression and substantial or total loss of vision by 4th or 5th decade of life (Eichers *et al*., 2002).

There are other syndromic forms that involve pigmentary retinopathy along with the disorders of the other organs. Examples are Leigh syndrome, Refsum syndrome, Kearns-Sayre syndrome, Battens disease, Alagille syndrome, Bassen-Kornzweig syndrome, Alstrom syndrome etc (Richards *et al*., 1994)

1.5.1b. Cone dystrophies

Cone dystrophies are a group of retinal dystrophies that are characterized by bilateral visual loss, color vision abnormalities, central scotomata, nystagmus, photophobia and abnormal cone electroretinograms. Cone dystrophies shows genetic as well as clinical heterogeneity, and can be inherited as autosomal dominant, autosomal recessive or X linked types. They can be divided into two subtypes, stationary and progressive.

1. Stationary cone dystrophies

The stationary sub-types of cone dystrophy are congenital and have normal rod function (Michaelides *et al*., 2004). Stationary cone dystrophies can be further divided into; complete achromatopsia, incomplete achromatopsia and oligicone trichromacy (Michaelides *et al*., 2004).

2. Progressive cone dystrophies

Progressive cone dystrophies, also referred to as cone-rod dystrophies, are a variant of RP, and show an involvement of cone photoreceptors along with rod photoreceptors. Cone-rod dystrophies are genetically heterogeneous and show a more central loss of visual field and greater degree of early changes in the cone-dominated central retina. Colour vision is also compromised. Other clinical features include photophobia, nystagmus and visual field abnormalities like central scotomata, peripheral field loss, and generalised depression of sensitivity and ring scotomata (a ring shaped area of diminished vision in the visual field). Fundus examination may show a bull's eye maculopathy (concentric alternating light and dark areas in the macular region), but in the later stages there may be peripheral atrophy and pigmentation (Simunovic *et al*., 1998).

1.5.1c. Macular dystrophies

Macular dystrophies are defined as a group of disorders that are characterized by central visual loss with the atrophy of the macula and the underlying retinal pigment epithelium. They mostly develop in the 1st and 2nd decades of life. Macular dystrophies show clinical and genetic heterogeneity. Autosomal dominant, autosomal recessive, X-linked and mitochondrial modes of inheriance have been reported. Types of of the macular dystrophies include Bests-vitelliform dystrophy, Sorsby fundus dystrophy, Stargardts

disease, fundus flavimaculatus, Doyne honeycomb retinal dystrophy, North Carolina macular dystrophy, progressive bifocal chorioretinal atrophy, central areolar choroidal dystrophy, butterfly shaped macular dystrophy and dominant cystoid macular dystrophy (Richards *et al*., 1994).

1.5.1d. Leber Congenital Amaurosis (LCA)

LCA is a severe form of retinal dystrophy that is congenital in onset. It is mostly inherited as an autosomal recessive form and is genetically heterogeneous. Autosomal dominant inheritance has also been reported in LCA (Sohocki *et al*., 1998, Bowne *et al*., 2006). Patients often have nystagmus (involuntary movements of eye ball) resulting from inability to fix due to very poor vision. The characteristic feature of LCA is a diminished electroretinographic (ERG) response recordable within the first year of life. The fundus may be initially normal, but shows abnormalities in the form of salt and pepper pigmentation, attenuation of retinal vessels, atrophy of RPE and choriocapillaris (Perrault *et al*., 1999) Syndromic forms of LCA exist and these are Refsum disease (Russell-Eggitt *et al*., 1989), Senior-Loken syndrome (Ehara *et al*., 1997) and Joubert syndrome (Parisi *et al*., 2007)

1.6 Genetics of RP

1.6.1 Overview of genes causing RP

This section provides an overview of genetics of RP, with a more detailed discussion on the genes known to cause ARRP, since this form was the major focus of this study.

RP is genetically heterogeneous and can occur with the following types of inheritance:

Autosomal Dominant

Autosomal Recessive

X linked

Digenic

Mitochondrial

There are 18 genes identified so far for ADRP, 23 genes for ARRP, 2 for XLRP and atleast 3 mitochondrial genes. Details of the genes are summarized in Tables 1.1-1.4.

Table 1.1. Genes involved in ADRP.

#	Gene	Location	Function	First report
1	*RHO* *	3q22.1	Photosensitive pigment in phototransduction (Nathans *et al*., 1992)	Dryja *et al*., 1990
2	*PRPH2*	6p21.2	OS disc structure (Molday *et al*., 1994)	Kajiwara *et al*.,

				1991
3	*ROM1*	11q12.3	Regulation of disk morphogenesis and the viability of mammalian rod photoreceptors (Clarke G *et al*., 2000).	Sakuma *et al*., 1995
4	*CRX*	19q13.32	Transcription factor (Furukawa *et al*., 1997)	Freund *et al*., 1998, Sohocki *et al*., 1998
5	*NRL* *	14q11.2	Transcription factor (Bessant *et al*., 1999)	Bessant *et al*., 1999
6	*RP1* *	8q12.1	Likely role either in the transportation of protein from inner segments to outer segments or in the maintenance of cilial structure (Liu *et al*., 2002)	Sullivan *et al*., 1999
7	*PRPF8*	17p13.3	Pre-mRNA splicing (Luo *et al*., 1999)	Mckie *et al*., 2001
8	*PRPF31*	19q13.42	Pre-mRNA splicing (Vithana *et al*., 2001)	Vithana *et al*., 2001
9	*FSCN2*	17q25.3	Likely role in the assembly of actin microfilaments associated with photoreceptor discs (Tubb *et al*., 2000)	Wada *et al*., 2001
10	*IMPDH1*	7q32.1	Catalyzes the formation of xanthine monophosphate from inosine monophosphate (Aherne *et al*., 2004)	Bowne *et al*., 2002
11	*PRPF3*	1q21.2	Pre-mRNA splicing (Wang *et al*., 1997)	Chakarova *et al*., 2002
12	*PAP1*	7p14.3	Unknown	Keen *et al*., 2002
13	*CA4*	17q23.2	Reversible hydration of carbon dioxide (Yang *et al*., 2005)	Rebello *et al*., 2004
14	*GUCA1B*	6p21.1	Activates photoreceptor guanylyl cyclase in a calcium-dependent manner (Gorczyca *et al*., 1995)	Sato *et al*., 2005**a**
15	*SEMA4A*	1q22	Likely role in cell cell interactions between photoreceptors and RPE (Rice *et al*., 2004)	Abid *et al*., 2005
16	*NR2E3*	15q23	Acts synergistically with other transcription factors like NRL and CRX and activates rod-specific genes essential for differentiation of rod photoreceptors (Cheng *et al*., 2004)	Coppieters *et al*., 2007
17	*TOPORS*	9p21.1	Likely role as as a ubiquitin ligase for transcription factors (Rajendra *et al*., 2004)	Chakarova *et al*., 2007
18	*RDH12*	14q24.1	Catalyzes reduction of all-*trans* retinal and its 9-*cis*, 11-*cis* , and 13-*cis* retinal isomers in the presence of NADPH (Maeda *et al*., 2006).	Fingert *et al*., 2008

Genes marked with astrisk (*) are also involved in ARRP. Gene symbols used are- rhodopsin (*RHO*), retinal degeneration slow (*RDS*), retinal outer segment membrane protein (*ROM1*), cone-rod homeobox (*CRX*), neural retina zipper (*NRL*), retintis pigmentosa 1 (*RP1*), pre-mRNA processing factor 8 homolog (*PRPF8*), pre-mRNA processing factor 31 homolog (*PRPF31*), fascin homolog 2 (*FSCN2*), inosine monophosphate

dehydrogenease 1 (*IMPDH1*), pre-mRNA processing factor 3 homolog (*PRPF3*), pim1 associated protein (*PAP1*), carbonic anhydrase IV (*CA4*), guanylate cyclase activator 1B (*GUCA1B*), semaphorin (*SEMA4A*), nuclear receptor subfamily 2, group E, member 3 (*NR2E3*), topoisomerase I binding, arginine/serine-rich (*TOPORS*), retinol dehydrogenase 12 (*RDH12*)

Table 1.2. Genes involved in ARRP.

#	Gene	Location	Function	First report
1	*PDE6B*	4p16.3	Hydrolysis of cGMP in phototransduction (Jindrova *et al*., 1998)	McLaughlin *et al*., 1993
2	*CNGA1*	4p12	Forms a cGMP-gated cation channel in the plasma membrane, allowing depolarization of rod photoreceptors (Dhallan *et al*., 1992)	Dryja *et al*., 1995
3	*PDE6A*	5q33.1	Hydrolysis of cGMP in phototransduction (Ionita *et al*., 2007)	Huang *et al*., 1995
4	*RLBP1*	15q26.1	Facilitates conversion of all-*trans* retinyl esters to 11-*cis* retinol and prevents esterification of 11-*cis* retinol (Noy *et al*., 2000)	Maw *et al*., 1997
5	*ABCA4*	1p22.1	Transports all-*trans* retinylidene-phosphatidylethanolamine across the disc membrane (Ahn *et al*., 2003)	Allikmets *et al*., 1997a
6	*RPE65*	1p31.2	Involved in the isomerization and hydrolysis of all-*trans* retinyl ester to 11-*cis* retinol (Moiseyev *et al*., 2005).	Gu *et al*., 1997
7	*SAG*	2q37.1	Inhibits activated phototransduction pathway, either by binding to the photoexcited phosphorylated rhodopsin or by inhibiting the cGMP phosphodiesterase (Yamaki *et al*., 1990)	Nakazawa *et al*., 1998
8	*TULP1*	6p21.31	Likely role in protein trafficking (Hagstorm *et al*., 1999).	Banerjee *et al*., 1998
9	*RGR*	10q23.1	Required in the conversion of all-*trans* retinal to 11-*cis* retinal (Chen *et al*., 2001).	Morimura *et al*., 1999a
10	*USH2A*	1q41	Tissue- specific extracellular matrix protein (Eudy *et al*., 1998).	Rivolta *et al*., 2000
11	*MERTK*	2q13	Phagocytosis of apoptotic cells (Scott *et al*., 2001)	Gal *et al*., 2000
12	*PNR*	15q23	Acts synergistically with other transcription factors like NRL and CRX and activates rod-specific genes essential for differentiation of rod photoreceptors (Cheng *et al*., 2004).	Gerber *et al*., 2000
13	*PROM1*	4p15.32	Likely role in the morphogenesis of disc (Zelhof *et al*. 2006)	Maw *et al*., 2000
14	*CNGB1*	16q13	Forms a cGMP-gated cation channel in the plasma membrane, allowing depolarization of rod photoreceptors (Dhallan *et al*., 1992)	Bareil *et al*., 2001

15	*CRB1*	1q31.3	Likely role in the neuronal development of retina, presumably through protein-protein interaction (den Hollander *et al*., 1999)	den Hollander *et al*., 2001, Lotery *et al*., 2001
16	*LRAT*	4q32.1	Catalyses the conversion of the membrane-associated form of RPE65 to the soluble form of RPE65 (Xue *et al*., 2004)	Thompson *et al*., 2001
17	*CERKL*	2q31.3	Converts ceramide into ceramide-1 phosphate, which is a key mediator of cellular apoptosis and survival (Tuson *et al*., 2004)	Tuson *et al*., 2004
18	*PRCD*	17q25.1	Unknown	Zangerl *et al*., 2006
19	*EYS*	6p12	Likely role in disc morphogenesis (Collin *et al*., 2008)	Abd El-Aziz *et al*., 2008, Collin *et al*., 2008
20	*IDH3B*	20p13	Catalyze the oxidative decarboxylation of isocitrate into alpha-ketoglutarate in the citric acid cycle (Hartong *et al*., 2008)	Hartong *et al*., 2008

Genes *NRL*, *RHO* and *RP1* are involved in both ARRP and ADRP. Gene symbols are-phosphodiesterase 6B, cGMP specific beta subunit (*PDE6B*), cyclic nucleotide gated channel alpha 1 (*CNGA1*), phosphodiesterase 6A cGMP specific alpha subunit (*PDE6A*), retinaldehyde binding protein 1 (*RLBP1*), ATP binding cassette transporter retinal (*ABCA4*), retinal pigment epithelium specific protein 65kDa (*RPE65*) arrestin (*SAG*), tubby-like protein 1 (*TULP1*), retinal G protein coupled receptor (*RGR*), usher syndrome 2A (*USH2A*), c-mer proto-oncogene tyrosine kinase (*MERTK*) photoreceptor cell-specific nuclear receptor gene (*PNR*), prominin 1 (*PROM1*), cyclic nucleotide gated channel, β1 subunit (*CNGB1*), crumbs homolog 1 (*CRB1*), lecithin retinol acyltransferase (*LRAT*), ceramide kinase like (*CERKL*), progressive rod-cone degeneration (*PRCD*) eyes Shut, Drosophila, homolog of, (*EYS, SPAM*), isocitrate dehydrogenase 3 (NAD+) beta (*IDH3B*)

Table 1.3. Genes involved in XLRP.

#	Gene	Location	Function	First report
1	*RPGR*	Xp11.4	Ciliary protein (Hong *et al*., 2003)	Meindl *et al*., 1996
2	*RP2*	Xp11.23	Unknown	Schwahn *et al*., 1998

Gene symbols refer to retinitis pigmentosa GTPase regulator (*RPGR*), retinitis Pigmentosa gene 2 (*RP2*)

Table 1.4. Mitochondrial genes associated with RP.

#	Gene	Function	First report
1	*MT-ATP6*	ATP synthesis (Santorelli *et al*., 1993)	Santorelli *et al*., 1993

2	*MT-TS2*	mitochondrial translation (Mansergh *et al*., 1999)	Mansergh *et al*., 1999
3	*MT-TH*	oxidative phosphorylation (Crimi *et al*., 2003)	Crimi *et al*., 2003

Gene symbols refers to mitochondrially encoded ATP synthase 6 (*MT-ATP6*), mitochondrially encoded tRNA serine 2 (*MT-TS2*), mitochondrially encoded tRNA histidine (*MT-TH*)

Table 1.5. Genes involved in autosomal dominant LCA.

#	Gene	Location	Function	First report
1	*CRX*	19q13.32	Transcription factor (Furukawa *et al*., 1997)	Sohocki *et al*., 1998
2	*IMPDH1*	7q32.1	catalyzes the formation of xanthine monophosphate from inosine monophosphate (Aherne *et al*., 2004)	Bowne *et al*., 2006

Gene symbols- cone-rod homeobox (*CRX*), inosine monophosphate dehydrogenease 1 (*IMPDH1*)

Table 1.6. Genes involved in autosomal recessive LCA.

#	Gene	Location	Function	First report
1	*GUCY2D*	17p13.1	Catalyses the conversion of guanosine triphosphate to cyclic 3', 5'- guanosine monophosphate (Perrault *et al*., 1999).	Perrault *et al*., 1996
2	*RPE65*	1p31.2	Involved in the isomerization and hydrolysis of all-*trans* retinyl ester to 11-*cis* retinol (Moiseyev *et al*., 2005).	Marlhens *et al*., 1997
3	*CRX*	19q13.32	Transcription factor (Furukawa *et al*., 1997)	Swaroop *et al*., 1999
4	*AIPL1*	17p13.2	Chaperone-like function (Spuy *et al*., 2004)	Sohocki *et al*., 2000
5	*RPGRIP1*	14q11.2	involved in the disk morphogenesis (Gerber *et al*., 2001)	Dryja *et al*., 2001
6	*CRB1*	1q31.3	Likely role in the neuronal development of retina, presumably through protein-protein interaction (den Hollander *et al*., 1999)	Lotery *et al*., 2001
7	*LRAT*	4q32.1	Catalyses the conversion of the membrane-associated form of RPE65 to the soluble form of RPE65 (Xue *et al*., 2004)	Thompson *et al*., 2001
8	*RDH12*	14q24.1	Catalyzes reduction of all-*trans* retinal and its 9-*cis*, 11-*cis*-, and 13-*cis* retinal isomers in the presence of NADPH (Maeda *et al*., 2006).	Perrault *et al*., 2004
9	*TULP1*	6p21.31	Likely role in protein trafficking (Hagstorm *et al*., 1999).	Hanein *et al*., 2004
10	*RD3*	1q32.3	Likely role in cellular processes and influence the	Friedman *et*

			function of subnuclear bodies (Friedman *et al*., 2006)	*al*., 2006
11	*CEP290*	12q21.32	Involved in G protein trafficing (McEwen *et al*., 2007)	den Hollander *et al*., 2006
12	*LCA5*	6q14.1	Associated with centrosomal or ciliary function (den Hollander *et al*., 2007c).	den Hollaner *et al*., 2007c
13	*SPATA7*	14q31.3	Unknown	Wang *et al*., 2009

Gene symbols refer to- retinal guanylate cyclase 2D (*GUCY2D*), retinal pigment epithelium specific protein 65kDa (*RPE65*), cone-rod homeobox (*CRX*), aryl hydrocarbon receptor interacting protein like 1 (*AIPL1*), RPGR interacting protein (*RPGRIP1*), crumbs homolog 1 (*CRB1*), lecithin retinol acyltransferase *(LRAT*), retinol dehydrogenase 12 (*RDH12*), tubby like protein 1 (*TULP1*), chromosome 1 open reading frame 36 (*RD3, C1ORF36*), centrosomal protein 290 (*CEP290*), spermatogenesis associated protein 7 (*SPATA7*)

1.6.2 Genes involved in ARRP

1. Rhodopsin (*RHO*, RP4)

The rhodopsin gene is located on chromosome 3q21-q24. The gene codes for a 348 amino acid protein. Rhodopsin belongs to a family of G-protein coupled receptors, also known as 7-transmembrane (7-TM) domain receptors. It is localized on the disc membranes as well as on the plasma membrane of the rod outer segments. The N-terminal part of the protein is enclosed in the intradiscal space; the C-terminal region and the intracellular loops face the cytoplasm (Nathans *et al*., 1992). Rhodopsin has two components, a chromophore 11-*cis* retinal and an opsin protein. 11-*cis* retinal is bound to opsin at lysine 296 by protonated Schiff-base linkage. The 11-*cis* retinal is the light-absorbing unit of rhodopsin that allows rhodopsin to mediate vision in dim light.

Phototransduction starts with the absorption of a photon of light by rhodopsin. This induces *cis* to *trans* isomerisation of the rhodopsin chromophore 11-*cis* retinal, and a conformational change of rhodopsin to its active state known as metarhodopsin (II, R*) which activates the rhodopsin. The R* catalytically stimulates the G-protein transducin. The transducin mediates the signal transmission between the rhodopsin and cGMP specific phosphodiesterase (Nathans *et al*., 1992). The R* is inactivated by its phosphorylation with rhodopsin kinase and subsequently by the binding of arrestin.

Mutations in the rhodopsin gene are a predominant cause of ADRP in American and European populations with mutations occurring in 10 to 30% of patients with ADRP from these populations (Inglehearn *et al*., 1992, Bareil *et al*., 1999, Bunge *et al*., 1993, Sung *et al*., 1991). Mutations in rhodopsin are also associated with congenital stationary night blindness (Dryja *et al*., 1993) and recessive RP (Rosenfeld *et al*., 1992). Mutation of proline-23 to histidine is found in 12.7% and mutation of proline-347 to leucine is found in 5.3% of the US population (Vaithinathan *et al*., 1994). The presence of the uncommon CA allele repeat polymorphism in the first intron of the rhodopsin gene in patients with the proline-23 to histidine mutation suggests it to be a founder mutation (Dryja *et al*., 1991) and less likely to be a mutational hotspot. Absence of linkage disequilibrium between the mutation of proline-347 to leucine and CA repeat polymorphism in the patients with this mutation is suggestive of a mutational hot spot (Dryja *et al*., 1991).

2 & 3. Rod cGMP phosphodiesterase type 6 (*PDE 6*) (α and β subunits)

PDE6 belongs to a family of cyclic nucleotide phosphodiesterases and is an important enzyme of phototransduction pathway hydrolyzing cGMP. PDE6 is a membrane-associated heterotetrameric enzyme and consists of α-, β- and γ-subunits. The α- and β-subunits (encoded by the *PDE6A* and *PDE6B* genes, respectively) form the catalytic core of the enzyme while the 2 identical γ-subunits (encoded by the *PDE6G* gene) are the inhibitory subunits which keep the enzyme in inactive state (Ionita *et al*., 2007). Mutations in the β-subunit cause ARRP (McLaughlin *et al*. 1993) or autosomal dominant CSNB (Gal *et al*., 1994). 3 to 5% of patients with ARRP have mutations in the *PDE6B* gene (McLaughlin *et al*. 1993, Bayes *et al*., 1995). 2.4% of patients with ARRP are known to have mutations in the *PDE6A* gene (Dryja *et al*., 1999). Till date no mutations have been reported in the *PDE6G* gene in patients with any form of retinal dystrophy, although *PDE6G* mouse model shows features similar to human patients with retinitis pigmentosa (Tsang *et al*., 1996).

4. Cyclic nucleotide gated channel alpha 1 (*CNGA1*)

Cyclic nucleotide gated channels are tetramers in their native form and composed of two subunits, A and B, that adopt a 3A:1B stoicometry (Zhong *et al*., 2002). The A-subunit (α-subunit) is encoded by *CNGA1* gene and the B-subunit (β-subunit) is encoded by *CNGB1* gene and are expressed in the outer segments of rod and cone photoreceptors. The *CNGA1* gene is located on chromosome 4p12. CNG channel subunit A has carboxy terminal leucine zipper domain that helps in the interaction of the two subunits (Zhong *et*

al., 2002). The CNG channels are opened by the direct binding of 3'-5'cyclic guanosine monophosphate (cGMP). *CNGA1* gene mutations cause 2.3% of autosomal recessive RP (Dryja *et al*., 1995).

5. Cellular retinaldehyde binding protein 1 (*RLBP1*, *CRALBP*)

The *CRALBP* gene is located on chromosome 15q26. *CRALBP* protein is a 317 amino acid protein expressed in the neural retina, RPE, ciliary body, cornea, optic nerve, pineal gland and brain (Noy *et al*., 2000). Within the RPE and neural retina it shows a high affinity for 11-*cis* retinoids. *CRALBP* is known to have two functions- first, it facilitates the conversion of all-*trans* retinyl esters to 11-*cis* retinol. Second, it prevents the esterification of 11-*cis* retinol and stimulates its oxidation to 11-*cis* retinal (Noy *et al*., 2000). Mutations in *CRALBP* are causative of a range of retinal phenotypes namely ARRP (Maw *et al*., 1997), retinitis punctata albescens, Newfoundland rod-cone dystrophy (a severe form of retinitis punctata albescens) (Eichers *et al*., 2002) and Bothnia dystrophy (Morimura *et al*., 1999).

6. ATP binding cassette transporter retinal (*ABCA4*, RP19)

The *ABCA4* gene is located on chromosome 1p22.3-p22.2. The 2273 amino acid protein product is known as the Rim protein (Allikmets *et al*., 1998). The *ABCA4* gene is exclusively expressed in the retina and the protein is localized to the disc membrane of rod outer segments (Sun *et al*., 2000) as well as in the peripheral and foveal cones

(Molday *et al*., 2000). *ABCA4* protein consists of two multispanning membrane domains (MSD), that serve as a pathway for the translocation of substrate across the membrane and two ATP-binding cassettes or nucleotide binding domains (NBD) that provide energy for substrate transport. *ABCA4* protein transports all-*trans* retinylidene-phosphatidylethanolamine across the disc membrane by utilizing energy from ATP hydrolysis (Ahn *et al*., 2003). The *ABCA4* gene is involved in the pathogenesis of Stargardts disease, cone rod dystrophy and recessive RP, and is being suggested to be a major risk factor in the pathogenesis of AMD by some studies (Allikmets *et al*., 1997) but not by others (De La Paz *et al*., 1999, Webster *et al*., 2001). 74% to 79% of patients with Stargardts disease have mutations in the *ABCA4* gene (Lewis *et al*., 1999, Rivera *et al*., 2000). *ABCA4* gene is found to be involved in 23.6% to 65% (Ducroq *et al*., 2002, Fishman *et al*., 2003) of patients with cone rod dystrophy. Mutations in the *ABCA4* have also been reported in families with ARRP (Martínez-Mir *et al*., 1998, Cremers *et al*., 1998, Rozet *et al*., 1999, Fukui *et al*., 2002, Klevering *et al*., 2004b). 2% (2/96) of patients with ARRP are found to have mutations in the *ABCA4* gene (Fukui *et al*., 2002). ABCA4 mutation screening is facilitated by a microarray chip which includes ~400 known disease causing variants as well as polymorphisms in *ABCA4* gene (Jaakson *et al*., 2003). This chip was found to be 98% effective in detecting the known variants. Genetic testing through this chip is available commercially with Asper Ophthalmics, Estonia (http://www.asperophthalmics.com/ABCRgenetest.htm). The chip has now been upgraded by them to detect 496 known disease-causing variants.

Cremers and co-workers (1998) have hypothesized that a combination of 2 *ABCA4* null alleles results in ARRP, a severe phenotype, while a combination of a null allele with a second mutation with residual *ABCA4* function leads to the less severe phenotype of CRD. Similar genotype-phenotype correlation has been observed by Klevering and coworkers (2004) in two Dutch families. In both the families patients with Stargardts disease were compound heterozygous for a mild mutation (2588G>C) and a severe mutation (768G>T or IVS33+1G>A), while patients with RP were homozygous for a severe *ABCA4* mutation (768G>T).

7. Retinal pigment epithelium specific protein 65kDa (*RPE65*, RP20)

RPE65 gene is located on chromosome 1p31 and codes for a protein of 533 amino acids. This protein is expressed exclusively in the retinal pigment epithelium (Nicoletti *et al*., 1995). *RPE65* protein exists in two forms; a membrane associated form and a soluble form. The membrane- associated form is triply palmitoylated. It is a chaperone for all-*trans* retinyl esters and allows their entry into the visual cycle for processing into 11-*cis* retinal. The soluble form of *RPE65* is not palmitoylated and is a chaperone for vitamin A. The palmitoylation of *RPE65* controls its ligand binding selectivity. The membrane associated form and the soluble form can be interconverted by lecithin retinol acyltransferase (*LRAT*) enzyme (Xue *et al*., 2004). Within the visual cycle *RPE65* is an isomerohydrolase, and functions in the isomerization and hydrolysis of all-*trans* retinyl ester to 11-*cis* retinol (Moiseyev *et al*., 2005). Mutations in *RPE65* gene are known to cause two phenotypes- autosomal recessive RP and LCA. *RPE65* gene mutations occur in

2% of ARRP patients (Morimura *et al*. 1998, 1999) and 6.8% to 16% of LCA patients (Lotery *et al*., 2000; Morimura *et al*. 1998).

8. Arrestin (S-Antigen (*SAG*))

The gene *SAG* (S antigen)/arrestin) is located on chromosome 2q37.1 and is expressed exclusively in the retina and pineal gland. Arrestin inhibits the activated phototransduction pathway, either by binding to the photoexcited phosphorylated rhodopsin and quenching the activation of light-dependent cGMP phosphodiesterase or by directly inhibiting the cGMP phosphodiesterase (Yamaki *et al*., 1990). Loss of the arrestin gene leads to continuous activation of the phototransduction cascade and it is hypothesized that this induces a Ca^{2+} stress that signals apoptosis in the cell (Fain *et al*., 1999). Mutations in the arrestin gene cause recessive RP (Nakazawa *et al*. 1998) and recessive Oguchi disease (Fuchs *et al*., 1995). Oguchi disease is characterized by congenital stationary night blindness associated with fundus discoloration and delayed dark adaptation (Maw *et al*., 1995). Nakazawa and coworkers (1998) screened 120 unrelated ARRP patients for the c.1147delA mutation, a frequent cause of Oguchi disease (Fuchs *et al*., 1995). They found a homozygous c.1147delA change in 3 unrelated families with ARRP, showing variable expressivity of the arrestin gene mutation. No mutations in the arrestin gene were found in the Canadian/American patients with ADRP (n=177) or ARRP (n=85) or stationary night blindness (n=10) (Sippel *et al*., 1998).

9. Tubby-like protein 1 (*TULP1*, RP14)

TULP1 gene is located on chromosome 6p21.3. *TULP1* gene sequence is conserved across species suggesting its vital cellular function (North *et al*., 1997). Expression of *TULP1* protein is restricted to the retina. *TULP1* knockout mice show degeneration of both rods and cones. Hagstrom and coworkers (1999) have observed accumulation of vesicular structures in the interphotoreceptor matrix and mislocalization of cone and rod opsins in *TULP1*-/- mice. They have speculated that *TULP1* has an essential role in the protein trafficking pathway (Hagstrom *et al*., 1999). Mutations in the *TULP1* gene are found in 2.2% of patients with ARRP (Gu *et al*., 1998, Hagstrom *et al*., 1998, Paloma *et al*., 2000, Mandal *et al*.,2005) and 3.7 % of patients with LCA (Hanein *et al*., 2004, Li *et al*., 2009) . It is interesting to note that Li and coworkers (2009) have found Q301X mutation in the *TULP1* gene in 5 unrelated families with LCA from Saudi Arabia. A founder effect was not investigated in the study.

10. Retinal G protein coupled receptor (*RGR*)

The *RGR* gene is located on chromsome10q23 and codes for a protein of 295 amino acids. *RGR* is a G-protein coupled receptor homologous to rhodopsin. It is found exclusively in the RPE and Muller cells. It is required in the conversion of all-*trans* retinal to 11-*cis* retinal in the RPE. It was proposed to act in a light-dependent manner (Chen *et al*., 2001) as a photoisomerase. Another study has suggested that it acts independent of light, presumably by influencing the isomerohydrolase activity in the RPE

(Wenzel *et al*., 2005). Mutations in *RGR* protein cause ARRP in about 0.5% of cases (Morimura *et al*., 1999).

11. Usher syndrome 2A (*USH2A*, RP39)

USH2A gene is located on chromosome 1q41 and codes for a protein of 1546 amino acids. The *USH2A* protein also known as usherin, which is known to interact with type 4 collagen and is a part of the basement membrane in cochlea, retina and many other tissues (van Wijk *et al*., 2004). The *USH2A* protein is thought to be a tissue-specific extracellular matrix protein or a cell adhesion molecule due to its similarity to laminins and cell adhesion molecules, a potential N-glycosylation site and a stretch of 20 residues of hydrophobic amino acids at the amino-terminus (Eudy *et al*., 1998). A mutation cysteine-759 to phenylalanine was found to be the most prevalent mutation in north American and Spanish populations (Rivolta *et al*., 2000). It was found in 4.5% (10 out of 224) (Rivolta *et al*., 2000) and 7% (10 out of 146) (Seyedahmadi *et al*., 2004) of patients with non-syndromic ARRP. These studies suggest that *USH2A* gene is likely to be involved in more than 4.5% to 7% of patients with ARRP as all the exons were not screened for mutations in these studies (Seyedahmadi *et al*., 2004, Rivolta *et al*., 2000).

12. c-mer proto-oncogene tyrosine kinase (*MERTK*, RP38)

The *MERTK* gene codes for a protein of 999 amino acids. *MERTK* protein has a putative transmembrane segment, a tyrosine kinase domain, N-glycosylation sites and tyrosine

phosphorylation sites (Graham *et al*., 1994). Studies on *MERTK* knockout mice showed that *MERTK*- null mice are extremely sensitive to the endotoxin lipopolysaccharide (LPS). The mice exhibit excessive TNFα production and increased susceptibility to septic shock. Thus it has been hypothesized that the *MERTK* gene is involved in modulating and dampening of cell activation in response to LPS endotoxin by downregulating the production of cytokines like TNFα (Camenisch *et al*., 1999). *MERTK* protein is also involved in the phagocytosis of apoptotic cells and thus has been suggested to maintain tissue homeostasis and the prevention of autoimmunity (Scott *et al*., 2001). 1% (3 of 328 patients) of patients with various retinal dystrophies were found to have mutations in the *MERTK* gene; the 3 patients with *MERTK* gene mutations had a diagnosis of ARRP (Gal *et al*., 2000). Tada and coworkers (2006) have analysed the *MERTK* gene in 96 patients with ARRP, and a disease-causing mutation was identified in a single patient with ARRP.

13. Photoreceptor cell-specific nuclear receptor gene (*PNR, NR2E3*, RP37)

The protein encoded by the *PNR* gene is a part of a large family of nuclear receptor transcription factors that are involved in signaling pathways (Gerber *et al*., 2000). It is expressed preferentially in the rod photoreceptors. *PNR* acts synergistically with other transcription factors like *NRL* and *CRX* and activates rod-specific genes essential for differentiation of rod photoreceptors (Cheng *et al*., 2004). *PNR* has also been reported as a repressor of cone specific genes in rods (Chen *et al*., 2005). Mutations in the *PNR* gene

cause enhanced S-cone syndrome (abnormal increase in the number of short wave type of cones) (Cheng *et al*., 2004) and ARRP (Gerber *et al*., 2000).

14. Prominin 1 (*PROM1*, RP41)

PROM1 gene is located on the short arm of chromosome 4 at 4p15.32. It codes for a 865-amino acid protein (Maw *et al*., 2000). *PROM1* is known as an antigenic marker (AC133 antigen) in human hematopoietic stem cells. Its expression is observed in retina and retinoblastoma cell lines (Miraglia *et al*., 1997) and the protein is localized to the base of outer segments (Maw *et al*., 2000). In Drosophila *prominin* is known to interact with spacemaker and a cell adhesion molecule called chaoptin and results in the formation of open type of rhabdomere system in which rhabdomeres are separated from each other (Zelhof *et al*., 2006). It has been suggested that in humans *prominin* may play a role in the morphogenesis of discs (Zelhof *et al*., 2006). Mutations in the *PROM1* gene are associated with autosomal recessive RP (Maw *et al*., 2000), and autosomal recessive RP with macular degeneration (Zhang *et al*., 2007), autosomal dominant Stargardts disease, autosomal dominant cone rod dystrophy and autosomal dominant bull's eye macular dystrophy (Yang *et al*., 2008)

15. Cyclic nucleotide gated channel, β1 subunit (*CNGB1*)

CNGB1 protein has a unique bipartite structure, consisting of a membrane spanning region (β part) and a large cytosolic amino-terminal region known as GARP (glutamic

acid rich protein). GARPs are localized in the rod outer segments and have high affinity towards alpha and beta subunits of phosphodiesterase, guanylate cyclase and *ABCA4* (Korschen *et al*., 1999). In contrast to *CNGA1*, *CNGB1* does not form functional channels alone, but in combination with *CNGA1* forms heteromeric *CNGA1*/*CNGB1* channels. The N-terminal region of *CNGB1* interacts with the C-terminal region of the *CNGA1* subunit and forms a functional cyclic nucleotide gated channel (Trudeau *et al*., 2002). Mutations in the *CNGB1* gene are known to cause ARRP (Bareil *et al*., Kondo *et al*., 2004).

16. Crumbs homolog 1 (*CRB1*, RP12)

Human CRB1 protein is a 1376 amino acid single transmembrane protein with a large extracellular part, containing 3 laminin A globular-like domains, 19 epidermal growth factor (EGF)-like domains and a cytoplasmic domain of 37 amino acids (McKay *et al*., 2005). The function of *CRB1* in humans is not known. In drosophila, *CRB1* protein co-localizes with the zonula adherens (a belt-like structure encircling the apex of epithelial cells) in the apical plasma membrane and drosophila mutant of the *CRB1* gene shows mis-localization of the apical proteins which is suggestive of a role of the CRB1 in localization of apical proteins (Wodarz *et al*., 1995). The EGF-like domain interacts with other transmembrane proteins containing EGF repeats (De Celis *et al*., 1993). The combination of EGF-like domains, which are present in proteins involved in neuronal development and laminin A globular-like domain in *CRB1* and its preferential expression in the retina suggests that it may be involved in the neuronal development of retina (den Hollander *et al*., 1999). *CRB1* also functions in the maintenance of zonula adherens and

protection against light-induced retinal degeneration in drosophia (Meuleman *et al*., 2004). Mutations in the *CRB1* gene cause LCA and RP with Coats-like exudative vasculopathy. Mutations in *CRB1* gene are found in 9% of patients with LCA (Lotery *et al*., 2001) and in 55.6% of patients with RP with Coats-like exudative vasculopathy (den Hollander *et al*., 2001).

17. Lecithin retinol acyltransferase (*LRAT*)

The *LRAT* gene is located on chromosome 4q31. LRAT protein is a 230 amino acid palmitoyl transferase, which catalyses the conversion of the membrane-associated form of *RPE65* to the soluble form of *RPE65* (Xue *et al*., 2004). Screening of *LRAT* gene in patients with different form of retinal dystrophies such as RP/flecked retinal dystrophies resulted in the identification of *LRAT* gene mutations in patients with LCA (Senechal *et al*., 2006) and ARRP (Thompson *et al*., 2001). No mutations were found in the *LRAT* gene upon screening 82 patients with LCA and 190 patients with ARRP, suggestiong it to be a rare cause of LCA and ARRP (Sweeney *et al*., 2007)

18. Ceramide kinase-like (*CERKL*, RP26)

The *CERKL* gene code for a protein of 557 amino acids. Within the retina, *CERKL* is predominantly expressed in the retinal ganglion cells (Tuson *et al*., 2004) and has a role in phosphorylation of an unknown lipid substrate (Graf *et al*., 2008). It has been shown that in oxidative stress conditions CERKL prevents cells (COS-7 cells) from undergoing

apoptosis (Tuson *et al*., 2009). *CERKL* gene mutations are reported in families with autosomal recessive retinitis pigmentosa (Tuson *et al*., 2004, Avila-Fernandez *et al*., 2008) and in families with ARRP with macular involvement (Auslender *et al*., 2007, Ali *et al*., 2008). Known mutation screening through microarray based on array primer extension technology resulted in the identification of *CERKL* gene mutaions in 3.3% (7 of 210) of patients with non-syndromic RP (Avila-Fernandez *et al*., 2008).

19. Neural retina leucine zipper (*NRL*, RP27)

NRL is a member of basic motif-leucine zipper (bZIP) family of transcription factors. It is expressed exclusively in the rod photoreceptors and pineal gland. It interacts with the retina-specific homeodomain protein *CRX* (cone-rod homeobox) and regulates the expression of genes including rhodopsin (Bessant *et al*., 1999) and α and β subunits of rod cGMP phosphodiesterase (Yoshida *et al*., 2004). In mouse models Mears and coworkers (2001) have shown that *NRL* has a role in the differentiation of the rods and in its absence immature photoreceptors adopt the short-wave cone phenotype. The *NRL* gene is involved in autosomal dominant RP (Bessant *et al*., 1999) as well as recessive form of clumped pigmentary retinal degeneration (Nishiguchi *et al*., 2004). Bessant and coworkers (2000) found a mutation of serine-50 to threonine in four unrelated families from south-eastern England Possibly arising from a founder effect. 2% (4/200) of British patients with autosomal recessive RP carry a *NRL* gene mutation (Bessant *et al*., 2000).

20. Retinitis pigmentosa 1 (*RP1*) (Oxygen regulated photoreceptor protein 1)

The *RP1* gene is located on chromosome 8q12 and codes for a protein of 2156 amino acids. It is expressed exclusively in the photoreceptors and its expression levels are modulated by oxygen levels *in vivo* (Pierce *et al*., 1999). The N-terminal sequence of RP1 is similar to doublecortin. Doublecortin is a protein of the central as well as peripheral nervous system (Gleeson *et al*., 1999), which helps in neuronal migration during development. Hence it is believed that RP1 may have a role in neuronal migration (Liu *et al*., 2002). The RP1 protein is present in the connecting cilium of both rod and cone photoreceptors, which is suggestive of its role either in the transportation of protein from inner segments to outer segments or in the maintenance of cilial structure (Liu *et al*., 2002). The *RP1* gene was first known to be involved in the pathogenesis of ADRP. However, mutations have subsequently been reported in ARRP families from Pakistan (Khaliq *et al*., 2005, Riazuddin *et al*., 2005). 6.8% of patients with ADRP have mutations in the *RP1* gene. A nonsense mutation at arginine-677 (forming an Opal codon) is one of the more prevalent *RP1* mutations, found in 2 to 3.7% of the north American patients with ADRP. It is not likely to be a result of a founder effect since a common haplotype was not observed in individuals carrying the mutation (Pierce *et al*., 1999, Bowne *et al*., 1999).

21. Progressive rod-cone degeneration (*PRCD*, RP36)

PRCD gene mutations are a common cause of hereditary retinal disease leading to blindness in dogs (Acland *et al*., 1998). The *PRCD* gene is located on human

chromosome 17q25.1. The *PRCD* gene codes for a protein of 54 amino acids (Zangeri *et al*., 2006). PRCD gene is highly conserved in the vertebrates and no homologue has been identified in the invertebrates, thus it has been hypothesized that the protein may be important for those aspects of photoreceptors structure or metabolism which are unique to vertebrate visual cycle (Zangeri *et al*., 2006). The expression of *PRCD* is mainly seen in retina, RPE and choroid. *PRCD* does not show any similarity with the known gene families and hence the function of this protein is not known (Zangeri *et al*., 2006). Screening for *PRCD* mutations in 1863 patients with retinitis pigmentosa and other inherited retinal degenerations, revealed a homozygous disease-causing mutation in one individual with autosomal recessive RP (Zangeri *et al*., 2006).

22. Eyes Shut homolog (Drosophila) (*EYS*, *SPAM*, RP25)

The *EYS* gene is located on chromosome 6q12. It codes for a protein of 3165 amino acids. (Collin *et al*., 2008). The gene is expressed abundantly in the retina. The EYS protein is localized in the outer segments of photoreceptors (El-Aziz *et al*., 2008). EYS protein contains 28 epidermal growth factor (EGF)-like domains and five laminin A G-like domains. The EYS protein is the ortholog of Drosophila spacemaker protein encoded by the *eys* (eyes shut) gene, hence it was given the name. On the basis of established functions of the insect orthologs, *EYS* is proposed to have a role in maintaining the integrity of photoreceptors (El-Aziz *et al*., 2008). Mutations in the *EYS* gene cause autosomal recessive RP (Collin *et al*., 2008, El-Aziz *et al*., 2008).

23. Isocitrate dehydrogenase 3 (NAD^+) beta (*IDH3B*)

IDH3B catalyzes the conversion of isocitrate to α-ketogluterate in the Krebs cycle by using a molecule of NAD^+. *IDH3B* gene is located on 20p13 and codes for a protein of 385 amino acids. Screening of 261 individuals with recessive RP and 265 individuals with simplex RP, revealed pathogenic mutations in 2 patients with autosomal recessive RP. Although *IDH3B* catalyses an essential step of metabolic pathway, patients with *IDH3B* gene mutations had no evident pathology other than retinitis pigmentosa (Hartong *et al*., 2008).

1.6.3. Genotype-phenotype correlations

Genotype-phenotype correlation in retinal dystrophies have been derived for some genes based characteristic features (Heckenlively *et al*., 1982, Morimura *et al*., 1999, Burstedt *et al*., 1999, Eichers *et al*., 2002). However, genotype-phenotype correlations are not always possible due to the overlap of clinical features in different forms of RP (Kajiwara *et al*., 1993, Souied *et al*., 1996) clinical heterogeneity of RP, and due to loss of both rod and cone function in advanced stages of disease (Richard *et al*., 1994, Cremers *et al*., 1998).

1. Rhodopsin

Genotype-phenotype correlations have been proposed for patients with rhodopsin gene mutations (Sandberg *et al*., 1995). Severity of phenotype was found to be correlated with the position of the mutated amino acid. Patients (n=60) with mutations in the intradiscal domain of rhodopsin had significantly better visual acuities (mean VA=20/24) than patients (n=26) with mutations in transmembrane domain (mean VA=20/30) or patients (n=42) with mutations in the cytoplasmic domain (mean VA=20/34). Similarly visual fields were significantly better in patients (n=60) with mutations in intradiscal domain (mean diameter=91.6$\pm$4.4) than those with mutations in the transmembrane domain (mean diameter=81.1$\pm$6.6, n=26), or with mutations in the cytoplasmic domain (n=41; mean diameter=64.4$\pm$5.3). ERG amplitudes also show similar trends, and the best ERG amplitudes were observed in patients with mutations in the intradiscal domain (10μV, n=59) (Sandberg *et al*., 1995). Thus patients with mutations in the transmembrane domain of RHO protein have an intermediate phenotype, as compared with patients that have mutations in the intradiscal and cytoplasmic domains of RHO protein (Sandberg *et al*., 1995). It was also observed in other studies that patients with mutations in intradiscal domain, Pro23His, Thr17Met (Richards *et al*., 1991, Fishman *et al*., 1992), had a less severe phenotype as compared to patients with mutation in the transmembrane domain Lys296Glu (Keen *et al*., 1991) and cytoplasmic domain, Pro347Leu (Berson *et al*., 1991a, Berson *et al*., 1991b). On the contrary a retrospective review of 119 families (Gal *et al*., 1997) with rhodopsin gene mutations suggest a wide range of severity of phenotype associated with the mutations in the 3 major domains of rhodopsin gene.

2. RLBP1

RLBP1 gene mutations result in small yellow deposits subretinally as well as in the RPE and RPE atrophy in the form of patches in the periphery with well-defined round margins. This phenotype is designated as retinitis punctata albescens (RPA) (Morimura *et al*., 1999, Katsanis *et al*., 2001, Fishman *et al*., 2004). A similar phenotpye was also reported for mutations in the *PRPH2* (Kajiwara *et al*., 1993) and *RHO* genes (Souied *et al*., 1996) in dominant forms of the disease.

In addition to signs of retintis punctata albescens, maculopathy with central pigment deposits in the early stages followed by areolar maculopathy has been observed in patients from northern Sweden in association with *RLBP1* gene mutations (Morimura *et al*., 1999, Burstedt *et al*., 2001, Gränse *et al*., 2001). This is the phenotype of Bothnia dystrophy. It is termed Bothnia dystrophy, an autosomal recessive rod-cone disorder with an estimated frequency of 1 per 4500 of the population (Burstedt *et al*., 2001). The R234W mutation in *RLBP1* underlies this disorder and is due to a founder effect in the area adjacent to the gulf of Bothnia in northern Sweden (Burstedt *et al*., 1999). At least 63 unrelated affected individuals have been identified to carry the R234W mutation in the above geographical area (Morimura *et al*., 1999b, Burstedt *et al*., 2001, Gränse *et al*., 2001).

Similarly in the island of New Foundland, Eichers and coworkers (2002) identified 26 patients from 6 families with a variant of retinitis punctata albescens. This variant has been termed New Foundland Rod Cone Dystrophy (NFRCD). Phenotype of NFRCD is

similar to that of retintis punctata albescens but with an early age of onset (1st decade), absence of bone spicules and rapid progression. NFRCD is associated with two splice site mutations in the *RLBP1* gene (Eichers *et al*., 2002).

It has been observed that mutations in the *RLBP1* gene result in different phenotypes. For example, mutation of R150Q in the *RLBP1* gene is known to cause phenotypes ranging from ARRP (Maw *et al*., 1997) to fundus albipunctatus (Katsanis *et al*., 2001) to retinitis punctata albescens (Katsanis *et al*., 2001). Similarly the R233W mutation has been associated with Bothnia dystrophy (Burstedt *et al*., 1999) as well as with retinitis punctata albescens (Morimura *et al*., 1999).

3. PRPF31

Pre-mRNA processing factor 31 (*PRPF31)* gene mutations have been observed in at least 13 families with autosomal dominant form of RP (Al-Maghtheh *et al*. 1996, McGee *et al*., 1997, Waseem *et al*., 2007, Xia *et al*., 2004, Sato *et al*., 2005, Wang *et al*., 2003). Families (n=12) with the *PRPF31* gene mutations have been reported to have incomplete penetrance. (Al-Maghtheh *et al*. 1996, McGee *et al*., 1997, Waseem *et al*., 2007, Xia *et al*., 2004, Sato *et al*., 2005). In families with *PRPF31* gene mutation clinical examination did not show any sign of disease in asymptomatic mutation carriers while symptomatic individuals showed signs of night blindness, extensive peripheral retinal degeneration with macular atrophy, reduced visual fields, and reduced ERG responses (rod-cone type) (Evans *et al*., 1995). Vithana and coworkers (2003) determined the molecular mechanism

of pathogenesis in a family with 11-bp deletion in the exon 11 of *PRPF31* gene. The asymptomatic mutation carriers (n=7) had similar levels of wild type *PRPF31* mRNA as compared to control individuals while symptomatic carriers (n=8) had much lower levels of wild type *PRPF31* mRNA as compared to control individuals (Vithana *et al*., 2003). Similar findings were made by Rivolta and coworkers (2006).

4. ABCA4

Mutations in the *ABCA4* gene cause a wide spectrum of phenotypes ranging from Stargardts disease to cone rod dystrophy to retinitis pigmentosa (Lewis *et al*., 1999, Ducroq *et al*., 2002, Birch *et al*., 2001. Genotype-phenotype correlations have been proposed for *ABCA4* mutations based on the predicted severity of the mutations. This was discussed in the section above under 'Genes causing ARRP'

Genotype-phenotype correlation with respect to age of onset has been proposed for Stargardts disease (Lewis *et al*., 1999, Yatsenko *et al*., 2001). Late onset (>35 years) Stargardts disease, was found in patients with missense mutations outside the functional ATP-binding (codons 965 to 1093 and codons 1975 to 2102) and the transmembrane domains (codons 648 to 855 and 1674 to 1898), whereas early onset was associated with missense mutations in the 1st transmembrane domain (codons 648 to 855).

5. X-linked RP

Two genes have been identified for XLRP, namely *RP2* and *RP3* (known as retinitis pigmentosa GTPase regulator, RPGR) (http://www.sph.uth.tmc.edu/Retnet/).

It has been observed that mutations in *RP2* gene result in a more severe phenotype as compared to RP3 gene mutations (Kaplan *et al*. 1992, Wright *et al*., 1991, Sharon *et al*., 2003). Severity of the phenotype has been described on the basis of early age of onset (Kaplan *et al*. 1992, Wright *et al*., 1991) and poorer visual acuity (Wright *et al*., 1991) in patients with *RP2* gene mutations compared to patients with *RP3* gene mutations. It is found that patients with *RP2* gene mutations (19 affected individuals of 5 families) show symptoms at a mean age of 3.5 years while patients with *RP3* gene mutations (11 patients, 5 families) show onset of symptoms at a mean age of 10.6 years (Kaplan *et al*. 1992, Wright *et al*.). Similarly patients with *RP2* gene mutations (n=16, 9 families) have significantly lower visual acuities (mean VA =20/210) as compared to the visual acuities (mean VA = 20/82) of patients with *RP3* gene mutations (n=156, 98 families) (Sharon *et al*., 2003). Genotype-phenotype correlation has been observed within the *RPGR* gene as well. It has been observed that compared to mutations in *RPGR* exon 1-14, patients with mutations in exon 15 have a better prognosis, larger visual fields, ERG amplitudes and better pan-retinal function (Sharon *et al*., 2003). Although the phenotype of *RPGR* gene mutations is milder than the phenotype associated with *RP2* gene mutations, it has been observed that patients with *RPGR* gene mutations (n=113) show faster rate of progression and tend to lose visual acuity at twice the mean rate of patients with RP due to rhodopsin gene mutations (Sandberg *et al*., 2007).

1.7 Animal models of retinal dystrophy

The course of progression of retinal dystrophies can be characterized on the basis of clinical manifestations and changes in the retina that are evident on eye examination although this is not always achievable in practice because patients may present at the clinic only at more advanced stages of disease or may not be available for periodic monitoring during the course of disease progression. The end point stage of the disease is more likely to be documented in humans but since different types of retinal dystrophies ultimately lead to the loss of both types of photoreceptors, they have overlapping manifestations especially in the end stages. Thus, it may be difficult to distinguish one type of retinal dystrophy from another in advanced stages of disease.

Secondly, the study of mechanism through which a particular pathogenic mutation causes retinal degeneration requires experimental model systems and cannot be learnt directly on humans. Hence animal models are a valuable resource in answering these questions. Apart from this, molecular investigations in animal models yield new potential candidate genes for human disease or even lead to the identification of the previously unrecognized retinal genes like *MERTK* (Dowling *et al*., 1962), *C1ORF36* (Friedman *et al*., 2006) and Peripherin/*RDS* (Sanyal *et al*., 1980).

Animal models can be spontaneous or induced. Both spontaneous and induced animal models for available in retinal dystrophies. The rodents have been used extensively as a model system for retinal dystrophies, although canine, porcine, feline

and avian model systems are also available. The animal models for different genes known to cause retinal dystrophy are discussed here.

1. Beta subunit of cGMP phosphodiesterase-6 gene (*PDE6B)*

Retinal degeneration mice (rd) are one of the oldest known animal models for retinal dystrophies. The disease phenotype in rd mouse arises due to a mutation in the beta subunit of the cGMP-phosphodiesterase (*Pde6b*) gene (Bowes *et al*., 1990). In rd mice the rod cells degenerate earlier and faster than the cone cells. It has been observed that in rd mice, rods and cones in the peripheral retina survive for a longer time than in the posterior retina. 98% of the rod cells are lost by the postnatal day 17. At this age most of the cone nuclei are present. By the postnatal day 36 only the cone photoreceptors are left, along with a few rod cells. Number of cone cells starts decreasing from day 17 onwards and by postnatal day 36 their number is reduced to half. By the age of 18 months only 1.5 % of original cone cell population remains in the posterior retina and 5% in the peripheral retina. In the posterior retina rod nuclei could be seen through at least 47 days (Carter-Dawson *et al*., 1978).

A spontaneous mutation in the beta subunit of cGMP phosphodiesterase gene has also been observed in Red Irish Setters dog with retinal degeneration. This locus is also known as rod cone dysplasia (RCD). The eyes appear normal till 15 to 20 days after birth. After this age the nuclei of outer nuclear layer starts degenerating and there is a progressive loss of night vision. The night vision is totally lost by 3-4 months of age,

which is suggestive of almost total rod cell loss. During this stage there is a loss of secondary blood vessels. The day vision starts deteriorating from 3 months onward. By 3 years of age there is a complete loss of vision. The cataract can appear from 1 to 4 years of age. By 4 years of age the blood vessels completely disappears. The RPE inner nuclear layer and ganglion cell layers are almost normal (Parry *et al*., 1953).

2. Retinal pigment epithelium 65 (*RPE65*)

Retinal dystrophy in the Swedish Briard/Briard-Beagle dogs is caused because of the *RPE65* gene mutation. Affected Briard dogs show membrane bound lipofuscin-like inclusions bodies in the RPE in the central fundus primarily, which spreads to the periphery with age. Outer segments show disorganization followed by degeneration and ultimately lead to the loss of complete rod and cone cells. The degeneration process of photoreceptors starts from the peripheral retina and extends to the central retina with age. The fundus appears normal till 3 years of age, however ERG can detect the degeneration process by 5 weeks of age. Through ERG, rod responses are barely recordable while cone responses are weak (Narfstrom *et al*., 2003).

In the *Rpe65* knockout mice it has been observed that at 7 weeks of age the outer segments of rod photoreceptors start disorganising while the loss of photoreceptor nuclei becomes evident by 15 weeks of age. At this age the RPE show increased number of lipid inclusions (Redmond *et al*.,1998).

3. Retinal degeneration slow (*RDS*)/Peripherin

Retinal degeneration slow (RDS) phenotype in mice is caused due to a spontaneous mutation in the peripherin gene (Ma *et al*., 1995). Peripherin transgenic mice are also available which represent a model for autosomal dominant type of retinal dystrophy. The photoreceptor degeneration is slower in the heterozygotes compared to homozygote mutants. The outer segments of rod and cone photoreceptors are shorter and disorganized (whorl-like) in the retina of heterozygous mice while outer segments are not at all formed in the homozygous mutant mice. In the high peripherin expressing background, of the 10 to 11 rows of photoreceptor nuclei 6-7 rows remain after 1 month and 2 rows by 7 months. In the low peripherin expressing background, there is slower photoreceptor degeneration, 6-7 rows of photoreceptor nuclei remain after 6 months. The development of inner nuclear, inner plexiform and ganglion cell layers appear to be normal (Sanyal *et al*., 1980, Kedzierski *et al*., 1997).

4. Rhodopsin (*RHO*)

English Mastiff dogs are a natural model for autosomal dominant type of retinal dystrophy, caused due to mutation in the rhodopsin gene. Electrophysiology measurements show that by 3 to 6 months of age ERG responses are normal in both *RHO*+/- and *RHO*-/- dogs. The ERG responses become severely abnormal by 18 months of age. The degeneration of photoreceptors is not uniform. Degeneration is more in the

area surrounding the optic nerve head, while the region beyond this area have relatively preserved photoreceptors in an 11-month old *RHO*+/- dog (Kijas *et al*., 2002).

In rhodopsin transgenic mice, at postnatal day 15 the nuclei of rods and cones appear normal, while the outer segments are absent in the *Rho* -/- retinas while they are ~50% shorter in *Rho* +/- retinas. By 30 days in the *Rho* -/- mice the nuclei of photoreceptors starts degenerating and outer nuclear layer thickness decreases by 1 to 2 layers. The degeneration of outer nuclear layer completes by 90th day. In *Rho* +/- mice the outer nuclear layer starts degenerating by 90th day (Lem *et al*., 1999).

The degeneration is relatively uniform from the periphery to the central retina. At 13 weeks of age *Rho* +/- and *Rho* +/+ mice show similar ERG response for rods and cones and bipolar cells. While at the same age rods and cones of *Rho*-/- mice show no response in ERG while a very mild response is seen for the bipolar cells. In *Rho*-/- mice at 7 weeks of age cone cells response are nearly normal and rod cells response are extinguished (Humphries *et al*., 1997).

In a transgenic pig model, the outer nuclear layer becomes thinner at 4 weeks of age. The rod cells show degeneration while the cone cells and RPE are unaffected at this age. At 6-8 weeks of age the degeneration process accelerates. Most of the rod nuclei disappear and cone cells also become a part of degeneration. The RPE is normal till this point. Mild proliferative reaction of RPE is noted at 24 weeks of age and cone cells degeneration progresses slowly after this. The degeneration process of rods and cones in

the peripheral retina is more severe compared with that of posterior pole (Tso *et al*., 1997).

5. Mer tyrosine kinase protooncogene (*MERTK*)

Royal College of Surgeon (RCS) rats represent a spontaneous model of retinal dystrophy (D'Cruz *et al*., 2000). The first degenerative sign is seen at 12 days of age in the form of accumulation of the extra outer segment like lamellae between the ends of developing rods and the pigment epithelium. Till 18 days of age the photoreceptors are normal in appearance and function. By 22 days the inner segments and some nuclei of photoreceptors begins to degenerate and ERG starts diminishing. By 32 days the inner segments disappear completely. By second month after birth the degeneration spreads to other parts of retina. By the 40th day of age the RPE cells break the Bruch's membrane and migrates towards the outer segment debris. By 1 year of age the debris zone completely disappears and retina displays an intact Bruch's membrane (Dowling *et al*., 1962).

6. Guanylate cyclase-1 (*GC1*)

Retinal degeneration chicken (rd) carries a spontaneous recessive mutation in the guanylate cyclase (*GC1*) gene. Histology results in a 1-day-old chicken show no signs of degeneration but rod and cone cell response is not measurable through ERG. The photoreceptors start degenerating in the central retina from 7-10 days after hatch. The

degeneration then follows to the periphery. By 6 to 8 months the photoreceptor layer is almost completely lost. The degeneration of RPE and inner retina follows after the degeneration of photoreceptors. The levels of cGMP are significantly reduced in the retina of *rd*-/- chicken (Semple-Rowland *et al*., 1998).

7. Chromosome 1 open reading frame 36 (*C1ORF36*)

Retinal degeneration-3 (rd3) mouse is a spontaneous model for autosomal recessive type of retinal dystrophy, which is caused due to mutation in *C1ORF36* gene (Friedman *et al*., 2006). In rd3/rd3 mice the photoreceptors are normal at 2 weeks of age but quickly degenerate there after. At 3 weeks the outer nuclear thickness is reduced, at 4 weeks only cones are observed and at 8 weeks of age almost no photoreceptors can be observed. At no age rod and cone ERG responses are normal in rd3/rd3 mice. The maximal ERG response is detectable at 4 weeks of age, which is 25% of normal. The ERG responses reduce further with age and at 7 weeks of age ERG responses becomes undetectable (Chang *et al*., 1993).

8. ATP binding cassette, subfamily A, member 4 (*ABCA4*)

The photoreceptor degeneration starts slowly in *Abcr* knockout mice. The cone cells degeneration start first followed by degeneration of rod cells. The rod cells remain normal till 13 weeks of age while the cone cells are normal till 8 weeks of age. By one year there is 35% reduction in the photoreceptors as shown by ERG. A2E (*N*-

retinylidene-*N*-retinylethanol-amine) a major fluorophore of lipofuscin is significantly elevated in the RPE and electron micrographs show a significant thickening of the Bruch's membrane (Weng *et al*., 1999).

9. Cone rod homeobox containing gene (*CRX*)

Crx gene knockout mouse is a model for autosomal dominant form of retinal dystrophy. Homozygous *Crx*-/- mice do not develop outer segments and the outer nuclear layer show thinning and dislocation at postnatal day 21. Heterozygous *Crx*+/- mice at postnatal day 21 are similar to wild type mice except for smaller outer segments. Functional defects are evident by 1 month in *Crx*+/- mice, since cone ERG responses are not detectable while rod responses are reduced. The cone responses, which were absent, start developing again by 2 months of age in *Crx*+/- mice. The homozygous knockout mice have both responses extinguished by 1 month of age (Furukawa *et al*., 1999). In the *Crx*-/- mice the nuclei of photoreceptors show further progressive degeneration and at 6 months the photoreceptor layer thickness reduces to 1 to 3 rows compared to 14 to 16 rows in normal mice. (Furukawa *et al*., 1999).

10. Gamma subunit of cGMP phosphodiesterase (*PDE6G*)

Tsang and coworkers (1996) first generated the homozygous knockout mouse for the gamma subunit of cGMP phosphodiesterase gene through the gene targeting approach. The knockout mouse shows that the outer segments fail to develop normally and are lost

by postnatal day 13, while the nuclear layer is intact till this time. From the postnatal day 14 to 21 the nuclear layer also degenerates and the loss is more prominent in the central relative to peripheral portion of retina. Single row of photoreceptors remain by 3 weeks of age and the retina is almost completely devoid of photoreceptors by 8 weeks of age. Tsang and coworkers have observed that before photoreceptor degeneration, levels of cGMP in the retinal tissue rise to about five-fold and after degeneration cGMP levels in the retinal tissue reduce to below normal levels (Tsang *et al*., 1996).

11. Interphotoreceptor retinoids binding protein gene (*IRBP*)

Irbp gene knockout mouse is a model for the recessive form of retinal dystrophy. At postnatal day-11 *Irbp*-/- mice show poorly oriented and significantly shorter outer segments and reduction in the thickness of the outer nuclear layer. However at this stage the RPE and the other cell layers like inner nuclear layer, ganglion cell layer and plexiform layers appear normal. The thickness of outer nuclear layer further reduces with age. Liou and coworkers (1998) were able to detect photoreceptor responses through ERG in *Irbp-/-* mice, inspite of photoreceptor cell loss with age. This suggests that even at late stages of the disease, outer segments in *Irbp-/-* mice contain the light sensitive pigment to initiate electrical response (Liou *et al*., 1998).

12. Tubby-like protein 1 (*TULP1*)

Ikeda and coworkers (2000) for the first time generated knockout mouse for tubby-like protein 1 (*Tulp1*). Homozygous *Tulp1*-/- mice at 3 weeks of age show normal thickness of the outer nuclear layer. The outer segments are shorter, fragmented and photoreceptor lamellae are distorted. The RPE and inner retina is normal at this stage. By 4 weeks of age thickness of outer nuclear layer starts reducing. It is reduced to 1-2 layers by 12 weeks of age. By 20 weeks of age there is apparently no outer nuclear layer in some areas and some areas retain 1-2 layers of outer nuclear layer. This variability in thickness of outer nuclear layer is random.

TULP1 and *tub* proteins belong to TULP family. The TULP1 protein resembles *tub* protein in its structure and expression- hence it is believed that both may have similar function. Tub-/- mice show progressive retinal degeneration along with hearing loss and obesity. However, Ikeda and coworkers have observed that the hearing ability and body weight of *Tulp1*-/- mice is comparable to that of normal mice (Ikeda *et al*., 2000).

13. Arrestin (*SAG*)

Arrestin knockout mouse is a model for the slowly progressing retinal dystrophy. The degenerative changes start at postnatal day 100. The outer segments appear shorter and disorganized. The outer nuclear layer starts reducing in thickness at postnatal day 100. By 1 year of age the outer nuclear layer is reduced to less than 50% of normal thickness. The degenerative changes are more severe in the inferior than the superior hemisphere (Chen *et al*., 1999).

1.8 Therapeutic approaches in retinal dystrophies

1.8.1 Gene therapy approaches

Gene therapy is a procedure in which a disease is treated by transfer of the desired gene into the diseased tissue. Success of gene therapy depends on the efficient delivery of the gene to the target cell as well as its long-term expression in the required tissue (Strachan *et al*., 1999). Genetic material can be delivered to the cells either by viral vectors or by non-viral vectors. Viral vectors have evolved as an efficient means of transferring genetic material but because of the pathogenic risk associated with the viruses, non-viral vectors are also being considered. Although non-viral vectors are non-pathogenic compared to viruses they are less efficient in delivery of genetic material to the cell. The viral vectors that have been used in gene therapy are retrovirus, lentivirus, HSV-1, adeno-associated virus (AAV) and adenovirus (Robbins *et al*., 1998). In retinal gene therapy adeno-associated viruses have been used most commonly because of their ability to transfect non-dividing cells and non-pathogenic and non-inflammatory nature (Bennett *et al*., 2000). The main disadvantage of AAV is its small packaging capacity (<5kb). Adenoviruses and lentiviruses which have a larger packaging capacity (8 kb) have also been used in retinal gene therapy but adenoviruses are known to cause an inflammatory response (Byrnes *et al*., 1995) and lentiviruses are known to induce oncogenesis (Themis *et al*., 2005) hence they have been used less in retinal gene therapy. The non-viral gene delivery methods mainly includes electroporation, ultrasound, gene gun, liposomes, and polymer mediated gene delivery. In electroporation the cell membrane is permeabilized

for the DNA uptake by the application of controlled electric field (Widera *et al*., 2000). Gene delivery through electroporation has been used to deliver DNA to the tumor tissue (Li *et al*., 2001, Heller *et al*., 2001). In ultrasound approach of gene delivery permeability of cell membrane is increased to macromolecules such as DNA by irradiating ultrasonic waves to the tissue after injection of DNA. Microbubbles have also been used in combination with ultrasound to increase the gene expression levels (Teupe *et al*., 2002, Song *et al*., 2002). In gene gun method DNA is loaded onto microscopic gold beads and shot into the cells with a helium gas gun this results in the delivery of DNA into the nucleus. However, a disadvantage of this method is the shallow penetration of DNA into the tissue (Kuriyama *et al*., 2000). Liposomes are spherical colloidal particles which can entrap DNA molecules, protect them from environmental factors and can deliver to the target cells. Liposomes are of two types anionic and cationic. Cationic liposomes are more commonly used as they are easy to prepare and show high transfection efficiency over anionic liposomes (Gao *et al*., 1995, Liu *et al*., 1996). In polymer mediated gene delivery DNA is complexed with cationic polymers such as polyethylenimine (PEI). The polymer/DNA complex is taken up by the cells and lead to gene expression (Goula *et al*., 1998). Among the non-viral gene delivery methods gene delivery through liposomes is most widely used as the liposomes are cheap and easy to make (Robbins *et al*., 1998).

One of the important reasons to do genetic testing on patients with retinal dystrophy is to identify patients suitable for future gene therapy trials. Since the molecular bases of diseases vary, gene therapy approaches that can be applied will also vary depending on the type of inheritance and the gene mutation present. In recessively

inherited disease, mutations generally lead to loss of function, and hence the aim of gene therapy is to introduce the required gene to the diseased tissue which will induce the local production of the missing protein. In case of dominantly inherited diseases, the pathogenic mechanism could be due to haploinsufficiency or abnormal accumulation of the mutant protein which is toxic for the cell or the mutant protein may interfere with the normal protein. Thus in disorders with mutations leading to gain of function the aim of gene therapy is to silence the mutant allele by using ribozymes or siRNA. Due to extensive mutational heterogeneity in genes causing RP, it is simpler to have one molecule (siRNA etc) to target a specific gene and all mutant versions of it. This would involve destruction of the normal (wild type) allele as well. Hence simultaneous replacement of the wild type allele of the gene is also carried out (Bennett *et al*., 2000).

In retinitis pigmentosa and related disorders gene therapy trials have been done mostly on animal models by mainly using adeno-associated viruses and adenoviruses. The approaches used in the gene therapy are discussed in this section.

A. Gene/mutation dependent approach

In this approach photoreceptors are targeted to rescue from degeneration by directly replacing the diseased gene. In this section outcomes of the gene replacement in the different models of retinal degeneration are discussed.

1. *PDE6B* gene

One of the first gene therapy trials in retinitis pigmentosa was done on rd mice, which lack the beta subunit of cGMP phosphodiesterase gene. Lem and coworkers showed that it is possible to rescue the photoreceptors in rd mice through the introduction of *Pde6b* gene in a 1-cell mouse embryo (Lem *et al*., 1992). Subsequently, photoreceptor rescue effects in rd mice have also been shown by sub-retinal injections of adenovirus, adeno-associated virus or lentivirus containing the *Pde6b* gene (Bennett *et al*., 1996, Jomary *et al*., 1997, Takahashi *et al*., 1999).

2. Peripherin/*RDS* gene

Travis and coworkers have shown that injection of *Rds* gene in the pronucleus of fertilized egg of rds mouse results in preservation of photoreceptor degeneration (Travis *et al*., 1992). Ali and coworkers have shown a rescue effect in this mouse model even in post-natal stages when the degeneration has not progressed fully. They found that sub-retinal delivery of the transgene by an adeno-associated virus (AAV) vector at post-natal day-10 also had a rescue effect in the rds mice. The treated mice showed successful expression of the transgene in its normal location, preservation of the disc structure and significantly improved ERG b waves (Ali *et al*., 2000).

3. *RPE65* gene

Swedish Briard dogs are a natural *RPE65* knockout model for retinal dystrophy. Thus they are very good model to check the potential of gene therapy in higher mammals. It has been shown in the above dog model that recombinant AAV-mediated *RPE65*gene delivery into the sub-retinal space results in restoration of visual function, as assessed by improved ERG, pupillometric responses and by behavioral responses (Acland *et al*., 2001, Narfstrom *et al*., 2003). Success of gene therapy in the canine model paved the way for phase-I gene therapy trials on humans with Lebers congenital amaurosis due to *RPE65* gene mutations. Phase-I gene therapy trials have been done on a total of 9 patients (age 17 to 26 years) at 3 different centers (Bainbridge *et al*., 2008, Maguire *et al*., 2008, Hauswirth *et al*., 2008). All the 3 studies have demonstrated the safety of adeno-associated virus mediated sub-retinal *RPE65* gene delivery. Maguire and coworkers reported an improvement in the visual acuity in the treated eye as compared with the untreated eye in all the 3 patients from the study however the other two studies did not find an improvement in visual acuity. In these studies patients were followed up for a period of 3 months (Hauswirth *et al*., 2008), 1.25 to 4.75 months (Maguire *et al*., 2008) and 6 to12 months (Bainbridge *et al*., 2008).

4. *RPGRIP* gene

RPGRIP gene has also been subjected to gene therapy trials in mouse models and these experiments have shown success. Pawlyk and coworkers have shown that that AAV-mediated delivery of *Rpgrip* gene in the sub-retinal space of *Rpgrip* knockout mice at

postnatal day 18 to day 20 resulted in the formation of well-developed outer segements, thicker outer nuclear layer, and improved ERG b-wave amplitudes (Pawlyk *et al*., 2005).

5. *MERTK* gene

Royal College of Surgeons (RCS) rat strains have a defect in the *Mertk* gene, due to which the RPE is unable to phagocytose outer segments which eventually leads to progressive loss of photoreceptors. Vollrath and coworkers have shown that sub-retinal delivery (adenovirus mediated) of the *Mertk* gene in the RCS rats at postnatal day 22 to day 85 show correction of RPE phagocytosis defects, preservation of structure of outer segments and increased thickness of outer nuclear layer (Vollrath *et al*., 2001).

6. *RHO* gene

Gene therapy for the autosomal dominant form of retinitis pigmentosa has been applied on rats with *Rho* gene mutations. Lewin and coworkers have shown that rate of photoreceptor loss and the ERG decline can be slowed down in P23H mutant rats by the use of ribozymes directed against the mutant P23H transcripts (Lewin *et al*., 1998). Since more than 100 mutations are known in the rhodopsin gene, customizing ribozymes for each mutation is not a feasible option and hence approaches that knock down the endogenous rhodopsin mRNA are being used. In these approaches suppression is targeted to a site independent of the mutation, as a result both wild type and mutant alleles are suppressed, simultaneously another transcript modified at the recognition site of shRNA

by using degeneracy of the codon, is injected which replaces the knocked down endogenous protein (Farrar *et al*., 2002). O'Reilly and coworkers have used an AAV construct containing shRNA sequence targeted against the endogenous *Rho* transcript, in addition the construct also contained *Rho* transcript with degenerate codon at the shRNA target sequence. Injection of the AAV in the sub-retinal space of 10-day old *Rho*+/- mice resulted in better preservation of photoreceptors in the treated mice as compared to control mice as assessed by the increased thickness of the outer nuclear layer (O,Reilly *et al*., 2007).

B. Gene/mutation independent approaches

Mutation-independent approaches aim at photoreceptor rescue by delivering genes which are not directly involved in the degeneration of photoreceptors, but are known to have neuro-protective properties. In this section such methods will be discussed.

1. CNTF

Ciliary neurotrophic factor (CNTF) belongs to interleukin-6 family of cytokines. It has a role in the survival and differentiation of neurons (Lo, 1993). The photoreceptor rescue effect of adenovirus or adeno-associated virus mediated delivery of CNTF has been assessed in a variety of rodent models such as rds mice (Bok *et al*., 2002), *Rho* knock-out mice (Liang *et al*., 2001), rd mice (Cayouette *et al*., 1997) and *Rho* knock-out rats (Liang *et al*., 2001b). It has been shown that sub-retinal or intravitreal injection of AAV or

adenoviral-mediated delivery of CNTF can slow down the degeneration of photoreceptors as assessed by the thickness of outer nuclear layer but on the contrary these studies have found a decrease in scotopic a- and b-wave amplitudes and a decrease in photopic b-wave amplitude in the injected eye compared to uninjected eye (Cayouette *et al*., 1997, Bok *et al*.,2002, Liang *et al*., 2001, Liang *et al*., 2001b). A single study has shown functional rescue by intravitreal injection of AAV-mediated delivery of CNTF in rds mice at age 20-days (Cayouette *et al*., 1998). Schlichtenbrede and coworkers have studied the role of combination approach of neuroprotection and gene replacement by injecting AAV containing CNTF and AAV containing *Prph2* gene in the sub-retinal space of the rds mice. No functional rescue was observed in this study (Schlichtenbrede *et al*., 2003).

In addition CNTF has also been administered through direct intravitreal injection of CNTF peptide (Chong *et al*., 1999), and with encapsulated cell implants (Tao *et al*., 2002). Photoreceptor rescue effects of CNTF in different types of animal models such as RCD1 dogs (Tao *et al*., 2002), rd mice (Cayouette *et al*., 1997), as well as in a feline model of retinal degeneration (Chong *et al*., 1999) led to phase I clinical trials in human patients with RP. In a phase I trial, CNTF implants made by enclosing RPE cells in a semipermeable polymer-based outer membrane were used. The RPE cells were transfected with the CNTF gene and stable CNTF-expressing cell lines were enclosed in the implant. The implants were placed in the eyes of 10 RP patients and these were found to be safe for at least 6 months (Sieving *et al*., 2006). The visual acuity also showed

improvement in the study although a larger study would be required to make conclusion about changes in visual acuity.

2. GDNF

Glial cell line derived neurotrophic factor (GDNF) is a neurotrophic factor required for the survival and differentiation of dopaminergic neurons (Lin *et al*., 1993). The beneficial effects of AAV-mediated delivery of GDNF were studied by Buch and coworkers in 2 animal models of retinal degenerations, rds mice which lack functional *Prph2* gene and RCS rats which lack functional *Mertk* gene. They injected the AAV-GDNF gene construct into the sub-retinal space of 10-day old rds mice and 12-day old RCS rats. Sub-retinal delivery of GDNF resulted in enhanced survival of the photoreceptors as accessed histologically as well as there was functional rescue as assessed by enhanced b-wave amplitudes in the treated animals compared to control animals. The rescue effect was enhanced upon introduction of the replacement gene (i.e., *Mertk* in RCS rats and *Prph2* in rds mice) in combination with GDNF gene therapy (Buch *et al*., 2006).

Protective effect of GDNF have also been observed in rd mice and *Rho* knock-out rats by sub-retinal injections of GDNF peptide (Frasson *et al*., 1999) and intravitreous injection of GDNF encapsulated in poly (D,L-lactide-co-glycolide) (PLGA) microspheres (Andrieu-Soler *et al*., 2005). This led to an increase in the number of cells in the outer nuclear layer as well as increase in the ERG amplitudes. No major side effects were observed in these studies.

3. bFGF

Basic fibroblast growth factor (bFGF) is a neurotrophin involved in the regeneration, proliferation and survival of the neurons of the central nervous system (Eckenstein *et al*., 1994). bFGF is also expressed in the retina (Connolly *et al*., 1992), and is required for the survival of photoreceptors (Campochiaro *et al*., 1996).

Akimoto and coworkers have shown that adenovirus mediated delivery of bFGF into the sub-retinal space of 21-day old RCS rats resulted in the rescue of photoreceptors as indicated by the increased thickness of outer nuclear layer as compared to the control rats (Akimoto *et al*., 1999). Lau and coworkers have shown that AAV-mediated sub-retinal delivery of bFGF in the *Rho* knockout rats at postnatal day 15 resulted in the rescue of photoreceptors as assessed by increased outer nuclear layer thickness and better organization of outer and inner segments compared to control rats. ERG responses did not showed any functional rescue in the treated rats (Lau *et al*., 2000).

4. BDNF

Brain derived neurotrophic factor (BDNF) belongs to a family of neurotrophic factors and has a role in the neuronal development and survival (Binder *et al*., 2004). Hojo and coworkers have assessed the photoreceptor rescue effect of BDNF in rats with light induced photoreceptor damage. They transduced autologous iris pigment epithelial (IPL)

cells with AAV-mediated BDNF, the modified IPL cells expressing BDNF were transplanted into the sub-retinal space of the Sprague-Dawley rats of age 3 months. After transplantation the rats were subjected to phototoxicity by one week of constant illuminance of 2000 to 2500 lux. Photoreceptor rescue in the form of increased outer nuclear layer thickness was observed in the treated eye compared to control eye (Hojo *et al*., 2004). Lawrence and coworkers modified the Schwann cells by transfecting them with the plasmids containing BDNF c.DNA. They injected the modified Schwann cells into the sub-retinal space of the RCS rats of age 23-25 days. Photoreceptor rescue was observed in the form of increased outer nuclear layer thickness and better head tracking to the moving stimulus in the treated eye compared to the control eye (Lawrence *et al*., 2004)

5. Anti-apoptotic genes

Photoreceptor cell death in retinitis pigmentosa animal models has been shown to occur by apoptosis (Portera-Cailliau *et al*., 1994). The process of apoptosis often involves a family of cysteine proteases known as caspases that cleave key cellular targets leading to cell death (Nicotera, 2002). It has been shown that inhibitors of apoptosis (IAPs), which interfere with the activity of caspases can block cell death (Liston *et al*., 1996). X-chromosome linked inhibitor of apoptosis protein (XIAP) has been shown to be a potent inhibitor of caspase-3 activation and apoptosis (Liston *et al*., 1996). Leonard and coworkers have assessed the potential of *XIAP* gene therapy in the animal models of inherited retinal degeneration. They have found that sub-retinal injection of AAV-

mediated *XIAP* gene delivery in *Rho* knock-out rats of age 14 to 17 days resulted in the structural and functional rescue of photoreceptors as assessed through preservation outer nuclear layer thickness as well as greater preservation of a-wave amplitudes over control rats (Leonard *et al*., 2007).

Bcl2 is another anti-apoptotic protein which is capable of preventing apoptosis in neuronal cells dying through apoptosis (Allsopp *et al*., 1993). Bennett and coworkers tested the role of *Bcl2* in halting the process of apoptosis in the rodent model of retinal degeneration and found that adenovirus-mediated delivery of *Bcl2* in the sub-retinal space of 4-day old rd mice resulted in the rescue of photoreceptors. The photoreceptor rescue was indicated by lesser pigmentary deposition in the fundus and greater thickness of outer nuclear layer as compared to control mice (Bennett *et al*., 1998).

6. Channelopsin-2 gene

Bi and coworkers have explored the feasibility of genetically converting the inner retinal neurons into photosensitive cells by the introduction of microbial channel rhodopsin-2 (*Chop2*) gene. They have shown that AAV-mediated delivery of Chop2 gene into the sub-retinal space of 2 to 12 month old rd mice resulted in restoration of the ability of retina to transmit light signals to the visual cortex (Bi *et al*. 2006). Tomita and coworkers have shown that intravitreal AAV-mediated delivery of *Chop2* gene in 10 month old RCS rats resulted in the partial rescue of the visual response as assessed by the better amplitudes of the VEP (visually evoked potentials) (Tomita *et al*., 2007). Although the

light evoked responses were seen in rd mice and RCS rats, *Chop2* treated retinas only responded to light of highest intensities of 10^{14}–10^{15} photons $cm^{-2}s^{-1}$ compared to normal threshold of 10^{6} to 10^{10} photons $cm^{-2}s^{-1}$ of rods and cones respectively.

1.8.2. Non-genetic therapeutic approaches

The majority of genes involved in the retinal degenerations belong to the functional classes of phototransduction cascade, Vitamin A metabolism, structural proteins of rod and cone photoreceptors, development pathway or transcription factors. In retinal dystrophies, it is evident that whatever the causative gene photoreceptors die through the final common pathway of apoptosis (Pierce *et al*., 2001). Thus it has been hypothesized that therapies that can prevent apoptosis or slow down the process of apoptosis will be of advantage in that they are applicable to patients regardless of gene mutations involved in the disease. Other approaches that are under investigation are aimed at enhancing photoreceptor survival in retinal dystrophies, such as treatment with growth factors, and nutritional supplements. Another approach involves cell transplantation in order to replace the dying cells. The retinal prosthesis is another kind of treatment option where an electronic device is used to replace the function of photoreceptors and are used to convert light into electrical signal that stimulates neurons in visual pathway. The present status of advancements in these areas is discussed below.

1.8.2a. Growth factors

Some of the growth factors that have been successfully tested in experimental models for rescue of the photoreceptors in retinal degenerations are discussed in this section.

Mullen and coworkers in 1976 while studying chimeric rats (cells from RCS rat embryo and normal rat embryo) observed that photoreceptors lying opposite as well neighboring the wild type RPE cells were protected from degeneration whereas photoreceptors lying opposite to mutant RPE cells show severe degeneration. They attributed this rescue to the probable diffusion of trophic factor/s from the wild type RPE cells. This led to the first experimental attempt of the therapeutic use of growth factor and to the identification of the rescue effect of basic fibroblast growth factor (bFGF) in RCS rats (Faktorovich *et al*., 1990). The rescue effect was also observed in other studies involving intravitreal injection of encapsulated bFGF secreting fibroblasts in RCS rats (Uteza *et al*., 1999) as well as through direct intravitreal injection of bFGF in light-induced retinal degeneration mouse model (Driscoll *et al*., 2007). However, side effects in the form of macrophage invasion, neovascularization and cataractogenesis were also observed (Faktorovich *et al*., 1990, Uteza *et al*., 1999). These studies suggest that bFGF has a protective effect on photoreceptors but the side effects make it unsuitable for therapeutic purpose. The success with bFGF triggered the identification of other factors. In 1992 Lavail and coworkers evaluated the protective role of various growth factors, cytokines and neutrophin-3 through intravitreal injections in the light-induced rat retinal damage model. Through light microscopy they measured the thickness of the outer

nuclear layer and observed that bFGF (basic fibroblast growth factor), BDNF (brain derived neurotrophic factor), CNTF (ciliary neurotrophic factor), interleukin 1 beta and aFGF (acidic fibroblast growth factor) have a protective role in light-induced retinal damage. Lavail and coworkers in 1998, in a subsequent study used animal models of retinal degeneration the rd mice and rds mice, in order to examine the efficacy of survival factors CNTF, Neutrophin-3 and 4, human insulin-like growth factor, human leukemia inhibitor and mouse nerve growth factor in rescuing photoreceptors. They found that only CNTF had a protective role in rd mice.

Ciliary neurotrophic factor is effective in photoreceptor rescue in different types of animal models such as RCD1 dogs (Tao *et al*., 2002), rd mice (Cayouette *et al*., 1997), as well as in a feline model of retinal degeneration (Chong *et al*., 1999). CNTF has been administered through different approaches such as direct intravitreal injection of CNTF peptide (Chong *et al*., 1999), intravitreal adenovirus-mediated CNTF gene delivery (Cayouette *et al*., 1997) as well as with encapsulated cell implants (Tao *et al*., 2002). Rescue effect of CNTF observed in animal models led to phase-I clinical trials in human patients with RP. In a phase-I trial, CNTF implants made by enclosing RPE cells in a semipermeable polymer-based outer membrane were used. The RPE cells were transfected with CNTF gene containing plasmids and stable CNTF expressing cell lines were enclosed in the implant. The implants were placed in the eyes of 10 RP patients and these were found to be safe for at least 6 months (Sieving *et al*., 2006). The visual acuity also showed improvement in the study although it was not powered to make conclusions

about changes in visual acuity. Further studies are required in order to determine the functional effectiveness of CNTF in humans.

In vitro as well as in vivo studies have shown protective effects of glial cell line-derived neurotrophic factor (GDNF) on dopaminergic neurons (Lin *et al*., 1993). Through in situ hybridization Nosrat and coworkers (1996) have shown the expression of GDNF in the retina. It was hypothesized that if GDNF is expressed in neurons and has a protective role then it may have a similar protective role in retina as it is expressed in the retina. This led to multiple *in vivo* studies on different animal models such as rd mice as well as on mutant rhodopsin rats, which have shown a protective effect of GDNF in the form of increase in the number of cells in the outer nuclear layer as well as increase in the ERG amplitudes (Sanftner *et al*., 2001, Frasson *et al*., 1999, Andrieu-Soler *et al*., 2005). These studies have used different modes of GDNF transfer including subretinal injection of adeno-associated viral vectors (Sanftner *et al*., 2001), direct subretinal injections of GDNF peptide (Frasson *et al*., 1999) and intravitreous injection of GDNF encapsulated in poly(D,L-lactide-co-glycolide) (PLGA) microspheres (Andrieu-Soler *et al*., 2005). No major side effects were observed in these studies. Clinical trials of this factor require studies on the appropriate dose in larger animal models.

1.8.2b. Ca channel blockers

It has been observed in rd mice and rcd1 dogs that mutation in the *PDE6B* gene lead to abnormal accumulation of cGMP (Pierce *et al*., 2001). cGMP gates cationic channels that are responsible for the flow of light-sensitive current in photoreceptors. In the presence of excess of cGMP these channels remains open continuously and lead to metabolic overload by demanding continuous activity of Na^+/K^+ ATPase to maintain electrochemical gradients (Pierce *et al*., 2001). It has been hypothesized that this abnormal increase could be the reason for the death of photoreceptors (Farber *et al*., 1974). Frasson and coworkers in 1999 proposed that diltiazem, a known Ca channel blocker in cardiac diseases, may also block cGMP gated channels and this blocking of cGMP channels will prevent photoreceptor degeneration. They observed that photoreceptors in rd mice were rescued (both structurally and functionally) by the regular use of intraperitoneal injection of diltiazem. However, the results could not be replicated in canine rcd 1 model (*PDE6B* mutant) (Kelling *et al*., 2001), and in the rd mouse model (Pawlyk *et al*., 2002). It has been speculated that diltiazem action may be a species-specific phenomenon (Frasson *et al*., 1999, Pawlyk *et al*., 2002).

1.8.2c Anti-oxidant/nutrient supplementation

Oxidative stress has been shown to be one of the causes of death of photoreceptors (Carmody *et al*., 1999). Lutein and zeaxanthins are known to be powerful antioxidants

and filter high energy blue light, they belong to the xanthophyll family of carotenoids and form a major component of the macular pigments (Lutein and zeaxanthin. Monograph. 2005). It has been observed that higher dietary intake of lutein and zeaxanthin is associated with lower relative risk for AMD (Seddon *et al*., 1994) and persons with higher amount of lutein and zeaxanthin pigments are at a lower risk to AMD (Bone *et al*., 2001). Pilot studies done on patients with retinal degeneration in order to study the effect of lutein supplementation on the visual acuity have shown beneficial (Dagnelie *et al*., 2000) as well as no effect (Aleman *et al*., 2001) on the visual function. A double masked randomized placebo controlled trial has shown that lutein supplementation (10 mg/day for 12 weeks followed by 30 mg/day for 12 weeks) had some beneficial effect on the visual activity, contrast sensitivity and visual field radius but the effects were not found to be statistically significant (Bahrami *et al*., 2006). Through studies on the rd1 mouse model it has been observed that a combined dose of lutein, zeaxanthin, alpha-lipoic acid and L-glutathione slowed the degeneration of the rod photoreceptors as evident by the significant decrease in the number of TUNEL positive cells at postnatal day 11 in the outer nuclear layer of treated animals. This effect was not observed when these antioxidants were administered singly (Sanz *et al*., 2007).

Berson and coworkers in 1985 studied the natural course of retinitis pigmentosa and observed that patients taking vitamin A and vitamin E supplements in their diet show relatively slow decline in ERG with time. This led them to do a randomized control trial. They made four treatment groups- group A received 15,000 IU of vitamin A, group E received 400 IU of vitamin E, group A+E received 15,000 IU of vitamin A and 400 IU of

vitamin E while the fourth control group received trace amounts of both vitamins. The main outcome measure was ERG amplitudes. It was observed that the rate of progression of disease as evident by decline in ERG amplitudes was slower in group A (6.1%) and group A+E (6.3%) compared to control group (7.1%) or group E (7.9%). Consumption of 400 IU of vitamin E without vitamin A led to faster progression of the disease. The visual acuity declined by almost 1 letter per year in all the four groups (group A 1.1 letter per year, control group 0.9 letter, group A+E and group E 0.7 letter per year) (Berson *et al*., 1993).

Long-term daily use of vitamin A has been found to be safe in retinitis pigmentosa patients (Sibulesky *et al*., 1999).

1.8.2d Cell/tissue Transplantation

Several studies using RCS rats, rd mice as well as light-induced models of retinal degeneration have shown photoreceptor rescue through the transplantation of retinal pigment epithelial cells of adult rat into RCS rats as well as transplantation of human fetal RPE into RCS rats (Lopez *et al*., 1989), transplanting of photoreceptor sheets from adult rat retina to the subretinal space of rat (Silverman *et al*., 1992), and transplantation of intact sheet of fetal tissue to the subretinal space of the of rat retina in the light-induced retinal degeneration model (Seiler *et al*., 1998). The success of these approaches relies on the release of trophic factors from the healthy transplanted cells or due to transplanted cells making appropriate connections with the functional part of the retina (Aramant *et*

al., 2002). Fetal retinal cells have been transplanted to RP patients in a study done at LV Prasad Eye Institute in India (Das *et al*., 1999) as well at Johns Hopkins University (Del Cerro *et al*., 2000). The Indian group has shown some subjective improvement in the change in visual acuity from light perception to hand motion in some patients, change in counting fingers at 15 cm to counting fingers at 50 cm in some patients and one patient showed improvement in visual fields. The Johns Hopkins group did not observe any improvement in the vision of treated patients. No adverse effect or rejection was reported in either of the two studies. Kaplan and coworkers (1997) transplanted sheets of human cadaveric photoreceptors into the subretinal space of 2 RP patients. No improvement in vision or adverse effects or rejection were reported in these patients (Kaplan *et al*., 1997).

Takahashi and coworkers (1998) first transplanted rat hippocampus derived neural progenitor cells into the vitreous cavity of the healthy rat eye. They found that these cells localize to a wide variety of heterologous environments and express some of the features of retinal cells. Similarly, there are reports of transplantation of progenitor cells derived from murine brain (Van Hoffelen *et al*., 2003), as well as from rat fetal retina (Chacko *et al*., 2000) and they have shown the integration of retinal progenitor cells into the retina of Brazilian opossums (Van Hoffelen *et al*., 2003) and of rats (Chacko *et al*., 2000) respectively but without any demonstration of synaptic connections with other neurons or restoration of visual acuity. A recent report from MacLaren and coworkers (2006) has shown using rd, RDS and rhodopsin- mutant mice that if cells are taken from the developing retina at a time coincident with the peak of rod genesis then

these transplanted cells are able to differentiate and form connections and improve visual function.

1.8.2e. Retinal prosthesis

The retinal prosthesis is an electronic device that converts light into electrical signals that in turn stimulate neurons in the visual pathway. The neuronal signal is then processed by the brain to generate a visual response (Winter *et al*., 2007). There are two basic types of retinal prosthetic devices namely multiphotodiode array (MPDA) (Chow *et al*., 2004) and microelectrode arrays (MEAs) (Humayun *et al*., 2003). MPDA is implanted into the subretinal space. MPDA devices have a very limited electrical output which is insufficient to activate diseased neurons as they have higher than normal activation thresholds. MPDA devices have been used in patients with advanced RP, and have been found to be safe, however visual acuity has shown only subjective improvement in some patients in the form of gain of letters on ETDRS charts (Chow *et al*., 2004). More studies are required in order to comment on the improvement in visual acuity through MPDA devices. MEAs consist of planar microelectrode arrays connected to an implantable signal processor. The MEA can be implanted in the epiretinal or subretinal space. Epiretinal implantation of MEAs with 16 microelectrodes in a patient with advanced RP with no light perception has shown success in the form of perception of light at all the 16 electrodes as well as detection of motion and direction (Humayun *et al*., 2003).

The implanted devices to date have 16 functional electrodes which provides a vision of 20/1200. It is estimated that 256 to 625 electrodes are required to yield visual acuity of 20/420 and 20/30 respectively (Winter *et al*., 2007).

1.9. Approaches and potential uses of molecular diagnostic testing

Genetic testing for molecular diagnostics in retinal dystrophies is important because it may serve to confirm the clinical diagnosis made by an ophthalmologist and allow prediction of prognosis. Genotype-phenotype correlations can be determined by means of classification of sufficiently large numbers of patients with specific mutations and their corresponding clinical features. If suitable correlations are developed for different genes, this information can be used in prediction of prognosis for individual patients and as a guide to genetic screening based on phenotypic features. Genetic testing can help in providing genetic counseling and can offer an option of prenatal screening for those desiring it. For those already born with the disease, genetic testing can help in identifying the disease-causing gene and guide the way towards suitable therapy if it is available. Gene therapy has shown success in animal models in case of several different genes as discussed in the preceding section but few have reached clinical trials so far.

In retinal dystrophies application of genetic testing in molecular diagnostics is challenging because of the fact that retinal dystrophies are genetically heterogeneous, have multiple inheritance patterns and a large number of mutations per gene. In order to

minimize the cost and labour involved in genetic testing, various approaches such as the screening genes based on their frequency in causing disease in the specific population, or screening for the most frequent mutations causing retinal dystrophy, may be used. The known mutations can be screened efficiently in a short time period by using microarray based technology (Zernant *et al*., 2005, Henderson *et al*., 2007, Vallespin *et al*., 2007, Yzer *et al*., 2006). This is available commercially for the genes involved in autosomal recessive RP, autosomal dominant RP and LCA. Genes for which microarray-based screening is available are *ABCA4, CERKL, CNGA1, CNGB1, MERTK, PDE6A, PDE6B, PNR, RDH12, RGR, RLBP1, SAG, USH2A, USH3A, CA4, FSCN2, IMPDH1, NRL, PRPF3, PRPF31, PRPF8, RDS, RHO, ROM1, RP1, RP9, CRX, AIPL1, CRB1, GUCY2D, LRAT, TULP1, CEP290, LCA5* and *RPE65* (http://www.asperophthalmics.com/index_testing.htm). Other shortcut approaches are based on sorting the families based on their mode of inheritance and the use of homozygosity testing for families with recessive disease (Singh *et al*., 2006, Kondo *et al*., 2004) or by the co-segregation of a haplotype with the disease phenotype in families with dominant mode of inheritance (Kondo *et al*., 2003). This approach can only be applied to identify known retinal dystrophy genes in families with 2 or more affected individuals. SNP microarrays have also been reported to be successful in identifying even new genes in families with only 2 affected family members through whole genome homozygosity screening (Ramprasad *et al*., 2008, den Hollander *et al*., 2007).

1.10 Objectives of the study

This study was designed with the following objectives:

1. To identify genes causing autosomal recessive disease in affected families by screening for homozygosity at known candidate gene loci.

2. To map and identify the disease locus in a family with autosomal dominant RP.

3. To directly screen candidate genes for mutations in a pool of unrelated patients with retinal dystrophy.

Chapter 2

Materials and Methods

CHAPTER 2: MATERIALS AND METHODS

2.1 Recruitment of patients and sample collection

The study protocol was approved by the Institutional Review Board and adhered to the guidelines of the Declaration of Helsinki. Eligible patients with retinal dystrophy seen at the outpatient clinic of the retina service of LVPEI were recruited for the study. Patients and subjects recruited were in the following categories- 1) Families with ARRP as ascertained through history and with two or more affected individuals were included. In these families first-degree relatives of probands were also called to participate in the study. 2) Probands with a diagnosis of autosomal dominant/autosomal recessive/sporadic RP and LCA were included. 3) Large families with dominant or recessive RP with multiple affected members available in 2 or more generations (at least 10 children in autosomal dominant inheritance and at least 6 affected offspring in autosomal recessive inheritance). All subjects underwent a complete ocular examination and diagnostic features were reviewed and confirmed independently by two ophthalmologists. Diagnostic criteria are detailed below.

2.1.1 Inclusion criteria

2.1.1a Inclusion criteria for RP

Patients who presented with at least two of the signs listed below were included

a. Bilateral diffuse and widespread (defined as involving the retina beyond the posterior pole) retinal pigment epithelium (RPE) degeneration (appear as fine, white or grayish discoloration of deeper retinal layers)

b. Visual field loss commensurate with clinical lesions or with advanced disease.

c. Visual acuity <6/60 or fields not possible.

d. Electroretinogram (ERG) criteria: Extinguished or b-wave < 50 μV in maximal response.

e. Arterial narrowing

f. Progressive visual loss

Other clinical signs that may be present but were not essential for the diagnosis were:

a. Pigment migration including bone corpuscular pigmentation.

b. Vitreous opacities and vitreous pigments.

c. Associated RPE atrophic changes in the macular area.

d. Diffuse disc pallor.

e. Stellate opacities in the crystalline lens.

f. Nyctalopia.

2.1.1b Inclusion criteria for LCA

a. Visual loss since birth defined on the basis of history if present within the first 6 months of life.

b. Diffuse and widespread RPE degeneration.

c. Nystagmus since birth/infancy.

Additional signs that may or may not be present were:

Eye poking, arterial narrowing, disc pallor, no progression of disease, extinguished ERG, visual acuity <20/200 in better eye, hyperopia >4.0 sph.

2.1.2 Exclusion criteria

2.1.2a Exclusion criteria for RP

Unilateral disease, macular retinal dystrophy with no evidence of widespread retinal photoreceptor involvement, evidence of ocular trauma, retinal vascular occlusion, retinal detachment surgery, exudative retinal detachment, retinal vasculitis, chorioretinitis or any other secondary cause of pigmentary retinal changes, involvement of any other systems, patients not willing to participate in the study.

2.1.2b Exclusion criteria for LCA

Absence of nystagmus, patchy retinal involvement, no loss of vision at birth, patients not willing to participate in the study.

2.1.3 Sample collection

Patients who fulfilled the above inclusion criteria were explained the purpose of the study. Patients/families that were willing to participate were asked to sign a consent form, the contents of which were explained to them. Family histories were taken and complete pedigrees were drawn. 4-5 ml of blood was drawn in sodium heparin vacuettes [Greiner bio-one, Kremsmuenster, Austria] by venipuncture from the arm. Blood samples were then stored frozen at -20°C.

2.1.4 Details of patients and families

1. A total of 34 families with autosomal recessive retinitis pigmentosa with 76 affected and 88 unaffected individuals were included, out of which 24 families were consanguineous and 10 were non-consanguineous.

2. 100 probands with a diagnosis of autosomal recessive (n=55), autosomal dominant (n=14), and sporadic (n=31) forms of RP and 3 probands with a diagnosis of LCA, autosomal recessive (n=2) or sporadic (n=1) were included for candidate gene screening.

3. One family with autosomal dominant retinitis pigmentosa with 9 affected individuals was recruited. Blood samples were collected from 8 affected, 17 unaffected and 7 individuals with mild RPE/pigmentary changes with normal best-corrected visual acuities. Electroretinography and visual field data could not be obtained in these patients and hence their status was not conclusive of RP. Hence their affection status for the purpose of analysis was treated as unknown.

2.1.5 Controls

Blood samples from the control individuals were collected after obtaining informed written consent. More than 100 control individuals were included in the study. All the control individuals were examined in the clinics of LVPEI and were without any history of retinal disease.

2.2 Molecular genetic analysis

2.2.1 Extraction of genomic DNA from blood leukocytes

Blood samples were first thawed at room temperature and were then transferred to 50ml polypropylene centrifuge tubes. Four volumes of buffer A (Sucrose (Sigma – Aldrich, St. Louis, USA) – 320mM, $MgCl_2$ (Sigma–Aldrich, St. Louis, USA)–5mM, Triton X 100 (Sigma–Aldrich, St. Louis, USA)–1%, Tris-HCl (pH-8)-10 mM) was added to the blood sample and mixed gently till the solution became clear. Tubes were then centrifuged at

3000 rpm for 8 minutes, so as to obtain a white blood cell (WBC) pellet. The supernatant containing the lysed red blood cells (RBCs) were decanted. The WBC pellet was disturbed thoroughly and half the volume (as that of blood) of buffer B (400 mM Tris-HCl (pH-8), 60 mM Na-EDTA (Sigma–Aldrich, St. Louis, USA), 150 mM NaCl (Sigma–Aldrich, St. Louis, USA), 1% SDS (USB, Cleveland, USA)) was added, pellet was then gently mixed and kept for incubation at 37ºC for 10 minutes. Buffer C (5 mM sodium perchlorate (MERCK, NJ, USA) was then added at one-fourth the volume of blood taken for extraction and the solution was mixed gently for 3-4 minutes. This was followed by addition of equal volume (as that of blood) of phenol (Ambion, Texas, USA) and chloroform (Qualigens, Mumbai, India). Solution was mixed well gently and centrifuged at 3000 rpm for 10 minutes so as to separate three layers namely, aqueous layer, interface and organic layer. The aqueous phase was transferred to fresh 15 ml polypropylene centrifuge tubes, and an equal volume of chloroform was added, mixed gently and centrifuged at 3000 rpm for 5 minutes. The aqueous phase was transferred to another fresh 15 ml polypropylene centrifuge tube. 2 volumes of chilled absolute ethanol was added for precipitation of DNA. DNA was spooled out in a fresh 1.5 ml centrifuge tube and was washed twice with 70% ethanol and air dried to remove alcohol. The DNA pellet was dissolved in 200 µl of sterile deionised water. DNA was then incubated at 56ºC for 1 hour to dissolve and then at 37ºC overnight. DNA samples were quantified on UV spectrophotometer. Tubes containing DNA were labeled with codes depicting family and patient number, and concentration of DNA, and were stored at -20ºC.

2.2.2 Quantitation of DNA

To estimate the concentration of DNA, 5 µl of the sample was transferred to a fresh microfuge tube and diluted to 1 ml with deionised water. Absorbance was measured at wavelengths 260 nm and 280 nm in a spectrophotometer (UV-1601, Shimadzu). An optical density (OD) value of 1 corresponds to 50 micrograms (µg/ml) for double-stranded DNA. The concentration of DNA was calculated using the given formula:

Concentration (µg/ml) = OD260 X 50 (concentration of double stranded DNA at OD 260 value of 1) X 200 (dilution factor)

2.2.3 Polymerase chain reaction (PCR)

PCR amplifications were carried out for genotyping of microsatellite markers as well as for amplifying coding regions of genes for mutational screening. Reaction volumes for PCR were 30 µl for genotyping and 25 µl for exon-specific PCR. Primers were designed by using Webprimer software [http://seq.yeastgenome.org/cgi-bin/web-primer] for exon-specific amplifications so as to be complementary to flanking intronic regions. For microsatellite markers, primer sequences were obtained from databases such as UniSTS (http://www.ncbi.nlm.nih.gov/sites/entrez?db=unists) and Human Genome Database. The primer sequences are listed in appendix 1, Table 1. PCR reactions were carried out with 50 ng of genomic DNA, 5-10 pmol each of forward and reverse primers, 1.0 -3.5 mM magnesium chloride, 1X PCR buffer (100 mM Tris (pH9.0), 500 mM potassium chloride,

0.1% gelatin), 200 mM dNTPs and 1unit of *Taq* polymerase (Bangalore Genei, Bangalore, India). Dimethyl sulphoxide (DMSO, Sigma–Aldrich, St. Louis, USA) was used at a concentration of 5% to 10% for GC-rich templates. Annealing temperature and concentration of $MgCl_2$ standardized for each primer pair are listed in Table 2.2. PCR conditions used were: initial denaturation at 95 ºC for 4 minutes, followed by 30-34 cycles with denaturation at 94 ºC for 30 sec, annealing at 51 ºC-69 ºC for 15 sec , extension at 72ºC for 30 sec and one cycle of final extension at 72 ºC for 5 minutes.

2.2.4 Genotyping and Linkage analysis

i. Genotyping for ARRP

Candidate gene loci listed in Table 2.1 were tested for homozygosity. Markers for genotyping of these loci were selected based on proximity to the gene and on heterozygosity. Information on the microsatellite markers, including heterozygosity, location and primer sequences was obtained from public databases such as the UniSTS (http://www.ncbi.nlm.nih.gov/sites/entrez?db=unists), Human Genome Database and NCBI Mapview, (http://www.ncbi.nlm.nih.gov/mapview/) databases. Primers were commercially synthesized with one of each pair having fluorescent tags of Fam, Hex or Tet for detection on the ABI system. Sequences of primers used for genotyping of microsatellite markers are listed in Appendix 1, Table 1.

Table 2.1: Genes selected for homozygosity screening.

#	Gene name	Gene symbol
1	Guanylate cyclase 2D, membrane (retina-specific)	*GUCY2D*
2	Phosphodiesterase 6A, cGMP-specific, rod, alpha	*PDE6A*
3	Phosphodiesterase 6B, cGMP-specific, rod, beta	*PDE6B*
4	Phosphodiesterase 6G, cGMP-specific, rod, gamma	*PDE6G*
5	Guanylate cyclase activator 1A (retina)	*GUCA1A*
6	Rhodopsin	*RHO*
7	Cyclic nucleotide gated channel alpha 1	*CNGA1*
8	Cyclic nucleotide gated channel beta 1	*CNGB1*
9	Peripherin 2 (retinal degeneration, slow)	*PRPH2*
10	Retinal outer segment membrane protein 1	*ROM1*
11	Crumbs homolog 1 (Drosophila)	*CRB1*
12	Retinitis pigmentosa 1	*RP1*
13	Cone-rod homeobox	*CRX*
14	Neural retina leucine zipper	*NRL*
15	ATP-binding cassette, sub-family A (ABC1), member 4	*ABCA4*
16	Retinol binding protein 1, cellular	*RBP1*
17	Retinaldehyde binding protein 1	*RLBP1*
18	Retinal pigment epithelium-specific protein 65kDa	*RPE65*
19	Retinal G protein coupled receptor	*RGR*
20	Tubby like protein 1	*TULP1*
21	Prominin 1	*PROM1*
22	Aryl hydrocarbon receptor interacting protein-like 1	*AIPL1*
23	Retinitis pigmentosa GTPase regulator interacting protein 1	*RPGRIP1*

Table 2.2. Microsatellite markers used in multiplex PCR.

Pool	Marker	Label	Product Size	Annealing temp	$MgCl_2$
1	D1S406	Fam	205 bp	57ºC	2.5 mM
	D1S236	Tet	190-218 bp		
	D3S3584	Tet	143-147 bp		
	D4S432	Tet	224-272 bp		
2	D3S3552	Hex	161-177 bp	58ºC	2.5 mM
	D19S219	Tet	160-190 bp		
	D3S2302	Tet	295 bp		
	D1S1170	Fam	120		
3	D6S1575	Fam	88-110 bp	55ºC	1.25 mM
	D19S540	Fam	182-190 bp		
	D15S972	Tet	222-236 bp		
	D17S948	Tet	125 149 bp		
4	D1S2806	Fam	133-163 bp	55ºC	2.5 mM

	D15S1046	Hex	116-148 bp		
	D5S2090	Tet	189-205 bp		
5	D3S3607	Fam	144-164 bp	55ºC	1.25 mM
	D1S219	Hex	154-176 bp		
	D17S796	Tet	144-174 bp		
	D11S1883	Fam	224-266 bp		
6	D17S1810	Fam	108-122 bp	55ºC	1.25 mM
	D11S4017	Hex	178-179 bp		
	D1S2829	Tet	177-225 bp		
7	D15S202	Fam	226-247 bp	53ºC	2.5 mM
	D2S2228	Hex	191-215 bp		
8	D11S4357	Tet	157 bp	57ºC	2.5 mM
	D17S1161	Fam	175 bp		
	D6S936	Tet	308-368 bp		
9	D1S2779	Hex	229-247 bp	53ºC	3.75 mM
	D17S1832	Hex	151-195 bp		
10	D6S1568	Hex	84-110 bp	55ºC	1.25 mM
	D14S1042	Hex	253-267 bp		
	D14S123	Tet	365-423 bp		
	D4S405	Fam	250 bp		
11	D6S388	Fam	60-160 bp	57ºC	1.25 mM
	D6S273	Tet	101-201 bp		
	D4S251	Hex	100-110 bp		
	D4S1518	Fam	177 bp		
12	D4S2971	Tet	133-155 bp	55ºC	1.25 mM
	D17S1353	Hex	184-222 bp		
	D17S1791	Fam	232- 290 bp		
	D1S1726	Tet	261-279 bp		
13	D1S2622	Hex	165-189 bp	58ºC	2.5 mM
	D14S72	Fam	250 bp		
	D14S972	Fam	201-211 bp		
14	D17S786	Tet	135-157 bp	57ºC	1.8 mM
	D1S373	Fam	283-330 bp		
15	D15S972	Tet	222-236 bp	55ºC	1.25 mM
	D3S3607	Fam	144-164 bp		
	D3S1671	Hex	136 bp		
	D11S1883	Fam	224-266 bp		
16	D10S1753	Tet	223-279	55ºC	2.5 mM
	D16S3080	Hex	269-285		
17	D16S682	Fam	292	55ºC	2.5mM
	D8S285	Fam	108-124		
18	D16S3120	Tet	216-262	55ºC	3.5 mM
	D4S403	Hex	217-231		

Shown above are the list of microsatellite 57 markers and their PCR conditions in the 18 multiplex PCR reactions.

2-4 primer sets were combined in each multiplex PCR reaction. 18 multiplex PCR reactions were standardized for a total of 57 primer pairs. The markers amplified in each multiplex PCR along with PCR conditions used are given in Table 2.2. PCR reactions were carried out in 30 µl volume as described in the previous section. Cycling conditions used were: initial denaturation at 95ºC for 4 minutes, 10 cycles of 94ºC for 15 sec, 55ºC for 15 sec and 72ºC for 30 sec. This was followed by 20 cycles with denaturation at 89ºC for 15 sec, annealing at 55ºC for 15 sec , extension at 72ºC for 30 sec and one cycle of final extension at 72ºC for 10 minutes. The PCR products were electrophoresed on ABI 310 automated DNA sequencer (Applied Biosystems Inc, Foster City, California, USA).

ii). Genotyping for ADRP

In the ADRP family (family RP161) studied, known ADRP loci were genotyped using a set of 28 markers (Table 2.3) selected from the ABI linkage mapping set (ABI PRISM linkage mapping set, version 2.5-MD10), based on their proximity to the known gene loci in retinal dystrophies. These markers were flanking the 14 known ADRP genes (*GUCA1B, PRPH2, PAP1, RHO, NRL, ROM1*, *IMPDH1, CA4, FSCN2, PRPF8, PRPF31, TOPORS, RP1* and *CRX),* 5 genes for autosomal dominant cone/cone rod dystrophy *(GUCA1A, RIMS1, AIPL1, PITPNM3, UNC119*), 2 mapped loci (*RCD1, CORD4*) for autosomal dominant cone/cone-rod dystrophy for which genes are not yet

identified and a gene for Refsum disease (*PEX7*). Distances of the markers from the genes were taken from the NCBI Map Viewer (http://www.ncbi.nlm.nih.gov/mapview/). Fine mapping was done by genotyping 7 additional markers (D6S434, D6S287, D6S408, D6S270, D6S1009, D6S1649, D6S1637) which were selected based on location within the interval in which evidence of linkage was obtained by genotyping the 28 markers mentioned above. Allele frequencies for relevant markers showing positive LOD scores were calculated by genotyping 30 control individuals. The markers were amplified individually in a 7.5 µl PCR reaction. The PCR products were electrophoresed on ABI 3130XL automated DNA sequencer (Applied Biosystems Inc, Foster City, California, USA).

Table 2.3. Shortlisted markers corresponding to ADRP loci from the ABI linkage panels.

Gene/ locus Name	Phenotype	Panel Marker	Distance from the gene	Label	Allele size range	Pools for loading
RCD1	CRD	D6S264	1 Mb	Fam	108-130	Pool-I
GUCA1A/GUCA1B/ PRPH2	CRD	D6S1610	5 Mb	Fam	200-214	
RP9/ PAP1	RP	D7S517	2 Mb	Fam	243-261	
RIMS1	CRD	D6S460	6 Mb	Fam	279-303	
PEX7	Refsum disease	D6S308	4 Mb	Fam	326-354	
RHO	RP	D3S1292	5 Mb	Ned	111-145	
GUCA1B/GUCA1A/ PRPH2	RP	D6S257	4 Mb	Ned	167-195	
NRL	RP	D14S261	1 Mb	Ned	273-305	
PEX7	Refsum disease	D6S262	4 Mb	Vic	169-189	
ROM1	RP	D11S4191	5 Mb	Vic	89-119	
IMPDH1	RP	D7S486	1 Mb	Fam	221-235	Pool-II
RCD1	CRD	D6S1581	2 Mb	Fam	257-271	
RP9/PAP1	RP	D7S484	2 Mb	Fam	97-115	
IMPDH1	RP	D7S640	3 Mb	Ned	110-150	
CA4/CORD4/FSCN2	RP	D17S785	1 Mb	Ned	165-193	
PAP1/RP9	RP	D7S657	1 Mb	Ned	244-270	

RP1/RP9	RP	D8S285	1 Mb	Ned	314-330	
CA4/CORD4/FSCN2	CRD	D17S784	1 Mb	Vic	230-244	
PAP1/RP9	RP	D7S630	2 Mb	Vic	327-355	
CA4/CORD4/FSCN2	CRD	D17S949	1 Mb	Fam	210-228	
GUCY2D/PITPNM3 /PRPF8/AIPL1	CRD	D17S938	1 Mb	Fam	238-258	
GUCY2D/PITPNM3 /PRPF8/AIPL1	CRD	D17S1852	1 Mb	Fam	279-310	
CA4/CORD4/FSCN2	RP	D17S944	1 Mb	Ned	318-334	Pool-III
TOPORS	RP	D9S171		Ned	160-186	
TOPORS	RP	D9S285		Ned	80-110	
CRX/PRPF31	RP/CRD	D19S210	1 Mb	Vic	172-192	
UNC119	CRD	D17S798	5 Mb	Vic	298-322	
CRX/PRPF31	RP/CRD	D19S418	1 Mb	Vic	87-107	

Gene symbols refer to; *AIPL1*, aryl hydrocarbon receptor interacting protein-like 1; *CA4* carbonic anhydrase IV; CORD 4, cone rod dystrophy 4; *CRX*, cone-rod homeobox; *FSCN2* fascin homolog 2 actin-bundling protein, retinal; *GUCA1A*, guanylate cyclase activator 1A retina; *GUCA1B*, guanylate cyclase activator 1B retina; *GUCY2D*, guanylate cyclase 2D, *IMPDH1*, IMP inosine monophosphate dehydrogenase 1; *NRL*, neural retina leucine zipper; *PAP1*, PIM1-associated protein; *PEX7*, peroxisomal biogenesis factor 7; *PRPF31*, pre-mRNA processing factor 31 homolog; *PRPF8*, pre-mRNA processing factor 8 homolog; *PRPH2*, peripherin 2; *RCD1*, retinal cone dystrophy 1; *RHO*, rhodopsin; *RIMS1*, regulating synaptic membrane exocytosis 1; *ROM1*, retinal outer segment membrane protein 1; *RP1*, retinitis pigmentosa 1; *TOPORS*, topoisomerase I binding, arginine/serine-rich; *UNC119*, unc-119 homolog; *PITPNM3*, PITPNM family member 3.

For loading, PCR products were diluted 20 times (Fam, Tet, Vic labeled) or 10 times (Hex, Ned labeled). In case of 28 markers from the ABI panels, loading was done in 3 pools (shown in Table 2.3). A loading mix consisting of 0.25 μl per reaction of Tamra/Liz size standard and 10 μl per reaction of deionised formamide was prepared. To the above mix, 2 μl of diluted PCR product was added. The mix was then denatured at 95^{o}C for 5 minutes and immediately transferred to ice and then loaded in ABI 310/ ABI 3130 XL. Alleles were detected using GeneScan v 3.7 and GeneMapper v 4.0 software (Applied Biosystems Inc, Foster City, California, USA).

Linkage analysis for the ADRP family was done by using EasyLinkage package v 5.08 (Lindner TH et al., 2005). Two-point LOD score was calculated using SuperLink v 1.6. The disease model used was autosomal dominant with full penetrance and a frequency of disease gene of 0.0001. Linkage was determined using equal allele frequencies for all markers. Subsequently, allele frequencies of markers having positive LOD scores were determined in the control population (30 unrelated individuals) and LOD scores were re-calculated based on these allele frequencies. Multipoint analysis was done for 9 microsatellite markers using the GeneHunter program in the above software package. Multipoint analysis was done under the assumption of fully penetrant autosomal dominant disease gene locus with the frequency of disease allele as 0.0001.

2.2.5 Gel electrophoresis

2.2.5a Agarose gels

PCR products were checked by electrophoresis on 1.5% agarose gels to determine their amplification and quality. Agarose gels (1.5- 2.0% (w/v agarose; Colloids Implex, Madrid, Spain) were prepared by dissolving the required quantity of agarose in 1X Tris-Acetate-EDTA (TAE; 0.04M tris-acetate, 0.001M EDTA) electrophoresis buffer by heating in a microwave oven, followed by addition of 0.25 µg/ml ethidium bromide. The agarose solution was poured into a gel tray containing a comb, allowed to cool and solidify, and then placed in an electrophoresis tank and submerged in 1X TAE buffer.

The DNA samples were mixed with DNA loading buffer (0.25% bromophenol blue, 0.25% xylene cyanol, 40% w/v sucrose). Samples were loaded on the gel along with DNA size standard (MBI Fermentas, Lithuania). Horizontal electrophoresis was carried out at approximately 80-100V. DNA fragments were detected by staining with ethidium bromide and visualized on a UV transilluminator (UVITec, Cambridge, UK).

2.2.5b. Polyacrylamide gels

PCR products digested with the restriction enzymes were resolved on polyacrylamide gels. 8-10% of polyacrylamide gels were prepared from the 30% acrylamide stock solution (29:1; acrylamide:bisacrylamide; Sigma–Aldrich, St. Louis, USA) with 1X Tris-borate-EDTA (TBE) buffer (0.09M tris-borate, 0.002M EDTA). Final volume was adjusted with autoclaved deionized water to a 50 ml. Polymerization was done with the addition of 300 µl of 10% ammonium persulfate (APS) (Sigma, St. Louis, MO, USA) and 30 µl of N,N,N',N'-Tetramethylethylenediamine (TEMED) (USB, Cleveland, USA). The mix was then poured between glass plates (20X16 cm) with 1.5 mm spacers. After polymerization samples were loaded along with the 6X loading dye (0.25% bromophenol blue, 0.25% xylene cyanol, 40% w/v sucrose) and electrophoresis was done in an vertical electrophoretic unit (Hoefer SE 600 Series, electrophoretic unit, Amersham Biosciences, San Francisco, USA) at a voltage of 80-100 V. The polyacrylamide gels were stained with ethidium bromide (0.5 µg/ml in 1X TBE) and DNA fragments were visualized on a UV transilluminator (UVITec, Cambridge, UK).

2.2.6 DNA sequencing

i. Purification of PCR products

PCR products were purified to remove primers and dNTPs prior to sequencing by using Ultraclean ™ PCR clean up DNA purification kit (MOBIO Laboratories, Carlsbad, California, USA) according to the protocol given by the manufacturer.

The eluted DNA (50 µl) in the collection buffer was the precipitated by adding 2 µl of 5M sodium chloride and 100 µl of ethanol and centrifuged at 13000 rpm for 5 minutes. The DNA pellet was air-dried and dissolved in 15 µl of autoclaved deionized water. The PCR products were checked by agarose gel electrophoresis after column purification and subjected to sequencing.

ii. Sequencing

PCR products were sequenced using Sanger's dideoxy chain-termination method using fluorescent labeled ddNTPs, available with Big Dye version 3.1 cycle sequencing kit (Applied Biosystems Incorporated, Foster city, CA). Sequencing reactions were carried out in a 10 µl reaction volume with 0.8 µl of Big Dye reaction mix v 3.1 (Applied Biosystems Incorporated, Foster City, CA), 3.2 pmol of primer and 50-100 ng of amplified template. Cycle sequencing was done with initial denaturation at 96 ºC for 1 minute, followed by 25 cycles of 96 ºC for 10 sec, 50 ºC for 5 sec and 60 ºC for 4

minutes. The amplified products were purified by sodium acetate/ethanol precipitation according to the ABI instructions (given in manual "Automated DNA sequencing, chemistry guide" part no. 4305080B, year 2000, page 3-41). Briefly, PCR products were diluted to 100 µl with deionised water followed by the addition of 3 µl of 3M sodium acetate pH 4.6 (0.09M final concentration,) and 250 µl of ethanol. Samples were incubated on ice for 15 minutes followed by centrifugation at 12,000 rpm for 20 minutes at room temperature. The pellets were then washed twice with 70% ethanol, air dried and dissolved in 15 µl of deionised formamide (Applied Biosystems Incorporated, Foster city, CA) and were analyzed on the ABI 310 or ABI 3130XL genetic analyzer.

2.2.7 PCR-RFLP

PCR-RFLP (Polymerase chain reaction-Restriction fragment length polymorphism) analysis was used to screen for the presence of sequence variants in the control population as well as to ascertain segregation of sequence changes in the family members of probands. Sequence changes that led to the creation or abolition of recognition sites for restriction enzymes were tested by this method. Restriction enzyme sites were searched using the web-based program from New England Biolabs NEBcutter v. 2.0 (http://tools.neb.com/NEBcutter2/index.php). PCR products were digested with 2.5 units of the restriction enzyme in a final volume of 20 µl using the recommended buffer. Reactions were incubated overnight at 37 ^{o}C or another temperature as recommended. Polyacrylamide gel electrophoresis was used to resolve the restriction enzyme digested PCR products. Depending on the size difference between the digested products, 8 to 10%

non-denaturing gels were prepared for electrophoresis and separated DNA fragments were visualized on a UV transilluminator (UVITec, Cambridge, UK).

2.2.8 Gene sequences and nomenclature

Genomic or cDNA sequences of the genes screened for mutations were obtained from Ensembl database (http://www.ensembl.org). The sequences obtained were compared with the publicly available sequence of the gene. Ensembl transcript IDs of the genes tested in this study are listed in Table 2.4. For nomenclature of sequence changes, numbering of residues was with reference to cDNA sequences and started with the first base of the initiation codon (ATG).

Table 2.4. Transcript IDs of the genes selected for mutation screening

Gene Name	Transcript ID
ABCA4	ENST00000370225
CNCG1	ENST00000358519
CRB1	ENST00000367400
NRL	ENST00000396997
PDE6B	ENST00000255622
RDS	ENST00000230381
RD3	ENST00000367002
RGR	ENST00000358110
RLBP1	ENST00000268125
ROM1	ENST00000278833
RP1	ENST00000220676
RPE65	ENST00000262340

TULP1	ENST00000229771

2.2.9 Multiple sequence alignment

Multiple sequence alignment of protein sequences was done to evaluate the degree of conservation of amino acid residues found to have mutations. Protein sequences were obtained from the NCBI protein database (http://www.ncbi.nlm.nih.gov/sites/entrez). Homologous protein sequences were aligned using ClustalW2 software (http://www.ebi.ac.uk/Tools/clustalw2/).

2.2.10. SIFT

The SIFT (sorting intolerant from tolerant) tool was also used to predict the effect of sequence changes on the protein's function, based on homology search and the physical properties of amino acids. For calculating SIFT scores, the protein sequence of the candidate gene was downloaded from NCBI in the FASTA format. This SIFT scores of <0.05 suggest that the amino acid change is not tolerated (Ng and Henikoff; 2003).

Chapter 3

Identification of Genes in Families with ARRP by Homozygosity Screening

CHAPTER 3: IDENTIFICATION OF GENES IN FAMILIES WITH ARRP BY HOMOZYGOSITY SCREENING

3.1 Introduction

This chapter describes the screening of candidate gene loci in 34 families with ARRP. The strategy used was homozygosity mapping as described by Lander and Botstein (1987) to map the disease gene in families affected with recessive disease. A region spanning to several centimorgans surrounding the disease gene is almost always homozygous in the affected offspring of consanguineous marriages and such homozygosity can be used to map the disease gene. In this study microsatellite markers located close to known genes for RP were genotyped to detect homozygosity shared by affected members of a family with recessive disease. If one or more affected individuals of a family were found heterozygous for the marker alleles then that locus was considered as unlikely to be co-segregating with disease. If a parent or unaffected sibling was found homozygous at a marker locus in addition to homozygosity of the affected individuals then that marker was considered as uninformative. Markers found to be homozygous only in all the affected individuals of a family but not in unaffected siblings/parents were interpreted to be possibly co-segregating with the disease. Such results were confirmed by genotyping additional markers in this region. Families in which homozygosity was found at 2 or more markers at a given candidate gene locus specific for affected

individuals were further followed up by screening of the relevant candidate gene for pathogenic changes.

3.2 Results

3.2.1 Homozygosity screening

34 families with ARRP consisting of a total of 76 affected and 88 unaffected individuals were included (Table 3.1). Of these, 24 families were consanguineous and the rest were non-consanguineous. Genotyping was initially carried out with 57 microsatellite markers (Table 2.2). These markers flanked 23 different genes which are commonly linked with ARRP or related disorders. The genes included 14 known genes for ARRP (*PDE6A, PDE6B, RHO, CNGA1, CNGB1, CRB1, RP1, NRL, ABCA4, RLBP1, RPE65, RGR, TULP1, PROM1*); 7 genes for disorders such as digenic RP (*ROM1* and *RDS),* cone-rod dystrophy (*GUCA1A*), Lebers congenital amaurosis (*RPGRIP1*) and for both cone-rod dystrophy and Lebers congenital amaurosis (*GUCY2D*, *CRX* and *AIPL1*). Two genes, *PDE6G* and *RBP1*, were selected as they are candidates for retinal dystrophy since mouse models for *PDE6G* gene show features similar to human retinitis pigmentosa (Tsang *et al*., 1996) and *RBP1* is an intracellular carrier of retinol and mutations in the extracellular carrier of retinol (*RBP4*) are known to cause retinal dystrophy (Seeliger *et al*., 1999). The details of the genes are provided in Chapter 2, Table 2.1.

Table 3.1. Number of individuals screened in the 34 families.

#	Family code	No. of affected individuals	Number of unaffected individuals
1	RP149	2	5
2	RP141	2	4
3	RP173	2	4
4	RP192	2	5
5	RP145	3	4
6	RP168	3	4
7	RP119	2	2
8	RP147	2	3
9	RP157	2	3
10	RP170	2	3
11	RP171	2	3
12	RP200	2	3
13	RP225	2	3
14	RP184	2	3
15	RP201	2	3
16	RP142	3	3
17	RP220	3	3
18	RP136	3	3
19	RP198	1	2
20	RP126	2	2
21	RP129	2	2
22	RP152	2	2
23	RP199	2	2
24	RP205	2	2
25	RP215	2	2
26	RP213	2	2
27	RP128	3	2
28	RP172	4	2
29	RP169	2	1
30	RP153	2	1
31	RP160	2	1
32	RP121	2	1
33	RP207	2	1
34	RP135	3	1

34 families are shown along with numbers of affected and unaffected members that were genotyped for homozygosity.

Results of homozygosity screening at the 23 different loci are discussed below:

1. *ABCA4* locus (1p22.1-p21)

4 microsatellite markers, D1S406, D1S2779, D1S236 and D1S1170 located within an interval of 2 megabase (Mb) of the *ABCA4* gene were genotyped to test for homozygosity at this locus. Homozygosity was observed at this locus in family RP213 (Figure 3.1A). Marker D1S406 was uninformative in this family as the father (III:1, Figure 3.1A) was homozygous as well, while marker D1S2779 was not typed in individual (IV:3, Figure 3.1A) due to failure of amplification. Markers D1S236 and D1S1170 were homozygous in both the affected individuals (IV:3, IV:4, Figure 3.1A, Table 3.2) and heterozygous in unaffected individuals III:1, IV:6 (Figure 3.1A, Table 3.2), suggesting co-segregation with disease. This was further supported by genotypes for marker D1S188 (shown in Table 3.2).

No evidence of homozygosity was found in any of the other families at this locus. Hence this locus can be ruled out as a cause of disease in 33 families. Family RP213 was taken for further screening of the *ABCA4* gene to detect pathogenic mutations.

Table 3.2 Genotyping results at *ABCA4* locus in family RP213

Gene	Marker	III:1	IV:6	IV:3	IV:4	Interpretation
		Father	Unaffected	Affected	Affected	
ABCA4	D1S406	5/5	5/6	5/5	5/5	Uninformative
ABCA4	D1S2779	6/10	10/12	Not done	10/10	Incomplete
ABCA4	D1S236	6/12	6/13	6/6	6/6	Positive for homozygosity
ABCA4	D1S1170	7/8	7/9	7/7	7/7	Positive for homozygosity
ABCA4	D1S188	1/3	1/2	1/1	1/1	Positive for homozygosity

Shown above are the genotypes of markers tested in the members of family RP213.

2. *CRX* locus (19q13.32)

2 microsatellite markers, D19S540 and D19S219 located within a 1 Mb interval of the *CRX* gene were genotyped in 76 affected and 88 unaffected individuals of the 34 families. None of the families showed apparent co-segregation of marker alleles at the *CRX* gene locus with disease. Hence *CRX* gene locus is unlikely to have homozygous disease causing mutations in the affected individuals of the 34 families and was ruled out as a cause of disease in all families.

3. *GUCY2D* locus (17p13.1)

3 microsatellite markers (D17S796, D17S1810, D17S1832) located within a region of 1Mb flanking the *GUCY2D* gene were genotyped. In all the 34 families, genotypes of one or more affected individuals were heterozygous for one or more markers. Hence, it is

unlikely that affected individuals will carry homozygous mutations in the *GUCY2D* locus. Thus the *GUCY2D* gene was ruled out from further analysis in the 34 families.

4. *PDE6A* locus (5q33.1)

Two microsatellite markers, D5S594 and D5S2090, located within 1 Mb of the *PDE6A* gene, were genotyped at this locus. Homozygosity was not found to co-segregate with the disease phenotype in any of the families; hence the involvement of the *PDE6A* gene locus in these families was not considered further.

5. *PDE6B* locus (4p16.3)

3 microsatellite markers namely D4S3038, D4S412 and D4S432 were tested, all of which were located within 5 Mb of the *PDE6B* gene. In family RP119 (Figure 3.1B), the affected individuals (VI:1, VI:3, Figure 3.1B) were homozygous for markers D4S3038, D4S412 and D4S432 and the mother (V:1, Figure 3.1B) and the unaffected sibling (VI:2, Figure 3.1B) were heterozygous (Table 3.3). Three more markers D4S2936, D4S3023 and D4S2285 were genotyped in this family to confirm homozygosity, and a similar result was obtained (Table 3.3). Based on genotypes of 6 markers in this family, it was concluded that the *PDE6B* locus may be co-segregating with the disease in this family.

The genotypes of the 3 markers (D4S3038, D4S412 and D4S432) at the *PDE6B* locus in the remaining 33 families suggested that it is unlikely that mutations at this locus cause the disease phenotype.

Table 3.3 Genotyping results in family RP119

Gene	Marker	V:1	VI:1	VI:3	VI:2	Interpretation
		Mother	Affected	Affected	Unaffected	
PDE6B	D4S3038	13/17	17/17	17/17	13/17	Positive for homozygosity
PDE6B	D4S412	7/9	7/7	7/7	7/9	Positive for homozygosity
PDE6B	D4S432	5/22	22/22	22/22	5/22	Positive for homozygosity
PDE6B	D4S2936	9/11	11/11	11/11	9/11	Positive for homozygosity
PDE6B	D4S3023	18/19	18/18	18/18	18/19	Positive for homozygosity
PDE6B	D4S2285	9/11	11/11	11/11	10/11	Positive for homozygosity

Shown above are the genotypes of markers tested at the *PDE6B* gene locus in family RP119.

6. *PDE6G* locus (17q25)

Markers D17S1161 and D17S948, both within a 1 Mb interval of the *PDE6G* gene, were genotyped. One or more affected individuals of all the 34 families were found heterozygous for one or both the markers, and hence the *PDE6G* locus was ruled out as a cause of pathogenicity in these 34 families.

7. *RBP1* locus (3q21-q22)

This locus was screened by genotyping 3 microsatellite markers (D3S3552, D3S2302 and D3S3646). All the 3 markers are located within 1 Mb of the *RBP1* gene. In all the 34 families at least 2 out of 3 markers did not show co-segregation of homozygosity with the disease phenotype. Hence it is unlikely for the affected individuals in these families to inherit a disease causing homozygous mutation in the *RBP1* locus.

8. *RDS/GUCA1A* locus (6p21.1-p21.2)

Two microsatellite markers D6S1575 and D6S936 were genotyped in order to screen this locus. Both these markers are located within 1 Mb of the *GUCA1A* and *RDS* genes and marker D6S1575 is in a region of about 7 Mb of the *RDS* gene. The genotyping results suggest that this locus can be ruled out as a cause of pathogenicity in the 34 families as one or more affected individuals of these families were heterozygous for one or both markers.

9. *RHO* locus (3q22.1)

The *RHO* locus was screened for homozygosity by genotyping 2 microsatellite markers D3S3584 and D3S3607. Both the markers are within a region of 1 Mb flanking the *RHO* gene. The heterozygous genotypes of the affected individuals in all families negate the likely involvement of *RHO* locus in the pathogenesis in these families.

10. *RLBP1* locus (15q26)

Three microsatellite markers D15S972, D15S1046 and D15S202, located within 4 Mb of the *RLBP1* gene, were genotyped to screen for homozygosity at this locus. In family RP169 (Figure 3.1C) both the affected individuals (IV:3, IV:5, Figure 3.1C) were homozygous and the mother (III:2, Figure 3.1C) was heterozygous for alleles of all the 3 markers (Table 3.4). To corroborate these results two more markers D15S111 and D15S963 were genotyped in this family, which also showed co-segregation of homozygosity with the disease phenotype (Table 3.4). As the homozygosity of 5 markers co-segregated with the disease phenotype, the *RLBP1* gene was considered as a possible cause of disease in this family.

In the remaining 33 families either 2 or all the 3 markers did not show co-segregation of homozygosity with the disease phenotype. Hence it is unlikely for the affected individuals in these families to inherit a disease causing homozygous mutation in *RLBP1* gene locus.

Table 3.4. Genotyping results in family RP169

Gene	**Marker**	**III:2**	**IV:3**	**IV:5**	**Interpretation**
		Mother	**Affected**	**Affected**	
RLBP1	D15S972	23/26	26/26	26/26	Positive for Homozygosity
RLBP1	D15S1046	7/9	9/9	9/9	Positive for Homozygosity
RLBP1	D15S111	16/18	18/18	18/18	Positive for Homozygosity
RLBP1	D15S963	27/29	27/27	27/27	Positive for Homozygosity
RLBP1	D15S202	6/9	6/6	6/6	Positive for Homozygosity

Shown above are the markers tested at the *RLBP1* gene locus in family RP169.

11. *ROM1* locus (11q12.3)

This locus was screened by genotyping 3 microsatellite markers D11S4357, D11S1883 and D11S4017. All the markers are within 1 Mb of the *ROM1* gene. Genotyping results of the 3 markers at the *ROM1* locus indicated that involvement of this locus can be ruled out in the 34 families as one or more affected individual of these families was found to be heterozygous for the alleles of one or all markers tested.

12. *RPE65* locus (1p31)

3 microsatellite markers D1S2829, D1S806 and D1S219 were genotyped in order to screen this locus. All the 3 markers are within 1 Mb of the *RPE65* gene. In family RP205 (Figure 3.1D), both the affected individuals (IV:1, IV:2, Figure 3.1D) were homozygous for allele 14 of marker D1S2829 while both the parents (III:3, II:5, Figure 3.1D) were heterozygous with genotypes of 14/16 and 11/14 (Table 3.5). Markers D1S2806 and D1S219 were uninformative due to the presence of homozygous alleles in one of the parents as well as the affected individuals. Genotyping was done with 2 more markers, D1S1162 and D2S410 to confirm the above observations. Marker D1S1162 showed co-segregation of homozygosity with the disease phenotype and marker D1S410 was uninformative as father (II:5, Figure 3.1D) was homozygous for this marker (Table 3.5). These results suggest that the *RPE65* gene may be the disease locus in family RP205.

In the remaining 33 families, this locus was ruled out as a possible cause of disease as homozygosity of marker alleles did not co-segregate with the disease phenotype.

Table 3.5. Genotyping results in family RP205

Gene	Marker	II:5 Father	III:3 Mother	IV:2 Affected	IV:1 Affected	Interpretation
RPE65	D1S2829	14/16	11/14	14/14	14/14	Positive for Homozygosity
RPE65	D1S2798	9/12	9/12	9/9	Not done	Incomplete
RPE65	D1S2806	12/13	12/12	12/12	12/12	Uniformative
RPE65	D1S410	2/2	2/5	2/2	2/2	Uniformative
RPE65	D1S219	11/11	7/11	11/11	11/11	Uniformative
RPE65	D1S1162	2/5	2/5	2/2	2/2	Positive for Homozygosity

Shown above are the genotypes of markers at the *RPE65* gene locus in family RP205 along with their interpretation.

13. *TULP1* locus (6p21.3)

The *TULP1* locus was screened for homozygosity using 3 microsatellite markers D6S388, D6S1568 and D6S273. All the 3 markers are within 4 Mb of the *TULP1* gene. In family RP126 both the affected individuals (IV:1, IV:2, Figure 3.1E) were homozygous for markers D6S1568 and D6S273 and the parents (III:4, III:5, Figure 3.1E) were heterozygous for both the markers (Table 3.6, Figure 3.1E). Marker D6S388 was uninformative in this family (Table 3.6). In order to confirm the presence of homozygosity two more markers (D6S1583 and D6S1629) were genotyped in this family, both of which were found to be positive for homozygosity (Table 3.6). The results suggest that the *TULP1* gene is likely to cause disease in family RP126 due to the presence of co-segregation of homozygosity with the disease phenotype.

Heterozygous genotypes were obtained for 2 or more markers in the affected individuals of the remaining 33 families, suggesting that it is unlikely that homozygous mutations at this locus are responsible for the disease phenotype in these families.

Table 3.6. Genotyping results in family RP126

Gene	Marker	III:4	III:5	IV:1	IV:2	Interpretation
		Father	Mother	Affected	Affected	
TULP1	D6S388	30/30	30/31	30/30	30/30	Uninformative
TULP1	D6S1568	3/8	8/10	8/8	8/8	Positive for homozygosity
TULP1	D6S1629	7/16	15/16	16/16	16/16	Positive for homozygosity
TULP1	D6S1583	22/27	22/27	22/22	22/22	Positive for homozygosity
TULP1	D6S273	22/24	22/23	22/22	22/22	Positive for homozygosity

Shown above are the genotyping results of markers tested at the *TULP1* locus in family RP126.

14. *NRL* locus (14q11.1-q11.2)

Genotyping was done with 2 microsatellite markers D14S1042 and D14S123, within 5 Mb of the *NRL* gene. In family RP153 (Figure 3.1F), the affected individuals (IV:1, IV:2, Figure 3.1F) were homozygous for marker D14S1042 (genotype 9/9) while the parent (III:1, Figure 3.1F) was heterozygous with a genotype of 9/12. Marker D14S123 was uninformative as all the individuals were homozygous (Table 3.7). Three more markers (D14S972, D14S64 and D14S990) were genotyped in this family in order to determine the involvement of this locus. Homozygosity only in affected siblings was found for marker D14S990 while markers D14S972 and D14S64 were uninformative (Table 3.7).

Based on the genotyping results in family RP153 the *NRL* gene was selected for further testing of its involvement in disease in this family by mutational screening.

Genotypes of the remaining 33 families suggested that the *NRL* gene locus is unlikely to be involved in the disease.

Table 3.7. Genotyping results in family RP153

Gene	Marker	III:1	IV:1	IV:2	Interpretation
		Father	Affected	Affected	
NRL	D14S1042	9/12	9/9	9/9	Positive for homozygosity
NRL	D14S972	1/1	1/1	1/1	Uninformative
NRL	D14S123	15/15	15/15	15/15	Uninformative
NRL	D14S64	2/2	2/2	2/2	Uninformative
NRL	D14S990	4/8	8/8	8/8	Positive for homozygosity

Shown above are the genotypes of of markers at *NRL* gene locus in family RP153, along with the interpretation of genotyping results.

15. *CNGA1* locus (4p12)

This locus was screened for homozygosity by genotyping 4 microsatellite markers D4S405, D4S251, D4S1518 and D4S2971, all within an interval of 8 Mb from the *CNGA1* gene. In family RP200, markers D4S405 and D4S2971 were homozygous in both the affected individuals (IV:1, IV:2, Figure 3.1G) while the parents (III:1, III:2, Figure 3.1G) were of heterozygous genotype (Table 3.8). The other 2 markers D4S251 and D4S1518 were uninformative in this family due to the presence of homozygosity in one of the parents in addition to the affected individuals. To corroborate the results of markers D4S405 and D4S2971, two more markers (D4S174 and D4S2996) were

genotyped in this family. Both the markers were positive for homozygosity as indicated by the co-segregation of the homozygosity with the disease phenotype (Table 3.8). The results suggest that in family RP200, *CNGA1* gene may have a homozygous pathogenic mutation. This locus was ruled out from further consideration based on genotypes obtained in the remaining 33 families.

Table 3.8. Genotyping results in family RP200

Gene	Marker	III:1	III:2	IV:1	IV:2	Interpretation
		Father	Mother	Affected	Affected	
CNGA1	D4S405	20/21	18/20	20/20	20/20	Positive for Homozygosity
CNGA1	D4S251	13/13	10/13	13/13	13/13	Uninformative
CNGA1	D4S1518	9/12	9/9	9/9	9/9	Uninformative
CNGA1	D4S174	7/13	7/10	7/7	7/7	Positive for Homozygosity
CNGA1	D4S2996	25/27	25/26	25/25	25/25	Positive for Homozygosity
CNGA1	D4S2971	5/10	5/9	5/5	5/5	Positive for Homozygosity

Shown above are the markers tested at the *CNCA1* gene locus in family RP200 and their genotypes and interpretation.

16. *AIPL1* locus (17p13.2)

Three markers D17S1353, D17S786, and D17S1791 were genotyped in order to screen this locus. All the 3 markers are within a region of 1 Mb of the *AIPL1* gene. Presence of heterozygous genotypes for one or more of these markers in the affected individuals suggest that this locus is unlikely to be pathogenic in the 34 families.

17. *CRB1* locus (1q31-q32.1)

This locus was screened for homozygosity by genotyping 2 microsatellite markers D1S1726 and D1S373, located within an interval of 3 Mb of the *CRB1* gene. In families RP126 (Figure 3.1E) and RP160 (Figure 3.1H) affected individuals were homozygous while the parents were heterozygous for both the markers D1S1726 and D1S373. Thus to confirm the presence of homozygosity in these two families, 3 more markers (D1S2622, D1S1181 and D1S2853) were genotyped. All the 3 markers were found to be positive for homozygosity in family RP126 (Table 3.10). In family RP160, markers D1S2622 and D1S1181 were positive for homozygosity while the marker D1S2853 was uninformative due to the presence of homozygous genotype in the father (IV:6, Figure 3.1H). In families RP126 (Table 3.10) and RP160 (Table 3.9) homozygosity co-segregated with the disease phenotype, and thus the *CRB1* gene was considered as the possible cause of disease in the 2 families. In the presence of heterozygous genotypes for one or more markers in the affected individuals of the remaining 32 families, the *CRB1* locus was interpreted as unlikely to be the cause of the disease in these families.

Table 3.9 Genotyping results in family RP160

Gene	Marker	IV:6	V:4	V:5	Interpretation
		Father	Affected	Affected	
CRB1	D1S1726	27/28	28/28	28/28	Positive for Homozygosity
CRB1	D1S2622	11/16	11/11	11/11	Positive for Homozygosity
CRB1	D1S1181	31/33	31/31	31/31	Positive for Homozygosity
CRB1	D1S2853	13/13	13/13	13/13	Uninformative
CRB1	D1S373	13/14	14/14	14/14	Positive for Homozygosity

Shown above are the markers tested at the *CRB1* in family RP160 along with the genotypes and their interpretation.

Table 3.10. Genotyping results in family RP126

Gene	Marker	III:4	III:5	IV:1	IV:2	Interpretation
		Father	Mother	Affected	Affected	
CRB1	D1S1726	14/17	14/17	17/17	17/17	Positive for homozygosity
CRB1	D1S373	17/21	18/21	21/21	21/21	Positive for homozygosity
CRB1	D1S1181	5/22	22/33	22/22	22/22	Positive for homozygosity
CRB1	D1S2853	9/15	7/15	15/15	15/15	Positive for homozygosity
CRB1	D1S2622	11/14	11/14	11/11	11/11	Positive for homozygosity

Shown above are the markers tested at the *CRB1* gene locus in family RP126.

18. *RGR* locus (10q23)

Two markers D10S1765 and D10S1753 were genotyped at this locus in order to screen for homozygosity. Both the markers lie within a region of 7 Mb of the *RGR* gene. In families RP160 (Figure 3.1H) and RP184 (Figure 3.1I), affected individuals were homozygous for both the markers while the parents were heterozygous. Three more markers (D10S215, D10S1744, D10S1755) were screened in these families. All the 3 markers were positive for homozygosity in RP160 while in family RP184 marker D10S1744 was positive for homozygosity (Table 3.11, 3.12). The markers D10S215 and D10S1755 were uninformative in family RP184 either due to homozygous genotypes in all the individuals (marker D10S215) as well as in one of the parents (II:3, Figure 3.1I, Table 3.11). The present genotyping results in families RP160 (Table 3.12) and RP184 (Table 3.11) suggest that disease causing homozygous mutation may be present in the

RGR gene locus, thus *RGR* gene was selected for screening of mutations in families RP160 and RP184.

In the absence of co-segregation of homozygosity with the disease phenotype in the remaining 32 families, it was interpreted as unlikely that the *RGR* locus is the cause of disease in any of them.

Table 3.11. Genotyping results in family RP184.

Gene	Marker	III:1	II:3	IV:1	IV:5	IV:2	Interpretation
		Mother	Father	Unaffected	Affected	Affected	
RGR	D10S1765	11/15	11/15	11/15	15/15	15/15	Positive for Homozygosity
RGR	D10S215	1/1	1/1	1/1	1/1	1/1	Uninformative
RGR	D10S1753	24/27	24/27	24/24	27/27	27/27	Positive for Homozygosity
RGR	D10S1744	1/9	1/9	1/9	9/9	9/9	Positive for Homozygosity
RGR	D10S1755	1/4	4/4	1/4	4/4	4/4	Uninformative

Shown above are the genotypes at the RGR gene locus in family RP184, along with interpretation of the results.

Table 3.12. Genotyping results in family RP160.

Gene	Marker	IV:6	V:4	V:5	Interpretation
		Father	Affected	Affected	
RGR	D10S1765	9/15	15/15	15/15	Positive for Homozygosity
RGR	D10S215	19/29	29/29	29/29	Positive for Homozygosity
RGR	D10S1753	28/30	28/28	28/28	Positive for Homozygosity
RGR	D10S1744	1/9	1/1	1/1	Positive for Homozygosity
RGR	D10S1755	1/3	1/1	1/1	Positive for Homozygosity

Shown above are the markers tested at the RGR locus in family RP160.

19. *CNGB1* locus (16q13)

This locus was screened for homozygosity by genotyping 3 microsatellite markers D16S682, D16S3120 and D16S3080, all within 1 Mb of the *CNGB1* gene. The absence of co-segregation of homozygosity with the disease phenotype in all 34 families, suggests that the *CNGB1* locus can be ruled out as the cause of disease in these families.

20. *PROML1* locus (4p15.3)

2 markers D4S2942 and D4S403, both within a region of 1 Mb of the *PROML1* gene, were genotyped to screen for homozygosity at this locus. No homozygosity was found that was specific for the presence of disease in any of the families. Hence this locus is unlikely to be involved in the pathogenicity in all 34 families.

21. *RP1* locus (8q11-q13)

This locus was screened for homozygosity by genotyping 2 microsatellite markers D8S285 and D8S1718. Both the markers are within a region of 9 Mb of the *RP1* gene. In family RP170 (Figure 3.1J), both the markers were homozygous in affected members but not in unaffected members (Table 3.13). These findings were confirmed by genotyping 3 more markers (D8S166, D8S1763, D8S1696) in this family. Marker D8S1696 was positive for homozygosity as affected individuals (II:1, II:2, Figure 3.1J) were homozygous for allele 14 while the parents (I:1, I:2, Figure 3.1J) and unaffected sibling (II:3, Figure 3.1J) were heterozygous with genotype (14/20, 14/20, 14/20) (Table 3.13). Markers D8S166 and D8S1763 were uninformative due to homozygosity in one of the

parents and affected individuals. The genotyping results suggest that homozygous disease causing mutation in the *RP1* gene locus may be present in family RP170. The *RP1* gene was selected for mutation screening in family RP170.

In the presence of heterozygous genotypes for one or more markers in the affected individuals of the remaining 33 families it was taken as unlikely for the affected individuals of these families to have homozygous disease causing mutations in the *RP1* locus.

Table 3.13. Genotyping results in family RP170

Gene	Marker	I:1	I:2	II:3	II:1	II:2	Interpretation
		Father	Mother	Unaffected	Affected	Affected	
RP1	D8S285	6/9	6/8	6/9	6/6	6/6	Positive for homozygosity
RP1	D8S166	9/12	9/9	9/12	9/9	9/9	Uninformative
RP1	D8S1718	4/13	4/6	4/13	4/4	4/4	Positive for homozygosity
RP1	D8S1763	4/4	2/4	4/4	4/4	4/4	Uninformative
RP1	D8S1696	14/20	14/20	14/20	14/14	14/14	Positive for homozygosity

Shown above are the genotypes of markers tested at the *RP1* gene locus in family RP170 and the interpretation.

22. *RPGRIP1* locus (14q11.2)

This locus was screened for homozygosity by genotyping 2 microsatellite markers D14S72 and D14S122, both within 5 Mb interval of the *RPGRIP1* gene. All the 34 families were considered unlikely to have homozygous disease causing mutations in the *RPGRIP1* locus due to the absence of co-segregation of homozygosity with the disease phenotype.

Table 3.14. Families with autosomal recessive RP and loci showing homozygosity.

Family	Chromosomal location	Gene	Informative markers	Distance of the furthest marker from the gene (Mb)
RP205	1p31	*RPE65*	D1S2829, D1S1162	0.6
RP126, RP160	1q31-q32.1	*CRB1*	D1S1726, D1S373, D1S1181, D1S2853, D1S2622	2.8
RP213	1p22.1-p21	*ABCA4*	D1S236, D1S1170, D1S188	1.9
RP119	4p16.3	*PDE6B*	D4S3038, D4S412, D4S432, D4S2936, D4S3023, D4S2285	4.5
RP200	4p12-cen	*CNCG1*	D4S405, D4S174, D4S2996, D4S2971	7.5
RP126	6p21.3	*TULP1*	D6S1568, D6S1629, D6S1583, D6S273	3.7
RP170	8q11-q13	*RP1*	D8S285, D8S1718, D8S1696	8.3
RP160, RP184	10q23	*RGR*	D10S1753, D10S1744, D10S1755, D10S1765	6.3
RP153	14q11.1-q11. 2	*NRL*	D14S1042, D14S990	4.7
RP169	15q26	*RLBP1*	D15S972, D15S1046, D15S111, D15S963, D15S202	3.8

Families and the gene loci are shown with corresponding markers at which homozygosity was identified with the distance of the furthest marker from the gene.

3.2.2 Screening of candidate genes

Genotyping in the 76 affected and 88 unaffected individuals of 34 families resulted in the identification of homozygosity specific for the disease phenotype at 12 loci of 10 families (Table 3.14). Candidate genes at these loci were subjected to mutation screening. Eight families showed homozygosity at one locus each while in 2 families, families RP126 and RP160 homozygosity was observed at more than one gene locus. Screening at all the gene loci shown in Table 3.14 was done for the respective families.

In a previous study from our group, homozygosity was observed in 4/10 families based on a similar screen (Lalitha *et al*., 2002). Three gene loci, *ABCA4* (families RP109 and RP111), *RDS/GUCA1A* (families RP102 and RP107) were found to be homozygous and were therefore candidates for mutational screening. Thus mutation screening was also carried out in these 3 genes in the 4 families.

Results of mutation screening in the shortlisted families are discussed in this section.

1. Family RP205

In family RP205 (Figure 3.1D), screening of the *RPE65* gene in the affected individual IV:1, showed a homozygous single base deletion c.1060delA (Figure 3.2A, Table 3.16). This change co-segregated with the disease phenotype in the family (Figure 3.1D). 103

control individuals were screened by direct sequencing and none of the controls showed the presence of the change.

2. Family RP170

Affected individual II:2 (Figure 3.1J) of family RP170 was screened for sequence changes in the *RP1* gene. A total of four sequence changes were observed (Table 3.16, 3.17). A homozygous single base deletion, c.2847delT, co-segregated with the disease phenotype (Figure 3.2B, Figure 3.1J). c.2847delT is predicted to result in frameshift at codon 949 and will lead to premature termination after 32 amino acid residues (p.Asn949LysfsX32). This change was not observed in any of 202 control chromosomes screened for this deletion by direct sequencing. Three other homozygous sequence changes identified in this gene are reported SNPs- rs444772, rs414352 and rs441800 (Table 3.17). None of these reported variants co-segregated with the disease phenotype.

3. Family RP126

In family RP126 (Figure 3.1E) 2 genes, *TULP1* and *CRB1* were selected for the mutation screening.

Screening of the *CRB1* gene in the individual (IV:1, Figure 3.1E) showed 3 homozygous sequence changes (Table 3.17). Arg905Arg is a novel synonymous change

that co-segregated with the disease. Changes rs58879207 (intronic) and rs3902057 (Leu470Leu) are reported SNPs and did not co-segregate with the disease.

5 homozygous sequence changes were identified in the *TULP1* gene in affected individual (IV:1, Figure 3.1E) (Table 3.16, 3.17). c.1199G>A is a novel homozygous change which resulted in missense change of Arg400Gln, and co-segregated with the disease phenotype (Figure 3.1E, 3.2C). The c.1199G>A change creates a restriction site for *Eco57I* enzyme. 109 control individuals were screened for this change using enzyme *Eco57I* and none were positive for the change. The conservation of the arginine at position 400 of the TULP1 protein was evaluated among different species. Arg400 is conserved among different species (Figure 3.4). SIFT analysis yielded a score of 0.00 predicting this change to be possibly damaging to the protein. The remaining 4 homozygous changes observed are reported SNPs namely rs7764472 (Thr67Arg), rs58984224 (intronic), rs2064317 (Ile259Thr), rs2064318 (Lys261Asn). None of the 4 changes, except Ile259Thr (rs2064317), co-segregated with the disease phenotype.

4. Family RP169

Screening of the affected individual IV:5 (Figure 3.1C) for mutations in the *RLBP1* gene showed a novel homozygous sequence change at c.451C>T (Figure 3.2D, Table 3.16) which predicts a missense change of Arg151Trp. This change co-segregated with the disease phenotype (Figure 3.1C). c.451C>T change abolishes a restriction site for enzyme *Hpy188III*. 108 control individuals were tested for the presence of this change by

digestion with *Hpy188III* and none of the control chromosomes were found to have the change. This residue is conserved among different species (Figure 3.5) indicating towards its importance in the protein function. SIFT analysis gave a score of 0.00 predicting this change to be probably damaging.

5. Families RP109, RP111, RP213

Screening of the *ABCA4* gene in the families (RP109, RP111, RP213) showed 3 pathogenic changes (Table 3.15). The pathogenicity was inferred by virtue of the nature of the change, co-segregation within the family and absence in 100 unrelated controls. A total of 9 sequence changes were identified in the 3 families (Table 3.15).

In family RP109, a homozygous nonsense mutation was found in exon 44 (c.6088C>T) corresponding to Arg2030X (Figure 3.2F). This mutation lead to gain of restriction enzyme site for *BseG*1 (Table 3.15). This mutation co-segregated with disease in the family (Figure 3.1K; Table 3.15) and was absent in 100 normal control individuals.

In family RP111, a single base deletion of an 'A' residue (c.1225delA) in exon 9 resulting in a frameshift at codon Arg409 (Figure 3.2G; Table 3.15). Due to c.1225delA mutation, there was a gain of *Mnl* 1 enzyme site. This change co-segregated with the disease phenotype (Figure 3.1L)

A change of Tyr665X was found in family RP213 that co-segregated with the disease (Figure 3.1A). This change leads to premature truncation of the ABCA4 protein and is predicted to result in complete loss of 2 ATP binding domains and 2nd transmembrane domain and partial loss of 1st transmembrane domain. Another novel change in family RP213 that is predicted to be benign, was a missense change of Met1419Thr (Table 3.15). 5/210 (2.4%) control chromosomes showed the Met1419Thr change (heterozygous in 5 normal controls). Mutiple sequence alignment showed that the Met1419 residue is not conserved among different species (not shown). SIFT analysis (score = 0.16) predicted this change to be tolerated. Other polymorphisms identified in *ABCA4* are listed in Table 3.15.

Table 3.15. Sequence changes identified in the *ABCA4* gene in families RP109, RP111 and RP213.

Family	Exon/Intron	Mutation in cDNA, protein	Consequence	Reported/ Novel	Co-segregation with disease	Restriction enzyme change
RP109	Exon 44	c.6088C>T, p.Arg2030X	Nonsense	Reported[†‡§]	Yes	*BseGI*+
RP111	Exon 9	c.1225delA, p.Arg409fs	Frameshift	Novel	Yes	*MnlI*+
RP213	Exon 14	c.1995C>A, p.Tyr665X	Nonsense	Novel	Yes	None
RP213	Exon 2	c.141A>G, p.Pro47Pro	Synonymous	rs4847281	No	NA
RP213	Exon 29	c.4256T>C, p.Met1419Thr	Missense	Novel	Yes	*NlaIII*-
RP213	IVS 29	c.4352+54A>G	Unknown	rs547806	No	NA
RP213	IVS 33	c.4774-16_17delGT	Unknown	rs55860151	No	NA
RP213	Exon 45	c.6249C>T, p.Ile2083Ile	Synonymous	rs1801359	Yes	NA
RP213	IVS 45	c.6282+7G>A	Unknown	rs17110761	No	NA

Sequence changes identified in ABCA4. '+' denotes gain of restriction site, ' –' denotes loss of restriction site. Numbering of the cDNA sequence is with respect to first base of ATG. *ABCA4* Ensembl transcript Id: ENST00000370225. Abbreviation: NA, not applicable. † Lewis *et al*., 1999, ‡ Papaioannou *et al*., 2000, § Webster *et al*., 2001. The dbSNP ids (http://www.ncbi.nlm.nih.gov/sites/entrez?db=snp) are given for reported SNPs.

6. Family RP119

Screening of the *PDE6B* gene in individual VI:3 (Figure 3.1B) showed 3 homozygous sequence changes and 1 heterozygous change (Table 3.17). A novel homozygous sequence change, c.2130-15G>A co-segregated with the disease phenotype. The c.2130-15G>A change abolishes a restriction site for *HpaII* and was absent in 216 control chromosomes screened by PCR-RFLP for *HpaII* . In order to assess the impact if any of

this sequence change on mRNA splicing, the mutant sequence was evaluated using the splice site prediction by neural network (www.fruitfly.org/seq-tools/splice.html). The introduction of the c.2130-15G>A sequence variant changes the accepter site prediction score from 0.90 to 0.89 and does not predict the creation of a new splice acceptor. This suggests that there is no effect of this change on splicing.

Two homozygous sequence changes c.*12A>G found in the 3'UTR region of *PDE6B* and c.958G>A (Val320Ile) both reported SNPs (details in Table 3.17), and a novel heterozygous intronic change c.1401+31C>A, were identified in this family.

7. Family RP184

Screening for mutations in the *RGR* gene showed a novel homozygous sequence change c.760-38 C>T in intron 6 (Table 3.17), that did not co-segregate with the disease in this family and was absent in 100 control individuals.

8. Family RP160

The *CRB1* and *RGR* genes were screened for mutations in family RP160. Screening of the *CRB1* gene in individual V:4 (Figure 3.1H) showed 2 reported homozygous sequence changes, rs59598360 (Leu470Leu) and rs12042179 (intronic) (Table 3.17). Neither of these sequence changes co-segregated with the disease in the family.

Screening of the *RGR* gene in individual RP160, V:4 (Figure 3.1H) showed 5 sequence changes (Table 3.17). These are either novel or reported SNPs and are listed in Table 3.17. Ser246Phe has been reported as a rare variant of unknown pathological significance (Morimura *et al*., 1999, Bernal *et al*., 2003). We screened 61 normal controls by direct sequencing and 9 individuals were found to have the Ser261Phe change (8 heterozygous and one homozygous). These observations suggest its benign nature.

9. Family RP200

In family RP200 (Figure 3.1G), the *CNGA1* was screened for pathogenic changes. A total of three sequence changes were observed in the *CNGA1* gene in individual IV:1 (Figure 3.1G**,** Table 3.17). All the three changes are reported SNPs, rs1972883 (homozygous), rs6819506 (homozygous) and rs59800634 (heterozygous). None of the homozygous changes co-segregated with the disease phenotype in the family.

10. Family RP153

In family RP153 (Figure 3.1F) the *NRL* gene was screened for sequence changes in the affected individual IV:2 (Figure 3.1F). No sequence change was detected in this gene.

11. Family RP102

Homozygosity was observed at the *RDS* gene locus in family RP102 (Lalitha *et al*., 2002). Mutation screening resulted in the identification of a novel homozygous missense change c.725A>G (Glu242Gly) in the affected individuals. The change led to the loss of a restriction site for *SacI* enzyme. This change was also present in homozygous form in one of the unaffected siblings (IV:3, Figure 3.1M) in this family. 2 of the 115 control individuals were heterozygous for the Glu242Gly change in *RDS* gene. *RDS* and *ROM1* genes are known to show digenic inheritance and hence it was thought that there could be a third allele in the *ROM1* gene that may be co-segregating with the disease phenotype and could be the cause of disease in this family. The *ROM1* gene was therefore screened in this family. No sequence change was detected in the *ROM1* gene.

12. Family RP107

In family RP107 (Figure 3.1N) homozygosity was observed at the *RDS*/*GUCA1A* locus (Lalitha *et al*., 2002). Screening of the *RDS* and *GUCA1A* genes in this family failed to show any sequence change.

Clinical features of patients with mutations:

Pathogenic sequence changes were identified in 5 genes in 7 families. The clinical features of the affected individuals of these 7 families are summarized in Table 3.18 and described below:

1. *RPE65* gene

Mutation c.1060delA in the *RPE65* gene was identified in family RP205 (Figure 3.1D). In both the affected individuals the initial symptom of night blindness was observed by 1 year of age. The fundus showed arterial narrowing and widespread white dots in periphery due to RPE atrophy (fundus picture of IV:1, Figure 3.3A). This family had a diagnosis of early onset RP (Table 3.18).

2. *RP1* gene

A homozygous sequence change, c.2847delT, in the *RP1* gene was identified as a cause of disease in family RP170. Both the affected individuals of this family reported symptoms of night blindness in their childhood followed by reduced visual acuity. The fundus showed equatorial RPE degeneration, pale disc, arterial narrowing, vitreous opacities and macular RPE degeneration (Figure 3.3B). Individual II:1 had a visual acuity of 20/60 in the right eye and counting fingers at 1 meter in the left eye, individual II:2 had a visual acuity of 20/50 in both eyes. This family had a diagnosis of RP with macular degeneration (Table 3.18).

3. *TULP1* gene

In family RP126, mutation of Arg400Gln in the *TULP1* gene was identified in both the affected individuals.The affected individuals showed initial symptoms of night blindness in their childhood which later progressed to reduced vision. At presentation, the older affected sibling had a visual acuity of 20/200 in both eyes while the younger affected individual had a visual acuity of 20/400 in right eye and 20/600 in the left eye. The fundus in these individuals showed diffuse RPE degeneration, pigment migration, arterial narrowing with prominent macular degeneration and optic disc pallor (Figure 3.3C). The ERG was extinguished in both the individuals. This family had a diagnosis of advanced typical RP (Table 3.18).

4. ***RLBP1*** **gene**

In family RP169, mutation of Arg151Trp was found in the *RLBP1* gene. The affected individuals of this family presented to our institution at the ages of 16 and 12 years. Both individuals experienced initial symptoms of night blindness in their childhood. The fundus showed diffuse RPE degeneration, pigment migration, arterial narrowing with macular sparing (Figure 3.3D). Visual fields detected an area of central scotoma (area of diminished vision) in both the individuals. A diagnosis of typical RP was made in this family (Table 3.18).

5. ***ABCA4*** **gene**

ABCA4 gene mutations were observed in 7 affected individuals of 3 families (RP109, RP111, RP213). The affected individuals of these families observed initial symptom of progressive vision loss in their $1^{st}/2^{nd}$ decades of life. All the individuals showed retinal degeneration with macular involvement, along with RPE changes and arterial narrowing (Figure 3.3 E-G). Pigmentary changes were seen in both the affected individuals of family RP111 as well as in one individual (IV:1, Figure 3.1K) of family RP109. Visual acuity was less than 20/200 in all the affected eyes. ERG was severely reduced or extinguished in the affected individulas of family RP213 and RP111 while ERG responses were recordable but grossly reduced in the affected individuals of family RP109. These families had a diagnosis of RP with atrophic maculopathy.

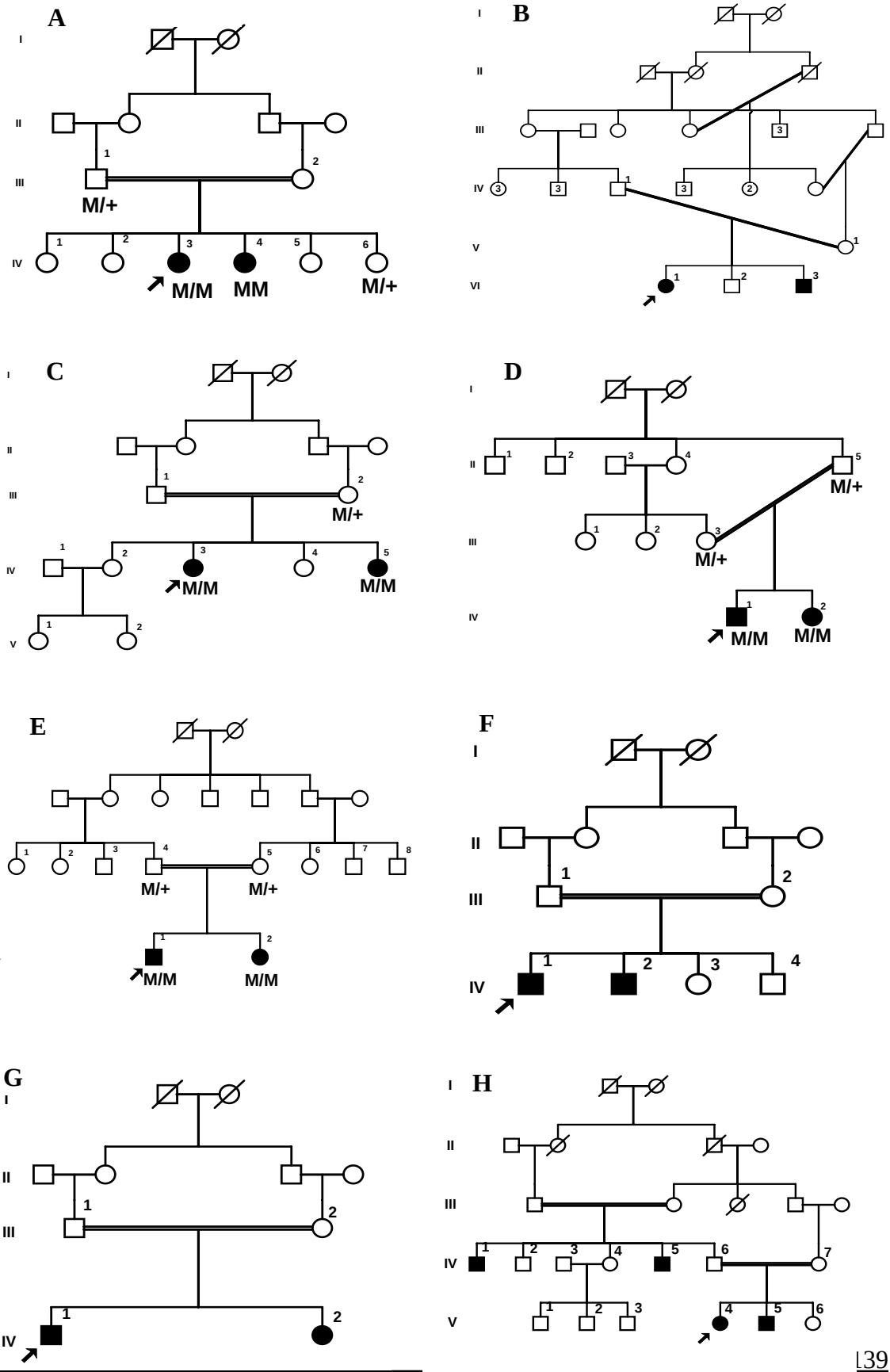
A
M/+
M/M
MM
M/+
B
C
M/+
M/M
M/M
D
M/+
M/+
M/M
M/M
E
M/+
M/+
M/M
M/M
F
G
H

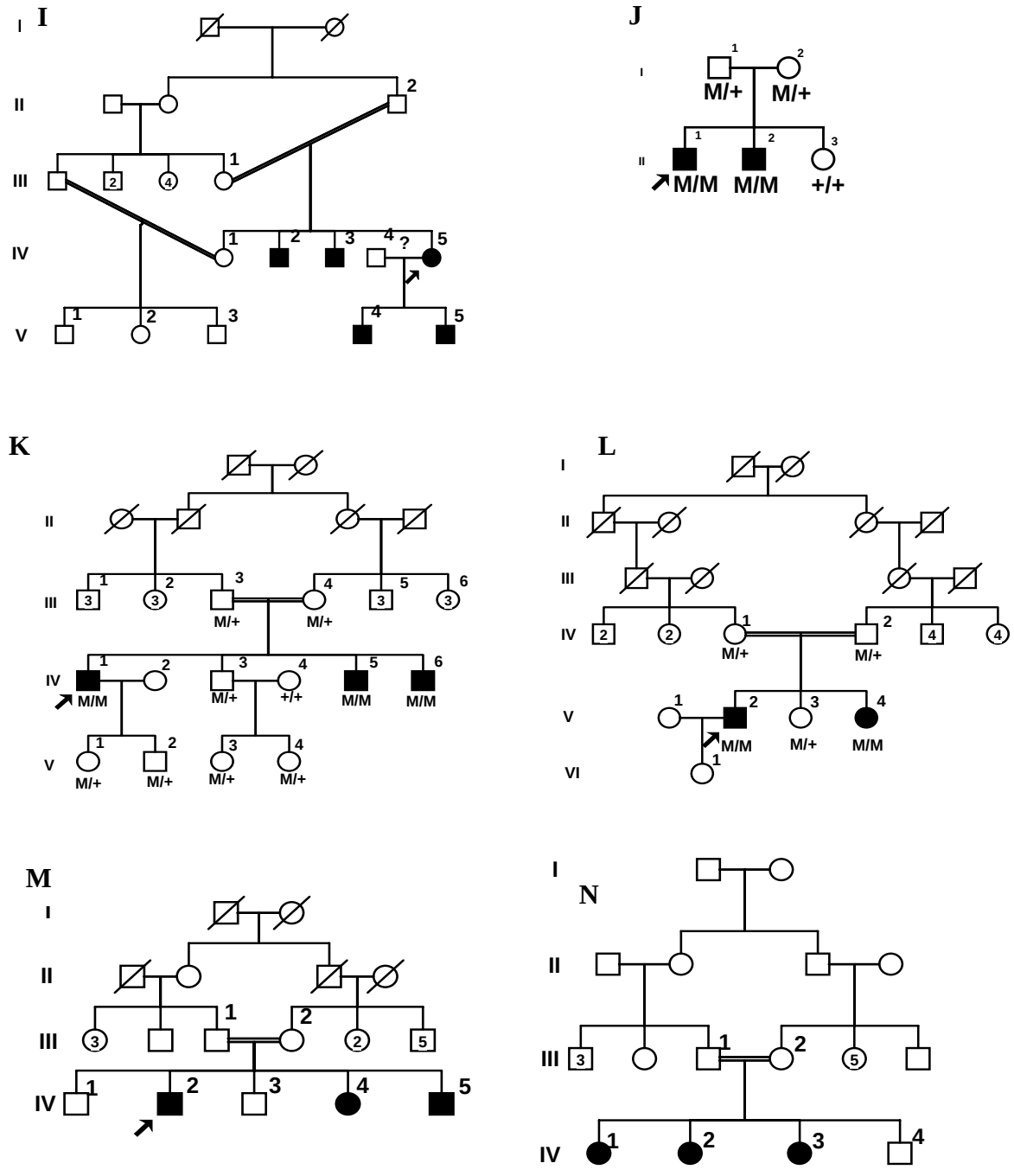

Figure 3.1. Pedigrees of families in which homozygosity was observed. M denotes mutant and plus sign (+) denotes the wild-type allele. (A) family RP213, (B) RP119, (C) RP169, (D) RP205, (E) RP126, (F) RP153, (G) RP200, (H) RP160, (I) RP184, (J) RP170, (K) RP109, (L) RP111, (M) RP102, (N) RP107.

(A) *RPE65*, c.1060delA

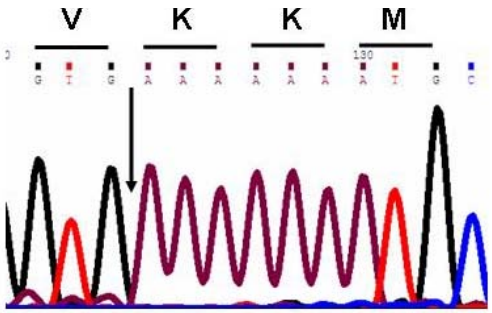

(B) *RP1*,c.2847delT

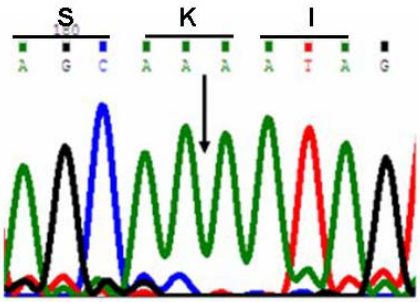

(C) *TULP1, c.1199G>A*

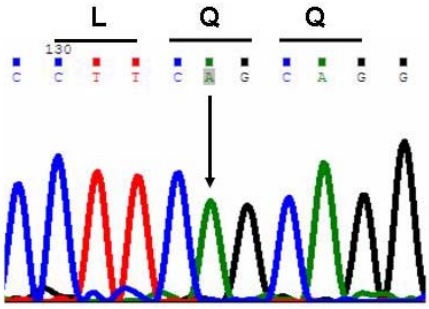

(D) *RLBP1,* c.451C>T

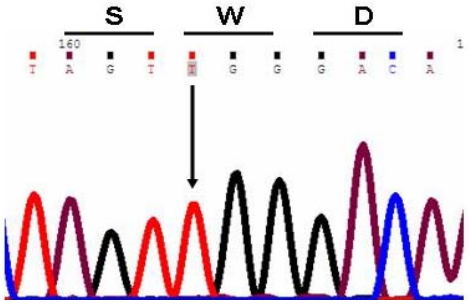

(E) *ABCA4,* c.1995C>A

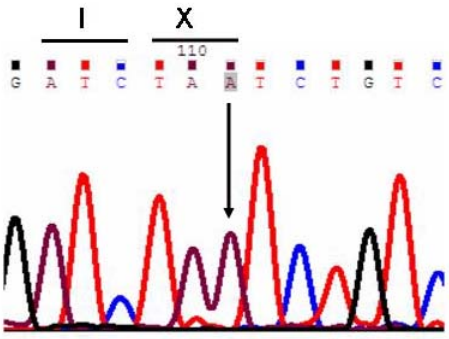

(F) *ABCA4,* c.6088C>T

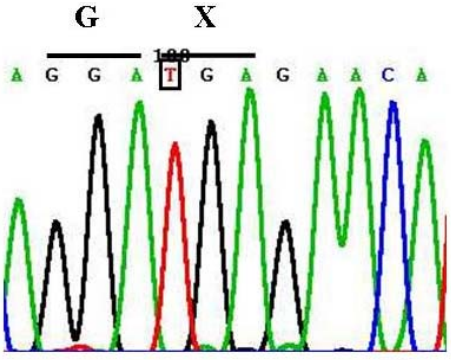

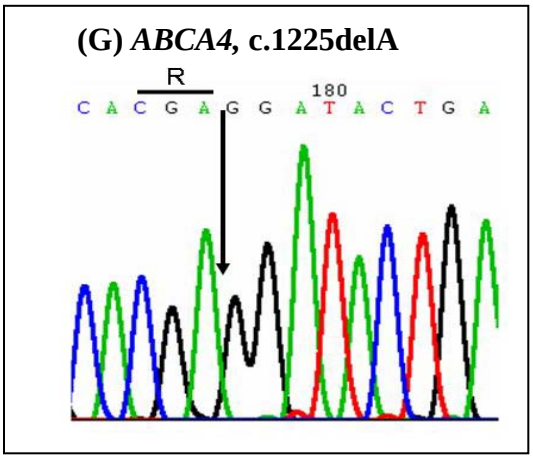

Figure 3.2. Sequence electropherograms showing pathogenic sequence changes in ARRP families. (A) family RP205, (B) family RP170, (C) family RP126, (D) family RP169, (E) family RP213, (F) family RP109, (G) family RP111.

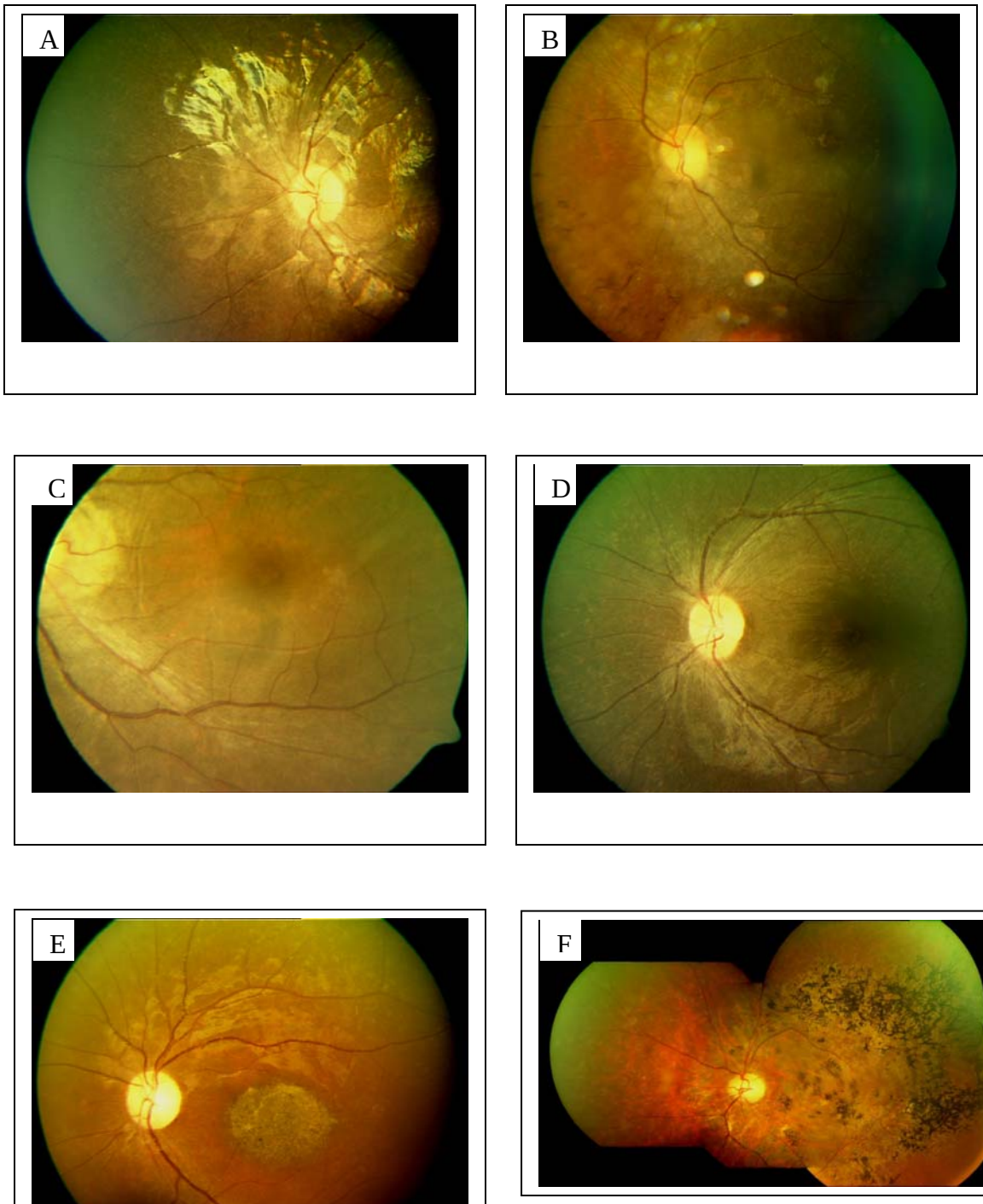
A
B
C
D
E
F

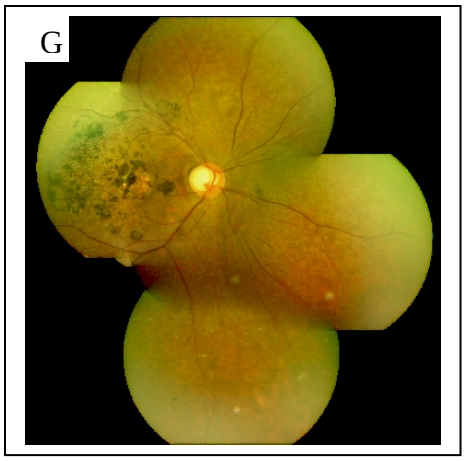

Figure 3.3. Representative fundus pictures of the patients from family RP205 (A), family RP170 (B), family RP126 (C), family RP169 (D), family RP213 (E), family RP109 (F), family RP111 (G).

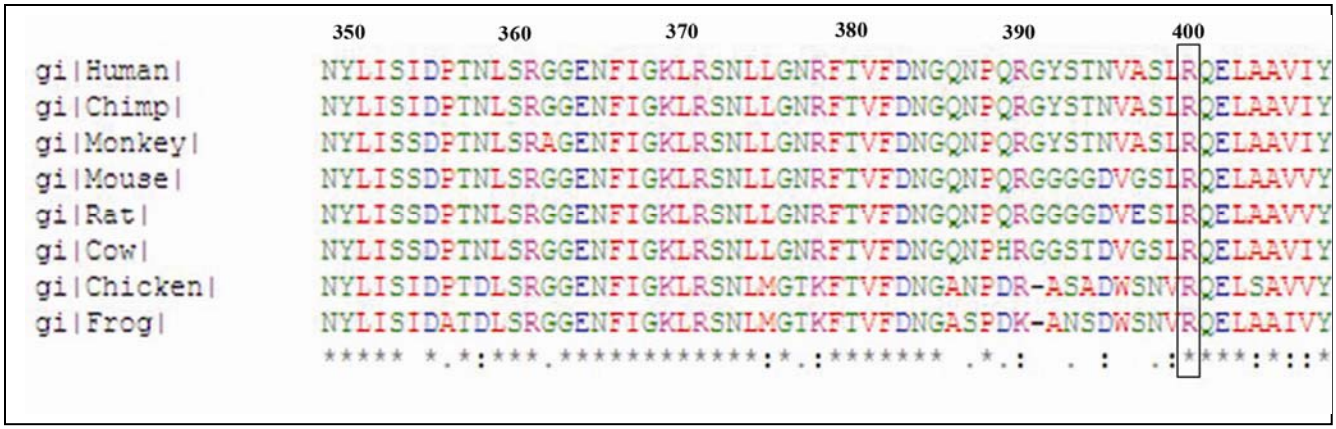

Figure 3.4. Multiple sequence alignment of TULP1 proteins from different species. Arginine residue at position 400, which is the site of mutation, is boxed.

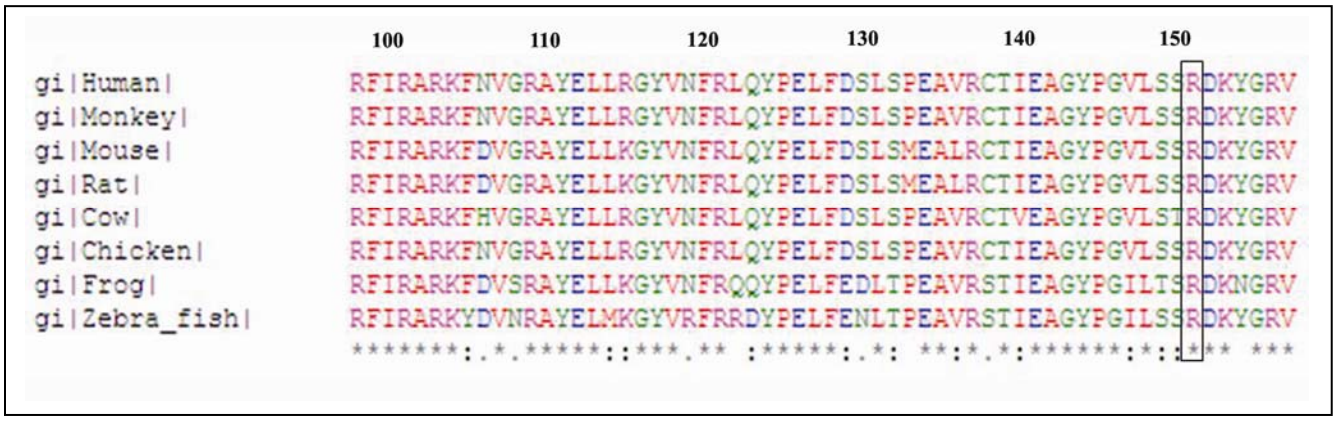

Figure 3.5. Multiple sequence alignment of the RLBP1 protein sequence in different species. Arginine residue undergoing mutation, at position 151 is boxed.

Table 3.16 Putative pathogenic changes found in autosomal recessive RP families.

Family	Gene	Location	Mutation cDNA, protein	Consequence	Reported/ Novel	Restriction site change, if any
RP205	*RPE65*	Exon 10	c.1060delA, p.Asn356fs	Frameshift	Reported*	None
RP170	*RP1*	Exon 4	c.2847delT, p.Asn949fs	Frameshift	Novel	None
RP126	*TULP1*	Exon 12	c.1199G>A, p.Arg400Gln	Missense	Novel	*Eco57I*+
RP169	*RLBP1*	Exon 6	c.451C>T, p.Arg151Trp	Missense	Novel	*Hpy188III* -
RP213	*ABCA4*	Exon 14	c.1995C>A, p.Tyr665X	Nonsense	Novel	None
RP109	*ABCA4*	Exon 44	c.6088C>T, p.Arg2030X	Nonsense	Reported†‡§	*BseGI*+
RP111	*ABCA4*	Exon 9	c.1225delA, p.Arg409fs	Frameshift	Novel	*MnlI*+

Pathogenic sequence changes identified. '+' denotes gain of restriction site, ' –' denotes loss of restriction site. Numbering is with respect to first base of ATG. Sequences referred to above have the following Ensembl transcript IDs: *RPE65*- ENST00000262340, *RP1*- ENST00000220676, *TULP1*- ENST00000229771, *RLBP1*- ENST00000268125, *ABCA4*- ENST00000370225, *PDE6B*- ENST00000255622. * Marlhens *et al*., 1997, † Lewis *et al*., 1999, ‡ Papaioannou *et al*., 2000, § Webster *et al*., 2001.

Table 3.17. Non-pathogenic/changes of uncertain significance identified in the 14 families

Family	Gene	cDNA, Protein	Location	Reported/Novel
RP170	*RP1*	c.2615G>A, p.Arg872Gln	Exon 4	rs444772
RP170	*RP1*	c.5071T>C, p.Ser1691Pro	Exon 4	rs414352
RP170	*RP1*	c.5175A>G, p.Gln1725Gln	Exon 4	rs441800
RP126	*CRB1*	c.849-35T>C	IVS 3	rs58879207
RP126	*CRB1*	c.2715G>A, p.Arg905Arg	Exon 8	Novel #
RP126	*CRB1*	c.1410A>G, p.Leu470Leu	Exon 6	rs3902057
RP126	*TULP1*	c.200C>G, p.Thr67Arg	Exon 4	rs7764472
RP126	*TULP1*	c.499+26C>T	IVS 5	rs58984224
RP126	*TULP1*	c.776T>C, p.Ile259Thr	Exon 8	rs2064317
RP126	*TULP1*	c.783G>C, p.Lys261Asn	Exon 8	rs2064318
RP213	*ABCA4*	c.141A>G, p.Pro47Pro	Exon 2	rs4847281
RP213	*ABCA4*	c.4256T>C, p.Met1419Thr	Exon 29	Novel #
RP213	*ABCA4*	c.4352+54A>G	IVS 29	rs547806
RP213	*ABCA4*	c.4774-16_17delGT	IVS 33	rs55860151
RP213	*ABCA4*	c.6249C>T, p.Ile2083Ile	Exon 45	rs1801359
RP213	*ABCA4*	c.6282+7G>A	IVS 45	rs17110761
RP119	*PDE6B*	c.958G>A, p.Val320Ile	Exon 6	rs10902758
RP119	*PDE6B*	c.1401+31C>A	IVS 10	Novel #
RP119	*PDE6B*	c.*12A>G	3' UTR	rs28675771
RP119	*PDE6B*	c.2130-15G>A	Intron 17	Novel #
RP200	*CNCG1*	c.237-33C>T	IVS 2	rs1972883
RP200	*CNCG1*	c.300-26G>C	IVS 3	rs6819506
RP200	*CNCG1*	c.557+28T>G	IVS 6	rs59800634
RP160	*CRB1*	c.71-12A>T	IVS 1	rs12042179
RP160	*CRB1*	c.1410A>G, p.Leu470Leu	Exon 6	rs3902057
RP160	*RGR*	c.27T>C, p.Thr9Thr	Exon 1	rs2279227
RP160	*RGR*	c.123C>T, p.Phe41Phe	Exon 2	Novel #
RP160	*RGR*	c.474C>T, p.Tyr158Tyr	Exon 4	rs1042454
RP160	*RGR*	c.737C>T, p.Ser246Phe	Exon 6	rs61730895
RP160	*RGR*	c.*65A>G	3'UTR	rs3526
RP184	*RGR*	c.760-38C>T	Intron 6	Novel #
RP102	*RDS*	c.725A>G, p.Glu242Gly	Exon 2	Novel #

This table shows reported non-pathogenic sequence changes as well as novel variants of unknown significance (marked with #). c.DNA numbers are given with A of ATG as +1. The following Ensembl transcript IDs apply: RP1- ENST00000220676, *CRB1*- ENST00000367400, *TULP1*- ENST00000229771, *ABCA4*- ENST00000370225, *PDE6B*- ENST00000255622, *CNCG1*- ENST00000358519, RGR- ENST00000358110, *RDS*- ENST00000230381

Table 3.18 Clinical features of the affected individuals with mutations identified.

Family/Gene mutation	Patient	Age at presentation	Age of onset	Initial symptoms	Fundus features	Visual acuity	ERG		Diagnosis
							Scotopic	**Photopic**	
RP205 ***RPE65***	IV:1	7 years	One year of age	Night blindness	Arterial narrowing; widespread white dots in periphery due to RPE atrophy	20/60 OD; 20/50 OS	Extinguished		Early onset RP
	IV:2	5 years				TAC: 20/63 OU	Not cooperative		
RP170 ***RP1***	II:1	19 years	NA, Childhood	Night blindness, progressively reduced vision	Equatorial RPE degeneration, pale disc, arterial narrowing; vitreous opacities and macular RPE degeneration	20/60 OD; CF 1 meter OS	Not done		RP with macular degeneration
	II:2	17 years	5 years			20/50 OU			
RP126 ***TULP1***	IV:1	22 years	NA, Childhood	Night blindness, progressively reduced vision	Diffuse RPE degeneration, pigment migration, arterial narrowing with prominent macular degeneration; optic disc pallor	20/200 OD; 20/200 OS	Extinguished		Advanced typical RP
	IV:2	19 years		Night blindness, progressively reduced vision; nystagmus		20/400 OD; 20/600 OS			
RP169 ***RLBP1***	IV:3	16 years	NA, childhood	Night blindness, progressively reduced vision	Diffuse RPE degeneration, pigment migration, arterial narrowing with macular sparing	20/50 OU	NA		Typical RP
	IV:5	12 years							
RP213 ***ABCA4***	IV:4	19 years	11 years	Progressive vision loss	Equatorial RPE degeneration, pale disc, arterial narrowing; vitreous opacities and large	20/200 OU	extinguished rods and severely reduced cone ERG		RP with atrophic maculopat

	IV:3	21 years	13 years					
RP109 ***ABCA4***	IV:1	28 years	5 years	Decreased vision	Macular degeneration and peripheral RP-like changes vitreous opacities, minimal disc pallor and pigmentary changes	6/60	Maximal retinal response, grossly reduced but recordable	Extinguished
	IV:5	23 years	5 years		Bronze reflex with RPE atrophy in macular arc, vessels & disc normal,.mild RPE degeneration, patches around arcades	Ambloypia, CF 1meter 20/100	Borderline responses	Borderline responses with recordable ERG, latency not increased
	IV:6	19 years	12 years		Mild disc pallor, macular RPE degenerative changes, peripheral RPE changes also developed after 6 years	20/800 20/200 A*T 15 degree	Borderline amplitude & delayed implicit time	Reduced amplitude with normal implicit time
RP111 ***ABCA4***	V:2	32 years	15 years	decreased vision, need more light	Nystagmus, diffuse RPE degeneration with more in macular area, arterial narrowing, pigmentary changes in macular area.	20/400 OU	Extinguished	
RP111 ***ABCA4***	V:4	24 years	14 years				Extinguished	

Abbreviations used: OU, both eyes; OD, right eye; OS, left eye, TAC, teller acuity card, A*T, alternating, CF, counting fingers. NA, not applicable.

3.3 Discussion

Homozygosity was detected at one or more loci in affected individuals of 10/34 families (in the present study) and 4/10 families earlier in our laboratory (Lalitha *et al*., 2002). Out of a total 14 families in which homozygosity was detected, homozygous pathogenic changes were identified in 7 families. A total of 3 frameshift, 2 missense, and 2 nonsense changes were observed (Table 3.16). In addition to these sequence changes several other known/novel polymorphisms were also detected (Table 3.17).

A homozygous single base deletion c.1060delA found in the *RPE65* gene in family RP205 is expected to result in frameshift at codon 356 (p.Asn356Metfs) with premature truncation at codon 371 (p.Asn356MetfsX16). It has been reported earlier in compound heterozygous form along with Arg234X mutation in a family with a diagnosis of LCA (Marlhens *et al*., 1997). The resultant protein is expected to be severely truncated and lose 33% of its C-terminal sequence, suggesting functional loss. Marlhens *et al*., (1997) reported this mutation in a family with LCA, whereas in the present study this mutation was associated with a diagnosis of early onset RP in family RP205 with typical signs of LCA being absent.

A homozygous single base insertion, c.2847delT in the *RP1* gene, observed in family RP170 is a novel change. c.2847delT is predicted to result in frameshift at codon 949 and lead to premature termination after 32 amino acid residues (p.Asn949LysfsX32). The length of RP protein is 2156 amino acids thereby this frameshift will cause 56% of

the RP1 protein to be lost from the C-terminus. This family had a diagnosis of retinitis pigmentosa with macular degeneration. The phenotype of patients in the present study is comparable with those reported in the Pakistani families, with typical fundus changes including disc pallor and vascular attenuation and an onset of disease in childhood. Similar to this study Khaliq and coworkers (2005) have also noted macular changes, but in the form of macular stippling in affected individuals with *RP1* gene mutations.

The Arg400Gln missense change (c.1199G>A) in the *TULP1* gene, reported for the first time in this study, involves a residue in the highly conserved tubby domain (243 aa to 505 aa) of the TULP1 protein (Boggon *et al*., 1999). All the reported missense mutations have been found in the tubby domain (Hagstrom *et al*., 1955, den Hollander *et al*., 2007b, Kondo *et al*., 2004). A previously described mutation Arg400Trp (Hanein *et al*., 2004) involves the same residue. The Arg400Gln change converts the positively charged side chain to a neutral one. It has been postulated that a positive surface charge has functional significance in the tubby domain, as it is required to interact with DNA and proteins (Boggon *et al*., 1999). The SIFT score of 0.00 adds further support for the pathogenic nature of this change. Multiple sequence alignment showed the conservation of this residue among different species (Figure 3.4). In addition, the Arg400 residue is also conserved in *TUB, TULP1, TULP3*, Drosophila king tubby and *C. elegans* tub-1 (den Hollander *et al*., 2007). This family had a diagnosis of advanced typical RP.

Arg151Trp is a novel change identified in the *RLBP1* gene in family RP169. Maw and coworkers **(**1997**)** reported substitution Arg151Gln in a family with autosomal

recessive RP. They showed that the Arg151Gln substituted RLBP1 protein is non-functional as it lacks the ability to bind 11-*cis* retinal. It is possible that Arg151Trp may behave similarly. Arginine at residue 178 is highly conserved through evolution (Figure 3.5) and the substitution of a positively charged hydrophilic amino acid (Arginine) with a neutral hydrophobic amino acid (tryptophan) would be expected to affect the function of protein. The SIFT score of 0.00 for the Arg151Trp substitution leads to a similar conclusion.

Two of the three mutations (c.1225delA/p.Arg409fs, c.1995C>A/ p.Tyr665X) identified in the *ABCA4* gene are novel. All the 3 identified mutations in the *ABCA4* gene are likely to be associated with a complete absence of ABCA4 activity. The c.1225delA mutation would be expected to result in a severely truncated protein with frameshift at codon 409. The Tyr701X is likely to result in premature truncation of the protein. Known functional domains such as two ATP binding domains and 2nd transmembrane domain are predicted to be lost and the 1st transmembrane domain is expected to be partially formed. The c.6088C>T/Arg2030X change has been reported as a heterozygous or compound heterozygous change in patients with a diagnosis of Stargardt's disease or cone-rod dystrophy (Lewis *et al*., 1999, Papaioannou *et al*., 2000, Webster *et al*., 2001). Arg2030X is predicted to form inactive protein, since the mutation affects the arginine-2030 residue located in the second nucleotide-binding domain of the ABCA4 protein. In addition it as also possible that all the mutations may also lead to instability of the mRNA due to non-sense mediated mRNA decay (Baker *et al*., 2004), due to the formation of premature nonsense codons. All the affected individuals of the 3 families manifested the symptoms

of severe retinal dystrophy in the form of onset of symptoms in the 1st or 2nd decade of life, visual acuities in the range of <20/200 to 20/400 and variably affected ERGs in the 2nd or 3rd decade of life. The genotype and phenotype in these 3 families is in agreement with the proposed model of residual protein activity and severity of phenotype (Rozet *et al.*, 1998, Lewis *et al.*, 1999) wherein severe form of retinal dystrophy is caused by 2 functionally null mutations in the *ABCA4* gene.

The novel homozygous sequence change, c.2130-15G>A observed in the intron 17 of the *PDE6B* gene in RP119 did not appear to predict a change in splicing of the mRNA. Despite this, absence in the control population of 108 unrelated individuals and co-segregation with the disease in the family suggest that this change should be further investigated in an experimental system to completely rule out that it is a pathogenic change.

Two other changes whose impact needs to be investigated further are the intronic variant c.760-38C>T in the *RGR* gene (RP184, Table 3.17) and the missense change Glu242Gly in the *RDS* gene (RP102, Table 3.17). The intronic variant in *RGR* gene was absent in the control population. The SIFT score for the Glu242Gly (*RDS* gene) change of 0.02, as well as the conservative nature of the Glu242 argue for a deleterious effect on the protein. Hence, further studies are required to confirm the nature of these two changes.

In summary we have identified disease causing mutations in 7/44 (16%) autosomal recessive RP families. Intronic changes found in genes *PDE6B* (family RP119) and *RGR* (family RP184) and a missense change found in *RDS* gene (family RP102) may have a role in the pathogenesis, which needs to be further investigated. In 4 families (RP153, RP107, RP200 and RP160) for which homozygosity was detected but no mutations identified, it is possible that the disease-causing mutation is present in the introns or promoter as these regions were not screened for mutations. Second, homozygosity screening identifies homozygosity extending to several centimorgans, and hence it is possible that another gene in the same region is actually the cause of disease in the 4 families. Third, it may also be possible that homozygosity identified in these families is not linked with the disease and there is another locus involved in the pathogenesis of these families. Familes in which no homozygosity was identified could have mutations at other loci than the ones screened in this study. Involvement of any of the 23 loci screened could have been missed in the event that there are mutations present in compound heterozygous form.

Chapter 4

Mapping of the Disease Locus in a Family with ADRP

CHAPTER 4: MAPPING OF THE DISEASE LOCUS IN A FAMILY WITH ADRP

4.1 Introduction

This chapter describes the results of gene mapping in family RP161 with autosomal dominant retinitis pigmentosa. Linkage analysis was aimed at screening pre-existing loci that are linked with autosomal dominant RP, cone dystrophy and cone-rod dystrophy (section 2.24).

Microsatellite markers from the ABI panel (ABI PRISM linkage mapping set, version 2.5-MD10), located in proximity to loci for retinal dystrophy were selected for genotyping. The genes included 14 known genes for ADRP, 5 genes for autosomal dominant cone/cone-rod dystrophy, 2 loci for autosomal dominant cone-rod dystrophy for which gene has not been identified and a gene for Refsum disease (Table 2.3). A total of 28 markers were genotyped in 23 individuals of the family RP161 (shown in Figure 4.1).

4.2 Results

4.2.1 Genotyping and linkage analysis

Microsatellite markers were genotyped as described in Chapter 2, section 2.24. Genotypes were obtained from the allele sizes called by the GeneMapper software. Genotypes were checked for errors and Mendelian inconsistencies both by visual

examination and by using the PedCheck software (O'Connell and Weeks, 1998). Parametric two-point linkage analysis was performed using the SuperLink v 1.6 program from the EasyLinkage package v 5.08 (Lindner and Hoffmann, 2005) with parameters specified in Chapter 2 section 2.24. Genotyping and linkage analysis of 23 individuals of the family (Figure 4.1) for 28 markers gave LOD scores of 2.5 at θ=0.0 for markers D6S262 and D6S308 on chromosome 6q23 (Table 4.1). Seven additional markers in this region were subsequently analyzed. These included D6S434, D6S287, D6S408, D6S270, D6S1009, D6S1649 and D6S1637 (Table 4.2) selected from the NCBI Map Viewer database (http://www.ncbi.nlm.nih.gov/mapview/). A maximum LOD score of 1.7 (θ=0.10) was obtained with marker D6S1637 while the remaining 6 markers gave LOD scores of less than 1 (Table 4.2, Figure 4.3). To confirm whether linkage was significant, 12 additional individuals of this family (shown in Figure 4.1) were genotyped for the 3 markers, D6S262, D6S308 and D6S1637 which had LOD scores of >1.5. Two-point linkage analysis with data from 35 individuals gave a LOD score of 3.2 (θ=0.0) for marker D6S262 confirming linkage with this locus (not shown). LOD scores for the 3 markers mentioned above were re-calculated using allele frequencies determined in the same population (30 normal individuals) and they remained significant (data not shown). Multipoint analysis using 9 markers gave a maximum multipoint LOD score of 1.8 for D6S262 (Figure 4.4), which is suggestive of a disease locus at or near this region.

Clinical features of the affected individuals of family RP161

Affected members of the family RP161 showed the initial symptom of night blindness in their 3rd, 4th or 5th decades. The fundus showed diffuse RPE degeneration, arterial narrowing and pigment migration (Figure 4.2 A, B). The visual fields, tested in individuals III:6, III:9, III:11, III:21 who were affected, were restricted to < 20 degrees and the visual acuity deteriorated with age and varied from 20/20 to PL/PR. 7 members of generation IV (Figure 4.1, symbols with cross) who were in the 1st, 2nd or 3rd decades of life showed mild RPE/pigmentary changes with normal best-corrected visual acuities. Electroretinography and visual field data could not be obtained in these patients and hence their status was not conclusive of RP. Hence their affection status for the purpose of analysis was treated as unknown. This family had a diagnosis of late-onset ADRP.

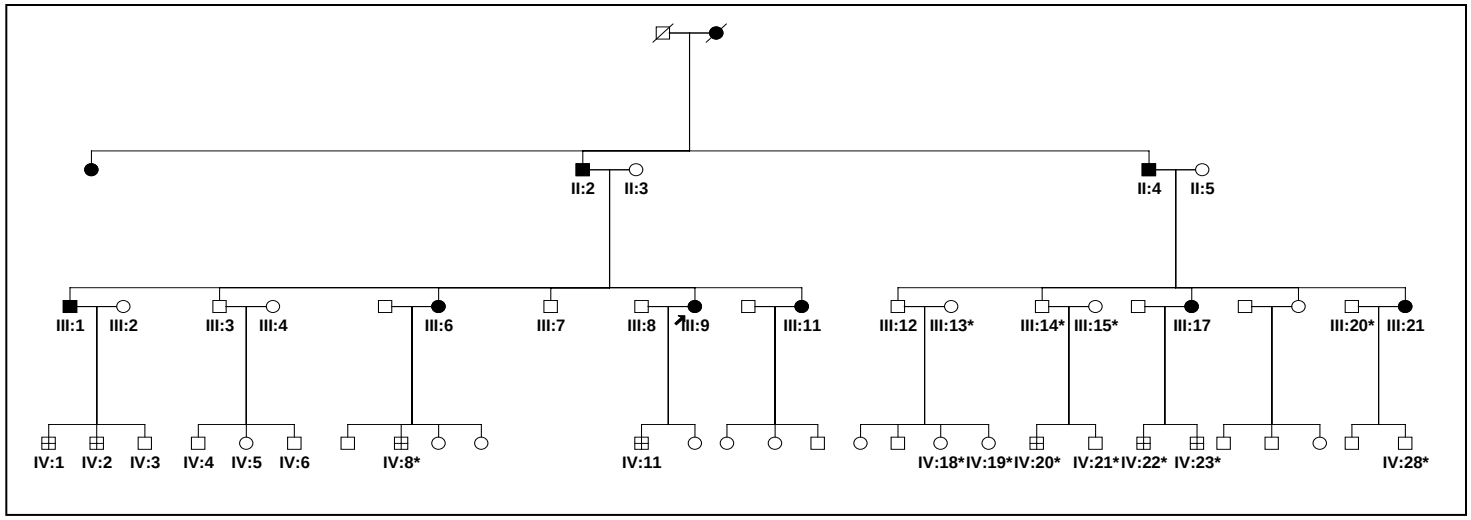

Figure 4.1. Pedigree of family RP161. Individuals analysed in the study are shown with codes below the symbols. Shaded symbols represent affected individuals. Symbols with cross represent individuals with unknown affection status. Individuals marked with asterisk were analysed only for 3 markers (D6S262, D6S308, D6S1637)

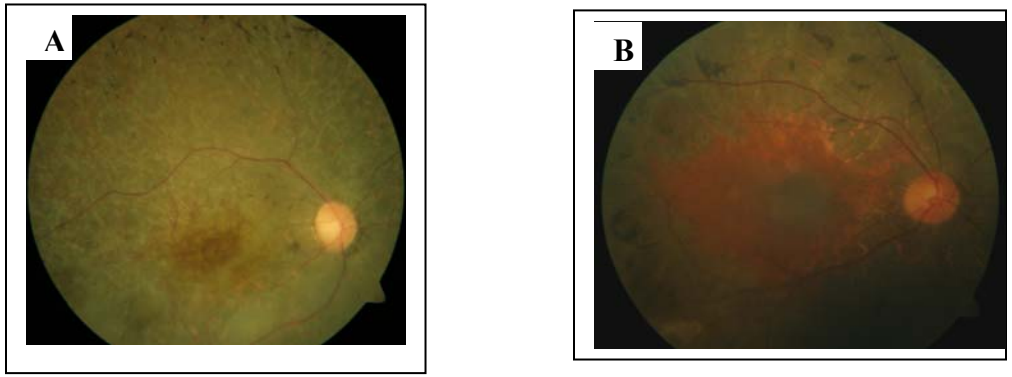

Figure 4.2. Representative fundus pictures of family RP161, showing pigment migration RPE atrophy and arterial narrowing. (A) fundus picture of III:21 (B) fundus picture of III:6.

Table 4.1. Linkage analysis in family RP161

MARKER	Z_{max}	Θ_{max}	LOD score at Θ =									
			0.00	0.05	0.10	0.15	0.20	0.25	0.30	0.35	0.40	0.45
D3S1292	0.1	0.0	0.1	0.1	0.1	0.1	0.0	0.0	0.0	0.0	0.0	0.0
D6S1610	0.1	0.3	-∞	-1.2	-0.5	-0.1	0.0	0.1	0.1	0.1	0.0	0.0
D6S257	0.4	0.2	-∞	-0.2	0.2	0.3	0.4	0.4	0.3	0.2	0.1	0.0
D6S460	0.0	0.5	-∞	-0.9	-0.6	-0.4	-0.3	-0.3	-0.2	-0.1	-0.1	0.0
D6S262	2.5	0.0	2.5	2.3	2.0	1.8	1.5	1.3	1.0	0.7	0.4	0.1
D6S308	2.5	0.0	2.5	2.3	2.0	1.8	1.5	1.3	1.0	0.7	0.4	0.1
D6S1581	0.3	0.3	-∞	-0.3	0.1	0.3	0.3	0.3	0.3	0.2	0.1	0.1
D6S264	0.1	0.3	-∞	-1.3	-0.6	-0.2	0.0	0.1	0.1	0.1	0.1	0.0
D7S517	0.0	0.5	-∞	-0.9	-0.6	-0.4	-0.3	-0.3	-0.2	-0.1	-0.1	0.0
D7S484	0.0	0.5	-∞	-2.7	-1.6	-1.1	-0.7	-0.4	-0.3	-0.1	-0.1	0.0
D7S630	0.0	0.5	-∞	-2.5	-1.5	-0.9	-0.6	-0.3	-0.2	-0.1	0.0	0.0
D7S657	0.0	0.5	-∞	-2.7	-1.7	-1.1	-0.7	-0.5	-0.3	-0.2	-0.1	0.0
D7S486	0.1	0.4	-∞	-1.6	-0.8	-0.5	-0.2	-0.1	0.0	0.0	0.1	0.0
D7S640	0.5	0.0	0.5	0.4	0.4	0.3	0.3	0.2	0.2	0.1	0.1	0.0
D8S285	0.0	0.3	-∞	-1.3	-0.6	-0.2	-0.1	0.0	0.0	0.0	0.0	0.0
D9S285	0.0	0.5	-∞	-2.3	-1.5	-1.0	-0.7	-0.5	-0.3	-0.2	-0.1	-0.1
D9S171	0.1	0.0	0.1	0.1	0.1	0.0	0.0	0.0	0.0	0.0	0.0	0.0
D11S4191	0.5	0.0	0.5	0.4	0.4	0.3	0.3	0.2	0.2	0.1	0.1	0.0
D14S261	0.1	0.4	-∞	-1.3	-0.5	-0.2	0.0	0.0	0.1	0.1	0.1	0.0
D17S938	0.0	0.0	0.0	0.0	0.0	0.0	0.0	0.0	0.0	0.0	0.0	0.0
D17S1852	0.0	0.5	-∞	-2.5	-1.4	-0.9	-0.5	-0.3	-0.1	0.0	0.0	0.0
D17S798	0.0	0.5	-3.7	-0.7	-0.4	-0.3	-0.2	-0.1	-0.1	0.0	0.0	0.0
D17S944	0.0	0.5	-∞	-1.6	-1.0	-0.6	-0.4	-0.3	-0.2	-0.1	0.0	0.0
D17S949	0.1	0.4	-∞	-1.3	-0.6	-0.2	0.0	0.0	0.1	0.1	0.1	0.0
D17S785	0.0	0.4	-∞	-2.3	-1.3	-0.7	-0.4	-0.2	-0.1	0.0	0.0	0.0
D17S784	0.0	0.4	-∞	-1.5	-0.8	-0.4	-0.2	-0.1	0.0	0.0	0.0	0.0
D19S418	0.0	0.5	-∞	-1.9	-1.1	-0.7	-0.4	-0.2	-0.1	0.0	0.0	0.0
D19S210	0.0	0.5	-∞	-3.3	-2.1	-1.5	-1.0	-0.7	-0.5	-0.3	-0.2	-0.1

The table shows two-point LOD scores of 28 markers genotyped in 23 individuals of family RP161. The LOD scores are shown at different values of the recombination fraction (Θ). Z_{max} indicates maximum LOD score, Θ_{max} indicates the value of Θ at which the LOD score is maximum.

Table 4.2. Linkage analysis of markers on chromosome 6q23 in family RP161.

MARKER	deCODE location (cM)	Z_{max}	Θ_{max}	LOD score at Θ =									
				0.00	**0.05**	**0.10**	**0.15**	**0.20**	**0.25**	**0.30**	**0.35**	**0.40**	**0.45**
D6S434	106.2	0.3	0.3	-∞	-0.9	-0.2	0.1	0.3	0.3	0.3	0.2	0.2	0.1
D6S287	119.6	0.1	0.0	0.1	0.1	0.1	0.0	0.0	0.0	0.0	0.0	0.0	0.0
D6S408	125.5	0.1	0.4	-∞	-0.6	-0.3	-0.2	-0.1	0.0	0.0	0.1	0.1	0.0
D6S262 *	130.7	2.5	0.0	2.5	2.3	2.0	1.8	1.5	1.3	1.0	0.7	0.4	0.1
D6S270	134.9	0.3	0.2	-2.8	0.1	0.3	0.3	0.3	0.3	0.2	0.2	0.1	0.1
D6S1009	138.8	0.1	0.2	-3.1	-0.2	0.0	0.1	0.1	0.1	0.1	0.1	0.0	0.0
D6S308 *	144.8	2.5	0.0	2.5	2.3	2.0	1.8	1.5	1.3	1.0	0.7	0.4	0.1
D6S1649	147.9	0.0	0.5	-3.5	-0.5	-0.3	-0.2	-0.1	0.0	0.0	0.0	0.0	0.0
D6S1637	150.6	1.7	0.1	-1.1	1.6	1.7	1.6	1.4	1.2	1.0	0.7	0.4	0.1

The table shows the two-point LOD scores for 9 markers on chromosome 6q23 genotyped in 23 individuals of family RP161. The LOD scores are shown at different values of the recombination fraction (Θ). Z_{max} indicates the maximum LOD score, Θ_{max} indicates the value of Θ at which LOD score is maximum. Asterisk (*) marked markers belong to the set of 28 shortlisted markers initially tested.

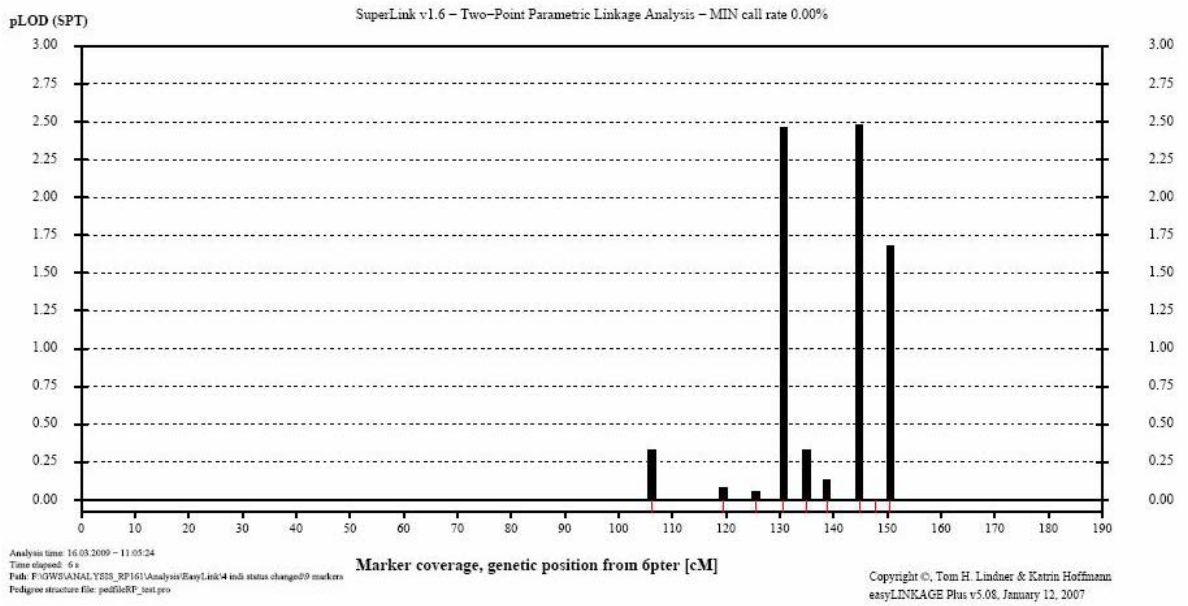

Figure 4.3. Two-point LOD scores with 9 markers. Plotted are the Z_{max} values for the 9 markers. The markers are ordered according to their location from 6pter to 6qter (left to right); D6S434, D6S287, D6S408, D6S262, D6S270, D6S1009, D6S308, D6S1649, D6S1637.

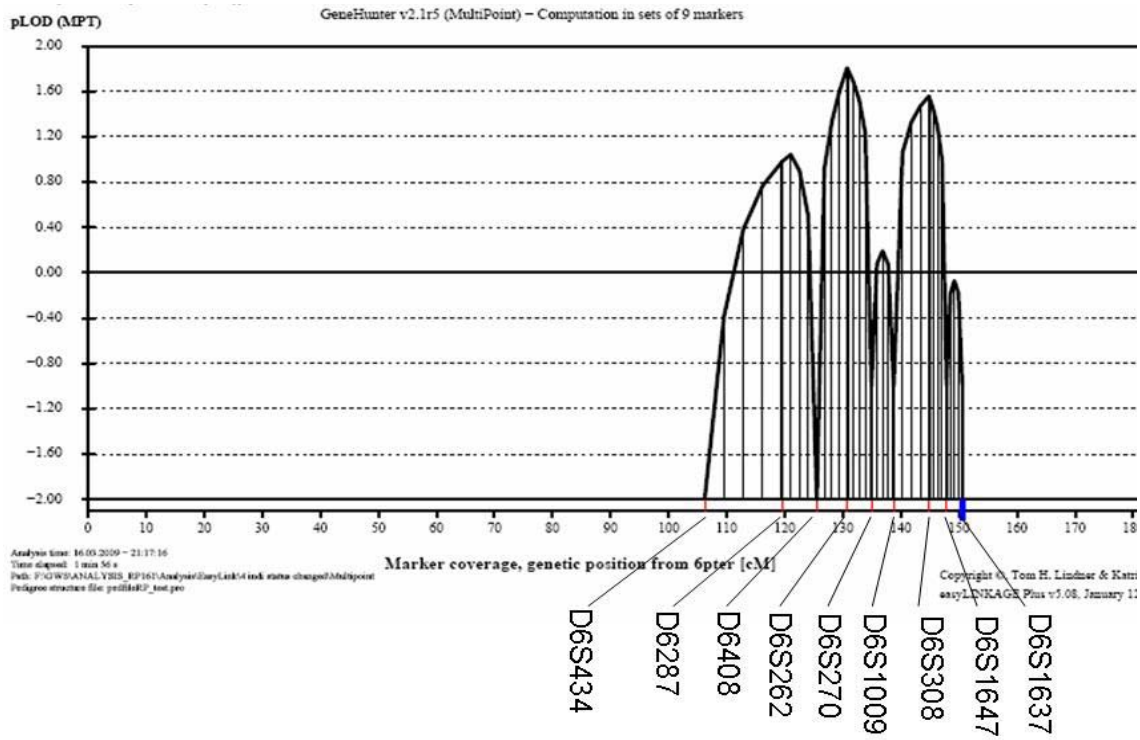

Figure 4.4. Multipoint linkage analysis. Shown above are the parametric LOD score curves (pLOD) for the 9 markers used for multipoint analysis in 23 individuals of family RP161.

4.3. Discussion

Linkage analysis in a family with ADRP (RP161) showed significant linkage of disease to chromosome 6q23 with a two-point LOD score of 3.2 for marker D6S262 located at 131.77 Mb/130.7 cM on 6q23. This was confirmed with multipoint linkage which gave a maximum LOD score of 1.8 for marker D6S262. *AHI1* (Abelson helper integration site 1) and *PEX7* (Peroxisomal biogenesis factor-7) are 2 candidate genes in this region located at a distance of 3.8 Mb and 5.4 Mb respectively from marker D6S272. *AHI1* gene mutations cause Joubert syndrome, which is associated with RP/LCA and other systemic involvement such as hypotonia, ataxia, mental retardation, altered respiratory pattern, abnormal eye movements, and brain malformation (Parisi *et al*., 2006). *PEX7* gene mutations cause Refsum disease, which is characterized by progressive adult retinitis pigmentosa, peripheral neuropathy, anosmia, and cerebellar ataxia (van dan Brink *et al*., 2003). Several other genes in the mapped region that are expressed in the retina/RPE are also candidates for the disease in this family. Examples are (*LAMA2* (Laminin, alpha 2), *TSPYL1* (Testis specific protein, Y-linked, like-1), *ENPP1* (Ectonucleotide pyrophosphatase/phosphodiesterase 1), *MYB* (v-myb myeloblastosis viral oncogene homolog (avian)), *IGNGR1* (interferon gamma receptor 1). Systematic screening of genes in this interval would be required to identify the disease gene. The mapped locus has not been linked with non-syndromic ADRP previously and therefore represents a novel locus for this disorder.

Chapter-5

Candidate Gene Screening

CHAPTER 5: CANDIDATE GENE SCREENING

5.1 Introduction

The majority of the genes associated with non-syndromic retinal dystrophies are expressed exclusively/predominantly in the retina or in the retinal pigment epithelium. This can be explained on the basis that genes which are highly or differentially expressed in the retina have an important role in the functioning of the retina and their mutation would result in retinal disease. A number of studies have identified transcripts that are enriched/differentially expressed in the retina (Bortoluzzi *et al*., 2000, Stohr *et al*., 2000, Blackshaw *et al*., 2001, Sharon *et al*., 2002, Lavorgana *et al*., 2003). The Riken cDNA 3322402L07/C1orf36 is one such transcript which is preferentially/highly expressed in the human and murine retina (Lavorgana *et al*., 2003, Akimoto et al., 2006).

The *CIorf36* gene is located on chromosome 1q32.3. It has 3 exons, which code for a 195-amino acid protein (Lavorgna *et al*., 2003). Screening of the *C1orf36* gene in human patients with retinal dystrophy in this study was carried out in collaboration with Anand Swaroop and co-workers. Parallel work on the rd3 mouse model of retinal degeneration resulted in the identification of the *rd3* gene as the mouse homolog (*3322402L07Rik*) of the human gene c1orf36 (re-named as *rd3* and *RD3* in mouse and human respectively). This gene was selected as a candidate for the *rd3* locus as it was shown to be highly expressed in the retina in previous studies (Lavorgana *et al*., 2003, Akimoto et al., 2006). In mouse retina *C1orf36* is expressed particularly in inner nuclear

layer, outer nuclear layer and ganglion cell layer. A homozygous nonsense mutation was identified in rd3 mice by Swaroop and co-workers. To complement this effort and identify a possible role of the human *RD3* gene in retinal disease, the *C1orf36/RD3* gene was selected for screening of a cohort of patients with RP and LCA.

5.2 Results

5.2.1 Screening of *RD3* gene

103 unrelated patients with ARRP (n=55), ADRP (n=14), sporadic RP (n=31), autosomal recessive LCA (n=2) and sporadic LCA (n=1) were screened for mutations in the *RD3* gene. *RD3* gene has 3 exons, of which first exon is non-coding. The 2 coding exons were screened in the 103 probands by PCR amplification and bi-directional sequencing. Details of primers are given in Appendix-1, Table 2L. Direct sequencing of the coding regions of *RD3* gene resulted in the identification of 5 sequence changes in 103 patients. Sequence changes which co-segregated with the disease phenotype were tested in at least 100 normal controls.

Five sequence changes were identified in 5 unrelated patients. Four changes were heterozygous and one was homozygous (Table 5.1). Heterozygous changes found in the families RP102, RP120, RP121 and RP192 did not co-segregate with the disease phenotype and were not evaluated further. The homozygous change (c.296+1G>A) involved the splice donor site +1 position and co-segregated with the disease in family

RP146 (Figure 5.1 A). This splice site change leads to abolition of restriction site for *Hph1* enzyme. Upon digestion of PCR products from normal and mutation-bearing individuals, the normal allele showed digestion of the 436 bp PCR product into 2 fragments of 387 bp and 49 bp , while the homozygous mutant allele showed an uncut 436-bp product (Figure 5.1 C). 121 control individuals were screened for the c.296+1G>A change by restriction digestion with the enzyme *HphI*. It was found to be absent in the control population.

Table 5.1 Sequence changes identified in *RD3* gene in families with retinal dystrophy.

Family	Diagnosis	Mode of Inheritance	Sequence Change	Consequence	Location	Report
RP102	LCA	AR	c.139C>T p.Arg47Cys	Missense	Exon-2	rs34049451
RP120	RP	AD	c.139C>T p.Arg47Cys	Missense	Exon-2	rs34049451
RP121	RP	AD	c.103G>A p.Gly35Arg	Missense	Exon-2	Novel
RP192	RP	AR	c.202C>T Arg68Trp	Missense	Exon-2	Novel
RP146	LCA	AR	c.296+1G>A	Splice site	Intron-2	Novel

This table describes the sequence changes identified in the *RD3* gene in 5/103 families. Numbering is according to transcript (ENST00000367002) with +1 as the first base of the initiation codon ATG. Abbreviations refer to; autosomal recessive, AR; autosomal dominant, AD; retinitis pigmentosa, RP; Leber's congenital Amaurosis, LCA.

The pedigree of family RP146 is shown in Figure 5.1A. There are 2 affected individuals who presented at LVPEI at the ages of 25 and 28 years. Both the individuals had nystagmus and poor vision since birth at the time of presentation visual acuity in both the affected individuals was restricted to perception of light. Fundus showed atrophy in the macular area with pigment migration, diffuse RPE degeneration. Punctuate lesions were seen in the proband while these lesions were absent in the younger affected sibling. ERG was done in one affected individual (V:9). Both scotopic and phototic responses were found to be extinguished. Fundus photographs of the affected siblings are shown in (Figure 5.1 D, E**)**. Due to the presence of typical features of LCA such as nystagmus and poor vision since birth, this family had a diagnosis of LCA.

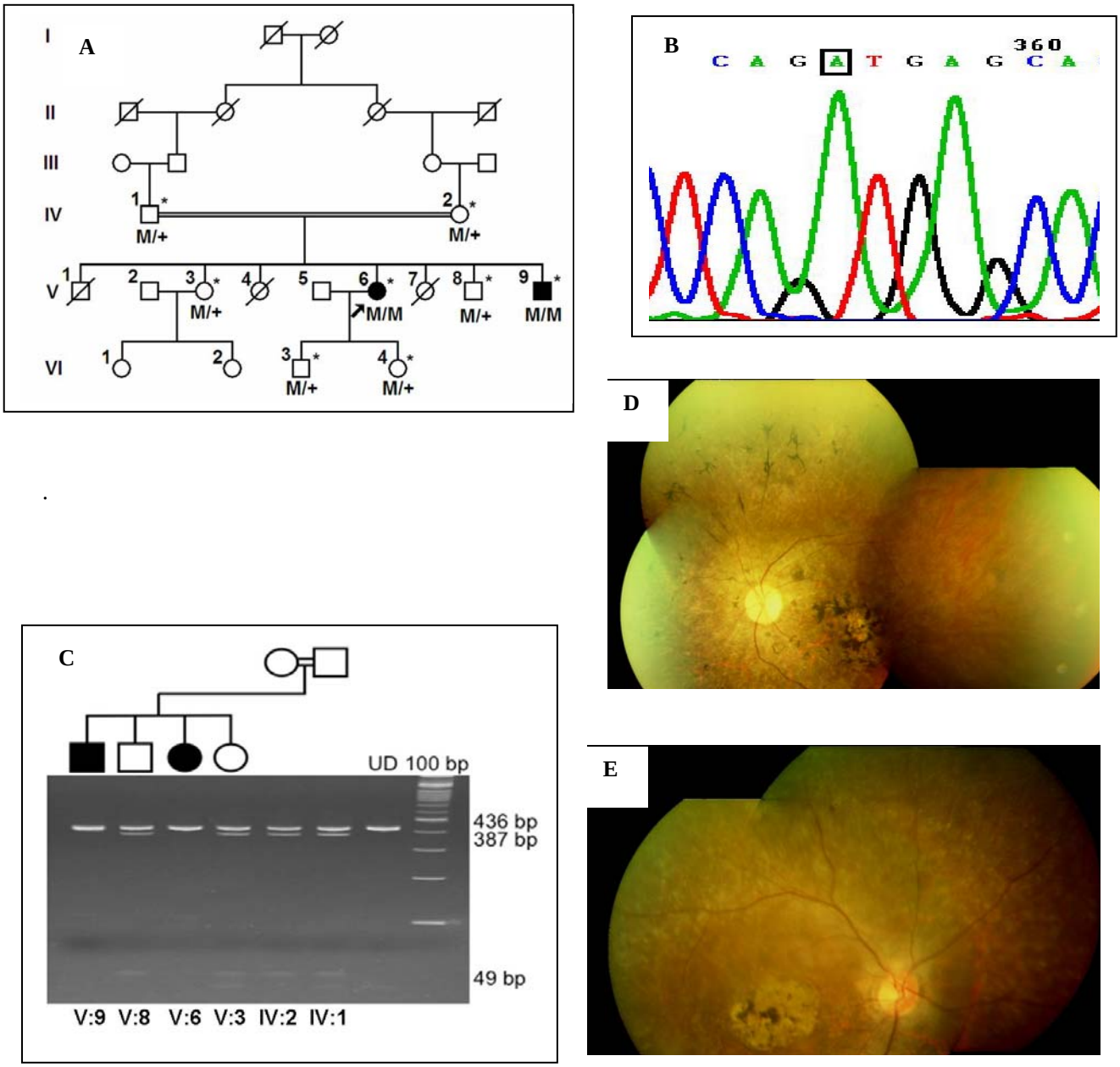

Figure 5.1: Details of family RP146. (A) Pedigree of family RP146. Astrisk (*) marked individuals were analysed for the genetic analysis. M denotes mutant and plus sign (+) denotes the wild-type allele. (B) chromatogram of the change at +1 of the splice donor site (indicated by boxed residue). (C) RFLP picture showing co-segregation of mutation. (D) fundus pictures of individuals V:6 (D) and V:9.(E) showing pigment migration, arterial narrowing, RPE atrophy and macular scar.

5.3 Discussion

This study was the first to identify mutation of the *RD3* gene in retinal dystrophy in humans . The G>A change at the +1 position of the conserved splice donor site is likely to disrupt normal splicing of the mRNA and thereby result in structurally abnormal protein or unstable mRNA or protein resulting in loss of function.

Due to the mutation it is possible that either exon skipping, intron retention or usage of a cryptic splice site may occur. All of these events would be expected to result in premature termination. Among the other changes identified, Arg47Cys sequence change found in families RP102 and RP120 is a reported SNP (rs34049451) while sequence changes found in families RP121 (Gly35Arg) and RP192 (Arg68Trp) are novel sequence changes that have unknown significance.

RD3 involvement in retinal degeneration in mouse and humans suggests the functional importance of the RD3 protein in the retina although its function is not clearly understood as yet. Friedman and coworkers (Friedman *et al*., 2006) have shown that in COS-1 cells, RD3 protein has a varied localization and the RD3 protein co-localizes with two sub-nuclear proteins namely SC35 (nuclear speckle marker) and promyelocytic leukemia gene product (PML body marker). They have speculated that varied localization of the protein is suggestive of its dynamic role in the cellular processes and its co-localization with subnuclear bodies suggest that it may influence the functions carried out by these sub-nuclear bodies.

The *RD3* gene was also screened by our collaborators (Swaroop and coworkers) and no mutation was identified in their cohort of 778 unrelated retinal dystrophy patients from north America, UK and Scandinavia (Friedman *et al*., 2006). An earlier study that screened 300 patients with RP for mutations in *RD3*/c1orf36 also failed to detect mutations (Lavorgana et al., 2003). These data suggest that mutations in *RD3* are a very rare cause of retinal dystrophy.

Chapter-6

Discussion and Conclusions

CHAPTER 6: DISCUSSION AND CONCLUSIONS

Retinal dystrophies are a group of disorders characterized by progressive loss of vision as well as by their clinically and genetically heterogeneous nature. The high degree of genetic heterogeneity in RP makes gene identification and genetic testing challenging. Thus it is important to devise approaches that are practically feasible for application in the clinic and for genetic counseling of patients.

A high frequency of consanguineous marriages in Andhra Pradesh as well as in South India is likely to be associated with a preponderance of recessive form of disease (Bittles *et al*, 1991). Hence one of the objectives of the present study was to identify the disease genes in families with recessive RP. Analysis of a total of 44 families (34 from the present study, 10 from a previous study in our laboratory) with ARRP resulted in the identification of mutations in 7/44 families in 5 different genes. Five mutations are novel and are previously not reported, while all 7 mutations c.1060delA (*RPE65*), c.2847delT (*RP1*), c.1199G>A (*TULP1*), c.451C>T (*RLBP1*), c.1995C>A (*ABCA4*), c.6088C>T (*ABCA4*), c.1225delA (ABCA4) are being reported for the first time from India. Two of these mutations c.1060delA (*RPE65*) and c.6088C>T (*ABCA4*) have been earlier reported in heterozygous/compound heterozygous forms in studies on patients from other regions of the world (Marlhens *et al*., 1997, Lewis *et al*., 1999, Papaioannou *et al*., 2000, Webster *et al*., 2001). The mutations identified in this study belong to different categories such as frameshift (n=3), missense (n=2) and nonsense (n=2). From the present study mutations in the 23 genes tested account for at least ~16% (7/44) of ARRP.

In addition novel variants of unknown significance were also found (Chapter 3, Table 3.17). The role of these variants in the pathogenesis or influencing the disease phenotype is not known at present. Similar homozygosity based screening in patients with ARRP has been done on Japanese patients (Kondo *et al*., 2004). Kondo and coworkers (2004) have analysed only probands for homozygosity while in the present study probands and family members were analysed as a result our success rate to identify mutations in the homozygous regions was more (7/14, 50%) as compared to Kondo and coworkers (3/33, 9%). This higher success rate in our study could be due to reduction in the false positives by analyzing multiple members of the family. We have identified mutations in ~16% of families with ARRP, while Kondo and coworkers have observed mutations in ~5% of their families with ARRP. One possible reason for the higher detection rate in our study could be the due to a higher rate of consanguinity in the families included in the present study (70%, 31/44) as compared to study by Kondo and coworkers who had 20% or 12/59 consanguineous families in their study. Recently SNP chips have been employed in identifying genes for recessive retinal dystrophy through homozygosity mapping (den Hollander *et al*., 2007b, Ramprasad *et al*., 2008). This approach has led to identification of novel genes for retinal dystrophy, such as Lebercilin (den Hollander *et al*., 2007c), Eyes shut *EYS* (Collins *et al*., 2008) and spermatogenesis-associated protein 7 (*SPATA7*; Wang *et al*., 2009).

A second aspect of this study that resulted in a novel finding was the mapping of the disease locus in a family (RP161) with ADRP to chromosome 6q23 (Chapter 4).

There are no known ADRP genes at this region. Since the disease in this family is non-syndromic ADRP and, it is possible that this represents a novel locus for ADRP.

The approach of direct candidate gene screening has resulted in the identification of the novel genes in the retinal dystrophies. Some of the examples are *RDS, ROM1, FSCN2, GUCA1B, CNGA1, PDE6A, SAG, USH2A, MERTK, RPGRIP, LRAT, RGR, SEMA4A*. *RD3* is a gene which is preferentially expressed in the retina and its involvement in the pathogenesis of retinal dystrophies was not known at the time of undertaking this study. Screening of the *RD3* gene (Chapter 5) for mutations in a cohort of patients with ARRP, ADRP, sporadic RP and LCA as part of this study provided evidence for the first time, for involvement of *RD3* in human retinal disease. A homozygous mutation splice site mutation in the *RD3* gene was identified as the cause of LCA as described in Chapter 3. The lack of detection of mutations in this gene in previous studies involving a cohort of cohort of 300 RP patients suggest that mutations in *RD3* are a rare cause of retinal dystrophy (Lavorgana *et al*., 2003).

Specific conclusions of the study:

1. Disease-causing mutations were identified in 7 families with ARRP. 5/7 mutations are reported for the first time.

2. About 16% of ARRP in the population studied is attributed to mutations in the 23 screened genes.

3. Autosomal dominant RP in a family was mapped to chromosome 6q23, which may represent a novel locus for ADRP.

4. Screening of >100 patients with retinal dystrophies resulted in finding of a mutation in the *RD3* gene as the cause of disease in a family with LCA. This is the first report of the involvement of *RD3* gene in the pathogenesis of LCA.

SPECIFIC CONTRIBUTIONS OF THE STUDY

1. Our study has identified novel causes of disease in Indian families with autosomal recessive retinitis pigmentosa. Mutations were detected in *RPE65, RP1, TULP1, RLBP1* and *ABCA4* genes, which support the genetically heterogeneous nature of retinitis pigmentosa in this region. The loci tested contributed to disease in about 16% (7/44) of Indian families with ARRP.

2. This is the first study that has identified the involvement of *RD3* gene in retinal dystrophy in humans.

3. A novel disease locus has been mapped to chromosome 6q23 in a family with ADRP.

LIMITATIONS OF THE STUDY

The screen for ARRP genes in this study was limited to only a subset of loci. Several other loci exist for ARRP. Screening of all genes would eventually be required to know the magnitude of disease due to known loci. A second limitation was that the approach used for screening families with ARRP, which does not enable the discovery of new genes for the disease since candidate loci were selected based on what was known at the time of starting the study. In the approach of homozygosity screening, false positives may arise due to random homozygosity unlinked with the disease, as may have been the case with 7 families in which homozygosity was detected at one or more loci but in which no mutations were detected. In addition, false negatives may arise due to recombination between the markers selected and the disease gene. The probability of this occurring was lowered by taking markers located within 5 cM of the candidate gene in most cases.

Mutation screening of candidate genes was confined to the coding regions as well as flanking intronic regions. In families where no mutations were identified it could be possible that mutations may be present in the deep intronic regions or in the promoter regions both of which were not screened in the present study.

FUTURE SCOPE OF THE STUDY

The approach of homozygosity screening employed in the study may be extended to cover other loci for recessive RP and applied to rapid screening of families. Knowledge of mutations in individual families can be applied in genetic testing and counseling of other family members of the probands. The results of this study have indicated that genome-wide screening approaches would be suitable in most of the families studied. The genome wide screening of these families has scope for the identification of novel genes/loci for ARRP. The results can be applied to genotype-phenotype correlations based on observations made in the families with mutations and the same can be tested in future screening efforts.

References

REFERENCES

Abd El-Aziz MM, Barragan I, O'Driscoll CA *et al. EYS*, encoding an ortholog of Drosophila spacemaker, is mutated in autosomal recessive retinitis pigmentosa. Nat Genet. 2008;40:1285-1287.

Abid A, Ismail M, Mehdi SQ, Khaliq S. Identification of novel mutations in SEMA4A gene associated with retinal degenerative diseases. J Med Genet. 2005;43:378-381.

Acland GM, Ray K, Mellersh CS *et al.* Linkage analysis and comparative mapping of canine progressive rod-cone degeneration (prcd) establishes potential locus homology with retinitis pigmentosa (RP17) in humans. Proc Natl Acad Sci. 1998;95:3048-3053.

Acland GM, Aguirre GD, Ray J, *et al.* Gene therapy restores vision in a canine model of childhood blindness. Nat Genet. 2001;28:92-95.

Aherne A, Kennan A, Kenna PF *et al.* On the molecular pathology of neurodegeneration in IMPDH1-based retinitis pigmentosa. Hum Mol Genet. 2004;13:641-50.

Ahn J, Beharry S, Molday LL, Molday RS. Functional interaction between the two halves of the photoreceptor-specific ATP binding cassette protein ABCR (*ABCA4*). J Biol Chem. 2003;278. 39600-39608.

Aleman TS, Duncan JL, Bieber ML *et al.* Macular pigment and lutein supplementation in retintis pigmentosa and usher syndrome. Invest Ophthalmol Vis Sci. 2001;42:1873-1881.

Akimoto M, Miyatake S, Kogishi J *et al.* Adenovirally expressed basic fibroblast growth factor rescues photoreceptor cells in RCS rats. Invest Ophthalmol Vis Sci. 1999;40:273-9.

Akimoto M, Cheng H, Zhu D *et al.* Targeting of GFP to newborn rods by Nrl promoter and temporal expression profiling of flow-sorted photoreceptors. Proc Natl Acad Sci. 2006;103:3890-3895.

Ali RR, Sarra GM, Stephens C, Alwis MD *et al.* Restoration of photoreceptor ultrastructure and function in retinal degeneration slow mice by gene therapy. Nat Genet. 2000;25:306-310.

Ali M, Ramprasad VL, Soumittra N *et al.* A missense mutation in the nuclear localization signal sequence of CERKL (p.R106S) causes autosomal recessive retinal degeneration. Mol Vis. 2008;14:1960-4.

Allikmets R, Shroyer N F, Singh N *et al.* Mutation of the Stargardt disease gene (ABCR) in age-related macular degeneration. Science. 1997;277:1805-1807.

Allikmets R, Singh N, Sun H *et al.* A photoreceptor cell-specific ATP-binding transporter gene (ABCR) is mutated in recessive Stargardt macular dystrophy. Nat Genet. 1997a;15:236-246.

Allikmets R, Wasserman WW, Hutchinson A, *et al.* Organization of the ABCR gene: analysis of promoter and splice junction sequences. Gene. 1998;215:111-122.

Allsopp TE, Wyatt S, Paterson HF, Davies AM. The proto-oncogene bcl-2 can selectively rescue neurotrophic factor-dependent neurons from apoptosis. Cell. 1993;73:295-307.

Al-Maghtheh M, Vithana E, Tarttelin E *et al.* Evidence for a major retinitis pigmentosa locus on 19q1 3.4 (RP11), and association with a unique bimodal expressivity phenotype. Am J Hum Genet. 1996;59:864-871.

Andrieu-Soler C, Aubert-Poussel A, Doat M *et al.* Intravitreous injection of PLGA microspheres encapsulating GDNF promotes the survival of photoreceptors in the rd1/rd1 mouse. Mol Vis. 2005;11:1002-1111.

Aramant RB, Seiler MJ. Retinal transplantation- advantages of intact fetal sheets. Prog Retin Eye Res. 2002;21:57-73.

Asper Ophthalmics. URL: http://www.asperophthalmics.com/index_testing.htm

Auslender N, Sharon D, Abbasi AH *et al.* A common founder mutation of CERKL underlies autosomal recessive retinal degeneration with early macular involvement among Yemenite Jews. Invest Ophthalmol Vis Sci. 2007;48:5431-8.

Avila-Fernandez A, Riveiro-Alvarez R, Vallespin E *et al.* A missense mutation in the nuclear localization signal sequence of CERKL (p.R106S) causes autosomal recessive retinal degeneration. Mol Vis. 2008;14:1960-1964.

Bahrami H, Mela M, Dagnelie G. Lutein supplementation in retinitis pigmentosa: PC-based vision assessment in a randomized double-masked placebo-controlled clinical trial (NCT00029289). BMC Ophthalmol. 2006;6:23.

Bainbridge JW, Smith AJ, Barker SS *et al.* Effect of gene therapy on visual function in Leber's congenital amaurosis. N Engl J Med. 2008;358:2231-2239.

Baker KE, Parker R . Nonsense-mediated mRNA decay: terminating erroneous gene expression. Curr Opin Cell Biol. 2004;16:293–299.

Banerjee P, Kleyn PW, Knowles JA *et al. TULIP1* mutation in two recessive extended Dominican kindreds with autosomal recessive retinitis pigmentosa. Nat Genet. 1998;18:177-179.

Bareil C, Hamel C, Pallares-Ruiz N, Arnaud B, Demaille J, and Claustres M. Molecular analysis of the rhodopsin gene in southern france: identification of the first duplication responsible for retinitis pigmentosa, c.998999ins4. Ophthalmic Genet. 1999;20:173-182.

Bareil C, Hamel CP, Delague V *et al.* Segregation of a mutation in *CNGB1* encoding the beta-subunit of the rod cGMP-gated channel in a family with autosomal recessive retinitis pigmentosa. Hum Genet. 2001;108:328-334.

Bayes M, Giordano M, Balcells S *et al.* Homozygous tandem duplication within the gene encoding the beta-subunit of rod phosphodiesterase as a cause for autosomal recessive retinitis pigmentosa. Hum Mutat. 1995;5:228-234.

Bennett J, Tanabe T, Sun D *et al.* Photoreceptor cell rescue in retinal degeneration (rd) mice by in vivo gene therapy. Nat Med. 1996;2:649-54.

Bennett J, Zeng Y, Bajwa R *et al.* Adenovirus-mediated delivery of rhodopsin-promoted bcl-2 results in a delay in photoreceptor cell death in the rd/rd mouse. Gene Ther. 1998;5:1156-64.

Bennett J, Maguire AM. Gene therapy for ocular disease. Mol Ther. 2000;1:501-5.

Berson EL, Sandberg MA, Rosner B *et al.* Natural course of retintis pigmentosa over a 3 year interval. Am J Ophthalmol. 1985;99:240-251.

Berson EL, Rosner B, Sandberg MA, Dryja TP. Ocular findings in patients with autosomal dominant retinitis pigmentosa and a rhodopsin gene defect (Pro-23-His). Arch Ophthalmol. 1991a;109:92-101.

Berson EL, Rosner B, Sandberg MA, Weigel-DiFranco C, Dryja TP .Ocular findings in patients with autosomal dominant retinitis pigmentosa and rhodopsin, proline-347-leucine. Am J Ophthalmol. 1991b;111:614-623.

Berson EL, Rosner B, Sandberg MA *et al.* A randomized trial of vitamin A and vitamin E supplementation for retinitis pigentosa. Arch Ophthalmol. 1993;111:761-772.

Bessant DAR, Payne AM, Mitton KP *et al.* A mutation in NRL is associated with autosomal dominant retinitis pigmentosa. Nat Genet. 1999;21:355-356.

Bessant DAR, Payne AM, Plant C *et al.* NRL S50T mutation and the importance of 'founder effects' in inherited retinal dystrophies. Eur J Hum Genet. 2000;8:783-787.

Bi A, Cui J, Ma YP, Olshevskaya E *et al.* Ectopic expression of a microbial-type rhodopsin restores visual responses in mice with photoreceptor degeneration. Neuron. 2006;50:23-33.

Binder DK, Scharfman HE. Brain-derived neurotrophic factor. Growth Factors. 2004;22:123-31.

Birch DG, Peters AY, Locke KL *et al.* Visual function in patients with cone-rod dystrophy associated with mutations in the *ABCA4* gene. Exp Eye Res. 2001;73:877-886.

Bittles AH, Mason WM, Greene J, Rao NA. Reproductive behavior and health in consanguineous marriages. Science. 1991;252:789-94.

Blackshaw S, Fraioli RE, Furukawa T, Cepko CL. Comprehensive analysis of photoreceptor gene expression and the identification of candidate retinal disease genes. Cell. 2001;107:579-589.

Blanks JC. The retina. 2nd ed. (Ed. Ryan SJ ed). Mosby; 1994.

Boggon TJ, Shan WS, Santagata S, Myers SC, Shapiro L. Implication of tubby proteins as transcription factors by structure-based functional analysis. Science. 1999;286:2119-25.

Bok D, Yasumura D, Matthes MT *et al.* Effects of adeno-associated virus-vectored ciliary neurotrophic factor on retinal structure and function in mice with a P216L rds/peripherin mutation. Exp Eye Res. 2002;74:719-35

Bone RA, Landrum JT, Mayne ST *et al.* Macular pigment in donar eyes with and without AMD: A case control study. Invest Opthalmol Vis Sci. 2001;42:235-240.

Bortoluzzi S, d'Alessi F, Danieli GA. A novel resource for the study of genes expressed in the adult human retina. Invest Ophthalmol Vis Sci. 2000;41:3305-3308.

Bowes C, Li T, Danciger M, Baxter LC. Retinal degenerations in the rd mouse is caused by a defect in the beta subunit of rod cGMP-phosphodiesterase. Nature. 1990;347:677-680.

Bowne SJ, Daiger SP, Hims MM *et al.* Mutations in the RP1 gene causing autosomal dominant retinitis pigmentosa. Hum Mol Genet.1999;11:2121-2128.

Bowne SJ, Sullivan LS, Blanton SH *et al.* Mutations in inosine monophosphate dehydrogenase 1 gene (*IMPDH1*) cause the RP10 form of autosomal dominant retinitis pigmentosa. Hum Mol Genet. 2002;11:559-568.

Bowne SJ, Sullivan LS, Mortimer SE *et al.* Spectrum and frequency of mutations in IMPDH1 associated with autosomal dominant retinitis pigmentosa and Leber congenital amaurosis. Invest Ophthalmol Vis Sci. 2006;47:34-42.

Bron AJ, Tripathi RC, Tripathi BJ. The retina. 8th edition. Chapman & Hall. UK. 1997.

Buch PK, MacLaren RE, Durán Y *et al.* In contrast to AAV-mediated Cntf expression, AAV-mediated Gdnf expression enhances gene replacement therapy in rodent models of retinal degeneration. Mol Ther. 2006;14:700-709.

Bundey S, Crews SJ. A study of retinitis pigmentosa in the City of Birmingham. I Prevalence. J Med Genet. 1984;21:417-420

Bunge S, Wedemann H, David D *et al.* Molecular analysis and genetic mapping of the rhodopsin gene in families with autosomal dominant retinitis pigmentosa. Genomics. 1993;17:230-233.

Bunker CH, Berson EL, Bromley WC, Hayes RP, Roderick TH. Prevalence of retinitis pigmentosa in Maine. Am J Ophthalmol. 1984;97:357-65.

Burns ME, Arshavsky VY. Beyond counting photons: trials and trends in vertebrate visual transduction. Neuron. 2005, 48:387-401.

Burstedt MS, Sandgren O, Holmgren G, Forsman-Semb K. Bothnia dystrophy caused by mutations in the cellular retinaldehyde-binding protein gene (*RLBP1*) on chromosome 15q26. Invest Ophthalmol Vis Sci. 1999;40:995-1000.

Burstedt MS, Forsman-Semb K, Golovleva I *et al.* Ocular phenotype of bothnia dystrophy, an autosomal recessive retinitis pigmentosa associated with an R234W mutation in the *RLBP1* gene. Arch Ophthalmol. 2001;119:260-7.

Byrnes AP, Rusby JE, Wood MJ, Charlton HM. Adenovirus gene transfer causes inflammation in the brain. Neuroscience. 1995;66:1015-24.

Calvert PD, Klenchin VA, Bownds MD. Rhodopsin kinase inhibition by recoverin. J Biol Chem. 1995, 270:24127:24129.

Camenisch TD, Koller BH, Earp HS, Matsushima GK. A novel receptor tyrosine kinase, Mer, inhibits TNF-a production and lipopolysaccharide-induced endotoxic shock1. J Immunol. 1999;162:3498-3503.

Campochiaro PA, Chang M, Ohsato M, *et al.* Retinal degeneration in transgenic mice with photoreceptor-specific expression of a dominant-negative fibroblast growth factor receptor. J Neurosci. 1996;16:1679–1688.

Carlson A, Bok D. Promotion of the release of 11-cis-retinal from cultured retinal pigment epithelium by interphotoreceptor retinoid-binding protein. Biochemistry. 1992;31:9056-9062.

Carmody RJ, McGowan AJ, Cotter TG. Reactive oxygen species as mediators of photoreceptor apoptosis in vitro. Exp Cell Res. 1999;248:520-30.

Carter-Dawson, LaVail MM, Sidman RL. Differential effect of rd mutation on rods and cones in the mouse retina. Invest Ophthalmol Vis Sci. 1978;17:489-498.

Cayouette M, Gravel C. Adenovirus-mediated gene transfer of ciliary neurotrophic factor can prevent photoreceptor degeneration in the retinal degeneration (rd) mouse. Hum Gen Ther. 1997;8:423-430.

Cayouette M, Behn D, Sendtner M, Lachapelle P, Gravel C. Intraocular gene transfer of ciliary neurotrophic factor prevents death and increases responsiveness of rod photoreceptors in the retinal degeneration slow mouse. J Neurosci. 1998;18:9282-9293.

Chacko DM, Rogers JA, Turner JE, Ahmad I. Survival and differentiation of cultured retinal progenitors transplanted in the subretinal space of the rat. Biochem Biophys Res Commun. 2000;268:842-846.

Chakarova CF, Hims MM, Bolz H *et al.* Mutations in the HPRP3, a third member of the pre-mRNA splicing factor genes, implicated in autosomal dominant retinitis pigmentosa. Hum Mol Genet. 2002;11:87-92.

Chakarova CF, Papaioannou MG, Khanna H *et al.* Mutations in TOPORS cause autosomal dominant retinitis pigmentosa with perivascular retinal pigment epithelium atrophy. Am J Hum Genet. 2007;81:1098-1103.

Chang B, Heckenlively, Hawes NL, Roderick. New mouse primary retinal degeneration (rd-3). Genomics. 1993;16:45-49.

Chen J, Makino CL, Peachey NS, Baylor DA, Simon MI. Mechanisms of rhodopsin inactivation in vivo as revealed by a COOH-terminal truncation mutant. Science. 1995;267:374-377.

Chen J, Simon MI, Matthes MT, Yasumura D, LaVail MM. Increased susceptibility to light damage in an arrestin knockout mousemodel of Oguchi disease (stationary night blindness). Invest Ophthalmol Vis Sci. 1999;40:2978-2982.

Chen J, Rattner A, Nathans J. The rod photoreceptor-specific nuclear receptor Nr2e3 represses transcription of multiple cone-specific genes. J Neurosci. 2005;25:118-129.

Chen P, Hao W, Rife L *et al.* A photic visual cycle of rhodopsin regeneration is dependent on Rgr. Nat Genet. 2001;28: 256-260.

Cheng H, Khanna H, Oh ECT *et al.* Photoreceptor-specific nuclear receptor NR2E3 functions as a transcriptional activator in rod photoreceptors. Hum Mol Genet. 2004;13:1563-1575.

Chong NH, Alexander RA, Waters L. Repeated injectons of a ciliary neurotrophic factor analogue leading to long term photoreceptor survival in heriditary retinal degeneration. Invest Ophthalmol Vis Sci. 1999;40;1298-1305.

Chow AY, Chow VY, Kirk BS *et al.* The artificial silicon retina microchip for the treatment of vision loss from retinitis pigmentosa. Arch Ophthalmol. 2004;122:460-469.

Clarke G, Goldberg AF, Vidgen D *et al.* Rom-1 is required for rod photoreceptor viability and the regulation of disk morphogenesis. Nat Genet. 2000;25:67-73.

Clinical trials. URL: http://clinicaltrials.gov/ct2/results?term=*RPE65*

Collin RW, Littink KW, Klevering BJ *et al.* Identification of a 2 Mb human ortholog of Drosophila eyes shut/spacemaker that is mutated in patients with retinitis pigmentosa. Am J Hum Genet. 2008;83:594-603.

Connolly SE, Hjelmeland LM, LaVail MM. Immunohistochemical localization of basic fibroblast growth factor in mature and developing retinas of normal and RCS rats. Curr Eye Res. 1992;11:1005–1017.

Coppieters F, Leroy BP, Beysen D *et al.* Recurrent mutation in the first zinc finger of the orphan nuclear receptor NR2E3 causes autosomal dominant retinitis pigmentosa. Am J Hum Genet. 2007;81:147-157.

Cremers FPM, Van de Pol DJR, Van Driel M *et al.* Autosomal recessive retinitis pigmentosa and cone-rod dystrophy caused by splice site mutations in the Stargardt's disease gene ABCR. Hum Mol Genet. 1998;7:355-362.

Crimi M, Galbiati S, Perini MP *et al.* A mitochondrial tRNA(His) gene mutation causing pigmentary retinopathy and neurosensorial deafness. Neurology. 2003;60:1200-3.

Dagnelie G, Zorge IS, McDonald TM. Lutein improves visual function in some patients with retinal degeneration: a pilot study via the internet. Optometry. 2000;71:147-164.

Dandona L, Dandona R, Srinivas M, *et al.* Blindness in the Indian state of Andhra Pradesh. Invest ophthalmol Vis Sci. 2001;42:908-916.

Das TP, delCerro M, Jalali S *et al.* The Transplantation of Human Fetal Neuroretinal Cells in Advanced Retinitis Pigmentosa Patients: Results of a Long-Term Safety Study. Exp Neurol. 1999;157:58-68.

D'Cruz PM, Yasumura D, Weir J *et al.* Early onset photoreceptor abnormalities induced by targeted disruption of the interphotoreceptor retinoid-binding protein gene. Hum Mol Genet. 2000;9:645-651.

De Celis JF, Barrio R, Del Arco A, Garcia-Bellido A. Genetic and molecular characterization of a Notch mutation in its Delta- and Serrate-binding domain in Drosophila. Proc Natl Acad Sci. 1993;90:4037-4041.

De La Paz MA, Guy VK, Abou-Donia S *et al.* Analysis of the Stargardt disease gene (ABCR) in age-related macular degeneration. Ophthalmology. 1999;106:1531-1536.

Del Cerro M, Humayun MS, Sadda SR *et al.* Histologic correlation of human neural retinal transplantation. Invest Ophthalmol Vis Sci. 2000;41:3142–3148.

den Hollander AI, ten Brink JB, de Kok YJ *et al.* Mutations in a human homologue of Drosophila crumbs cause retinitis pigmentosa (RP12). Nat Genet. 1999,23:217-221.

den Hollander AI, Heckenlively JR, van den Born I *et al.* Leber congenital amaurosis and retinitis pigmentosa with coats-like exudative vasculopathy are associated with mutations in the crumbs homologue 1 (*CRB1*) gene. Am J Hum Genet. 2001;69:198-203.

den Hollander AI, Koenekoop RK Yzer S *et al.* Mutations in the *CEP290* (NPHP6) gene are a frequent cause of Leber congenital amaurosis. Am J Hum Genet. 2006.79:556-561.

den Hollander AI, Koenekoop RK, Mohamed MD *et al.* Mutations in LCA5, encoding the ciliary protein lebercilin, cause Leber congenital amaurosis. Nat Genet. 2007a;39:889-895.

den Hollander AI, van Lith-Verhoeven JJ, Arends ML, Strom TM, Cremers FP, Hoyng CB. Novel compound heterozygous TULP1 mutations in a family with severe early-onset retinitis pigmentosa. Arch Ophthalmol. 2007b;125:932-935.

den Hollander AI, Lopez I, Yzer S *et al.* Identification of novel mutations in patients with Leber congenital amaurosis and juvenile RP by genome-wide homozygosity mapping with SNP microarrays. Invest Ophthalmol Vis Sci. 2007c;48:5690-5698.

Dizhoor AM, Lowe DG, Olshevskaya EV, Laura RP, Hurley JB. The human photoreceptor membrane guanylyl cyclase, RetGC, is present in outer segments and is regulated by calcium and a soluble activator. Neuron. 1994;12:1345-52.

Dhallan RS, Macke JP, Eddy RL *et al.* Human rod photoreceptor cGMP-gated channel: amino acid sequence, gene structure, and functional expression. J Neurosci. 1992;2:3248-56.

Dowling JE, Sidman RL. Inherited retinal dystrophy in the rat. J Cell Biol. 1962;14:73-109.

Driscoll C, Connor J, Brien CJ, Cotter TG. Basic fibroblast growth factor-induced protection from light damage in the mouse retina in vivo. J Neurochem. 2007;105:524-536.

Dryja TP, McGee TL, Reichel E *et al.* A point mutation of the rhodopsin gene in one form of retinitis pigmentosa. Nature. 1990;343:364-366.

Dryja TP, Hahn LB, McGee TL, Cowley GS, Berson EL. Mutation spectrum of the rhodopsin gene in patients with autosomal dominant retinitis pigmentosa. Proc Natl Acad Sci. 1991;88:9370-9374.

Dryja TP, Adams SM, Grimsby JL *et al.* Null *RPGRIP1* alleles in patients with Leber congenital amaurosis. Am J Hum Genet. 2001;68:1295-1298.

Dryja TP, Berson EL, Rao V, Oprian DD. Heterozygous missense mutation in the rhodopsin gene as the cause of congenital stationary night blindness. Nat Genet. 1993;4:280-283.

Dryja TP, Finn JT, Peng YW, *et al.* Mutations in the gene encoding the alpha subunit of the rod cGMP-gated channel in autosomal recessive retinitis pigmentosa. Proc Nat Acad Sci. 1995;92:10177-10181.

Dryja TP, Rucinski DE, Chen SH, Berson EL. Frequency of mutations in the gene encoding the alpha subunit of rod cGMP-phosphodiesterase in autosomal recessive retinitis pigmentosa. Invest Ophthalmol Vis Sci. 1999;40:1859-1865.

Ducroq D, Rozet JM, Gerber S *et al.* The *ABCA4* gene in autosomal recessive cone rod dystrophies. Am J Hum Genet. 2002;71:1480-1482.

Eckenstein FP. Fibroblast growth factors in the nervous system. J Neurobiol. 1994;25:1467–1480.

Ehara H, Nakano C, Ohno K, Goto YI, Takeshita K. New autosomal-recessive syndrome of Leber congenital amaurosis, short stature, growth hormone insufficiency, mental retardation, hepatic dysfunction, and metabolic acidosis. Am J Med Genet. 1997;71:258-66.

Eichers ER, Green J S, Stockton D W *et al.* Newfoundland rod-cone dystrophy, an early-onset retinal dystrophy, is caused by splice-junction mutations in *RLBP1*. Am J Hum Genet. 2002;70:955-964.

Eudy JD, Weston MD, Yao S *et al.* Mutation of a gene encoding a protein with extracellular matrix motifs in Usher Syndrome type IIa. Science. 1998; 280:1753-1758.

Evans K, al-Maghtheh M, Fitzke FW *et al.* Bimodal expressivity in dominant retinitis pigmentosa genetically linked to chromosome 19q. Br J Ophthalmol. 1995;79:841-6.

Fain GL, Lisman JE. Light, Ca2+, and photoreceptor death: new evidence for the equivalent-light hypothesis from arrestin knockout mice. Invest Ophthalmol Vis Sci. 1999;40:2770-2772.

Faktorovich EG, Steinberg RH, Yasumura D *et al.* Photoreceptor degeneration in inherited retinal dystrophy delayed by basic fibroblast growth factor. Nature. 1990;347:83-86.

Farber DB, Lolley RN. Cyclic guanosine monophosphate: elevation in degenerating photoreceptor cells of the C3H mouse retina. Science. 1974;186:449-451.

Farrar GJ, Kenna PF, Humphries P. On the genetics of retinitis pigmentosa and on mutation-independent approaches to therapeutic intervention. EMBO J. 2002;21:857-864.

Fingert JH, Oh K, Chung M *et al.* Association of a novel mutation in the retinol dehydrogenase 12 (RDH12) gene with autosomal dominant retinitis pigmentosa. Arch Ophthalmol. 2008;126:1301-1307

Fishman GA, Stone EM, Sheffield VC *et al.* Ocular findings associated with rhodopsin gene codon 17 and codon 182 transition mutations in dominant retinitis pigmentosa. Arch Ophthalmol. 1992;110:54-62.

Fishman GA, Stone EM, Eliason DA *et al. ABCA4* gene sequence variations in patients with autosomal recessive cone rod dystrophy patients. Arch Ophthalmol. 2003;121:851-855.

Fishman GA, Roberts MF, Derlacki DJ *et al.* Novel mutations in the cellular retinaldehyde-binding protein gene (*RLBP1*) associated with retinitis punctata albescens: evidence of interfamilial genetic heterogeneity and fundus changes in heterozygotes. Arch Ophthalmol. 2004;122:70-75.

Forrester JV, Dick AD, McMenamin PG. The Eye. Elsevier Health Sciences;2001.

Frasson M, Picaud S, Leveillard T *et al.* Glial cell line derived neurotrophic factor induces histologic and functional protection of rod photoreceptors in rd/d mouse. Invest Ophthalmol Vis Sci. 1999;40:2724-2734.

Freund CL, Wang QL, Chen S *et al.* De novo mutations in the CRX homeobox gene associated with Leber congenital amaurosis. Nat Genet. 1998;18:311-312.

Friedman JS, Chang B, Kannabiran C *et al.* Premature truncation of a novel protein, RD3, exhibiting subnuclear localization is associated with retinal degeneration. Am J Hum Genet. 2006;79:1059-1070.

Fuchs S, Nakazawa M, Maw M *et al.* A homozygous 1-base pair deletion in the arrestin gene is a frequent cause of Oguchi disease in Japanese. Nat Genet. 1995;10:360-362.

Fukui T, Yamamoto S, Nakano K, *et al. ABCA4* gene mutations in Japanese patients with Stargardt disease and retinitis pigmentosa. Invest Ophthalmol Vis Sci. 2002;43:2819-24.

Furukawa T, Morrow EM, Cepko CL. Crx, a novel otx-like homeobox gene, shows photoreceptor-specific expression and regulates photoreceptor differentiation. Cell. 1997;91:531-541.

Furukawa T, Morrow EM, Li T, Davis FC, Cepko CL. Retinopathy and attenuated circadian entrainment in Crx-deficient mice. Nat Genet. 1999;23:466-470.

Gal A, Orth U, Baehr W, Schwinger E, Rosenberg T. Heterozygous missense mutation in the rod cGMP phosphodiesterase beta-subunit gene in autosomal dominant stationary night blindness. Nat Genet. 1994;7:64-68.

Gal A, Xu S, Piczenik Y *et al.* Gene for autosomal dominant congenital stationary night blindness maps to the same region as the gene for the beta-subunit of the rod photoreceptor cGMP phosphodiesterase (PDEB) in chromosome 4p16.3. Hum Mol Genet. 1994;3:323-325.

Gal A, Apfelstedt-Sylla E, Janecke AR, Zrennert E. Rhodopsin mutations in inherited retinal dystrophies and dysfunctions. Prog Retin Eye Res. 1997;16:51-79.

Gal A, Li Y, Thompson DA *et al.* Mutations in *MERTK*, the human orthologue of the RCS rat retinal dystrophy gene, cause retinitis pigmentosa. Nat Genet. 2000;26:270-271.

Gao X. and Huang L. Cationic liposome-mediated gene transfer. Gene Ther. 1995;2:710–722.

Gehring WJ, Ikeo K. Pax 6: mastering eye morphogenesis and eye evolution. Trends Genet. 1999;15:371-7.

Gerber S, Rozet JM, Takezawa SI *et al.* The photoreceptor cell-specific nuclear receptor gene (*PNR*) accounts for retinitis pigmentosa in the Crypto-Jews from Portugal (Marranos), survivors from the Spanish Inquisition. Hum Genet. 2000;107:276-284.

Gerber S, Perrault I, Hanein S *et al.* RPGR-interacting protein (*RPGRIP*) gene allows the identification of mutations underlying Leber congenital amaurosis. Eup J Hum Genet. 2001;9:561-571.

Gleeson JG, Lin PT, Flanagan LA, Walsh CA. Doublecortin is a microtubule-associated protein and is expressed widely by migrating neurons. Neuron. 1999;23:257-271.

Gorczyca WA, Polans AS, Surgucheva IG *et al.* Guanylyl cyclase activating protein. A calcium-sensitive regulator of phototransduction. J Biol Chem. 1995;270:22029-36.

Goula D, Benoist C, Mantero S *et al.* Polyethylenimine-based intravenous delivery of transgenes to mouse lung. Gene Ther 1998; 5:1291–1295.

Graham DK, Dawson TL, Mullaney DL *et al.* Cloning and mRNA expression analysis of a novel human protooncogene, c-mer. Cell Growth Differ. 1994;5:647-657.

Graf C, Niwa S, Müller M, Kinzel B, Bornancin F. Wild-type levels of ceramide and ceramide-1-phosphate in the retina of ceramide kinase-like-deficient mice. Biochem Biophys Res Commun. 2008;373:159-63.

Gränse L, Abrahamson M, Ponjavic V, Andréasson S. Electrophysiological findings in two young patients with Bothnia dystrophy and a mutation in the *RLBP1* gene. Ophthal Genet. 2001;22:97-105.

Gu SM, Thompson DA, Srikumari CRS *et al.* Mutations in *RPE65* cause autosomal recessive childhood-onset severe retinal dystrophy. Nat Genet. 1997;17:194-197.

Gu S, Lennon A, Li Y *et al.* Tubby-like protein-1 mutations in autosomal recessive retinitis pigmentosa. Lancet. 1998;351:1103-1104.

Hagstrom SA, North MA, Nishina PM *et al.* Recessive mutations in the gene encoding the tubby-like protein TULIP1 in patients with Retinitis Pigmentosa. Nat Genet. 1998;18:174-176.

Hagstorm SA, Duyao M, North MA, Li T. Retinal Degeneration in *TULP1*$^{-/-}$ Mice: Vesicular Accumulation in the Interphotoreceptor Matrix. Invest Ophthalmol Vis Sci. 1999;40:2795-2802.

Hagstrom SA, Adamian M, Scimeca M, Pawlyk BS, Yue G, Li T. A role for the Tubby-like protein 1 in rhodopsin transport. Invest Ophthalmol Vis Sci. 2001;42:1955-1962.

Haim M, Holm NV, Rosenberg T. Prevalence of retinitis pigmentosa and allied disorders in Denmark. I Main results. Acta Ophthalmol (Copenh). 1992;70:178-86.

Hanein S, Perrault, Gerber S *et al.* Leber congenital amaurosis: Comprehensive survey of the genetic heterogeneity, refinement of the clinical definition, and genotype phenotype correlation as a strategy for molecular diagnosis. Hum Mut. 2004;23:306-317.

Hartong DT, Dange M, McGee TL *et al.* Insights from retinitis pigmentosa into the roles of isocitrate dehydrogenases in the Krebs cycle. Nat Genet. 2008;40:1230-1234.

Heckenlively JR. Preserved para-arteriole retinal pigment epithelium (PPRPE) in retinitis pigmentosa. Br J Ophthalmol. 1982;66:26-30.

Henderson RH, Waseem N, Searle R *et al.* An assessment of the apex microarray technology in genotyping patients with Leber congenital amaurosis and early-onset severe retinal dystrophy. Invest Ophthalmol Vis Sci. 2007;48:5684-5689.

Hojo M, Abe T, Sugano E *et al.* Photoreceptor protection by iris pigment epithelial transplantation transduced with AAV-mediated brain-derived neurotrophic factor gene. Invest Ophthalmol Vis Sci. 2004;45:3721-3726.

Hong DH, Pawlyk B, Sokolov M *et al.* RPGR isoforms in photoreceptor connecting cilia and the transitional zone of motile cilia. Invest Ophthalmol Vis Sci. 2003;44:2413-421.

Hope CI, Bundey S, Proops D, Fielder AR. Usher syndrome in the city of Birmingham--prevalence and clinical classification. Br J Ophthalmol. 1997;81:46-53.

Hauswirth W, Aleman TS, Kaushal S *et al.* Phase I Trial of Leber Congenital Amaurosis due to RPE65 Mutations by Ocular Subretinal Injection of Adeno-Associated Virus Gene Vector: Short-Term Results. Hum Gene Ther. 2008;19:979-990.

Heller L, Jaroszeski MJ, Coppola D *et al.* Electrically mediated plasmid DNA delivery to hepatocellular carcinomas in vivo. Gene Ther. 2000;7:826-9

Huang SH, Pittler SJ, Huang X *et al.* Autosomal recessive retinitis pigmentosa caused by mutations in the alpha subunit of rod cGMP phosphodiesterase. Nat Genet. 1995;11:468-471.

Humayun MS, Weiland JD, Fuji GY *et al.* Visual perception in a blind subject with a chronic microelectronic retinal prosthesis. Vis Res. 2003;43:2573-2581.

Humphries MM, Rancourt D, Farrar GJ *et al.* Retinopathy induced in mice by targeted disruption of the rhodopsin gene. Nat Genet. 1997;15:216-219.

Ikeda S, Shiva N, Ikeda A *et al.* Retinal degeneration but not obesity is observed in null mutants of the tubby-like protein 1 gene. Hum Mol Genet. 2000;9:155-163.

Inglehearn CF, Keen TJ, Bashir R, *et al.* A completed screen for mutations of the rhodopsin gene in a panel of patients with autosomal dominant retinitis pigmentosa. Hum Mol Genet. 1992;1:41-45.

Ionita MA, Pittler SJ. Focus on molecules: rod cGMP phosphodiesterase type 6. Exp Eye Res. 2007;84:1-2.

Jaakson K, Zernant J, Kulm M *et al.* Genotyping microarray (gene chip) for the ABCR gene. Hum Mut. 2003;22:395-403.

Jang G.F., McBee J.K., Alekseev A.M., Haeseleer F., Palczewski K. Stereoisomeric specificity of the retinoid cycle in the vertebrate retina. J Biol Chem. 2000, 275:28128-28138.

Jindrova H. Vertebrate phototransduction: Activation, recovery and adaptation. Physiol Res. 1998,47:155-168.

Jomary C, Vincent KA, Grist J, Neal MJ, Jones SE. Rescue of photoreceptor function by AAV-mediated gene transfer in a mouse model of inherited retinal degeneration. Gene Ther. 1997;4:683-690.

Kajiwara K, Hahn LB, Mukai S *et al.* Mutations in the human retinal degeneration slow gene in autosomal dominant retinitis pigmentosa. Nature. 1991;354:480-483.

Kajiwara K, Sandberg MA, Berson EL, Dryja TP. A null mutation in the human peripherin/*RDS* gene in a family with autosomal dominant retinitis punctata albescens. Nat Genet. 1993;3:208-212.

Kaplan HJ, Tezel HJ, Berger AS *et al.* Human photoreceptor transplantation in retinitis pigmentosa. A safety study. Arch Ophthalmol. 1997;115;1168–1172.

Kaplan J, Pelet A, Martin C, *et al.* Phenotype-genotype correlations in X-linked retinitis pigmentosa. J Med Genet. 1992;29:615–623.

Katsanis N, Shroyer NF, Lewis RA *et al.* Fundus albipunctatus and retinitis punctata albescens in a pedigree with an R150Q mutation in *RLBP1*. Clin Genet. 2001;59:424-429.

Kedzierski W, Lloyd M, Birch DG, Bok D, Travis GH. Generation and analysis of transgenic mice expressing P216L-substituted *RDS*/Peripherin in rod photoreceptors. Invest Ophthalmol Vis Sci. 1997;38:498-509.

Keen TJ, Inglehearn CF, Lester DH *et al.*Autosomal dominant retinitis pigmentosa: four new mutations in rhodopsin, one of them in the retinal attachment site. Genomics. 1991;11:199-205.

Keen TJ, Hims MM, McKie AB *et al.* Mutations in a protein target of the Pim-1 kinase associated with the RP9 form of autosomal dominant retinitis pigmentosa. Eur J Hum Genet. 2002;10:245-249.

Kelling SEP, Aleman TS, Nickle A *et al.* Calcium channel blocker D-cis-diltiazem does not slow retinal degeneration in the *PDE6B* mutant rcd1 canine model of retinitis pigmentosa. Mol Vis. 2001;7:42-47.

Khaliq S, Abid A, Ismail M *et al.* Novel association of *RP1* gene mutations with autosomal recessive retinitis pigmentosa. J Med Genet. 2005;42:436-438.

Kijas JW, Cideciyan AV, Aleman TS *et al.* Naturally occurring rhodopsin mutation in the dog causes retinal dysfunction and degeneration mimicking human dominant retinitis pigmentosa. Proc Natl Acad Sci. 2002;99:6328-6333.

Klevering JB, Yzer S, Rohrschneider K *et al.* Microarray-based mutation analysis of the *ABCA4* (ABCR) gene in autosomal recessive cone–rod dystrophy and retinitis pigmentosa. Eur J Hum Genet. 2004;12:1024-1032.

Kondo H, Tahira T, Mizota A *et al.* Diagnosis of autosomal dominant retinitis pigmentosa by linkage-based exclusion screening with multiple locus-specific microsatellite markers. Invest Ophthalmol Vis Sci. 2003;44:1275-1281.

Kondo H, Qin M, Mizota A *et al.* A Homozygosity-based search for mutations in patients with autosomal recessive retinitis pigmentosa, using microsatellite markers. Invest Ophthalmol Vis Sci. 2004;45:4433-4439.

Korchen HG, Beyermann M, Muller F *et al.* Interaction of glutamic-acid-rich proteins with the cGMP signalling pathway in rod photoreceptors. Nature. 1999;400:761-766.

Kuriyama S, Mitoro A, Tsujinoue H *et al.* Particle-mediated gene transfer into murine livers using a newly developed gene gun. Gene Ther. 2000;7:1132-6.

Lalitha K, Jalali S, Kadakia T, Kannabiran C. Screening for homozygosity by descent in families with autosomal recessive retinitis pigmentosa. J Genet. 2002;81:59-63.

Lamb TD, Pugh EN. Dark adaptation and the retinoid cycle of vision. Prog Retin Eye Res. 2004;23:307-380.

Lander ES, Botstein D. Homozygosity mapping: a way to map human recessive traits with the DNA of inbred children. Science. 1987;236:1567-70.

Lau D, McGee LH, Zhou S *et al.* Retinal degeneration is slowed in transgenic rats by AAV-mediated delivery of FGF-2. Invest Ophthalmol Vis Sci. 2000;41:3622-3633.

LaVail MM, Unoki K, Yasumura D *et al.* Multiple growth factors and neurotrophins rescue photoreceptors from the damaging effects of constant light. Proc Natl Acad Sci. 1992;89:11249-11253.

LaVail MM, Yasumura D, Matthes MT *et al.* Protection of mouse photoreceptors by survival factors in retinal degenerations. Invest Ophthalmol Vis Sci. 1998;39:592-602.

Lavorgna G, Lestingi M, Ziviello *et al.* Identification and characterization of C1ORF36, a transcript highly expressed in photoreceptor cells, and mutation analysis in retinitis pigmentosa. Biochem Biophys Res Commun. 2003;308:414-421.

Lawrence JM, Keegan DJ, Muir EM *et al.* Transplantation of Schwann cell line clones secreting GDNF or BDNF into the retinas of dystrophic Royal College of Surgeons rats. Invest Ophthalmol Vis Sci. 2004;45:267-74.

Lem J, Flannery JG, Li T *et al.* Retinal degeneration is rescued in transgenic rd mice by expression of the cGMP phosphodiesterase beta subunit. Proc Natl Acad Sci.1992;89:4422-4426.

Lem J, Krasnoperova NV, Calvert PD *et al.* Morphological, physiological, and biochemical changes in rhodopsin knockout mice. Proc Natl Acad Sci. 1999;96:736-741.

Leskov IB, Klenchin VA, Handy JW, *et al.* The gain of rod phototransduction: Reconciliation of biochemical and electrophsiological measurements. Neuron. 2000;27:525-537.

Levine EM, Fuhrmann S and Reh TA. Soluble factors and the development of rod photoreceptors. Cell Mol Life Sci. 2000;57:224–234.

Lewis RA, Shroyer NF, Singh N *et al.* Genotype/phenotype analysis of a photoreceptor-specific ATP-binding cassette transporter gene, ABCR, in Stargardt Disease. Am J Hum Genet. 1999;64:422-434.

Leonard KC, Petrin D, Coupland SG *et al.* XIAP protection of photoreceptors in animal models of retinitis pigmentosa. PLoS ONE. 2007;2:e314.

Lewin AS, Drenser KA, Hauswirth WW *et al.* Ribozyme rescue of photoreceptor cells in a transgenic rat model of autosomal dominant retinitis pigmentosa. Nat Med. 1998;4:967-71.

Li S, Zhang X, Xia X *et al.* Intramuscular electroporation delivery of IFN-alpha gene therapy for inhibition of tumor growth located at a distant site. Gene Ther. 2001;8:400-7.

Li Y, Wang H, Peng J *et al.* Mutation survey of known LCA genes and loci in the Saudi Arabian population. Invest Ophthalmol Vis Sci. 2009;50:1336-43.

Liang FQ, Dejneka NS, Cohen DR *et al.* AAV-mediated delivery of ciliary neurotrophic factor prolongs photoreceptor survival in the rhodopsin knockout mouse. Mol Ther. 2001a;3:241-8.

Liang FQ, Aleman TS, Dejneka NS *et al.* Long-term protection of retinal structure but not function using RAAV.CNTF in animal models of retinitis pigmentosa. Mol Ther. 2001b;4:461-72.

Lin LFH, Doherty DH, Lile JD *et al.* GDNF: a glial cell line derived neurotrophic factor for midbrain dopaminergic neurons. Science. 1993;260:1130-1132.

Lindner TH, Hoffmann K. easyLINKAGE: a PERL script for easy and automated two-/multi-point linkage analyses. Bioinformatics. 2005;21:405-407.

Liou GI, Fei Y, Peachey NS, Matragoon S *et al.* Early onset photoreceptor abnormalities induced by targeted disruption of the interphotoreceptor retinoid-binding protein gene. J Neurosci. 1998;18:4511-4520.

Liston P, Roy N, Tamai K *et al.* Suppression of apoptosis in mammalian cells by NAIP and a related family of IAP genes. Nature. 1996;379:349-353.

Liu F, Yang J, Huang L, Liu D. New cationic lipid formulations for gene transfer. Pharm Res. 1996;13:1856-1860.

Liu Q, Zhou J, Daiger SP *et al.* Identification and subcellular localization of the RP1 protein in human and mouse photoreceptors. Invest Ophthal Vis Sci. 2002;43: 22-32.

Lopez R, Gauras H, Kjeldbye H *et al.* Transplanted Retinal Pigment Epithelium Modifies the Retinal Degeneration in the RC5 Rat. Invest Ophthalmol Vis Sci. 1989;30:586-588.

Lotery AJ, Namperumalsamy P, Jacobson SG *et al.* Mutation analysis of 3 genes in patients with Leber congenital amaurosis. Arch Ophthalmol. 2000;118:538-543.

Lotery AJ, Jacobson SG, Fishman GA *et al.* Mutations in the *CRB1* gene cause Leber congenital amaurosis. Arch Ophthalmol. 2001;119:415-420.

Luo HR, Moreau GA, Levin N, Moore MJ. The human Prp8 protein is a component of both U2- and U12-dependent spliceosomes. RNA. 1999;5:893-908.

Lutein and zeaxanthin. Monograph. Altern Med Rev. 2005;10:128-135.

Ma J, Norton JC, Allen AC *et al.* Retinal degeneration slow (*RDS*) in mouse results from simple insertion of a t haplotype-specific element into protein coding exon II. Genomics. 1995;28:212-219.

MacLaren RE, Pearson RA, MacNeil A *et al.* Retinal repair by transplantation of photoreceptor precursors. Nature. 2006;444:203-207.

Maeda A, Maeda T, Imanishi Y *et al.* Retinol Dehydrogenase (*RDH12*) protects photoreceptors from light-induced degeneration in mice. J Biol Chem. 2006;281:37697-37704.

Maguire AM, Simonelli F, Pierce EA *et al.* Safety and efficacy of gene transfer for Leber's congenital amaurosis. N Engl J Med. 2008;358:2240-2248.

Mandal MN, Heckenlively JR, Burch T *et al.* Sequencing arrays for screening multiple genes associated with early-onset human retinal degenerations on a high-throughput platform. Invest Ophthalmol Vis Sci. 2005;46:3355-3362.

Mansergh FC, Millington-Ward S, Kennan A *et al.* Retinitis pigmentosa and progressive sensorineural hearing loss caused by a C12258A mutation in the mitochondrial MTTS2 gene. Am J Hum Genet. 1999;64:971-85.

Marlhens F, Bareil C, Griffoin JM *et al.* Mutations in *RPE65* cause Leber's congenital amaurosis. Nat Genet. 1997;17:139-141.

Martínez-Mir A, Paloma E, Allikmets R *et al.* Retinitis pigmentosa caused by a homozygous mutation in the Stargardt disease gene ABCR. Nat Genet. 1998;18:11-22.

Mata NL, Radu RA, Clemmons RS, Travis GH. Isomerization and oxidation of vitamin A in cone dominant retinas: A novel pathway for visual pigment regeneration in day light. Neuron. 2002, 36:69-80.

Maw MA, John S, Jablonka S *et al.* Oguchi disease: suggestion of linkage to markers on chromosome 2q. J Med Genet. 1995;32:396-8.

Maw MA, Kennedy B, Knight A *et al.* Mutation of the gene encoding cellular retinaldehyde-binding protein in autosomal recessive retinitis pigmentosa. Nat Genet. 1997;17:198-200.

Maw MA, Corbeil D, Koch J *et al.* A frameshift mutation in prominin (mouse)-like 1 causes human retinal degeneration. Hum Mol Genet. 2000;9:27-34.

McEwen DP, Koenekoop RK, Khanna H *et al.* Hypomorphic CEP290/NPHP6 mutations result in anosmia caused by the selective loss of G proteins in cilia of olfactory sensory neurons. Proc Natl Acad Sci. 2007;104:15917-15922.

McGee TL, Devoto M, Ott J, Berson EL, Dryja TP. Evidence that the penetrance of mutations at the RP11 locus causing dominant retinitis pigmentosa is influenced by a gene linked to the homologous RP11 allele. Am J Hum Genet. 1997;61:1059-1066.

McKay GJ, Clarke S, Davis JA *et al.* pigmented paravenous chorioretinal atrophy is associated with a mutation within the crumbs homolog 1 (*CRB1*) gene. Invest Ophthalmol Vis Sci. 2005;46:322-328.

McKie AB, McHale JC, Keen TJ *et al.* Mutations in the pre-mRNA splicing factor gene PRPC8 in autosomal dominant retintis pigmentosa (RP13). Hum Mol Genet. 2001;10:1555-1562.

McLaughlin ME, Sandberg MA, Berson EL, Dryja TP. Recessive mutations in the gene encoding the beta-subunit of rod phosphodiesterase in patients with retinitis pigmentosa. Nat Genet. 1993;4:130-134.

Mears AJ, Kondo M, Swain PK *et al.* Nrl is required for rod photoreceptor development. Nat Genet. 2001;29:447-452.

Meindl A, Dry K, Herrmann K *et al.* A gene (RPGR) with homology to the RCC1 guanine nucleotide exchange factor is mutated in X-linked retinitis pigmentosa (RP3). Nat Genet. 1996;13:35-42.

Meuleman J, van de Pavert SA, Wijnholds J. Crumbs homologue 1 in polarity and blindness. Biochem Soc Trans. 2004;32:828-830.

Michaelides M, Hunt DM, Moore AT. The cone dysfunction syndromes. Br J Ophthalmol. 2004;88:291-297.

Miraglia S, Godfrey W, Yin AH *et al.* A novel five-transmembrane hematopoietic stem cell antigen: isolation, characterization, and molecular cloning. Blood. 1997;90:5013-5021.

Moiseyev G, Chen Y, Takahashi Y *et al. RPE65* is the isomerohydrolase in the retinoid visual cycle. Proc Nat Acad Sci. 2005;102:12413-12418.

Molday RS. Peripherin/rds and rom-1: molecular properties and role in photoreceptor cell degeneration. Prog Retin Eye Res. 1994; 13, 271–299.

Molday LL, Rabin AR, Molday RS. ABCR expression in foveal cone photoreceptors and its role in Stargardts macular dystrophy. Nat Genet. 2000;25:257-258.

Morimura H, Fishman GA, Grover SA, Fulton AB *et al.* Mutations in the *RPE65* gene in patients with autosomal recessive retinitis pigmentosa or Leber congenital amaurosis. Proc Natl Acad Sci. 1998;95:3088-3093.

Morimura H, Saindelle-Ribeaudeau F, Berson EL, Dryja TP. Mutations in RGR, encoding a light-sensitive opsin homologue, in patients with retinitis pigmentosa. Nat Genet.1999a; 23:393-394.

Morimura H, Berson E L, Dryja T P. Recessive mutations in the *RLBP1* gene encoding cellular retinaldehyde-binding protein in a form of retinitis punctata albescens. Invest Ophthalmol Vis Sci. 1999b;40:1000-1004.

Moshiri A, Close J, Reh TA. Retinal stem cells and regeneration. Int J Dev Biol. 2004;48:1003-1014.

Nakazawa M, Wada Y, Tamai M. Arrestin gene mutations in autosomal recessive retinitis pigmentosa. Arch Ophthalmol. 1998;116:498-501.

Narfstrom K, Katz ML, Bragadottir R, Seeliger M *et al.* Functional and structural recovery of the retina after gene therapy in the *RPE65* null mutation dog. Invest Ophthalmol Vis Sci. 2003;44:1663-1672.

Nathans J. Rhodopsin: structure, function and genetics. Biochemistry. 1992;31:4923-4931.

Neumann CJ, Nuesslein-Volhard C. Patterning of the zebrafish retina by a wave of sonic hedgehog activity. Science. 2000;289:2137-2139.

Ng PC, Henikoff S. SIFT: Predicting amino acid changes that affect protein function. Nucleic Acids Res. 2003;31:3812-3814.

Nicoletti A, Wong D J, Kawase K. *et al.* Molecular characterization of the human gene encoding an abundant 61 kDa protein specific to the retinal pigment epithelium. Hum Mol Genet. 1995; 4: 641-649.

Nicotera P. Apoptosis and age-related disorders: role of caspase-dependent and caspase-independent pathways. Toxicol Lett. 2002;127:189-195.

Nishiguchi KM, Friedman JS, Sandberg MA *et al.* Recessive NRL mutations in patients with clumped pigmentary retinal degeneration and relative preservation of blue cone function. Proc Natl Acad Sci. 2004;101:17819-17824.

North MA, Naggert JK, Yan Yingzhuo, Noben-Trauth K. Molecular characterization of TUB, *TULP1*, and TULP2, members of the novel tubby gene family and their possible relation to ocular diseases. Proc Natl Acad Sci. 1997;94:3128-3133.

Nosrat CA, Tomac A, Lindqvist E, *et al.* Cellular expression of GDNF mRNA suggests multiple functions inside and outside the nervous system. Cell Tissue Res. 1996;286:191–207.

Noy N. Retinoid-binding proteins : mediators of retinoid action.Biochem. J. 2000; 348:481:495.

O'Reilly M, Palfi A, Chadderton N *et al.* RNA interference-mediated suppression and replacement of human rhodopsin in vivo. Am J Hum Genet. 2007;81:127-35

Paloma E, Hjelmqvist L, Bayés M *et al.* Novel mutations in the TULP1 gene causing autosomal recessive retinitis pigmentosa. Invest Ophthalmol Vis Sci. 2000;41:656-659.

Papaioannou M, Ocaka L, Bessant D *et al.* An analysis of ABCR mutations in British patients with recessive retinal dystrophies. Invest Ophthalmol Vis Sci. 2000;41:16-9.

Parisi MA, Doherty D, Chance PF, Glass IA. Joubert syndrome (and related disorders) (OMIM 213300). Eur J Hum Genet. 2007;15:511-521.

Parisi MA, Doherty D, Eckert ML *et al.* AHI1 mutations cause both retinal dystrophy and renal cystic disease in Joubert syndrome. J Med Genet. 2006;43:334-9.

Parry HB. Degenerations of the dog retina. Brit J Ophthalmol. 1953;37:487-502.

Pawlyk BS, Li T, Scimeca MS *et al.* Absence of Photoreceptor Rescue with D-cis-Diltiazemin the rd Mouse. Invest Ophthalmol Vis Sci. 2002;43:1912-1915.

Pawlyk BS, Smith AJ, Buch PK *et al.* Gene replacement therapy rescues photoreceptor degeneration in a murine model of Leber congenital amaurosis lacking *RPGRIP*. Invest Ophthalmol Vis Sci. 2005;46:3039-3045.

Perrault I, Rozet JM, Calvas P *et al.* Retinal-specific guanylate cyclase gene mutations in Leber's congenital amaurosis. Nat Genet. 1996;14:461-464.

Perrault I, Rozet JM, Gerber S, *et al.* Leber Congenital Amaurosis. Mol Genet Metab. 1999;68:200-208.

Perrault I, Hanein S, Gerber S *et al.* Retinal dehydrogenase 12 (*RDH12*) mutations in Leber congenital amaurosis. Am J Hum Genet. 2004;75:639-646.

Pierce EA, Quinn T, Meehan T *et al.* Mutations in a gene encoding a new oxygen-regulated photoreceptor protein cause dominant retinitis pigmentosa. Nat Genet. 1999;22:248-254.

Pierce EA. Pathways of photoreceptor cell death in inherited retinal degenerations. Bioessays. 2001;23:605-618.

Pittack C, Grunwald GB, Reh TA. Fibroblast growth factors are necessary for neural retina but not pigmented epithelium differentiation in chick embryos. Development. 1997;124:805-816.

Portera-Cailliau C, Sung CH, Nathans J, Adler R. Apoptotic photoreceptor cell death in mouse models of retinitis pigmentosa. Proc Natl Acad Sci. 1994;91:974-8.

Pugh EN Jr, Lamb TD. Amplification and kinetics of the activation steps in phototransduction. Biochim Biophys Acta. 1993;1141:111-149.

Rajendra R, Malegaonkar D, Pungaliya P *et al.* Topors functions as an E3 ubiquitin ligase with specific E2 enzymes and ubiquitinates p53. J Biol Chem. 2004;279:36440-3644.

Ramprasad VL, Soumittra N, Nancarrow D *et al.* Identification of a novel splice-site mutation in the Lebercilin (LCA5) gene causing Leber congenital amaurosis. Mol Vis. 2008;14:481-486.

Rando R.R. The biochemistry of the visual cycle. Chem. Rev. 2001, 101:1881-1896.

Rapaport DH, Wong LL, Wood ED, Yasumura D, LaVail MM. Timing and topography of cell genesis in the rat retina. J Comp Neurol. 2004;474:304-324.

Rebello G, Ramesar R, Vorster A *et al.* Apoptosis-inducing signal sequence mutation in carbonic anhydrase IV identified in patients with the RP17 form of retinitis pigmentosa Proc Natl Acad Sci. 2004;101:6617-6622.

Redmond TM, Yu S, Lee E *et al. RPE65* is necessary for production of 11-cis-vitamin A in the retinal visual cycle. Nat Genet. 1998;20:344-351.

Reh TA. The retina. 3rd ed. (Ed. Ryan SJ ed). Mosby; 2001.

Retinal information network available at http://www.sph.uth.tmc.edu/Retnet/

Riazuddin SA, Zulfiqar F, Zhang Q *et al.* Autosomal recessive retinitis pigmentosa is associated with mutations in RP1 in three consanguineous Pakistani families. Invest Ophthalmol Vis Sci. 2005;46:2264-2670.

Rice DS, Huang W, Jones HA *et al.* Severe retinal degeneration associated with disruption of semaphorin 4A. Invest Ophthalmol Vis Sci. 2004;45:2767-2777.

Richard GW. Retinitis Pigmentosa and allied disorders. Basic Science and inherited retinal disease. 2nd ed. (Ryan SJ, ed.) Mosby; 1994.

Richards JE, Kuo CY, Boehnke M, Sieving PA. Rhodopsin Thr58Arg mutation in a family with autosomal dominant retinitis pigmentosa. Ophthalmology. 1991;98:1797-1805.

Rivera A, White K, Stohr H, Steiner K *et al.* A comprehensive survey of sequence variation in the *ABCA4* (ABCR) gene in Stargardt disease and age-related macular degeneration. Am J Hum Genet. 2000;67:800-813.

Rivolta C, Sweklo EA, Berson EL Dryja TP. Missense mutation in the *USH2A* gene associated with recessive retinitis pigmentosa without hearing loss. Am J Hum Genet. 2000;66:1975-1978.

Rivolta C, McGee TL, Rio Frio T, *et al.* Variation in retinitis pigmentosa-11 (*PRPF31* or RP11) gene expression between symptomatic and asymptomatic patients with dominant RP11 mutations. Hum Mutat. 2006;27:644-653.

Robbins PD, Ghivizzani SC. Viral vectors for gene therapy. Pharmacol Ther. 1998;80:35-47.

Rosenfeld PJ, Cowley GS, McGee TL *et al.* A null mutation in the rhodopsin gene causes rod photoreceptor dysfunction and autosomal recessive retinitis pigmentosa. Nat Genet. 1992;1:209-213.

Rozet JM, Gerber S, Souied E *et al.* Spectrum of ABCR gene mutations in autosomal recessive macular dystrophies. Eur J Hum Genet. 1998;6:291-295.

Rozet JM, Gerber S, Souied E, *et al.* The ABCR Gene: A Major Disease Gene in Macular and Peripheral Retinal Degenerations with Onset from Early Childhood to the Elderly. Mol Genet Metab. 1999;68:310–315.

Russell-Eggitt IM, Taylor DS, Clayton PT *et al.* Leber's congenital amaurosis--a new syndrome with a cardiomyopathy. Br J Ophthalmol. 1989;73:250-254.

Sakuma H, Inana G, Murakami A *et al.* A heterozygous putative null mutation in *ROM1* without a mutation in peripherin/*RDS* in a family with Retinitis Pigmentosa. Genomics. 1995;27:384-386.

Sandberg MA, Weigel-DiFranco C, Dryja TP, Berson EL. Clinical expression correlates with location of rhodopsin mutation in dominant retinitis pigmentosa. Invest Ophthalmol Vis Sci. 1995;36:1934-1942.

Sandberg MA, Rosner B, Weigel-DiFranco C, Dryja TP, Berson EL. Disease course of patients with X-linked retinitis pigmentosa due to RPGR gene mutations. Invest Ophthalmol Vis Sci. 2007;48:1298-1304.

Sanftner LHM, Abel H, Hauswirth WW, Flannery JG. Glial cell line derived neurotrophic factor delays photoreceptor degeneration in a transgenic rat model of retinitis pigmentosa. Mol Therapy. 2001;4:622-629.

Santorelli FM, Shanske S, Macaya A, DeVivo DC, DiMauro S. The mutation at nt 8993 of mitochondrial DNA is a common cause of Leigh's syndrome. Ann Neurol. 1993;34:827-34.

Sanyal A, De Ruiter A, Hawkins RK. Development and degeneration of retina in *RDS* mutant mice: light microscopy. J Comp Neurol. 1980;194:193-207.

Sanz MM, Johnson LE, Ahuja S *et al.* Significant photoreceptor rescue by treatment with a combination of antioxidants in an animal model for retinal degeneration. Neuroscience. 2007;145:1120-1129.

Sato H, Wada Y, Itabashi T *et al.* Mutations in the pre-mRNA splicing gene, *PRPF31*, in Japanese families with autosomal dominant retinitis pigmentosa. Am J Ophthalmol. 2005;140:537-540.

Sato M, Nakazawa M, Usui T *et al.* Mutations in the gene coding for guanylate cyclase-activating protein 2 (*GUCA1B* gene) in patients with autosomal dominant retinal dystrophies. Graefe's Arch Clin Exp Ophthalmol. 2005a;243:235-242.

Schlichtenbrede FC, MacNeil A, Bainbridge JW *et al.* Intraocular gene delivery of ciliary neurotrophic factor results in significant loss of retinal function in normal mice and in the Prph2Rd2/Rd2 model of retinal degeneration. Gene Ther. 2003;10:523-527.

Schwahn U, Lenzner S, Dong J *et al.* Positional cloning of the gene for X-linked retinitis pigmentosa 2. Nat Genet. 1998;19:327-332.

Scott RS, McMahon EJ, Pop SM *et al.* Phagocytosis and clearance of apoptotic cells is mediated by MER. Nature. 2001;411:207-211.

Seddon JM, Ajani UA, Sperduto RD *et al.* Dietary carotenoids, vitamins A, C, and E, and advanced age-related macular degeneration. Eye Disease Case-Control Study Group. JAMA. 1994;272:1413-1420.

Seeliger MW, Biesalski HK, Wissinger B *et al.* Phenotype in retinol deficiency due to a hereditary defect in retinol binding protein synthesis. Invest Ophthalmol Vis Sci. 1999;40:3-11.

Seiler MJ, Aramant RB. Intact sheets of fetal retina transplanted to restore damaged rat retinas. Invest Ophthalmol Vis Sci. 1998;39:2121-2131.

Semple-Rowland SL, Lee NR, Van Hooser JP, Palczewski K, Baehr W. A null mutation in the photoreceptor guanylate cyclase gene causes the retinal degeneration chicken phenotype. Proc Natl Acad Sci. 1998;95:1271-1276.

Senechal A, Humbert G, Surget MO *et al.* Screening genes of the retinoid metabolism: novel *LRAT* mutation in Leber congenital amaurosis. Am J Ophthalmol. 2006;142:702-704.

Seyedahmadi BJ, Rivolta C, Keene JA *et al.* Comprehensive screening of *USH2A* gene in Usher syndrome type-II and non-syndromic recessive retinitis pigmentosa. Exp Eye Res. 2004;79:167-173.

Sharon D, Blackshaw S, Cepko CL, Dryja TP. Profile of the genes expressed in the human peripheral retina, macula, and retinal pigment epithelium determined through serial analysis of gene expression (SAGE). Proc Natl Acad Sci. 2002;99:315-20.

Sharon D, Sandberg MA, Rabe VW, *et al.* RP2 and RPGR mutations and clinical correlations in patients with X-linked retinitis pigmentosa. Am J Hum Genet. 2003;73:1131-1146.

Sibulesky L, Hayes KC, Pronczuk A *et al.* Safety of <7500 RE (<25000 IU) vitamin A daily in adults with retinitis pimentosa. Am J Clin Nutr. 1999;69:656-663.

Seiving PA, Caruso RC Tao W *et al.* Ciliary neutrophic factor (CNTF) for human retinal degeneration: Phase I trial of CNTF delivered by encapsulated cell intraocular implants. Proc Natl Acad Sci. 2006;103:3896-3901.

Silverman MS, Hughes SE, Valentino T, Liu Y. Photoreceptor transplantation: anatomic, electrophysiologic, and photoreceptor transplantation: anatomic, electrophysiologic, and behavioral evidence for the functional reconstruction of retinas lacking photoreceptors. Exp Neurol. 1992;115:87–94.

Simon A, Romert A, Gustafson AL, McCaffery JM, Eriksson U. Intracellular localization and membrane topology of 11-cis retinol dehydrogenase in the retinal pigment epithelium suggest a compartmentalized synthesis of 11-cis retinaldehyde. J Cell Sci. 1999;112:549-558.

Simunovic MP, Moore AT. The cone dystrophies. Eye. 1998; 12:553-565.

Singh HP, Jalali S, Hejtmancik JF, Kannabiran C. Homozygous null mutations in the *ABCA4* gene in two families with autosomal recessive retinal dystrophy. Am J Ophthalmol. 2006;141:906-913.

Sippel KC, DeStefano JD, Berson EL, Dryja TP. Evaluation of the human arrestin gene in patients with retinitis pigmentosa and stationary night blindness. Invest Ophthalmol Vis Sci. 1998;39:665-670.

Sohocki MM, Sullivan LS, Mintz-Hittner HA *et al.* A range of clinical phenotypes associated with mutations in CRX, a photoreceptor transcription factor gene. Am J Hum Genet. 1998;63:1307-1315.

Sohocki MM, Bowne SJ, Sullivan LS *et al.* Mutations in a new photoreceptor-pineal gene on 17p cause Leber congenital amaurosis. Nat Genet. 2000;24:79-83.

Song J, Chappell JC, Qi M *et al.* Influence of injection site, microvascular pressure and ultrasound variables on microbubble-mediated delivery of microspheres to muscle. J Am Coll Cardiol. 2002;39:726-31.

Souied E, Soubrane G, Benlian P, *et al.* Retinitis punctata albescens associated with the Argl35Trp mutation in the rhodopsin gene. Am J Ophthalmol. 1996;121:19-25.

Spuy J, Cheetham ME.The Leber congenital amaurosis protein *AIPL1* modulates the nuclear translocation of NUB1 and suppresses inclusion formation by NUB1 fragments. J Biol Chem. 2004;279:48038-48047.

Sullivan LS, Heckenlively JR, Bowne SJ *et al.* Mutations in novel retina-specific gene cause autosomal dominant retintis pigmentosa. Nat Genet. 1999;22:255-259.

Stöhr H, Mah N, Schulz HL *et al.* EST mining of the UniGene dataset to identify retina-specific genes. Cytogenet Cell Genet. 2000;91:267-277.

Strachan T, Read AP. Human molecular genetics. 2nd ed., UK: BIOS scientific publishers Ltd; 1999.

Steiner PA. Bardet-Biedl syndrome. J Am Optom Assoc. 1990;61:852-855.

Sun H, Smallwood PM, Nathans J. Biochemical defects in ABCR protein variants associated with human retinopathies. Nat Genet. 2000;26:242-246.

Sung CH, Davenport CM, Hennessey JC *et al.* Rhodopsin mutations in autosomal dominant retinitis pigmentosa Rhodopsin mutations in autosomal dominant retinitis pigmentosa. Proc Natl Acad Sci. 1991;88:6481-6485.

Swaroop A, Wang QL, W Wu *et al.* Leber congenital amaurosis caused by a homozygous mutation (R90W) in the homeodomain of the retinal transcription factor CRX: direct evidence for the involvement of CRX in the development of photoreceptor function. Hum Mol Genet. 1999;8:299-305.

Sweeney MO, McGee TL, Berson EL, Dryja TP. Low prevalence of lecithin retinol acyltransferase mutations in patients with Leber congenital amaurosis and autosomal recessive retinitis pigmentosa. Mol Vis. 2007;13:588-593.

Tada A, Wada Y, Sato H *et al.* Screening of the MERTK gene for mutations in Japanese patients with autosomal recessive retinitis pigmentosa. Mol Vis. 2006;12:441-444.

Takahashi M, Palmer TD, Takahashi J, Gage FH. Widespread integration and survival of adult-derived neural progenitor cells in the developing optic retina. Mol Cell Neurosci. 1998;12:340-348.

Takahashi M, Miyoshi H, Verma IM, Gage FH. Rescue from photoreceptor degeneration in the rd mouse by human immunodeficiency virus vector-mediated gene transfer. J Virol. 1999;73:7812-7816.

Tao W, Wen R, Goddard MB *et al.* Encapsulated cell based delivery of CNTF reduces photoreceptor degenration in animal model of retinitis pigmentosa. Invest Ophthalmol Vis Sci. 2002;43:3292-3298.

Teupe C, Richter S, Fisslthaler B *et al.* Vascular gene transfer of phosphomimetic endothelial nitric oxide synthase (S1177D) using ultrasound-enhanced destruction of plasmid-loaded microbubbles improves vasoreactivity. Circulation. 2002;105:1104-1109.

Themis M, Waddington SN, Schmidt M *et al.* Oncogenesis following delivery of a nonprimate lentiviral gene therapy vector to fetal and neonatal mice. Mol Ther. 2005;12:763-771.

Thompson DA, Christina YL, Mc Henry L *et al.* Mutations in the gene encoding lecithin retinol acyltransferase are associated with early-onset severe retinal dystrophy. Nat Genet. 2001;28:123-124.

Thompson DA, Gal A. Vitamin A metabolism in the retinal pigment epithelium: genes, mutations and disease. Prog Retin Eye Res. 2003, 22:683-703.

Tomita H, Sugano E, Yawo H *et al.* Restoration of visual response in aged dystrophic RCS rats using AAV-mediated channelopsin-2 gene transfer. Invest Ophthalmol Vis Sci. 2007;48:3821-3826.

Travis GH, Groshan KR, Lloyd M, Bok D. Complete rescue of photoreceptor dysplasia and degeneration in transgenic retinal degeneration slow (rds) mice. Neuron. 1992;9:113-119.

Trudeau MC, Zagotta WN. An intersubunit interaction regulates trafficking of rod cyclic nucleotide-gated channels ans is disrupted in an inherited form of blindenss. Neuron. 2002;34:197-207.

Tsang SH, Gouras P, Yamashita CK *et al.* Retinal degeneration in mice lacking the gamma subunit of the rod cGMP phosphodiesterase. Science. 1996;272:1026-1029.

Tso MOM, Li WWY, Zang C *et al.* A pathologic study of degeneration of the rod and cone populations of the rhodopsin Pro347Leu transgenic pigs. Tr Am Soc. 1997;95:467-483.

Tubb BE, Bardien-Kruger S, Kashork CD *et al.* Characterization of human retinal fascin gene (FSCN2) at 17q25: close physical linkage of fascin and cytoplasmic actin genes. Genomics. 2000;65:146-56.

Tuson M, Marfany G, Gonza`lez-Duarte R. Mutation of *CERKL*, a novel human ceramide kinase gene, causes autosomal recessive retinitis pigmentosa (RP26). Am J Hum Genet. 2004;74:128–138.

Tuson M, Garanto A, Gonzàlez-Duarte R, Marfany G. Overexpression of CERKL, a gene responsible for retinitis pigmentosa in humans, protects cells from apoptosis induced by oxidative stress. Mol Vis. 2009;15:168-180.

Uteza Y, Rouillot JS, Kobetz A *et al.* Intravitreous transplantation of encapsulated fibroblasts secreting the human fibroblast growth factor 2 delays photoreceptor degeneration in royal college of surgeon rats. Proc Natl Acad Sci. 1999;96:3126-3131.

Vaithinathan R, Berson EL and Dryja TP. Further screening of the Rhodopsin gene in patients with autosomal dominant retinitis pigmentosa. Genomics.1994;21:461-463.

Vallespin E, Cantalapiedra D, Riveiro-Alvarez R *et al.* Mutation screening of 299 Spanish families with retinal dystrophies by Leber congenital amaurosis genotyping microarray. Invest Ophthalmol Vis Sci. 2007;48:5653-5661.

van den Brink DM, Brites P, Haasjes J *et al.* Identification of PEX7 as the second gene involved in Refsum disease. Am J Hum Genet. 2003;72:471-477.

van Hoffelen SJ, Young MJ Shatos MA, Sakaguchi DS. Incorporation of murine brain progenitor cells into the developing mammalian retina. Invest Opththalmol Vis Sci. 2003;44:426-434.

van Wijk E, Pennings RJE, te Brinke H *et al.* Identification of 51 novel exons of the Usher syndrome type 2A (*USH2A*) gene that encode multiple conserved functional domains and that are mutated in patients with Usher syndrome type II. Am J Hum Genet. 2004;74:738-744.

Vithana EN, Abu Safieh L, Allen MJ *et al.* A Human Homolog of Yeast Pre-mRNA Splicing Gene, *PRP31*, Underlies Autosomal Dominant Retinitis Pigmentosa on Chromosome 19q13.4 (*RP11*). Mol Cell. 2001;8:375-381.

Vithana EN, Abu-Safieh L, Pelosini L, *et al.* Expression of *PRPF31* mRNA in patients with autosomal dominant retinitis pigmentosa: a molecular clue for incomplete penetrance? Invest Ophthalmol Vis Sci. 2003;44:4204-4209.

Vollrath D, Feng W, Duncan JL *et al.* Correction of the retinal dystrophy phenotype of the RCS rat by viral gene transfer of Mertk. Proc Natl Acad Sci. 2001;98:12584-12589.

Wang A, Forman-Kay J, Luo Y *et al.* Identification and characterization of human genes encoding Hprp3p and Hprp4p, interacting components of the spliceosome. Hum Mol Genet. 1997;6:2117-2126.

Wang H, den Hollander AI, Moayedi Y *et al.* Mutations in the SPATA7 causes Leber congenital amaurosis and juvenile retinitis pigmentosa. Am J Hum Genet. 2009 (early online).

Wang L, Ribaudo M, Zhao K *et al.* Novel deletion in the pre-mRNA splicing gene *PRPF31* causes autosomal dominant retinitis pigmentosa in a large Chinese family. Am J Med Genet. 2003;121A:235-239.

Wada Y, Abe T, Takeshita T *et al.* Mutation of Human Retinal Fascin Gene (*FSCN2*) Causes Autosomal Dominant Retinitis Pigmentosa. Invest Ophthalmol Vis Sci. 2001;42:2395-2400.

Waseem NH, Vaclavik V, Webster A *et al.* Mutations in the gene coding for the pre-mRNA splicing factor, *PRPF31*, in patients with autosomal dominant retinitis pigmentosa. Invest Ophthalmol Vis Sci. 2007;48:1330-4.

Webster AR, Heon E, Lotery AJ. An analysis of allelic variation in the *ABCA4* gene. Invest Ophthalmol Vis Sci. 2001;42:1179-1189.

Weng J, Mata NL, Azarian SM *et al.* Insights into the function of rim protein in photoreceptors and etiology of Stargardt's disease from the phenotype in abcr knockout mice. Cell. 1999;98:13-23.

Wenzel A, Oberhauser V, Pugh EN *et al.* The Retinal G Protein-coupled Receptor (RGR) enhances isomerohydrolase activity independent of light. J Biol Chem. 2005;280:29874–29884.

Widera G, Austin M, Rabussay D *et al.* Increased DNA vaccine delivery and immunogenicity by electroporation in vivo. J Immunol. 2000;164:4635-4640.

Winter JO, Cogan SF, Rizzo JF. Retinal prostheses: current challenges and future outlook. J Biomater Sci Polymer Edn. 2007;18:1031-1055.

Wodarz A, Hinz U, Engelbert M, Knust E. Expresion of crimbs confers apical character on plasma membrane domain of ectodermal epithelia of drosophila. Cell.1995;82:67-78.

Wright AF, Bhattacharya SS, Aldred MA *et al.* Genetic localisation of the RP2 type of X linked retinitis pigmentosa in a large kindred. J Med Genet. 1991;28:453-457.

Xia K, Zheng D, Pan Q *et al.* A novel *PRPF31* splice-site mutation in a Chinese family with autosomal dominant retinitis pigmentosa. Mol Vis. 2004;10:361-365.

Xu L, Hu L, Ma K, Li J, Jonas JB. Prevalence of retinitis pigmentosa in urban and rural adult Chinese: The Beijing Eye Study. Eur J Ophthalmol. 2006;16:865-866.

Xue L, Gollapalli D R, Maiti P, Jahng W J, Rando R R. A palmitoylation switch mechanism in the regulation of the visual cycle. Cell. 2004;61-771.

Yamaki K, Tsuda M Kikuchi T *et al.* Structural organization of the human S antigen. J Biol Chem. 1990;265:20757-20762.

Yang Z, Alvarez BV, Chakarova C, *et al.* Mutant carbonic anhydrase 4 impairs pH regulation and causes retinal photoreceptor degeneration. Hum Mol Genet. 2005;14:255–265.

Yang Z, Chen Y, Lillo C *et al.* Mutant prominin 1 found in patients with macular degeneration disrupts photoreceptor disk morphogenesis in mice. J Clin Invest. 2008;118:2908-2916.

Yatsenko AN, Shroyer NF, Lewis RA, Lupski JR. Late-onset Stargardt disease is associated with missense mutations that map outside known functional regions of ABCR (*ABCA4*). Hum Genet. 2001;108:346-355.

Yoshida S, Mears AJ, Friedman JS *et al.* Expression profiling of the developing and mature Nrl2/2 mouse retina: identification of retinal disease candidates and transcriptional regulatory targets of Nrl. Hum Mol Genet. 2004;13:1487-1503.

Yzer S, Leroy BP, De Baere E *et al.* Microarray-based mutation detection and phenotypic characterization of patients with Leber congenital amaurosis. Invest Ophthalmol Vis Sci. 2006;47:1167-1176.

Zaghloul NA, Yan B, Moody SA. Step-wise specification of retinal stem cells during normal embryogenesis. Biol Cell. 2005;97:321-337.

Zhang Q, Zulfiqar F, Xiao X *et al.* Severe retinitis pigmentosa mapped to 4p15 and associated with a novel mutation in the PROM1 gene. Hum Genet. 2007;122:293-299.

Zangerl B, Goldstein O, Philp AR *et al.* Identical mutation in a novel retinal gene causes progressive rod-cone degeneration in dogs and retinitis pigmentosa in humans. Genomics. 2006;88:551-563.

Zelhof AC, Hardy RW, Becker A, Zuker CS. Transforming the architecture of compound eyes. Nature. 2006;443:696–699.

Zernant J, Külm M, Dharmaraj S *et al.* Genotyping microarray (disease chip) for Leber congenital amaurosis: detection of modifier alleles. Invest Ophthalmol Vis Sci. 2005;46:3052-3059.

Zhong H, Molday LL, Molday RS, Yau KW. The heteromeric cyclic nucleotide-gated channel adopts a 3A:1B stoichiometry. Nature. 2002;420:193-198.

Appendix

APPENDIX

Table 1. Microsatellite markers genotyped in ARRP families.

#	Gene	Marker	Label	Heterozygosity	Type of Repeat	Sequence
1	*ABCR*	D1S 406-F	Fam	0.83	Tetranucleotide	AGGCAGCAGAGTGAGACTC
		D1S 406-R				GCTTTCTTAGGCCACACGTA
		D1S 2779-F	Hex	0.82	Dinucleotide	AACCATTAATATCTTNCCAGGT
		D1S 2779-R				AGTGCATACCACCATGCC
		D1S 236-F	Tet	0.80	Dinucleotide	AAACCACCTACCAATGTCTGTC
		D1S 236-R				GAAGCTGTCGTTATGGGGT
		D1S 1170-F	Fam	0.75	Tetranucleotide	GATAGCAAGGCCTCGTCTC
		D1S 1170-R				GAGGACTACAGGCATGTGC
		D1S188-F *	Hex	0.86	Dinucleotide	AACCAATCAAGGTGCCTGCA
		D1S188-R *				TCCCCTAGTGTCCTGGCAG
2	*RPE65*	D1S 219-F	Hex	0.83	Dinucleotide	TCCAGTCACTCTCTCTAGCC
		D1S 219-R				GAAGATGCTGATACCCAAGT
		D1S 2806-F	fam	0.78	Dinucleotide	CATTACATCACAGCCTGATTAGA
		D1S 2806-R				CCACCATGCCTGACCT
		D1S 2829-F	Tet	0.86	Dinucleotide	AGTGGTTTATATGACTTACTGTGGG
		D1S 2829-R				GCACNCCAGCCTAGGTA
		D1S410-F *	fam	0.75	Tetranucleotide	CACATCATGATTGGGCCAC
		D1S410-R *				AAAAGTGTGGATGGATATACC
		D1S2798-F *	Hex	0.74	Dinucleotide	GATCCTCTCTCAATCAATAAATAA
		D1S2798-R *				AAGAAGCCAACCAGAGTTAG
		D1S1162-F *	Tet	0.81	Tetranucleotide	CCACACTATCATTTACCAGA
		D1S1162-R *				GGTTTCCTATGTTCCAAGC
3	*CRB1*	D1S1726-F	Tet	0.74	Dinucleotide	TGCCAGTTGACCTCAAG
		D1S1726-R				TCCAGTTGCTCCTCACC
		D1S2622-F *	Hex	0.79	Dinucleotide	CTGCAACATAAGAACCTAGTGTAAC
		D1S2622-R *				AAACTGGTAGGCCATTGATAGA

		D1S373-F	Fam	0.88	Tetranucleotide	GGGTGACAGAGCAAGACTC
		D1S373-R				CCCTGACCTCCCTTACAGA
		D1S1181-F *	Hex	0.87	Dinucleotide	GTGACAGAGCAAAACTCTG
		D1S1181-R *				CCTGGCCTTTCTTTTTAAAAAA
		D1S2853-F *	Fam	0.78	Dinucleotide	TACGTGACATGCATTAACCT
		D1S2853-R *				GCAAACAGACCGGAAAT
4	*CNCG2*	D16S682F	Fam	0.64	Tetranucleotide	TGGGTGACAGAGTAAGACCT
		D16S682R				ATCCACAGCCCACACTTAC
		D16S3120F	Hex	not known	Dinucleotide	CTGGGTGCGATTGCTC
		D16S3120R				GGCCCCATGACAGAAC
		D16S3080F	Tet	0.80	Dinucleotide	GGATGCCTGCTCTAAATACC
		D16S3080R				CCCAGGGGTCAAACTTAAT
5	*RBP1*	D3S 3646-F	Fam	0.72	Dinucleotide	ATGCAAGGGCTCAGACTCC
		D3S 3646-R				GAAGCATGTTTGAAGCTGCG
		D3S 2302-F	Tet	0.81	Tetranucleotide	AATCGCTTGAACCTGGGAG
		D3S 2302-R				GGAAAATTTTTCAGAAAGGGC
		D3S 3552-F	Hex	0.79	Dinucleotide	GCCACTCCCAAATGTCTGTC
		D3S 3552-R				AACTTGATTGCCCCCCTG
6	*RHO*	D3S 3584-F	Tet	0.65	Dinucleotide	CTCTCAGGTGGCAGCCAG
		D3S 3584-R				TTGAAGTGGATCTCACTCTCAGG
		D3S 3607-F	Fam	0.70	Dinucleotide	ACAGGCTCAGGCCCAC
		D3S 3607-R				CTAAGAATAGCTTCCCAGAAACGG
		D3S1671-F	Hex	0.75	Dinucleotide	CAAAAATGCTGCAATGAACAG
		D3S1671-R				GAGAAATGTCTATTCATGCCC
7	*PDE6B*	D4S 3038-F	Fam	0.78	Dinucleotide	GAAGACCAGCATTCGG
		D4S 3038-R				GGTTTAATACACAGTAATTGTTCA
		D4S 412-F	Hex	0.78	Dinucleotide	ACTACCGCCAGGCACT
		D4S 412-R				CTAAGATATGAAAACCTAAGGGA
		D4S 432-F	Tet		Dinucleotide	ACTCTGAAGGCTGAGATGGG
		D4S 432-R				CTGAACCGCAGATCCCC
		D4S2936-F *	Hex	0.84	Dinucleotide	CACTCAAGCCTGGGGG
		D4S2936-R *				TGGCACATCACCAACAAC
		D4S3023-F *	Hex	0.7	Dinucleotide	ACCTCACTGGAAACTAAATGG
		D4S3023-R *				TGAACAGCAGCGGTCT

		D4S2285-F *	Tet	0.75	Tetranucleotide	ATGAGCTCCTCTGAGAGG
		D4S2285-R *				GGAAAGAGGGCAAGACTC
8	*CNCG1*	D4S1518-F	Fam	0.75	Dinucleotide	TTGGGTCAGCTGAATGGTC
		D4S1518-R				GGCAGAGTCAAGACCCTGT
		D4S251-F	Hex	0.83	Dinucleotide	GTCTGAGAACAGAAATGCCTCC
		D4S251-R				TATGTATATATGTGTGCGTGCG
		D4S2971-F	Tet	0.80	Dinucleotide	GGTAAAATAATGATGTNGGCTAAAG
		D4S2971-R				GGTAATGAAAATCAAGCCCA
		D4S405-F	Fam	0.87	Dinucleotide	ATCAGGAGATGTTGCCTTGC
		D4S405-R				CAGGGCTATGATTGGATGTC
		D4S174-F *	Tet	0.87	Dinucleotide	AAGAACCATGCGATACGACT
		D4S174-R *				CATTCCTAGATGGGTAAAGC
		D4S2996-F *	Tet	0.81	Dinucleotide	ACTCAGGGTATTTGGGGCTA
		D4S2996-R *				GTTGCTTTTACGGAATCCAT
9	*PDE6A*	D5S 1375-F	Hex	0.75	Dinucleotide	TCTTCTGCTACCCCCCACA
		D5S 1375-R				GGGTCAATGAAGTATTTGCAC
		D5S 2090-F	Tet	0.83	Dinucleotide	CATGGGCATGTTTCAAAAT
		D5S 2090-R				AGTACCTCCTTAGTAACTCTGGGC
		D5S 594-F	Fam	0.80	Tetranucleotide	TTCTGGGAGGTAGAGGCTG
		D5S 594-R				GGAGCTACAGACATGGGCA
10_11	*RDS/ GUCA1A*	D6S 1575-F	Fam	0.82	Dinucleotide	GCATCTCCCCAAACACAAAC
		D6S 1575-R				ACTATGCTTCTGGGTCCCTG
		D6S 1582-F	Tet	0.83	Dinucleotide	CTAGGTAGTCAGGTGGTCATAGTC
		D6S 1582-R				AGTAGGGCTGGAACCTTCT
		D6S 1689-F	Fam	0.85	Dinucleotide	AGTTGTTTGATGNCCAGG
		D6S 1689-R				AGCTCTCCTACTTCTAGCAGATGAC
		D6S 1689-F	Hex	0.85	Dinucleotide	AGTTGTTTGATGNCCAGG
		D6S 1689-R				AGCTCTCCTACTTCTAGCAGATGAC
		D6S 936-F	Tet	0.81	Tetranucleotide	CAGTGAGGCCAGATTGTGC
		D6S 936-R				CATTTCAGCTTCCGCAGTAG
12	*TULP1*	D6S1568-F	Hex	0.87	Dinucleotide	ACATGACCAGAACTTCCCAG
		D6S1568-R				AGCTAGGCCAGGCCGT
		D6S273-F	Tet	0.77	Dinucleotide	GCAACTTTTCTGTCAATCCA
		D6S273-R				ACCAAACTTCAAATTTTCGG

		D6S388-F	Fam	0.75	Dinucleotide	GAGGAAGATGATGGGAAGC
		D6S388-R				AGAGAGAATAAGGGGCACG
		D6S1583-F *	Fam	0.84	Dinucleotide	GCCCCTAACCTGCTTCTACTGA
		D6S1583-R *				GCAGATGGCCCCACTGAC
		D6S1629-F *	Tet	0.79	Dinucleotide	TGCTGAACCCATAGTGGATTTTTG
		D6S1629-R *				AGCTGAGGGCTGCTGATGC
13	*ROM1*	D11S 4017-F	Hex	not known	Dinucleotide	TCAAAAAGATAGACTTTAACCAGCC
		D11S 4017-R				CCCCTCAAATTCCACACATC
		D11S 4357 F	Tet	not known	Dinucleotide	AACTTTATTTGTGCTGTAAAGGGG
		D11S 4357 R				GGGAAGTAGTCTCGGGTATGC
		D11S1883-F	Fam	0.74	Dinucleotide	TTCAGTAACAGGAGACAAAAGG
		D11S1883-R				TGGTTTCGGATCTCTTCTCA
14	*NRL*	D14S123-F	Tet	0.75	Tetranucleotide	CCCAGCATTTATCAACCATG
		D14S123-R				ACCTGGCCACCTATTCCTA
		D14S1042-F	Hex	0.80	Dinucleotide	TACTTGTGCATAACCGAGCA
		D14S1042-R				AATTACAGGCACCTGCCATC
		D14S972-F *	Fam	0.75	Dinucleotide	TTAACGCATAACAGCCAAGA
		D14S972-R *				TCTGACTGCCTCCATGA
		D14S64-F *	Hex	0.76	Dinucleotide	GGGCAACACAGTGAGACTCT
		D14S64-R *				TGGGATAGAAGCAACACAGA
		D14S990-F *	Fam	0.85	Dinucleotide	GTCCACTTGGTCATGGAAAC
		D14S990-R *				AAGTTGCACTGTGACTGGG
15	*RPGRIP*	D14S122-F		0.86	Tetranucleotide	CCAGCCTGGGTGAGACTC
		D14S122-R				CGTTCATGTACCACTGCATG
		D14S72-F	Fam	0.83	Dinucleotide	TGTAAAGTTTTGTACATGGTGTAAT
		D14S72-R				TCCTAACATTCTGCTACCCA
		D14S781-F		0.75	Dinucleotide	CTGCTATATCATGTGCCTTG
		D14S781-R				CTGGATTTTCTGCCTAGTCA
16	*RLBP1*	D15S 1046-F	Hex	0.77	Dinucleotide	CACACTAAAGTTGGCCTCA
		D15S 1046-R				CCCTTTTAACACACAGGGT
		D15S 202-F	Fam	0.84	Dinucleotide	AACCTGGGTGGCACAGTGAG
		D15S 202-R				CAGGACCTTTGCACAGGC
		D15S 972-F	Tet	0.77	Dinucleotide	GTCTGCGAAATAGGCAAGT
		D15S 972-R				CAACAGTTCTCAGGATAGATTCA

		D15S111-F *	Fam	0.73	Dinucleotide	AGTTCAGTTAGCCCTTTTAACA
		D15S111-R *				CACTAAAGTTGGCCTCAATC
		D15S963-F *	Hex	0.76	Dinucleotide	CAGCAAATCTCTGGAGCAC
		D15S963-R *				GCAACTTCTTGTAAGTAGCCTAGC
17	*GUCY2D*	D17S 1810-F	Fam	0.79	Dinucleotide	TGTCCACTGTAACCCCTG
		D17S 1810-R				CCTAGTGAGGGCATGAAAC
		D17S 1832-F	Hex	0.82	Dinucleotide	ACGCCTTGACATAGTTGC
		D17S 1832-R				TGTGTGACTGTTCAGCCTC
		D17S 796-F	Tet	0.82	Dinucleotide	CAATGGAACCAAATGTGGTC
		D17S 796-R				AGTCCGATAATGCCAGGATG
18	*PDE6G*	D4S 432-F	Tet	0.74	Dinucleotide	ACTCTGAAGGCTGAGATGGG
		D4S 432-R				CTGAACCGCAGATCCCC
		D17S 1161-F	Fam	0.88	Tetranucleotide	GCCAAGATAATGCCATTGCA
		D17S 1161-R				TTCTCCCTGTGCCCTCTAA
		D17S 948-F	Tet	0.83	Dinucleotide	GTCTCTGTCCTTAGGGAGTTTA
		D17S 948-R				TATCTTTGCCCATTTCTTG
		D17S 949-F	Hex	0.80	Dinucleotide	ATAGAAACTCCACATTTGCATTA
		D17S 949-R				CTTTCCCACNCGTGTC
19	*AIPL1*	D17S1353-F	HEx	0.88	Dinucleotide	CTGAGGCACGAGAATTGCAC
		D17S1353-R				TACTATTCAGCCCGAGGTGC
		D17S1791-F	Fam	0.85	Dinucleotide	AGCTTTTGGTCAACCTG
		D17S1791-R				GGGTGGGTGGAGTTAC
		D17S786-F	Tet	0.77	Dinucleotide	TACAGGGATAGGTAGCCGAG
		D17S786-R				GGATTTGGGCTCTTTTGTAA
20	*CRX*	D19S 219-F	Tet	0.77	Dinucleotide	GTGAGCCAAGATTGTGCC
		D19S 219-R				GACTATTTCTGAGACAGATTCCCA
		D19S 540-F	Fam	0.71	Dinucleotide	CAACTCAGCTCCTGCTGCTC
		D19S 540-R				GCGCAGTGAGGTGACTCTTG
		D19S 562-F	Hex	0.83	Tetranucleotide	GGGAGGCGGAGTTTGCAGT
		D19S 562-R				GGAGAGGCGCGGTACGTAA
21	*RGR*	D10S215-F *	Fam	0.82	Dinucleotide	TGGCATCATTCTGGGGA
		D10S215R *				GCTTTACGTTTCTTCACATGGT
		D10S1753F	Tet	0.744	Dinucleotide	CTGCTGCCACCAACCTAA
		D10S1753R				CAAGTGGAGACTCGATGACA

		D10S1675F	Hex	0.68	Dinucleotide	AAGAGGCAGTGTCGTCG
		D10S1675R				ACCTGTTGGAGCCACC
		D10S1744-F *	Tet	0.83	Dinucleotide	TCTCGTGTCTGACTCCCACC
		D10S1744-R *				ACAATAGACTGCTGCTGCTGC
		D10S1755-F *	Hex	0.76	Dinucleotide	CCATAGTATCAATGTGAGGGTG
		D10S1755-R *				TGGCTAATTTTTTAAGGTGTGT
22	*RP1*	D8S285-F	Fam	0.78	Dinucleotide	GCATCACACAGAATCTTTG
		D8S285-R				ATGGGTTTATGGCCTTTAC
		D8S1718-F	Tet	not known	Dinucleotide	ACGTGTGAATGACATCAGCC
		D8S1718-R				TAACCCCTGGGCAGTTG
		D8S166-F *	Hex	0.84	Dinucleotide	GATTGTGTCATTGCACTCCA
		D8S166-R *				ACAAGGAAGTTCCTTTTTGG
		D8S1763-F *	Hex	0.73	Dinucleotide	CAATGAAAGCCTTTATCTACAGGT
		D8S1763-R *				TTCCATTCACGGAGTAAAAGT
		D8S1696-F *	Tet	0.73	Dinucleotide	CTGCCCTAGAAGGCTAACTACC
		D8S1696-R *				TGCCATTTGCTCACTGAGAT
23	*PROML1*	D4S2942F	Fam	0.74	Dinucleotide	CAAATGCCCATCAATCAAC
		D4S2942R				GGGTCCAGTCTCATCCAC
		D4S403F	Hex	0.78	Dinucleotide	AGGTGGCCCTGAGTAGGAGT
		D4S403R				TTTGAGGGAATGATTTGGGT

Twenty-three candidate gene loci are shown with corresponding markers. * Markers were screened in a subset of families to confirm homozygosity.

Table 2A. Primers for amplification of coding regions of *PDE6B* gene

#	Primer name	Sequence	Annealing temp °C	$MgCl_2$ conc. in mM	Product size (bp)
1	PDE6B-1a-F	TTCATTCCACAGGGTCTGGTT	57	1.25	418
	PDE6B-1a-R	TTGATGCTCTCCTGCATATCC			
2	PDE6B-1b-F	TCTGCCAGGTGGAGGAGAG	59	1.25	440
	PDE6B-1b-R	AGCCTGTGCCCTGACAAGA			
3	PDE6B-2F	AGAGCTTGACGACAACCCCA	61	1.25	316
	PDE6B-2R	GATGCGCAGCACAGAACAG			
4	PDE6B-3F	CGTGTCTGGGCACCCTCA	57	1.25	294
	PDE6B-3R	ACAAGACCACCTGCCACCA			
5	PDE6B-4,5F	ACCTGTGTCAGGCTTGAGTTAA	53	1.25	460
	PDE6B-4,5R	AGTTGGAGTCAGGGAAACAGA			
6	PDE6B-6F	ATGCGTGTGGCTGTGTGTAG	57	1.25	318
	PDE6B-6R	ACGGCACACAGAGCACCA			
7	PDE6B-7,8-F	ACAGACATCCAGTCCCTCTGA	53	1.25	514
	PDE6B-7,8-R	CGAATTCACTTCATCATCGC			
8	PDE6B-9F	ACGGCTCTAGGGGAGAAGA	59	1.25	366
	PDE6B-9R	CACACACATGAGCACACGC			
9	PDE6B-10F	GCACACAGGCACATGGGA	63	2.5	288
	PDE6B-10R	GTGACCCCTGGACGACCT			
10	PDE6B-11F	ACCTTGTCCCACATGCGAA	61	2.5	191
	PDE6B-11R	AATGCAGAACTCTTCCTCCCA			
11	PDE6B-12F	AGAAAGGATGAGAAGCAAGTGG	55	2.5	297
	PDE6B-12R	ACCTGAGGCCCTGATCACAT			
12	PDE6B-13F	TGTGAAGTCAGCCACAGGTGC	57	1.25	254
	PDE6B-13R	TGCTTGAGTGCTGCCCTTG			
13	PDE6B-14F	AACCCGACGCCTAGGTCA	55	3.75	289
	PDE6B-14R	TTCTACATAGCCTGCTATGCGA			
14	PDE6B-15F	ATCTGGGGGGGCTGCAGA	68	5% DMSO, 3.75	236
	PDE6B-15R	ATACGGCCCTGCCGTCCT			
15	PDE6B-16F	ACAGGCAGCCGAGGCGGAA	69	1	304
	PDE6B-16R	ACGGAATCCGGGGCTGCGT			
16	PDE6B-17F	TCCCTGCAGACGGGCGCTT	57	2.5	289
	PDE6B-17R	TTCCTGCTCCAGAGCGTCTGGG			
17	PDE6B-18F	TGGGCAACAGAGCAAGACTC	59	1.25	265
	PDE6B-18R	TGCAAACAATGGTCCGTTG			
18	PDE6B-19F	AGAAGACCGAGGCTCGGA	59	2.5, 5% DMSO	300
	PDE6B-19R	ACAAAGTGAGATAAGGACCCCA			
19	PDE6B-20F	TCCATGAGCACATCTGAGTGAG	57	2.5	306
	PDE6B-20R	CATCCCTACTCCAGTGAGGACA			
20	PDE6B-21F	TGGGGAAGGGCTATCTTACTC	55	1.25	281
	PDE6B-21R	TCATTTTGCCTTGGGAGAGT			

21	PDE6B-22F	CAGGGGTTGGTAGAGGTCACA	59	2.5	266
	PDE6B-22R	CAGTCATTTTCTTGGGCTTCC			

Table 2B. Primers for amplification of coding regions of *CNCG1* gene.

#	Primer name	Sequence	Annealing temp ^{o}C	$MgCl_2$ conc. in mM	Product size (bp)
1	CNCG1-1F rep	GCAGCATGAGGACAGACTAATACAT	61	2.5	373
	CNCG1-1R rep	GACAAGTTATGCAGTTCCAAAGTG			
2	CNCG1-2F	AATTGTCCCCCTAGTGAGGAAT	60	2.5	309
	CNCG1-2R	TACTGCTCAAGGTCATCACCAT			
3	CNCG1-3F	TGGAGAAGAATTTGTTTTTTCAGAC	60	2.5	386
	CNCG1-3R	CACAGAGAAAGTCAACTGCATGAAC			
4	CNCG1-4-5-F	CAGGTCTTTGAATGCAAAGC	60	2.5	454
	CNCG1-4-5-R	GTCTTTACACAGGGCTCTTTACTA			
5	CNCG1-6-F	CTTCTCCAGCTTACTTCCATTTCAT	60	2.5	354
	CNCG1-6-R	TTACCACCTGCAGTAGAGAAAGGA			
6	CNCG1-7-F	AGTGTGCTGTGCTTCTCATCA	60	2.5	349
	CNCG1-7-R	CTTCACCTGTGCCTTTTTCTCT			
7	CNCG1-8a-F	TGACCTCAACAAAGTTAATTGACA	59	2.5	569
	CNCG1-8a-R	CAACCACCACAAAGACATACTCA			
8	CNCG1-8b-F	ACAGCCTTTACTGGTCTACACTG	60	2.5	597
	CNCG1-8b-R	GAATGCTGATCTCACCGAAGTA			
9	CNCG1-8c-F	GCAGATGATGGAGTCACTCAGTTT	61	2.5	553
	CNCG1-8c-R	GTCAGTCATAGGATCAAAAGGATCA			

Table 2C. Primers for amplification of coding regions of *CRB1* gene.

#	Primer name	Sequence	Annealing temp ^{o}C	$MgCl_2$ conc. in mM	Product size (bp)
1	CRB1-1F	TGAAGGAGCTGTAAGTAGGGTG	59	2.5	433
	CRB1-1R	CCTGAATACCTATTGGAAATCA			
2	CRB1-2a-F	TTTGGTTGAGGCAGCACAAA	59	2.5	454
	CRB1-2a-R	GAATCTTCCAGCATATCCAGCA			
3	CRB1-2b-F	TTCCTGTGGCAAGAACTCCT	59	2.5	442
	CRB1-2b-R	TGATTCCTGTCAAGAACTTGGC			
4	CRB1-3F	GAACATTTGACAAGTGCTCTGG	59	2.5	394
	CRB1-3R	CGAGAACGTGAGAGCTCTAAAT			
5	CRB1-4F	ATGGGTCTTGGGTTGATAGACA	59	2.5	442
	CRB1-4R	TGGGCAGCTTGGTAACCTACTT			
6	CRB1-5F	AATGCCAGTATAGCAGTCAACC	59	2.5	366
	CRB1-5R	AGCTCTTCCTGCTAATACACCA			
7	CRB1-6a-F	GCTATTCATGCACTTCTGCAAG	59	2.5	402

	CRB1-6a-R	TCGCCCTCAAATGAAAGTGT			
8	CRB1-6b-F	ATTCAGCTGCCTATGTCCATCT	59	2.5	415
	CRB1-6b-R	TGATTGATCACTTTCAAGTGGA			
9	CRB1-6c-F	AATCGACGACTCCTGTAAGGAGA	59	2.5	447
	CRB1-6c-R	TTTGCTGTTTCTGCTCTGCTCT			
10	CRB1-7a-F	TCCATCCCTTCTGTCTTTTGAG	59	2.5	350
	CRB1-7a-R	GGCTTGATTTTCAAAGATATCAA			
11	CRB1-7b-F	TGACTCCAAACTCTCCCAAA	62	2.5	468
	CRB1-7b-R	TGGTGGGTCAGTAACATCATCT			
12	CRB1-8F	CAGATATGTGGTTTCACCGTCA	59	2.5	380
	CRB1-8R	TACTCGCATAGGGGAAACAA			
13	CRB1-9a-F	GCACAGTATGTAACATGTATCAAATA	59	2.5	639
	CRB1-9a-R	GAAACCATGAACATTTTCAAAG			
14	CRB1-9b-F	CCTGCAAGGGTGTCTAAGTACA	59	2.5	558
	CRB1-9b-R	GAGGAGAGAGCTTTCCAATTTG			
15	CRB1-10F	CTCCTCCAGCCTGAGTACTTAA	61	2.5	367
	CRB1-10R	CAGCATAGATTTTCCTATGGGA			
16	CRB1-11F	GGATGGGTAGATAAGACTGTGC	59	2.5	356
	CRB1-11R	TGTTCACCCCACTCAACAACT			
17	CRB1-12F	CCTGAGTAGTTCCATTGTCCTGA	61	2.5	407
	CRB1-12R	TTCCAGTGTAATCCCAGTTGCA			

Table 2D. Primers for amplification of coding regions of *TULP1* gene

#	Primer name	Sequence	Annealing temp ^{o}C	$MgCl_2$ conc. in mM	Product size (bp)
1	TULP1- 1,2-F	AGTTGAGATTCTTCCCCCAGT	57	2.5	476
	TULP1- 1,2-R	TACCCTGCGTGGGTTTACG			
2	TULP1- 3F	TTATTTCTGGCGGCTCAAGG	55	2.5	324
	TULP1- 3R	AATCCCTCCCCTCTCATCACT			
3	TULP1- 4F	TAGCGGGTAGAGGCGCTGC	69	2.5	296
	TULP1- 4R	GTCCAGCCAGCCCCTTCTC			
4	TULP1- 5F	CAGTCTGGAGGAACTGGGCT	59	2.5	317
	TULP1- 5R	TCAATCGCTGTGTCTCAGTGA			
5	TULP1- 6,7-F	TTGGAAGGCAGCCTTCAG	59	2.5	441
	TULP1- 6,7-R	TTGTATGCTGTAAGGACCCTCT			
6	TULP1- 8F	GGGCTCTAATAATAACATGGGG	59	2.5	309
	TULP1- 8R	TCTAGGCTCCCAAGTCCAGG			
7	TULP1- 9,10-F	ATGAGGGGCAGTGGCTTC	61	2.5	433
	TULP1- 9,10-R	AGAAATCAGGCCCGTTTGT			
8	TULP1- 11F	ATTTCTCCCTGCAGCTCACC	69	2.5	272
	TULP1- 11R	TACCAGGCACAGCAGGACA			
9	TULP1- 12,13-F	TTGGCTGTGTGGAAGGGG	59	2.5	451
	TULP1- 12,13-R	TCAGGGAGTTGGCTATTTCCTA			
10	TULP1- 14F	AGCCATCTCAGCCATCTCTAA	61	2.5	296
	TULP1- 14R	CTTGAATGAAGGTCAGCATCCT			

11	TULP1- 15F	ATGGGGGTCCAAGGAGGT	61	2.5	295
	TULP1- 15R	ACACAGGAGCAGTTTTCCGC			

Table 2E. Primers for amplification of coding regions of *RLBP1* gene.

#	Primer name	Sequence	Annealing temp ^{o}C	$MgCl_2$ conc. in mM	Product size (bp)
1	RLBP-3-4-F	CGGGTGATTCTGATGCAATT	60	2.5	673
	RLBP-3-4-R	TTTTCACAGGAGAGAGAATGCAG			
2	RLBP-5F	TCTAGCTCTGGCAGGAGACTCAT	61	2.5	400
	RLBP-5R	TTGCCCACAGTATGGAAGCA			
3	RLBP-6F	GGTCAGGTCTCTGAGTCCCACTA	61	2.5	354
	RLBP-6R	TGGAGAACCAGGAATGAGGG			
4	RLBP-7F	GAATGTACCAATTAGCTCTCCCC	60	2.5	346
	RLBP-7R	CAACTTCTCAGTTCCCTGCAA			
5	RLBP-8F	TGATGCTGGACAAGTCTGTTCT	56	2.5	321
	RLBP-8R	ATCCACATAGCTCAGGACCAT			
6	RLBP-9F	TCCCTCAACCCTCATCCTTAG	60	2.5	457
	RLBP-9R	CAAGGGCAGGTGGAAATATAAC			

Table 2F: Primers for amplification of coding regions of *RP1* gene.

#	Primer name	Sequence	Annealing temp ^{o}C	$MgCl_2$ conc. in mM	Product size (bp)
1	RP1-2a-F	TCCTGGATGTCTGCAGCTATAT	60	2.5	465
	RP1-2a-R	CTTTGTCCAGGTCTACAGGCT			
2	RP1-2b-F	TTGGAGTGAGGAACATCAGC	56	2.5	462
	RP1-2b-R	ACCATTCATATCCCACACGA			
3	RP1-3F	GCCTAGGAGGTTGTTGATTTGA	60	2.5	381
	RP1-3R	TTTCGTTTCTGTGGTGGAAGA			
4	RP1-4a-F	GCTGCCTCTTCCTTTGGATATT	60	2.5	593
	RP1-4a-R	TCCACAGTAGCATTCTCCCAA			
5	RP1-4b-F	AAGCAGTAATCAAGAGGGCAGT	60	2.5	585
	RP1-4b-R	CCAGTTTTGTTGTCCAATACCA			
6	RP1-4c-F	TGTCACATAATAATGGTTTGCCA	60	2.5	587
	RP1-4c-R	CTTGGAAATCGTGGAATTGAG			
7	RP1-4d-F	AGGAGGGATACTTTGTGAGGAAGA	61	2.5	609
	RP1-4d-R	GGATTTATGTTCTGCAACCAACTC			
8	RP1-4e-F	CAACCAGGGCAAATTCTTTAGC	60	2.5	599
	RP1-4e-R	AAGCATCAGGACTGGTAAGAGGT			
9	RP1-4f-F	AAAAAGGCAAAGTGTAGAGGCTG	57	2.5	596
	RP1-4f-R	ATGGAGAGCAAGTCACTTCCAA			
10	RP1-4g-F	CACAAGGAATCTCCTCTTTGGA	60	2.5	606
	RP1-4g-R	CATCCTGAAACTTCCTTAGTGAAC			
11	RP1-4h-F	GTGGCCTTTGCCTAAGTGAAA	60	2.5	605

	RP1-4h-R	ACTGTCACTGTCAGGCCGATA			
12	RP1-4i-F	GGAAGTTATTCAGAGTCCTCTCC	62	2.5	584
	RP1-4i-R	CACATGCCAGGATTTTCAGA			
13	RP1-4j-F	TGATAGCAGAATCCTCACAGACA	60	2.5	613
	RP1-4j-R	TTCCTCATTCATGGGTTGGA			
14	RP1-4k-F	TTCAGGAAGCTGACTCTTTGGA	56	2.5	551
	RP1-4k-R	GTTGAGATTTGTTCTTGAGCCC			
15	RP1-4L-F	TCAGCGGTCAGACAAATGAA	60	2.5	515
	RP1-4L-R	GAACCTGAGTCTGTAATTGTTGGA			

Table 2G: Primers for amplification of coding regions of *RGR* gene.

#	Primer name	Sequence	Annealing temp ^{o}C	$MgCl_2$ conc. in mM	Product size (bp)
1	RGR-1F	AACAGCCCAAGGTCCAACATAA	60	2.5	304
	RGR-1R	TTTGGGGACCTCTCCTCTCCT			
2	RGR-2F	GTCCAGGAGGTTGCTGATGTT	58	2.5	411
	RGR-2R	CAATCTGGAATTCAGCCCATT			
3	RGR-3F	ACCAATATTAAGGCCCTCTTCAG	58	2.5	392
	RGR-3R	TATGCATGCACACTCACACCTA			
4	RGR-4F	CACTTGAAGGGACACTCTTCGA	60	2.5	362
	RGR-4R	CGTTGACATTTCCCCATTTG			
5	RGR-5F	TTTCCCCACAACCGATCAT	60	2.5	315
	RGR-5R	CTGTTTGTGTGTGTCACATCCA			
6	RGR-6F	TGAAGCCTGGTCCATGCT	60	2.5	325
	RGR-6R	CTGACACAGAGGTCATAAATCCA			
7	RGR-7F	AATGATTGGCAGTTGTAGGTGG	58	1.25	376
	RGR-7R	AATCCTGTGTCCAGCCTAGGA			

Table 2H: Primers for amplification of coding regions of *NRL* gene.

#	Primer name	5' to 3' sequence	Annealing temp ^{o}C	$MgCl_2$ conc. in mM	Product size (bp)
1	NRL-3F	TTTGAGGGAAGAGGGACTTGGT	61	2.5	593
	NRL-3R	TGTCCCCTGTCCCAGTCCATA			
2	NRL-4F	TTCCGGTGAAGGTGGGAG	56	2.5	547

Table 2I: Primers for amplification of coding regions of *ABCA4* gene.

#.	Primer name	5' to 3' sequence	Annealing temp	$MgCl_2$ conc. in mM	Product

			°C		**size (bp)**
1	ABCA-1F	CGCTCTTAACGGCGTTTATG	58	3.75	210
	ABCA-1R	CCCACACTTCCAACCTGTTT	58	3.75	
2	ABCA-2F	AAGTCCTACTGCACACATGG	57	1.25	289
	ABCA-2R	ACACTCCCACCCCAAGATC			
3	ABCA-3F	CTGCATCCTGCTTGGTCTCC	66	2.5	256
	ABCA-3R	CACGTGAAGGGGTGTGCAA			
4	ABCA-4F	TGGGTGACAGAGCGAGATAA	55	2.5	285
	ABCA-4R	ATAGGTGAGGGAAATGATGCT			
5	ABCA-5F	TGTTTCCAATCGACTCTGGC	60	2.5	279
	ABCA-5R	TTCTTGCCTTTCTCAGGCTG			
6	ABCA-6F	TGGGTGTCTTTCCTACCACA	55	1.25	290
	ABCA-6R	CACCTTGCAATTGGCGAGC			
7	ABCA-7F	CAGACTGTGCCTATGTGTGT	58	2.5	230
	ABCA-7R	TGACATAAGTGGGGTAAATGG			
8	ABCA-8F	GAGCATTGGCCTCACAGCA	55	2.5	348
	ABCA-8R	AGAGGCCAATTTATAAGCAGG			
9	ABCA-9F	AGACATGTGATGTGGATACAC	58	2.5	270
	ABCA-9R	GGGAGGTCCAGGGTACACAA			
10	ABCA-10F	ACACAACCAAAAGTTCTCTCTC	51	2.5	284
	ABCA-10R	GCGATTAACTCTTTCCTGGG			
11	ABCA-11F	TCTAAGCAGAGCAGTGACTG	53	2.5	285
	ABCA-11R	CTCATGGGGCTATCTTCAAG			
12	ABCA-12F	CTCTCTCAACTTTGTGACTCT	58	2.5	270
	ABCA-12R	TTTGGAGAAATGCAGCGAGC			
13	ABCA-13F	GAGCTATCCAAGCCCGTTC	58	2.5	267
	ABCA-13R	CATTAGCGTGTCATGGAGGA			
14	ABCA-14F	CTCTACCAGGTACAGAGCAC	58	2.5	332
	ABCA-14R	AAAGGGGAAAGGAACCAAAGT			
15	ABCA-15F	AGGCTGGTGGGAGAGAGC	63	2.5	407
	ABCA-15R	AGTGGACCCCCTCAGAGG			
16	ABCA-16F	CATCTGGGTGCTGTTGCATTGG	59	1.25	329
	ABCA-16R	AGGGCTGGGGATCTGAAGAACT			
17	ABCA-17F	AACTGCGGTAAGGTAGGATAGGG	59	1.25	217
	ABCA-17R	GGGCCACCTCTGTGATCCATA			
18	ABCA-18F	CTCTCCCCTCCTTTCCTGCCTT	58	1.25	265
	ABCA-18R	GCTTCTTTCCACCCTTGCCAT			
19	ABCA-19F	TGGGGCCATGTAATTAGGC	55	1.25	322
	ABCA-19R	TGGGAAAGAGTAGACAGCCG			
20	ABCA-20F	TGAACCTGGTGTGGGGGTGG	61	1.25	304
	ABCA-20R	GCCTGGCACCCCTGAGCTG			
21	ABCA-21F	CAGCTGCTGGAAGTGGAAGTGC	63	1.25	267
	ABCA-21R	GCCTCCTGGGTGCACTGGG			
22	ABCA-22F	AAGGTACCCCCACAATGCCAC	63	1.25	307
	ABCA-22R	AATGGCAGGTGAGAGAGTGGG			
23	ABCA-23F	CTTTACCAACAATGCCCAACCC	63	1.25	315
	ABCA-23R	GCCCCGTGCTGTGTGCTC			

24	ABCA-24F	TGACAGCAGCTGGCATCAGG	59	1.25	211
	ABCA-24R	GGAGATGGCTGCCAGACGGA			
25	ABCA-25F	TCCTCTGAAAGAGTCACTGCCG	58	2.5	423
	ABCA-25R	AACGATGGCTTTTTGCTTTTACAA			
26	ABCA-26F	AATACCCAACAAAACAGAGCTTG	53	1.25	212
	ABCA-26R	CCAGCCCCTTAGACTTTCG			
27	ABCA-27F	GGCATTAGAGATCCAGACCTTA	58	1.25	383
	ABCA-27R	GGAAGGCTGGGAGAGGAG			
28	ABCA-28F	CGCGCACGTGTGACATCTCC	58	1.25	239
	ABCA-28R	TGACCCAGGTGCCCCAAA			
29	ABCA-29F	GCATGATGTTGGCACGCGCC	58	1.25	229
	ABCA-29F	CTGCCATCTTGAACCCACC			
30	ABCA-30F	GCCTAGGGATTTGTCAGCAAC	58	2.5	328
	ABCA-30R	AGACTCAGGAGATACCAG			
31	ABCA-31F	GTGAGAACTAGGGAGATGCCAG	59	2.5	291
	ABCA-31R	TTCTACAGGGAGCCAGGATAAA			
32	ABCA-32F	TTAACGGCACTGCTGTACTTGT	66	2.5	169
	ABCA-32R	GGTGTGCCTTTTAAAAGTGTGC			
33	ABCA-33,34F	TAGTAGGCGTGAAGTTCGTGGC	61	2.5	471
	ABCA-33,34R	CAGCAGGAGGAGGGATGGAAT			
34	ABCA-35F	CCTTCCTGCTTCTCAAATTTCC	59	2.5	345
	ABCA-35R	CGCGGTGGTGAGAATCCTC			
35	ABCA-36F	TCCTCCTTCTGCTCTTCCCTC	61	2.5	311
	ABCA-36R	TGGTCCTTCAGAGCACACACAA			
36	ABCA-37F	GCAGAGCTGGCAGCAGGTCT	70	1.25	276
	ABCA-37R	ACCACCACAGGACAGCCCAG			
37	ABCA-38F	TTGTAGGTGGAATGGAATGTGG	59	2.5	276
	ABCA-38R	GGCTCTGCTCGACCAACA			
38	ABCA-39F	GAGAGCATCTGGGCCCCACCTG	70	1.25	268
	ABCA-39R	CCCGGTAACCCTCCCAGCTT			
39	ABCA-40F	AGTGGGCCCTGTGCTGTGG	59	2.5	318
	ABCA-40R	AAAAACATTGTGGAGTGGGGCT			
40	ABCA-41F	CCCATGGAAAGGACAGTGCC	57	2.5	247
	ABCA-41R	CAACATCATGCCAACTGTGGAT			
41	ABCA-42F	CCCTCCTTGCTCTCACCCTG	70	2.5	190
	ABCA-42R	TATGGGGAGGAGAGGCAGGC			
42	ABCA-43F	CACTTACCCTGGGGCCTGAC	69	3.75	258
	ABCA-43R	GGTCTGATGATCACCCTTCCTAT			
43	ABCA-44F	GGTCATCCCTCCACTCCTTG	59	2.5	261
	ABCA-44R	GCACTCTCATGAAACAGGCTTG			
44	ABCA-45F	GGCTTTGAACTGGGGGAGGT	59	2.5	271
	ABCA-45R	ATTTCCCCAACCCAAGAGACC			
45	ABCA-46,47F	CCAGGGGGAAGCAGTAATCAG	60	2.5	389
	ABCA-46,47R	CAGGTGGATCCACAGAAGGCA			
46	ABCA-48F	GGATTACCTTAGGCCCAACCA	63	2.5	393
	ABCA-48R	CCTCCCTCTTATGGCAATTCC			
47	ABCA-49,50F	AGAGCAAAGTGGGTAGGTGGG	68	2.5	220
	ABCA-49,50R	GCTCTGAGCCAAGGAACTGC			

Table 2J: Primers for amplification of coding regions of *RPE65* gene.

#	Primer name	Sequence	Annealing temp ^{o}C	$MgCl_2$ conc. in mM	Product size (bp)
1	RPE-1F	GAGAGCTGAAAGCAACTTCTG	52	1.25	244
	RPE-1R	ATAGCACATTTATCATGAATCCATG			
2	RPE-2F	CTATCTCTGCGGACTTTGAGC	56	1.25	199
	RPE-2R	GCCAGAGAAGAGAGACTGAC			
3	RPE-3F	AGGACAAGCCTAGCCCAAG	56	1.25	263
	RPE-3R	CCAAGCTAGGCCCTACTTTG			
4	RPE-4,5F	CTGTACGGATTGCTCCTGTC	56	1.25	501
	RPE-4,5R	TTAGAATCATACATTCGCAGCATG			
5	RPE-6F	TTCAAGGGGTAGTGATGACCTC	56	1.25	341
	RPE-6R	TGCACAAAATGCTATTCTGACAT			
6	RPE-7F	AAAATGTGTTTCTTTGCCTGTA	57	2.5	253
	RPE-7R	GTATCAAAGGTAGGCAAAGCAA			
7	RPE-8,9F	GTCTGTGGCTTGAGAATCAGC	60	1.25	500
	RPE-8,9R	AAAACCCCGTAATTTCCAGG			
8	RPE-10F	AGAACAGGCAGGCACTTGTG	60	1.25	302
	RPE-10R	CATGAGGCAGGAGGACAATT			
9	RPE-11F	GCTGTTTGAATTCTTTCCTGC	56	1.25	216
	RPE-11R	AAGAAACATTTGTTCACTCCCG			
10	RPE-12-13F	TAGAGAAAACTTCACACGGGAG	53	1.25	455
	RPE-12-13R	GAACTAACATACAGAACTGCAG			
11	RPE-14F	AGCTTGGGCTTTTAAAAACTC	50	1.25	281
	RPE-14R	TTGAACAGAATTTGATTGCAGA			

Table 2K: Primers for amplification of coding regions of *RDS* gene

#	Primer name	Sequence	Annealing temp ^{o}C	$MgCl_2$ conc. in mM	Product size (bp)
1	RDS1a-F	CTCTGGGCTCGTTAAGGTTTGG	57	1.25	307
	RDS1a-R	TCCCAGCCAGCGAGTTGAAGA			
2	RDS1b-F	CCGAAAGAGGAGCGATGTGATG	57	1.25	367
	RDS1b-R	GCCGCAGCATTTGAACTCGA			
3	RDS1c-F	CCAAGGGCTCAAGAACGGCA	60	1.25	272
	RDS1c-R	GGGGAGAGGGGCTGGTCAGA			
4	RDS2-F	GGTTTCCAGAGGCAGGGGTTG	64	1.25	405
	RDS2-R	CTCCGCCCCCATTAGACCCA			
5	RDS3-F	GGTCCAGCTCCCAGCGATTCT	60	1.25	371
	RDS3-R	CCTTGGGAGATTCAGACTTTCGG			

Table 2L: Primers for amplification of coding regions of *RD3* gene

#	Primer name	Sequence	Annealing temp ^{o}C	$MgCl_2$ conc. in mM	Product size (bp)
1	RD3-2F	TTCCCAGGTTCCCCACTCTG	63	1.25	436
	RD3-2R	CCACTGCAGCCACCTTTCCT			
2	RD3-3F	GACGCCCGGGGTGCCAGAC	67	1.25	439
	RD3-3R	GTTCCAGGGCCCGGCGCT			

LIST OF PUBLICATIONS

1. **Hardeep Pal Singh**, Subhadra Jalali, J Fielding Hejtmancik and Chitra Kannabiran. Homozygous Null Mutations in the ABCA4 Gene in Two Families With Autosomal Recessive Retinal Dystrophy. *American Journal of Ophthalmology*. 2006;141:906-913.

2. James S. Friedman, B Chang, Chitra Kannabiran, Christina Chakarova, **Hardeep P. Singh**, Subhadra Jalali, Norman L. Hawes, Kari Branham, Mohammad Othman, Elena Filippova1, Debra A. Thompson, Andrew Webster, Sten Andréasson, Samuel G. Jacobson, Shomi S. Bhattacharya, John R. Heckenlively, and Anand Swaroop. Premature truncation of a novel protein, RD3, exhibiting sub-nuclear localization is associated with retinal degeneration. *American Journal of Human Genetics*. 2006;79:1059-1070.

3. **Hardeep Pal Singh**, Subhadra Jalali, Raja Narayanan, Chitra Kannabiran. Genetic analysis of Indian families with autosomal recessive retinitis pigmentosa by homozygosity screening. *Investigative Ophthalmology and Visual Science*. *2009 Apr 1. [Epub ahead of print]*

LIST OF PRESENTATIONS

1. Oral presentation in the Asia ARVO meeting, January 2009, Hyderabad, India.
2. Poster presentation in the Human Genome Organization Meeting, September 2008, Hyderabad, India.
3. Oral Presentation in the Indian Eye Research Group Annual Conference, July 2008. Aravind Eye Care Systems, Madurai.
4. Presented a poster and Hyde park presentation in the Annual conference of The All India Ophthalmological Society, February 2007, Hyderabad, India
5. Presented a poster in the Indian Society of Human Genetics annual conferences, January 2006. JNU Delhi.
6. Presented a poster in the Indian Eye Research Group Annual Conference, July 2006. LVPEI Hyderabad.
7. Presented a poster in the Indian Eye Research Group Annual Conference, July 2005. LVPEI Hyderabad.

LIST OF AWARDS

1. Awarded senior research fellowship from CSIR, India, for the PhD.

2. Awarded travel fellowship in the annual conference of Indian Eye Research Group, July 2008, Aravind Eye Care Systems, Madurai, India.

BRIEF BIOGRAPHY OF THE CANDIDATE

Academic Career

PhD degree (March 2004 – till date): Topic "Molecular Genetic Studies on Retinal Dystrophies" in the field of human genetics at the L. V. Prasad Eye Institute (LVPEI), Hyderabad, India.

Project fellow (October 2002- February 2004): Worked as a project fellow in a collaborative project of Anthropology and Human Genetics Unit of Indian Statistical Institute (ISI) Kolkata and Centre for Cellular and Molecular Biology (CCMB) Hyderabad. Title of project "DNA Polymorphisms in the Caste and Tribal Populations of Andhra Pradesh"

MSc, Human Genetics (2000-2002): Guru Nanak Dev University (GNDU) Amritsar. Dissertation topic "Chromosomal abnormalities in the gastrointestinal tract cancer patients"**.**

Publications

1. James S. Friedman, B Chang, Chitra Kannabiran, Christina Chakarova, **Hardeep P. Singh**, Subhadra Jalali, Norman L. Hawes, Kari Branham, Mohammad Othman, Elena Filippova1, Debra A. Thompson, Andrew Webster, Sten Andréasson, Samuel G. Jacobson, Shomi S. Bhattacharya, John R. Heckenlively, and Anand Swaroop. Premature truncation of a novel protein, RD3, exhibiting sub-nuclear localization is associated with retinal degeneration. *American Journal of Human Genetics*. 2006;79:1059-1070.
2. **Hardeep Pal Singh**, Subhadra Jalali, J Fielding Hejtmancik and Chitra Kannabiran. Homozygous Null Mutations in the ABCA4 Gene in Two Families With Autosomal Recessive Retinal Dystrophy. *American Journal of Ophthalmology*. 2006;141:906-913.

3. B. Mohan Reddy, Vikrant Kumar, Banrida T. Langstieh, Komal. V. Madhavi, Vegi. M. Naidu, **Hardeep Pal Singh**, Silpak Biswas, Kumarasamy Thangaraj & Lalji Singh. Global Patterns in Human Mitochondrial DNA and Y-Chromosome Variation Caused by Spatial Instability of the Local Cultural Processes. *PloS Genetics*. 2006;2:420-424.

4. Kamlesh Guleria, **Hardeep Pal Singh**, Jagmohan Singh, Harpreet Kaur, Vasudha Sambyal. Non-random chromosomal aberrations in peripheral blood leucocytes of gastrointestinal tract and breast cancer. *International Journal of Human Genetics*. 2005;5:205-211.

5. K. Guleria, **H. Singh**, H. Kaur and V. Sambyal. ABO Blood Groups in Gastrointestinal Tract (GIT) and Breast Carcinoma Patients. *The Anthropologist*. 2005;7:189-192.

6. B.Mohan Reddy, A.N. Srikar Reddy, T. Nagaraju, L.V.K.S Bhaskar, **H.P. Singh**, V.M.Naidu, K. Thangaraj, A. Govardhan Reddy, A.Nirmala, Lalji Singh. Anthropological Perspective of the single nucleotide polymorphisms in the NPY and DRD2 Genes among the Socio-Economically Stratified Populations of Andhra Pradesh, India. *International Journal of Human Genetics*. 2007; 7:277-284.

7. **Hardeep Pal Singh**, Subhadra Jalali, Raja Narayanan, Chitra Kannabiran. Genetic analysis of Indian families with autosomal recessive retinitis pigmentosa by homozygosity screening. *Invest Ophthalmol Vis Sci. April 1,* **[Epub ahead of print]**

BRIEF BIOGRAPHY OF THE SUPERVISOR

Name: Chitra Kannabiran

Educational background

1981 – 1984:	M.Sc. (Medical Biochemistry) JIPMER, University of Madras, Pondicherry.
1984 – 1989:	Ph.D. Indian Institute of Science, Banglore. Title of thesis: Antibodies to dpG: sequence-dependent binding to dsDNA. (Advisor: Prof. T. M. Jacob)

Research and Professional Experience

1989 – 1992:	Post-doctoral fellow, Cold Spring Harbor Laboratory, New York. Worked in the area of transcriptional regulation by adenoviral oncoproteins.
1992 – 1995:	Research Associate, Dept. of Biochemistry, University of Medicine and dentistry, New Jersey. Worked in the area of transcriptional regulation in mammalian cells.
1997 –1998:	Visiting Fellow, National Eye Institute, NIH, Bethesda, Maryland. Gained experience in ophthalmic molecular genetics and worked on identifying a gene causing congenital cataract and expression in transgenic mice.
1996 – present:	Scientist (Dept. of Molecular Genetics), L. V. Prasad Eye Institute, Hyderabad. Involved in setting up of molecular genetics facility (1998-1999) and initiation of work in molecular genetics of eye diseases.
Reviewer:	Reviewer of Indian Journal of Ophthalmology, Journal of Genetics, Molecular Vision, American Journal of Ophthalmology, Eye, Journal of Medical Genetics, BMC Medical Genetics, Orphanet J Rare Diseases, IOVS, etc.
Associate editor	Journal of Genetics

Publications in peer – reviewed journals

1. Genetic analysis of Indian families with autosomal recessive retinitis pigmentosa by homozygosity screening. Hardeep Pal Singh, Subhadra Jalali, Raja Narayanan, **Chitra Kannabiran**. Invest Ophthalmol Vis Sci (accepted March 2009).

2. Immunophenotypes of macular corneal dystrophy in India and correlation with mutations in CHST6. Sultana A, Klintworth GK, Thonar EJ, Vemuganti GK, **Kannabiran C**. Mol Vis. 2009;15:319-25.
3. Phenotypic Characterization of Retinoblastoma for the Presence of Putative Cancer Stem-like Cell markers by Flow Cytometry. Balla MM, Vemuganti GK, **Kannabiran C**, Honavar SG, Murthy R. Invest Ophthalmol Vis Sci. 2008 Nov 21. [Epub ahead of print]
4. Retintis pigmentosa: genetics and genetics and gene-based approaches to therapy. **Chitra Kannabiran**. Expert Rev Ophthalmol. 2008;3:417-429.
5. A missense mutation in LIM2 causes autosomal recessive congenital cataract. Ponnam SP, Ramesha K, Tejwani S, Matalia J, **Kannabiran C**. Mol Vis. 2008 Jun 23;14:1204-8.
6. Mutational spectrum of the SLC4A11 gene in autosomal recessive congenital hereditary endothelial dystrophy. Sultana A, Garg P, Ramamurthy B, Vemuganti GK, **Kannabiran C**. Mol Vis. 2007 Jul 26;13:1327-32.
7. Share, learn and get together: knowledge and information interactions at the XLV International Symposium of ISCEV - Hyderabad, India, 25-29 August 2007. Jalali S, Kondo M, Narayanan R, **Kannabiran C**, McCulloch DL. Doc Ophthalmol. 2007 Jul;115(1):1-2.
8. Mutation of the gap junction protein alpha 8 (GJA8) gene causes autosomal recessive cataract. Ponnam SP, Ramesha K, Tejwani S, Ramamurthy B, **Kannabiran C**. J Med Genet. 2007 Jul;44(7):e85.
9. Gene expression signatures in stem cells. Vemuganti GK and **Kannabiran, C**. *Int J Hum Genet* 2007; **7**(1): 83-89
10. Autosomal recessive corneal endothelial dystrophy (CHED2) is associated with mutations in SLC4A11. Jiao X, Sultana A, Garg P, Ramamurthy B, Vemuganti GK, Gangopadhyay N, Hejtmancik JF, **Kannabiran C**. J Med Genet. 2007 Jan;44(1):64-8.
11. Premature truncation of a novel protein, RD3, exhibiting sub-nuclear localization is associated with retinal degeneration. James S. Friedman, B Chang, **Chitra Kannabiran**, Christina Chakarova, Hardeep P. Singh, Subhadra Jalali, Norman L. Hawes, Kari Branham, Mohammad Othman, Elena Filippova1, Debra A. Thompson, Andrew Webster, Sten Andréasson, Samuel G. Jacobson, Shomi S. Bhattacharya, John R. Heckenlively, and Anand Swaroop. American Journal of Human Genetics. 2006;79:1059-1070.
12. TGFBI mutations in corneal dystrophies. **Kannabiran C**, Klintworth GK. Hum Mutat. 2006; 27(7), 615-625.
13. Homozygous Null Mutations in the ABCA4 Gene in Two Families With Autosomal Recessive Retinal Dystrophy. Hardeep Pal Singh, Subhadra Jalali, J Fielding Hejtmancik and **Chitra Kannabiran**. American Journal of Ophthalmology. 2006;141:906-913.
14. Allelic heterogeneity of the carbohydrate sulfotransferase-6 gene in patients with macular corneal dystrophy. Sultana A, Sridhar MS, Klintworth GK, Balasubramanian D, **Kannabiran C**. Clin Genet. 2005;68:454-60.

15. Genotype-phenotype correlation in 2 Indian families with severe granular corneal dystrophy. **Kannabiran C**, Sridhar MS, Chakravarthi SK, Vemuganti GK, Lakshmipathi M. Arch Ophthalmol. 2005;123:1127-33.
16. TGFBI gene mutations causing lattice and granular corneal dystrophies in Indian patients. Chakravarthi SV, **Kannabiran C**, Sridhar MS, Vemuganti GK. Invest Ophthalmol Vis Sci. 2005;46:121-5.
17. Novel mutations of the carbohydrate sulfotransferase-6 (CHST6) gene causing macular corneal dystrophy in India. Sultana A, Sridhar MS, Jagannathan A, Balasubramanian D, **Kannabiran C**, Klintworth GK. Mol Vis. 2003;22:730-4.
18. Mutational screening of the RB1 gene in Indian patients with retinoblastoma reveals eight novel and several recurrent mutations. Kiran VS, Chakravarthi K, **Kannabiran C**, Vemuganti GK, Honavar SG. Hum Mutat. 2003 Oct;22(4):339.
19. Screening for homozygosity by descent in families with autosomal recessive retinitis pigmentosa. Lalitha K, Jalali S, Kadakia T, **Kannabiran C**. J Genet. 2002;81:59-63.
20. Mutational analysis of the RB1 gene in Indian patients with retinoblastoma. Ata-ur-Rasheed M, Vemuganti G, Honavar S, Ahmed N, Hasnain S, **Kannabiran C**. Ophthalmic Genet. 2002;23:121-8.
21. Reliability of nested polymerase chain reaction in the diagnosis of bacterial endophthalmitis. Sharma S, Das D, Anand R, Das T, **Kannabiran C**. Am J Ophthalmol. 2002;133:142-4.
22. Molecular genetics of cataract. **Kannabiran C**, Balasubramanian D. Indian J Ophthalmol. 2000;48:5-13.
23. Dual action of the adenovirus E1A 243R oncoprotein on the human proliferating cell nuclear antigen promoter: repression of transcriptional activation by p53. **Kannabiran C**, Morris GF, Mathews MB. Oncogene. 1999;18:7825-33.
24. Autosomal dominant zonular cataract with sutural opacities is associated with a splice mutation in the betaA3/A1-crystallin gene. **Kannabiran C**, Rogan PK, Olmos L, Basti S, Rao GN, Kaiser-Kupfer M, Hejtmancik JF. Mol Vis. 1998;4:21.
25. The mammalian transcriptional repressor RBP (CBF1) regulates interleukin-6 gene expression. **Kannabiran C**, Zeng X, Vales LD. Mol Cell Biol. 1997;17:1-9.
26. Structure-function analysis of the TBP-binding protein Dr1 reveals a mechanism for repression of class II gene transcription. Yeung KC, Inostroza JA, Mermelstein FH, **Kannabiran C**, Reinberg D. Genes Dev.1994;8: 2097-109.
27. The adenovirus E1A 12S product displays functional redundancy in activating the human proliferating cell nuclear antigen promoter. **Kannabiran C**, Morris GF, Labrie GF, Mathews MB. J Virol. 1993;67:507-15.

Full text of Publications

Homozygous Null Mutations in the ABCA4 Gene in Two Families With Autosomal Recessive Retinal Dystrophy

HARDEEP PAL SINGH, MSc, SUBHADRA JALALI, MD, J. FIELDING HEJTMANCIK, MD, PhD, AND CHITRA KANNABIRAN, PhD

• PURPOSE: **To identify the genes causing autosomal recessive retinal dystrophy in Indian families and to characterize the associated phenotypes.**
• DESIGN: **Experimental and observational.**
• METHODS: **Families with autosomal recessive nonsyndromic retinal dystrophies were recruited. Complete ophthalmic evaluation, including visual acuity, visual fields, fundus examinations, and electroretinography, was performed on all members. Genotyping of 14 families for two or more microsatellite markers flanking each of 21 different genes causing retinal dystrophy was done by standard methods to screen for the presence of homozygosity by descent. Mutational screening of the ABCA4 gene was carried out on 18 members (five affected) of two families by amplification and direct automated sequencing of exons and flanking sequences. Sequence alterations identified were tested for cosegregation with disease in the families and for presence in 100 unrelated normal controls.**
• RESULTS: **Two of 14 families showed homozygosity shared by affected individuals for markers flanking the ABCA4 locus. A homozygous nonsense mutation in the ABCA4 gene of Arg2030Stop was found in one family and a homozygous single base deletion leading to frameshift at Arg409 was found in the second family. Both of these mutations were found to cosegregate with disease. Five affected individuals from the two families had early-onset visual loss, diminished rod and cone electroretinographic responses, and widespread atrophy of the retinal pigment epithelium.**
• CONCLUSION: **Homozygous null mutations in ABCA4 produced a severe widespread retinal degeneration that showed marked central retinal involvement.** (Am J Ophthalmol 2006;141:906–913. © 2006 by Elsevier Inc. All rights reserved.)

Accepted for publication Dec 8, 2005.

From the Kallam Anji Reddy Molecular Genetics Laboratory, L.V. Prasad Eye Institute, Hyderabad, India (H.P.S., C.K.); Smt. Kannuri Santhamma Retina-Vitreous Service, L.V. Prasad Eye Institute, Hyderabad, India (S.J.); and Ophthalmic Genetics and Visual Function Branch, National Eye Institute, Bethesda, Maryland (J.F.H.).

This study was supported by grant RO1 TW06231 from the Fogarty International Center, National Institutes of Health, Bethesda, Maryland, under the Global Health Research Initiative Program (C.K.), and by the Hyderabad Eye Research Foundation, Hyderabad, India.

Inquiries to Chitra Kannabiran, PhD, L.V. Prasad Eye Institute, L.V. Prasad Marg, Banjara Hills, Hyderabad 500 034, India; e-mail: chitra@lvpei.org

RETINAL DYSTROPHIES ARE A CLINICALLY AND GENETICALLY heterogeneous group of progressive, bilateral, hereditary disorders involving degeneration of the retinal or choroidal tissue, or both. They are inherited as single gene disorders with autosomal dominant, autosomal recessive, or X-linked modes of inheritance, and also as digenic disorders. They are genetically highly heterogeneous, and over 70 different loci are known for nonsyndromic retinal dystrophies.[1] Multiple mutations in each of the identified genes result in the same phenotype and, conversely, different phenotypes of retinal dystrophy can be caused by mutations in the same gene. One such gene associated with a range of phenotypes of retinal dystrophy is the ABCA4 gene (ATP-binding cassette, subfamily A member 4) on chromosome 1p22. The ABCA4 protein (also known as rim protein) is a membrane transporter located in the outer segment disks of rods[2] and cones.[3] It is implicated in the transport of the retinoid derivative N-retinylidene phosphatidyl ethanolamine across the photoreceptor outer segment disk membranes.[4] It is a 220-kD protein consisting of two tandem halves with each half having an extracellular (intradiskal) domain, a multispanning membrane domain, and a nucleotide-binding domain.[5] Mutations in ABCA4 are regarded as a major cause of retinal dystrophy and result in a variety of disorders, including Stargardt's macular dystrophy, autosomal recessive cone-rod dystrophy, and autosomal recessive retinitis pigmentosa.[6,7]

To identify genes causing disease in Indian families with autosomal recessive retinal dystrophies, we carried out a screen to test for possible involvement of the known retinal dystrophy genes in these families. Because there are numerous genes already identified for different types of retinal dystrophy, we used a rapid screening approach to

© 2006 BY ELSEVIER INC. ALL RIGHTS RESERVED.
0002-9394/06/$32.00
doi:10.1016/j.ajo.2005.12.009

test for homozygosity by descent at several of these loci.[8] We screened 14 families using two or more markers flanking each of 21 different retinal dystrophy genes. We found homozygosity among affected individuals of two families for microsatellite markers at the ABCA4 gene locus. Subsequent analysis of all 50 exons of the ABCA4 gene revealed two homozygous null mutations in the two families. Affected individuals of both families had a severe, early-onset disease that resulted in degeneration of the central and peripheral retina.

METHODS

FAMILIES WITH TWO OR MORE MEMBERS AFFECTED WITH retinal dystrophy and a pedigree pattern suggestive of autosomal recessive inheritance were included in the study. Informed consent for clinical investigations was obtained and blood samples were collected from all members after approval of the protocol by the Institutional Review Board of the L.V. Prasad Eye Institute. Patients with bilateral, symmetric, diffuse, primary retinal dystrophy were included in the study. Essential criteria included diffuse and widespread (defined as involving the retina beyond the posterior pole) retinal pigment epithelial degeneration (that appears as fine, white, or grayish discoloration of the deeper retinal layers); arterial narrowing; visual field loss commensurate with clinical lesions; and reduced amplitudes on electroretinogram (ERG) to less than 25% of the maximal retinal response in normal individuals, that is, less than 80 μV for b-wave and 30 μV for a-wave (normal amplitude of b-wave >350 μV and a-wave >110 μV). Other clinical signs that may be present but were not essential for diagnosis included pigment migration including bone-corpuscular pigmentation, vitreous opacities and vitreous pigments, associated retinal pigment epithelium atrophic changes in the macular area, diffuse disk pallor, and stellate opacities in the crystalline lens. Excluded were patients who had unilateral disease, absence of other affected members in autosomal recessive inheritance pattern, macular retinal dystrophy with no evidence of widespread retinal photoreceptor involvement, evidence or history of ocular trauma, retinal vascular occlusion, retinal detachment surgery, exudative retinal detachment, retinal vasculitis, chorioretinitis or any other secondary cause of pigmentary retinal changes, or involvement of any other systems (syndromic diseases). Patients were excluded if the ERG showed patterns consistent with localized retinal degeneration or loss of only cone function without involvement of rod functions, or evidence of a primary inner retinal dysfunction alone (negative ERG).

Genomic DNA was isolated from 5 ml to 10 ml of blood by standard procedures. Two or more markers flanking each of 21 different genes that are known to cause retinitis pigmentosa or related retinal dystrophies, or both, were

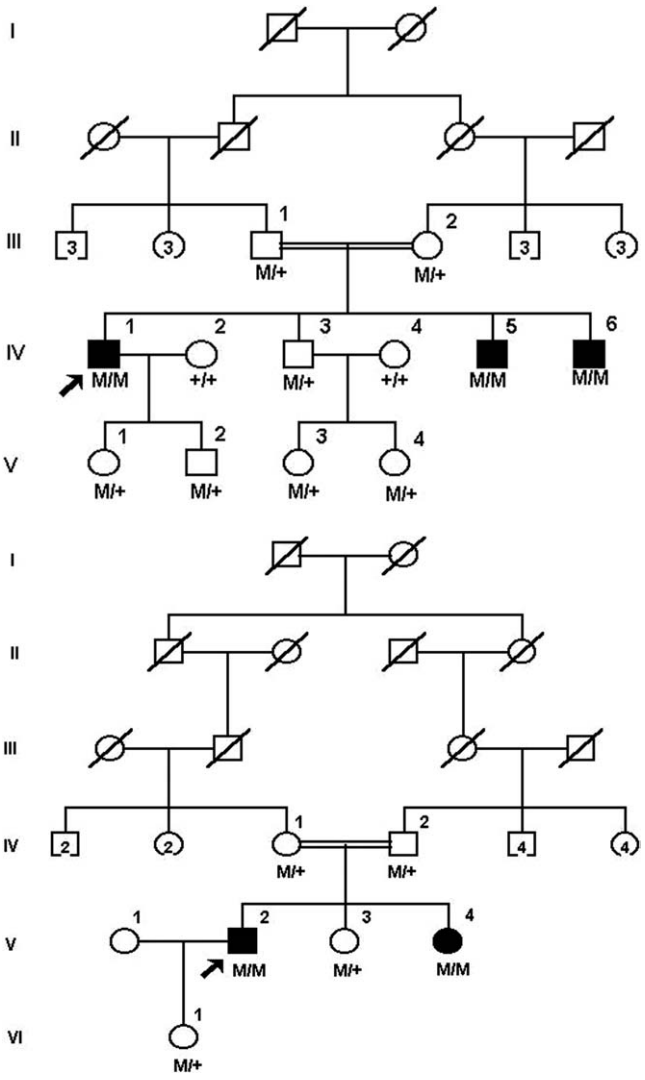

FIGURE 1. Pedigree drawings of families with autosomal recessive retinal dystrophy. Circles and squares represent females and males, respectively, with affected individuals indicated by darkened symbols. Double lines joining spouses indicate consanguinity. Top, family A. Bottom, family B. Roman numerals at the (Top) indicate the generation in the pedigree diagram, and individuals who were part of the study are designated by numbers below the corresponding symbols. Genotype for each individual is given below the symbol; M denotes mutant and plus sign (+) denotes the wild-type allele. Arrow at lower left of symbol denotes the proband.

screened for homozygosity by descent. Sequences of primers for amplifying each of the microsatellite markers were obtained from the genome database.[9] Information on marker locations and polymorphism was taken from the websites for the Human Genome Database and the Center for Medical Genetics.[9,10]

Genotyping was done by manual methods as described previously[8] and automated methods on the ABI310 genetic analyzer using fluorescently labeled custom-made

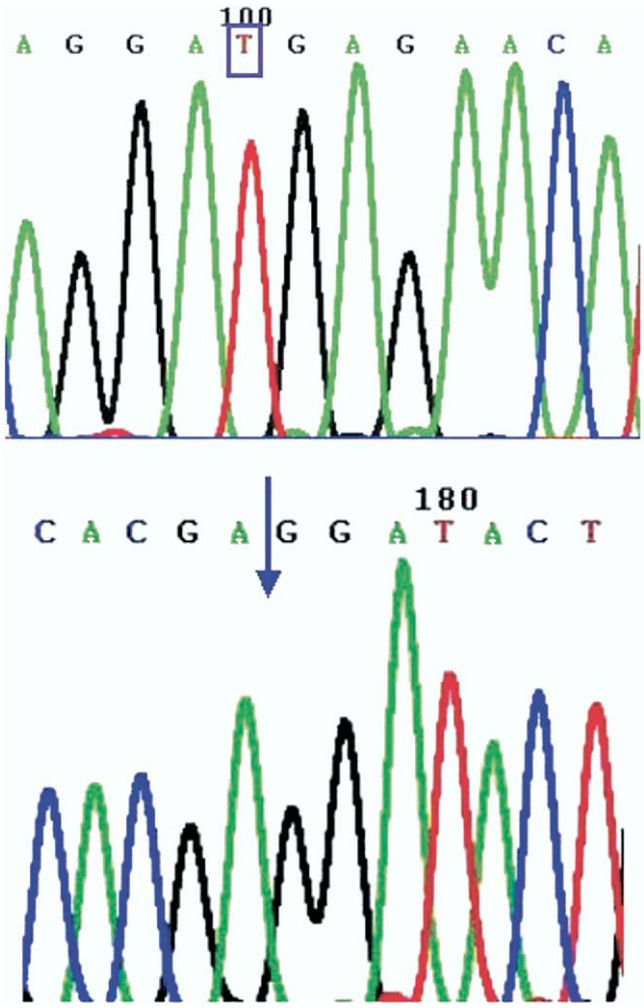

FIGURE 2. Sequence changes in the ABCA4 gene in affected individuals. Sequence electropherograms are shown for nonsense mutation c.6088C>T corresponding to Arg2030Ter found in family A (Top) and single base deletion c.1225delA leading to frameshift at Arg409 in family B (Bottom). The site of mutation is boxed (Top) or indicated by an arrow (Bottom).

primers and Genescan analysis software (Applied Biosystems Inc, Foster City, California, USA).

Sequences of primers specific for the ABCA4 gene were designed by us except for exons 1 to 15, which were previously reported.[11] Thermal cycling conditions included initial denaturation at 94°C for four minutes, followed by 34 cycles of denaturation at 94°C for 45 seconds, annealing at 53°C to 68°C (depending on primer) for 15 seconds, extension at 72°C for 45 seconds, with a final extension at 72°C for five minutes. Polymerase chain reaction (PCR) products were purified by MO BIO UltraClean PCR Clean-up kit (Mo Bio Laboratories Inc, Carlsbad, California, USA) and directly sequenced using forward and reverse PCR primers by automated methods.

Sequence changes identified were tested for cosegregation in the families and for presence in 100 unrelated normal control individuals by PCR-RFLP methods. Digested PCR products were resolved on 8% polyacrylamide gels and visualized after ethidium bromide staining. For the mutation c.6088C>T, there was a gain of restriction enzyme site for *Bse*G1. This resulted in digestion of the 261 bp PCR product of exon 44 into two fragments of 139 and 122 bp. For the c.1225delA mutation, there was a gain of *Mnl* 1 enzyme site. Exon 9 PCR products from normal individuals produced two fragments of 142 and 128 bp upon *Mnl* 1 digestion. In the presence of the mutation, the 128 bp fragment was further cut into 66 and 62 bp fragments.

RESULTS

14 FAMILIES WERE GENOTYPED FOR MICROSATELLITE MARKers flanking 21 different genes causing retinal dystrophies. Affected individuals from two families (shown in Figure 1) showed homozygosity for four markers (D1S406, D1S1170, D1S236, and D1S497) located in a 3.2 cM interval containing the ABCA4 gene locus. Homozygosity for these markers was shared by three affected offspring from family A and two affected offspring of family B (data not shown). Sequencing of all 50 exons of the ABCA4 gene was performed on DNA samples of the affected and unaffected individuals of these two families. A homozygous nonsense mutation was found in exon 44 (c.6088C>T) corresponding to Arg2030Stop change in the three affected individuals in family A (Figure 2, Top). This mutation cosegregated with disease in the family as shown by digestion of the PCR product with *Bse*G1 (data not shown). The genotypes of the remaining family members studied are shown in (Figure 1, Top).

In family B, both affected offspring were homozygous for a single base deletion of an A residue (c.1225delA) in exon 9 resulting in a frameshift at codon Arg409 (Figure 2, Bottom). The parents and unaffected sibling were heterozygous for the mutation as tested by digestion with *Mnl* 1 (not shown). The genotypes of the family members screened are indicated in (Figure 1, Bottom).

Both of the above changes were absent in 100 unrelated ethnically matched control individuals who were free of retinal disease.

In family A, the age at onset of symptoms was early childhood in two older siblings and late childhood for the youngest. All three had initial symptoms of reduced vision for distance and reading with no noticeable difference in dim vs bright illumination levels. There was no history of delayed or poor dark adaptation or nyctalopia or of glare sensitivity. Clinical features were bilaterally symmetric in all affected with the additional feature of strabismic amblyopia in one affected (Table 1). Best-corrected Snellen visual acuity was less than 20/200 (6/60) in all affected by the third decade. None of the eyes showed nystagmus. Fundus evaluation of all three affected showed features of diffuse retinal pigment epithelium changes in peripheral retina associated with arterial narrowing and disk pallor. The macular area, however, showed significant variation

TABLE 1. Clinical Features of Individuals Affected With Retinal Dystrophy From Families A and B

Family/ Individual	Gender	Age at Presentation (y)	Age at Onset (y)	Initial Symptoms	Fundus Features	ERG		VA
						Scotopic	Photopic	
A/IV-1	M	28	5	Decreased vision	Macular degeneration, pigment migration around arcades, RPE degeneration, arterial narrowing, vitreous opacities, slight disk pallor	Maximal retinal response, grossly reduced but recordable	Extinguished	OU 20/200
A/IV-5	M	23	5	Decreased vision for reading, squint (30 degree squint)	Bronze reflex with RPE atrophy in macular area, vessels and disk normal. Mild RPE degeneration, patches around arcades	Borderline responses	Borderline responses with recordable ERG, latency not increased	OD ambloypia, CF 1 m OS 20/100
A/IV-6	M	19	12	Decreased distance and reading vision	Mild disk pallor, macular RPE degenerative changes, no peripheral changes seen initially, peripheral RPE changes developed after 6 years	Borderline amplitude and delayed implicit time	Reduced amplitude with normal implicit time	OD 20/800 OS 20/200 A^{x}T 15 degree attenuating exotropia
B/V-2	M	32	15	Decreased vision, needs more light	Nystagmus, diffuse RPE degeneration all over, more in macular area, arterial narrowing, pigmentary changes in macular area	Extinguished	Extinguished	OU 20/400
B/V-4	F	24	14	Decreased vision, needs more light	Nystagmus, no disk pallor, arterial narrowing, pigmentary changes in macular area and periphery	Extinguished	Extinguished	OU 20/400

CF = counting fingers; ERG = electroretinogram; VA = visual acuity; A^{x}T = alternate exotropia.

FIGURE 3. Fundus photographs of affected siblings of family A showing diffuse primary retinal dystrophy. For subject IV: 1 (Top), pigment migration is seen as whorl-like pattern at the posterior pole and around the arcades with a paravascular pattern toward the periphery. For subject IV: 5 (Bottom), arterial narrowing, widespread retinal pigment epithelium degeneration, and macular involvement showing configuration of atrophic maculopathy with pigmentary changes were noted. Peripheral retina showed diffuse retinal pigment epithelium atrophy and arterial narrowing with no pigment migration.

though all of the three siblings were in the third decade of life (19 to 28 years of age). The oldest affected (individual IV:1; Figure 3) had striking pigment migration around the posterior pole and also beyond. This appeared in a whorl-like pattern at the posterior pole and around the arcades but had more of a paravascular pattern toward the retinal periphery. In the other two younger siblings (IV:5, IV:6; Figure 3, and data not shown), the macula showed a few pigment blotches and atrophic retinal pigment epithelium changes that were oval in configuration with the long axis horizontal. There were no significant changes in the vitreous in any of the affected eyes. Visual fields showed a temporal island of vision. ERG was nearly extinguished in one affected (Table 2) with unrecordable isolated rod and cone responses. The other two affected siblings had a cone-rod type of ERG response and had well-recordable maximal retinal response (Table 2). The parents (Figure 1, Top, III:1, III:2) who were carriers of the mutation were normal on clinical evaluation but showed subnormal cone ERG responses (Table 2).

In family B, the age at onset of symptoms was early teens in both affected siblings. Both had symptoms of reduced vision, more so in dim illumination. Clinical features were bilaterally symmetric in both. Best-corrected Snellen visual acuity was less than 20/400 (6/120) in both affected at ages 32 and 24 years. All of the eyes showed nystagmus. Fundus evaluation of both affected siblings showed features of diffuse retinal pigment epithelium changes in the peripheral retina associated with mild arterial narrowing in the younger affected sibling but no significant disk pallor (Figure 4). The retinal vessels were of normal caliber, and the disk was normal in the older affected sibling. The macular area, however, showed significant variation between both siblings, who were aged 32 and 24 years. The older affected sibling had striking blot-like pigment migration around the foveal area and also close to the arcade. There was also an area of bare sclera with punched-out area of chorioretinal atrophy around the foveal area. Pigment migration beyond the arcades was minimal. In the younger sibling, there was a metallic sheen–like appearance at the posterior pole due to what appeared to be confluent areas of retinal pigment epithelium atrophy, with a few areas of pigment migration just beyond the arcades. The retinal pigment epithelium atrophy in the periphery was widespread. Fundus fluorescein angiography showed retinal pigment epithelium window defects that were confluent at the posterior pole and more discrete and scattered toward the peripheral retina. Fundus fluorescein angiography showed up many more retinal pigment epithelium lesions than those seen clinically or on photography. There were no significant changes in the vitreous in any of the affected eyes. ERGs revealed diffuse photoreceptor involvement with both rod and cone systems but with rods affected more than cones (Table 2). Both ERG and visual field changes were more pronounced in the younger than in the older affected sibling. The mother (Figure 1, Bottom, IV:1), who was a heterozygous carrier, was normal upon funduscopy.

The clinical and ERG findings of affected individuals in both families were interpreted as bilaterally symmetric, diffuse photoreceptor dystrophy with a predominant macular involvement and some phenotypic variation. The ERG was of cone-rod pattern in family A, including the heterozygous carrier parents and rod-cone type in family B.

TABLE 2. ERG Data of Individuals From Families A and B

Family, individual*	Response	a-Wave		b-Wave	
		Amplitude	Latency	Amplitude	Latency
A, III-1	Isolated rod response			108.86	136.5
	Maximal retinal response	−109.21	22.0	282.65	47.00
	30 Hz Flicker			37.3	31.80
A, III-2	Isolated rod response			170.37	103.0
	Maximal retinal response	−165.83	21.5	475.17	47.00
	30 Hz Flicker			44.5	29.00
A, IV-1	Isolated rod response			Extinguished	
	Maximal retinal response	−20.66	31.5	57.8	55.5
	30 Hz Flicker			Extinguished	
A, IV-5	Isolated rod response	—	—	129.61	103.5
	Maximal retinal response	−191.09	22	291.2	45.00
	30 Hz Flicker			35.4	28.0
A, IV-6	Isolated rod response			72.4	118.5
	Maximal retinal response	−83.22	20.5	215.53	48.00
	30 Hz Flicker			26.7	28.6
B, V-2	Isolated rod response			69.81	160.00
	Maximal retinal response	−47.83	22.5	161.59	57.0
	30 Hz Flicker			15.2	41.1
B, V-4	Isolated rod response	—	—	Extinguished	—
	Maximal retinal response	−56.02	29	84.7	54.5
	30 Hz Flicker			20.6	41.7
Normal values†	Isolated rod response	—	—	150.0	90–110
	Maximal retinal response	110	20	350–450	45.00 ± 4
	Photopic cone response	—	—	120–180	27–31
	30 Hz Flicker	—	—	100–150	33–35

*For family A, data from unaffected parents (individuals III-1 and III-2) and affected offspring (IV-1, IV-5, and IV-6) are shown. For family B, data from the two affected offspring (V-2 and V-4) are shown.

†The normal values are supplied by the manufacturer (LKC Technologies, Gaithersburg, Maryland, USA) and confirmed by recordings in our laboratory on a normal patient population.

DISCUSSION

WE IDENTIFIED HOMOZYGOUS NULL MUTATIONS IN THE ABCA4 gene in five affected individuals from two families with autosomal recessive retinal dystrophy. Mutations found in both families cosegregated with disease and were absent in 100 unrelated normal controls. The c.1225delA resulting in frameshift at Arg409, to our knowledge, has not been previously reported, whereas the c.6088C>T change resulting in a stop codon at Arg2030 has been reported as a heterozygous or compound heterozygous change in patients with a diagnosis of Stargardt's disease or cone-rod dystrophy.[12–15] Both mutations identified are likely to be associated with a complete absence of ABCA4 activity. The Arg2030Stop mutation is predicted to either lead to instability of the messenger RNA due to nonsense-mediated mRNA decay or, in the event that the protein is expressed, to inactive protein, since the mutation affects the arginine-2030 residue located in the second nucleotide-binding domain of the ABCA4 protein.[5] The c.1225delA mutation would be expected to result in a severely truncated protein with frameshift at codon 409.

The mutational spectrum of the ABCA4 gene consists predominantly of missense mutations with approximately 75% or more of individuals tested having missense mutations.[16,17] Null mutations have been reported in fewer cases in heterozygous, compound heterozygous, or, less frequently, homozygous individuals. Mutations in the ABCA4 gene have been found in up to 50% to 60% of patients with Stargardt's disease and autosomal recessive cone-rod dystrophy.[12,17,18] In addition, heterozygous ABCA4 mutations have been associated with age-related macular degeneration.[12,19]

The phenotypes of the two families described herein involved degeneration of the central and peripheral retina. The initial symptoms were diminished central vision in affected individuals of both families, whereas the ERG patterns were different between the families, with two affected siblings in family A (Table 1) having ERGs suggestive of a cone-rod pattern of degeneration (Table 1),

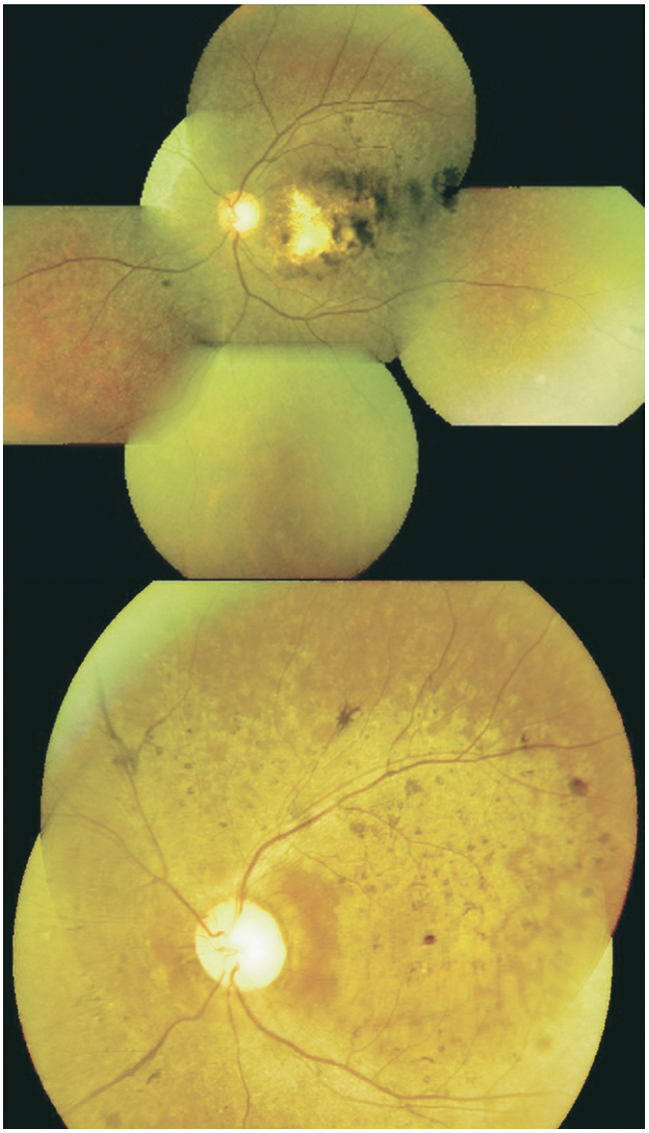

FIGURE 4. Fundus photographs of affected siblings of family B showing retinal dystrophy phenotype. Photographs shown are for subject V: 2 (Top) and V: 4 (Bottom). Note diffuse retinal pigment epithelium atrophy with predominant macular involvement in both, but associated punched-out chorioretinal macular atrophic patch in the older sibling V:2 (Top), whereas the younger sibling V:4 (Bottom) had no such lesion in the macular area but showed pigment migration extending along the retinal vessels.

and those of family B having a rod-cone pattern. From the available data, it appears that the disease, at least in family B, may represent a different entity than "typical" forms of retinitis pigmentosa or cone-rod dystrophy. It is also possible that the sequence of degenerative changes may have been different in different members of each of the families, because there was variability in fundus features between the affected members of both families (Figures 3 and 4). Essentially, all affected from both families manifested severe retinal dystrophy with onset of symptoms in the first-second decades, variably affected ERG patterns, and visual acuities in the range of <20/200 to 20/400 by the third decade.

The presence of two null alleles in ABCA4 has been proposed to result in the most severe forms of disease. In families showing more than one phenotype associated with ABCA4 mutations, patients with two null mutations had an atypical retinitis pigmentosa with onset within the first decade.[7,20,21] Null mutations in ABCA4 have also been found in patients with other diagnoses, including Stargardt's disease[16,22,23] and cone-rod dystrophy.[17,23] In these cases of null mutations in ABCA4, the patients' phenotypes progressed in the advanced stages to severe panretinal degeneration with low or absent rod and cone ERGs, regardless of whether the initial diagnosis was Stargardt's disease[22,23] or cone-rod dystrophy.[17,23] It is possible that individuals with homozygous null mutations have common features related to disease severity and progression as compared with patients having missense or other "mild" mutations. Identification of both mutant alleles in patients and evaluation and follow-up during various stages of the disease will aid in developing genotype-phenotype correlations.

An additional observation that may have a bearing on the ABCA4 mutational status is that we found that the heterozygous parents of the affected individuals in family A (aged 55 and 45 years) had reduced cone ERG amplitudes (Table 2), though they were normal upon fundus examination. This raises the question of whether the subnormal ERGs are related to the presence of one null ABCA4 allele. Earlier studies have suggested that the presence of heterozygous mutations in ABCA4 may lead to milder or late-onset disease. The role of heterozygous changes in ABCA4 in age-related macular degeneration has remained controversial. Studies on cohorts of patients with age-related macular degeneration[19] and on first-degree relatives of patients with Stargardt's disease[12,24] have reported an association of heterozygous mutations in ABCA4 and age-related macular degeneration, although others have not confirmed this.[14,25] A heterozygous null ABCA4 mutation has been proposed to be responsible for late-onset fundus flavimaculatus.[26] It is conceivable that a long-standing deficiency of ABCA4 activity could trigger the development of disease, although there is no conclusive evidence.

In summary, we identified homozygous null mutations in the ABCA4 gene in five affected individuals from two Indian families with severe autosomal recessive retinal dystrophy. Screening of a larger number of families with retinal dystrophies will be required to determine whether ABCA4 mutations are a major cause of retinal dystrophy in Indian patients.

REFERENCES

1. Retinal information network. URL: http://www.sph.uth.tmc.edu/RetNet/. Access date: September 1, 2005

2. Illing M, Molday LL, Molday RS. The 220-kDa rim protein of retinal rod outer segments is a member of the ABC transporter superfamily. J Biol Chem 1997;272:10303–10310.
3. Molday LL, Rabin AR, Molday RS. ABCR expression in foveal cone photoreceptors and its role in Stargardt macular dystrophy. Nat Genet 2000;25:257–258.
4. Beharry S, Zhong M, Molday RS. N-retinylidene-phosphatidylethanolamine is the preferred retinoid substrate for the photoreceptor-specific ABC transporter ABCA4 (ABCR). J Biol Chem 2004;279:53972–53979.
5. Bungert S, Molday LL, Molday RS. Membrane topology of the ATP binding cassette transporter ABCR and its relationship to ABC1 and related ABCA transporters: identification of N-linked glycosylation sites. J Biol Chem 2001;276: 23539–23546.
6. Allikmets R, Singh N, Sun H, et al. A photoreceptor cell-specific ATP-binding transporter gene (ABCR) is mutated in recessive Stargardt macular dystrophy. Nat Genet 1997;15:236–246.
7. Cremers FP, van de Pol DJ, van Driel M, et al. Autosomal recessive retinitis pigmentosa and cone-rod dystrophy caused by splice site mutations in the Stargardt's disease gene ABCR. Hum Mol Genet 1998;7:355–362.
8. Lalitha K, Jalali S, Kadakia T, Kannabiran C. Screening for homozygosity by descent in families with autosomal recessive retinitis pigmentosa. J Genet 2002;81:59–63.
9. The Human Genome Database. URL: http://gdbwww.gdb.org. Access date: September 1, 2005.
10. The Center for Medical Genetics, Marshfield Clinic. URL: http://research.marshfieldclinic.org/genetics/. Access date: September 1, 2005.
11. Ocular Molecular Genetics Institute. ABCR primer sequences. URL: http://eyegene.meei.harvard.edu/OMGI/ABCR/primers.html. Access date: September 1, 2005.
12. Lewis RA, Shroyer NF, Singh N, et al. Genotype/phenotype analysis of a photoreceptor-specific ATP-binding cassette transporter gene, ABCR, in Stargardt disease. Am J Hum Genet 1999;64:422–434.
13. Papaioannou M, Ocaka L, Bessant D, et al. An analysis of ABCR mutations in British patients with recessive retinal dystrophies. Invest Ophthalmol Vis Sci 2000;41:16–19.
14. Webster AR, Heon E, Lotery AJ, et al. An analysis of allelic variation in the ABCA4 gene. Invest Ophthalmol Vis Sci 2001;42:1179–1189.
15. September AV, Vorster AA, Ramesar RS, et al. Mutation spectrum and founder chromosomes for the ABCA4 gene in South African patients with Stargardt disease. Invest Ophthalmol Vis Sci 2004;45:1705–1711.
16. Rivera A, White K, Stohr H, et al. A comprehensive survey of sequence variation in the ABCA4 (ABCR) gene in Stargardt disease and age-related macular degeneration. Am J Hum Genet 2000;67:800–813.
17. Briggs CE, Rucinski D, Rosenfeld PJ, Hirose T, Berson EL, Dryja TP. Mutations in ABCR (ABCA4) in patients with Stargardt macular degeneration or cone-rod degeneration. Invest Ophthalmol Vis Sci 2001;42:2229–2236.
18. Fishman GA, Stone EM, Eliason DA, Taylor CM, Lindman M, Derlacki DJ. ABCA4 gene sequence variations in patients with autosomal recessive cone-rod dystrophy. Arch Ophthalmol 2003;121:851–855.
19. Allikmets R, Shroyer NF, Singh N, et al. Mutation of the Stargardt disease gene (ABCR) in age-related macular degeneration. Science 1997;277:1805–1807.
20. Klevering BJ, van Driel M, van de Pol DJ, Pinckers AJ, Cremers FP, Hoyng CB. Phenotypic variations in a family with retinal dystrophy as result of different mutations in the ABCR gene. Br J Ophthalmol 1999;83:914–918.
21. Rozet JM, Gerber S, Ghazi I, et al. Mutations of the retinal specific ATP binding transporter gene (ABCR) in a single family segregating both autosomal recessive retinitis pigmentosa RP19 and Stargardt disease: evidence of clinical heterogeneity at this locus. J Med Genet 1999;36:447–451.
22. Fukui T, Yamamoto S, Nakano K, et al. ABCA4 gene mutations in Japanese patients with Stargardt disease and retinitis pigmentosa. Invest Ophthalmol Vis Sci 2002;43: 2819–2824.
23. Simonelli F, Testa F, Zernant J, et al. Association of a homozygous nonsense mutation in the ABCA4 (ABCR) gene with cone-rod dystrophy phenotype in an Italian family. Ophthalmic Res 2004;36:82–88.
24. Simonelli F, Testa F, de Crecchio G, et al. New ABCR mutations and clinical phenotype in Italian patients with Stargardt disease. Invest Ophthalmol Vis Sci 2000;41:892–897.
25. Schmidt S, Postel EA, Agarwal A, et al. Detailed analysis of allelic variation in the ABCA4 gene in age-related maculopathy. Invest Ophthalmol Vis Sci 2003;44:2868–2875.
26. Souied EH, Ducroq D, Rozet JM, et al. A novel ABCR nonsense mutation responsible for late-onset fundus flavimaculatus. Invest Ophthalmol Vis Sci 1999;40:2740–2744.

Premature Truncation of a Novel Protein, RD3, Exhibiting Subnuclear Localization Is Associated with Retinal Degeneration

James S. Friedman, Bo Chang, Chitra Kannabiran, Christina Chakarova, Hardeep P. Singh, Subhadra Jalali, Norman L. Hawes, Kari Branham, Mohammad Othman, Elena Filippova, Debra A. Thompson, Andrew R. Webster, Sten Andréasson, Samuel G. Jacobson, Shomi S. Bhattacharya, John R. Heckenlively, and Anand Swaroop

The *rd3* mouse is one of the oldest identified models of early-onset retinal degeneration. Using the positional candidate approach, we have identified a C→T substitution in a novel gene, *Rd3,* that encodes an evolutionarily conserved protein of 195 amino acids. The *rd3* mutation results in a predicted stop codon after residue 106. This change is observed in four *rd3* lines derived from the original collected mice but not in the nine wild-type mouse strains that were examined. *Rd3* is preferentially expressed in the retina and exhibits increasing expression through early postnatal development. In transiently transfected COS-1 cells, the RD3-fusion protein shows subnuclear localization adjacent to promyelocytic leukemia-gene-product bodies. The truncated mutant RD3 protein is detectable in COS-1 cells but appears to get degraded rapidly. To explore potential association of the human *RD3* gene at chromosome 1q32 with retinopathies, we performed a mutation screen of 881 probands from North America, India, and Europe. In addition to several alterations of uncertain significance, we identified a homozygous alteration in the invariant G nucleotide of the *RD3* exon 2 donor splice site in two siblings with Leber congenital amaurosis. This mutation is predicted to result in premature truncation of the RD3 protein, segregates with the disease, and is not detected in 121 ethnically matched control individuals. We suggest that the retinopathy-associated RD3 protein is part of subnuclear protein complexes involved in diverse processes, such as transcription and splicing.

Retinitis pigmentosa (RP [MIM #268000]) encompasses a group of retinal degenerative diseases (RDs) that severely compromise the quality of life of affected individuals. RP is genetically heterogeneous, with mutations in multiple genes; to date, 168 retinal-disease loci have been mapped, and 117 retinal disease–associated genes have been identified (RetNet Web site).[1] A majority of RP-causing genes encode proteins involved in phototransduction, photoreceptor morphogenesis, trafficking, gene regulation, and/or splicing.[2] Mutations in some of the genes are suggested to cause a prolonged and/or increased phototransduction, followed by decreased Ca^{++} levels, leading to photoreceptor-cell death.[3] Despite major advances, genetic defects have not been determined for a significant proportion of subjects with RP (RetNet Web site).[4–6]

One approach for identification of additional human retinopathy genes is to elucidate the molecular basis of retinal degeneration in animal models. At least 35 strains of mice exhibit retinal degenerative disease.[7,8] Some examples of retinal degeneration (rd) mice include *rd1* (*Pde6b*), *Rds* (*peripherin*), *rd7* (*Nr2e3*), and *rd16* (*Cep290/NPHP6*), and their known and putative biological functions closely correspond to genes involved in human retinal disease.[9–13] Mutations in their human orthologs are associated with retinopathies.[14–18]

The retinal degeneration 3 (*rd3*) mice were originally collected in Switzerland in 1969, were sent to the Jackson Laboratory, were bred as different lines to establish their Robertsonian translocation, and were later identified as having retinal degeneration.[19] Different strains of *rd3* have variable phenotypes, with photoreceptors starting to degenerate at age 2–3 wk and complete loss of photoreceptors at age 8–16 wk.[19] Electroretinography (ERG) studies have demonstrated that the loss of retinal response was dependent on the genetic background, with ERGs becoming extinguished at age 6–16 wk in some strains.[19] Hence, at least one modifier locus appears to slow down the rate of degeneration in the pigmented mice compared with the albino mice. A detailed morphological examination of three *rd3* strains demonstrated the degeneration of photoreceptors through apoptosis and has confirmed the slower rate of degeneration in pigmented *rd3* mice compared with albino strains.[20]

The *rd3* genetic locus was mapped to mouse chromosome 1 between markers *D1Mit292* and *D1Mit510* and was excluded as being a mouse ortholog of one of the human

From the Departments of Ophthalmology and Visual Sciences (J.S.F.; K.B.; M.O.; E.F.; D.A.T.; J.R.H. A.S.) and Human Genetics (A.S.), W. K. Kellogg Eye Center, University of Michigan, Ann Arbor; the Jackson Laboratory, Bar Harbor, Maine (B.C.; N.L.H.); Kallam Anji Reddy Molecular Genetics Laboratory (C.K.; H.P.S.) and Kannuri Santhamma Retina-Vitreous Services (S.J.), L. V. Prasad Eye Institute, Banjara Hills, Hyderaba, India; Department of Molecular Genetics, Institute of Ophthalmology, University College London (C.C.; A.R.W.; S.S.B.), and Moorfield Eye Hospital (A.R.W.), London; Department of Ophthalmology, University Hospital of Lund, Lund, Sweden (S.A.); and Department of Ophthalmology, Scheie Eye Institute, University of Pennsylvania, Philadelphia (S.G.J.)

Received August 21, 2006; accepted for publication October 6, 2006; electronically published October 23, 2006.

Address for correspondence and reprints: Dr. Anand Swaroop, W. K. Kellogg Eye Center, University of Michigan, 1000 Wall Street, Ann Arbor, MI 48105. E-mail: swaroop@umich.edu

Am. J. Hum. Genet. 2006;79:000–000. © 2006 by The American Society of Human Genetics. All rights reserved. 0002-9297/2006/7906-00XX$15.00

Usher syndrome loci.[21,22] Herein, we report the identification of the genes (*3322402L07Rik* and *C1orf36*—renamed "*Rd3*" and "*RD3*," respectively) responsible for the *rd3* retinopathy. We show that *Rd3* is preferentially expressed in the retina and that the *rd3* mutation leads to a truncated and relatively unstable protein in COS-1 cells. The RD3 protein is associated with promyelocytic leukemia-gene-product (PML) bodies in the nucleus. We also describe a large *RD3*-screening effort involving 881 probands with retinopathy, revealing at least one putative disease-causing mutation and several changes of uncertain significance.

Material and Methods

Histological and Electroretinogram Analysis of rd3 *Mice*

The studies involving mice were performed after approval from institutional committees was obtained. Histology and electroretinograms were performed as described elsewhere.[23]

Mouse Mutation Screen

We examined genes in the published *rd3* (RBF/DnJ) critical region by direct sequencing. We additionally screened other *rd3* lines (RBJ/DnJ, STOCK Rb(11.13)4Bnr/J, and STOCK In(5)30Rk/J), as well as wild-type (WT) mouse strains, to verify the alteration. The following primers were used: for Rd3 exon 2, 5′-cgcctctctctttcttg-gtg-3′ (forward) and 5′-gcgactccagtcaccttctc-3′ (reverse); for Rd3 exon 3 5′-caagagcaaggttgggagtt-3′ (forward) and 5′-tccagcattcaagg-actcag-3′ (reverse). Exon amplification and sequencing of another gene, *Rcor3,* was initiated but was halted when the stop codon in *3322402L07Rik* was identified. PCR was performed from mouse-tail DNA with use of standard conditions, and amplified products were evaluated by agarose gel electrophoresis and were sequenced at the University of Michigan sequencing core facility.

RT-PCR and Northern-Blot Analysis

RT-PCR analysis was performed using WT mouse retinal RNA at time points ranging from embryonic day 12 (E12) to age 4 mo and from postnatal day 2 (P2) and 4-wk-old (4W) adult $Nrl^{-/-}$ and $Crx^{-/-}$ mice.[24,25] The primers used were Hprt 5′-caaactttgctttccctggt-3′ (forward), Hprt 5′-caagggcatatccaaacaaca-3′ (reverse), Rd3rt 5′-gagagaggtggagcgacaac-3′ (forward), and Rd3rt 5′-cacatcctccgagatggttc-3′ (reverse). A human multiple-tissue northern blot (BD Biosciences Clontech) and a mouse retina northern blot were probed with radiolabeled full-length *Rd3* cDNA or β-actin cDNA, as described elsewhere.[26]

Immunoblot Analysis

Rd3 cDNA was amplified and cloned into the pEGFPN1 vector (BD Biosciences Clontech) with use of primers N1 5′-gacgacaagctt-atagtggccctgaaggaggt-3′ (forward) and N1 5′-cagcagggatccgagtcgg-cctggggcgccctgaa-3′ (reverse). Mutagenesis was performed, as described elsewhere,[27] with primers W6R 5′-atgtccctcatcccgcggctccg-gtggaacg-3′ (forward), W6R 5′-cgttccaccggagccgcgggatgagggacat-3′ (reverse), E23D 5′-cggaccccggccgacatggtgctggagacg-3′ (forward), E23D 5′-cgtctccagcaccatgtcggccggggtccg-3′ (reverse), K130M 5′-gccc-tggagaagatgatgcaggaggaggaggcc-3′ (forward), and K130M 5′-ggcct-cctcctcctgcatcatcttctccagggc-3′ (reverse). Primers used to transfer *Rd3* into pcDNA4c (Invitrogen) were Rd3pc 5′-gacgacggatccatgtcc-ctcatcccgtgg-3′ (forward) and Rd3pc 5′-cagcaggcggccgccttgatgggtc-tcctggttg-3′ (reverse). Primers (Rd3mut 5′-gctgctggctgaatgagagccc-gaggtg-3′ [forward] and Rd3mut 5′-cacctcgggctctcattcagccagcagc-3′ [reverse]) were used to introduce the *rd3* mutation into the mouse *Rd3* cDNA. The *rd3* cDNA construct was then used as a PCR template with Rd3pcF and Rd3pcR primers. The amplified PCR product was digested and cloned into pcDNA4. Each *Rd3* mutant cDNA clone was completely sequenced. Mouse *Mef2c* in pcDNA4 was used as a transfection control in some experiments. Expression constructs were transfected into COS-1 cells with Fugene 6 (Roche), according to the manufacturer's instructions. Cells were harvested after 48 h, with use of PBS and protease inhibitors (Roche), and extracts were fractionated by SDS-PAGE and were transferred to nitrocellulose membrane. The blots were probed with rabbit anti-Green Fluroescent Protein (GFP) polyclonal antibody (1:2,000) and mouse anti-beta tubulin antibody (1:10,000) or with mouse-anti Xpress antibody (1:4,000) (Invitrogen) and were visualized using appropriate secondary antibodies and luminescence (Pierce).

Localization in COS-1 Cells

Cells were washed with PBS 48 h after transfection, were fixed using 4% paraformaldehyde/PBS for 15 min, and were washed again in PBS. Cells were permeabilized using 0.05% Triton X-100/PBS (PBS-T) for 10 min. After washing, a 5% BSA/PBS solution was applied, and the cells were blocked for 30 min. The primary antibodies used were anti-coilin antibody ab11822 (1:50) (Abcam), anti-SC-35 antibody ab11826 (1:50) (Abcam), anti-PML antibody sc-5621 (1:50) (Santa Cruz Biotechnology), and anti-Xpress antibody (1:400) (Invitrogen). The cells were incubated for 1 h in 1% BSA/PBS with primary antibody, were washed with 1% BSA/PBS, and were incubated with the appropriate secondary: anti-rabbit IgG Alexa fluor 546, anti-mouse IgG Alexa fluor 546, or anti-mouse IgG Alexa fluor 488 (Molecular Probes) (1:750 dilution). Cells were washed with 1% BSA/PBS, were counterstained with bisbenzimide to stain nuclei, and were examined by fluorescent microscopy.

Human-Mutation Screen

All human studies were performed in a manner consistent with the Declaration of Helsinki and were approved by the respective institutional review boards. Appropriate informed consent was obtained from study subjects. We performed a three-continent (North America, Asia [India], and Europe [United Kingdom and Scandinavia]) human-mutation screen of the *RD3* gene. Clinical phenotypes observed among the North American patient pool included simplex RP, multiplex RP, juvenile (early-onset) RP, recessive RP, cone-rod dystrophy (CRD), Leber congenital amaurosis (LCA [MIM #204000]), partial cone degeneration, fundus albipunctatus, atypical pattern dystrophy, macular degeneration, Stargardt disease, autoimmune retinopathy, achromatopsia, congenital stationary night blindness, and enhanced S-cone syndrome. For the North American and European screen, the following primers were used: for exon 2, RD3 5′-ctgttagggcagagcaggtc (forward) and RD3 5′-ctctagtcctggtggcctca (reverse); for exon 3, RD3 5′-ggactaattggccatgagga (forward) and RD3 5′-ctttgtggccagag-gaagag (reverse). The screen in India used exon 2 5′-ttcccaggttcc-ccactctg-3′ (forward) and 5′-ccactgcagccacctttcct-3′ (reverse) and exon 3 5′-gacgcccggggtgccagac-3′ (forward) and 5′-gttccagggcccgg-cgct-3′ (reverse). PCR was performed using standard conditions, and products were subjected to direct sequencing. Sequencing

was performed at the University of Michigan sequencing core, at Bangalore Genei (Bangalore, India), and at the Institute of Ophthalmology (London). We performed RFLP analysis to determine segregation of a splice-site change within the LCA-affected family and to examine 121 unrelated ethnically matched unaffected controls. This change leads to the abolition of a restriction site for *Hph*1. The normal allele in a 436-bp amplified PCR product is digested into 387 bp and 49 bp fragments, whereas the homozygous mutated allele shows a 436-bp product.

Results

rd3 Mouse Strains and Visual-Function Analysis

The *rd3* mutation has been bred into different strains of mice and now exists in five separate strains—RBF/DnJ, STOCK In(1)Rk/J, STOCK In(5)30Rk/J, RBJ/DnJ, and STOCK Rb(11.13)4Bnr/J (hereafter termed "4Bnr"). An updated pedigree of *rd3*-bearing mice is shown in figure 1.[19] Histologically, STOCK In(5)30Rk/J mice have a modest reduction in outer nuclear layer (ONL) thickness, with 3–5 rows of nuclei left at age 35 d. In contrast, the RBF/DnJ albino strain has a fully degenerated retina at the same age. The 4Bnr albino strain had the least degenerate retina of the three assessed *rd3/rd3* mice, but some degeneration was observed at the earlier time point of 27 d (fig. 2*A*).

For comprehensive evaluation of rod and/or cone photoreceptor dysfunction, we performed dark-adapted (rod photoreceptor derived) and light-adapted (cone photoreceptor derived) ERG tests on STOCK In(5)30Rk/J, 4Bnr, and RBF/DnJ *rd3*/*rd3* strains, with C57BL/6J mice as controls. In a previous study, rod derived ERG showed progressive retinal functional loss in *rd3* mice; no cone ERG was reported.[19,28] We found that the amplitude of the loss of dark-adapted ERG varied, depending on the mouse strain. The In(5)30Rk/J (pigmented) strain had dark-adapted ERG closer to the WT at both age 24 d and age 32 d. The 4Bnr (albino) strain had a large response at day 17, but ERG was reduced at day 24. Lastly, the ERG in the RBF/DnJ (albino) strain was almost undetectable at age 24 d and was completely abolished by age 31 d (fig. 2*B*, top panel). All three strains of *rd3*/*rd3* mice had greatly reduced or nondetectable light-adapted ERGs by age 24 d (fig. 2*B*, bottom panel, and data not shown). These results demonstrate that both rod and cone photoreceptors in the *rd3* homozygotes are functionally affected.

Mutation Screen of rd3 *Mice*

To identify the *rd3* mutation, we screened candidate genes in the mapped *rd3* region (fig. 3*A*) that had been defined elsewhere.[21] The critical genomic region was ~1 Mb and contained 13 genes or expressed sequences (National Center for Biotechnology Information [NCBI] Map Viewer build 36.1). To select candidates for mutation analysis, we first examined the expression profile of all genes *in silico* and through our microarray profiling, as reported elsewhere.[29] The Riken cDNA *3322402L07* showed a twofold increase in expression from P2 to P10 in purified rod photoreceptors[29] (A. Swaroop, M. Akimoto, and H. Cheng, unpublished data). Hence, we selected it as a candidate gene for the *rd3* mutation screen. Complete sequencing of all exons and intron-exon boundaries (fig. 3*B*) revealed a homozygous c.319C→T transition in the third exon. This change alters codon 107 from CGA to TGA, thus converting arginine to a stop codon, and is predicted to result in premature truncation of the RD3 protein. The mutation was detected in all *rd3* lines tested (RBF/DnJ, RBJ/DnJ, 4Bnr, and STOCK In(5)30Rk/J) but not in the nine control WT mouse lines (C57BL/6J, A/J, AE/J, BALB/cJ, C3H/HeJ, CBA/J, DBA/2J, MOLC/RkJ, and NON/LtJ) (fig. 3*C*). To further confirm whether this is indeed the causative mutation in *rd3*-containing strains, we generated haplotypes using markers spanning the *rd3* locus.[21] The three markers—

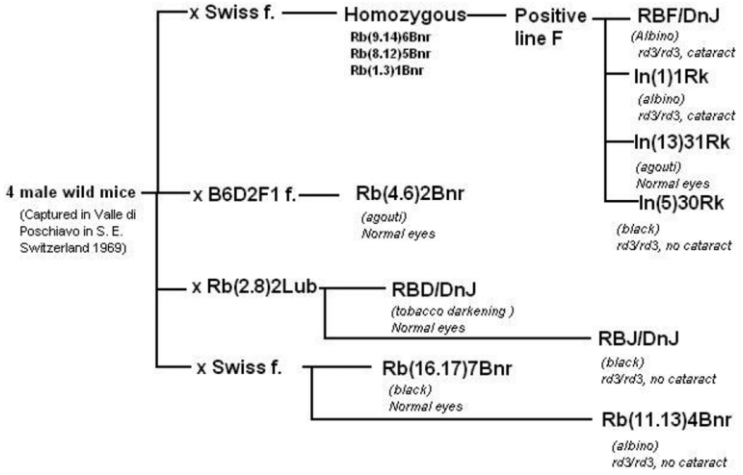

Figure 1. Pedigree of the *rd3* mouse strains. Four male mice were collected in Switzerland in 1969 and were genetically fixed to several lines. The mouse strains are currently housed at the Jackson Laboratory. This pedigree was updated from an earlier version,[19] with the kind permission of Springer Science and Business Media.

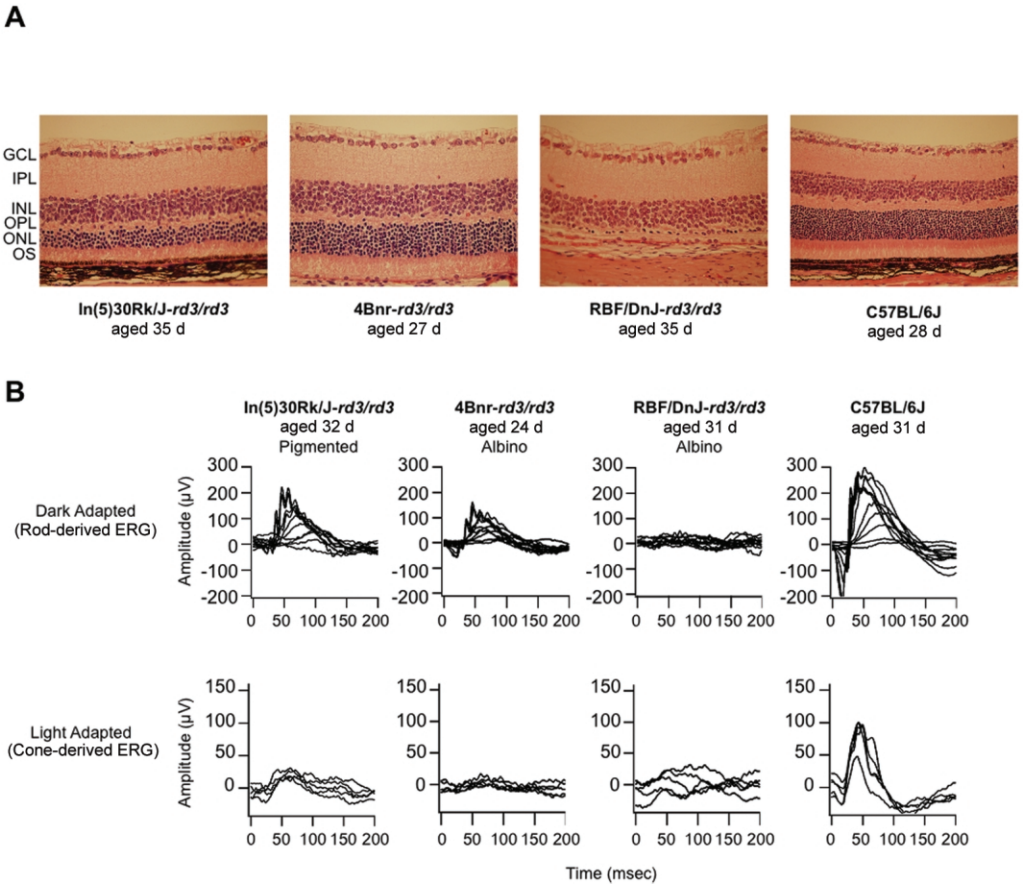

Figure 2. *A,* Histology of *rd3/rd3* mice. We examined STOCK In(5)30Rk/J, 4Bnr, RBF/DnJ (all *rd3/rd3*), and control C57BL/6J mice at ages 35, 27, 35, and 28 d, respectively. *B, top,* ERG responses under dark-adapted conditions: STOCK In(5)30Rk/J(*rd3/rd3*) mice (aged 32 d), 4Bnr(*rd3/rd3*) mice (aged 24 d), RBF/DnJ(*rd3/rd3*) mice (aged 31 d), C57BL/6J mice (aged 31 d). *Bottom,* Light-adapted ERG responses of the same mice.

D1Mit292.1, D1Mit462.2, and *D1Mit511*—revealed identical alleles in the three tested *rd3* lines (data not shown), which is consistent with the presence of the *rd3* mutation in this genetic background.

Analysis of the Rd3 *Gene*

To determine the expression profile of the *Rd3* transcript, we performed northern-blot and RT-PCR analysis using RNA from human and mouse tissues. The *Rd3* transcript of 1.9 kb was enriched in adult-mouse retinal tissues and had no detectable expression in nonretinal adult-human tissues, as revealed by human multiple-tissue northern-blot analysis (data not shown). We then examined its expression using WT, $Nrl^{+/-}$, and $Nrl^{-/-}$ mouse retinal RNA by northern-blot analysis. WT mice and $Nrl^{+/-}$ mice have a rod/photoreceptor–dominated retina, whereas $Nrl^{-/-}$ mice lack rods and instead have a cone-dominant retina.[24] *Rd3* is transcribed as a single RNA in these strains, with no obvious difference (data not shown).

To elucidate developmental expression of *Rd3,* we performed RT-PCR experiments using mouse retinal RNA from E12 to age 4 mo (fig. 4*A*). The *Rd3* transcript is detected at very low levels at E12 but was more noticeable beginning at E18, with subsequent increase in expression at P2 and P6. After P6, the levels of *Rd3* transcript remained high. Additional RT-PCR experiments were performed using retinal RNA from $Nrl^{-/-}$ (aged P2 and 4W), $Crx^{-/-}$ (aged P2 and 4W), *rd1* (adult), and *rd16* (adult) mice. The $Nrl^{-/-}$ mouse lacks rod photoreceptors, whereas the $Crx^{-/-}$ mouse exhibits a lessening of rod and cone gene expression at P10 and exhibits photoreceptor degeneration at age 2 mo.[24,25] The *rd1* and *rd16* homozygotes exhibit early-onset degeneration of photoreceptors.[9,13] The detection of the *Rd3* transcript in all mutant mouse strains suggests that it is also expressed in inner retina cell types (fig. 4*B*). Our data are consistent with the expression profile for C1orf36 (Hs.632495 [NCBI Expression Profile Viewer]) and previous in situ hybridization experiments,[30,31] which demonstrate high expression of *3322402L07Rik* cDNA in the ONL in addition to the other cellular layers of the retina.

Clustal analysis of the RD3 protein orthologs suggests its strong conservation in vertebrates, from human to ze-

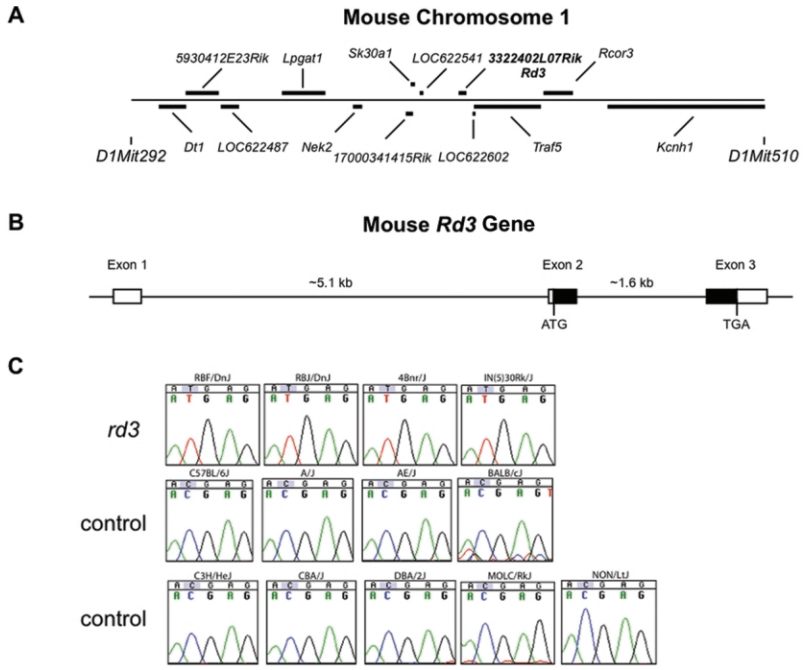

Figure 3. *A,* Critical genomic region encompassing the *rd3* mutation, between markers *D1Mit292* and *D1Mit510*.[21] Genes within the critical region are indicated. *B,* Genomic structure of the mouse *Rd3* gene. *C,* Chromatogram showing the region of the *Rd3* (*3322402L07Rik*) molecular defect in *rd3/rd3* strains RBF/DnJ, RBJ/DnJ, STOCK Rb(11.13)4Bnr/J, STOCK In(5)30Rk/J, and WT control strains C57BL/6J, A/J, AE/J, BALB/cJ, C3H/HeJ, CBA/J, DBA/2J, MOLC/RkJ, and NON/LtJ. The homozygous C→T change in the *rd3*-bearing mice is indicated. It generates a stop codon after aa 106.

brafish (fig. 4*C*). An *in silico* analysis of the mouse and human RD3 proteins reveals a coiled-coil domain at aa 22–54 and another weaker coiled-coil domain at aa 121–141.[32] The RD3 protein also has several putative protein kinase C and consensus Casein kinase II phosphorylation sites and one predicted sumoylation site. The mouse and human RD3 orthologs are basic proteins, with isoelectric points of 8.9 and 7.7, respectively.

Immunoblot analysis of COS-1 cells transfected with an *Rd3*-expression construct in the EGFPN1 vector demonstrated an expected RD3-GFP–fusion protein of ~45 kDa (predicted molecular mass of RD3 is ~22 kDa and that of GFP is ~23 kDa) (fig. 4*D*).

Localization of the RD3 Protein in Transfected COS-1 Cells

In transfected COS-1 cells, the RD3-GFP–fusion protein primarily exhibited nuclear or nuclear/cytoplasmic localization (fig. 5*A*–5*D* and data not shown). Some cells also contained a putative aggresome-like staining adjacent to the nucleus—likely because of the overexpression of the RD3 protein (data not shown). The most striking pattern was the presence of subnuclear spots, henceforth named "RD3 bodies," of different sizes (fig. 5*A*–5*C*). We examined whether RD3 bodies colocalized with other subnuclear proteins, such as coilin (Cajal body marker), SC-35 (Nuclear Speckle marker), and promyelocytic leukemia gene product (PML body marker). Coilin staining did not localize near RD3 bodies in a consistent manner, suggesting that they are not associated (fig. 5*A*). SC-35 staining tended to be diffuse and localized near RD3 bodies (fig. 5*B*). PML staining also existed near RD3 bodies, with an occasional overlap (fig. 5*C* and 5*G*). To further confirm close PML proximity, we performed the same experiment using an Xpress-tagged *Rd3* plasmid. The Xpress-RD3 protein demonstrated a more highly varied localization pattern than did RD3-GFP, suggesting that the size of the tag may impact the distribution of transfected RD3 protein (fig. 5*E* and 5*F*). Nonetheless, we observed many cells with similar RD3 bodies in close proximity to PML bodies in Xpress-*Rd3*–transfected cells (fig. 5*E* and 5*H*).

Analysis of the rd3 *Mutation*

To determine the consequence of the *rd3* mutation, we introduced this sequence alteration into the *Rd3*-pcDNA4 construct. Immunoblot analysis of COS-1–transfected cells revealed a truncated mutant RD3 protein (~11 kDa + ~4 kDa Xpress epitope), which was consistently detected at reduced levels compared with the WT protein (~22 kDa + ~4 kDa Xpress epitope) (fig. 6*A*). The mutant truncated protein therefore appears to be unstable and prematurely degraded. The mouse *Mef2c*-pcDNA4 construct was used as an internal control for transfection and was detected in roughly equal amounts in all experiments (fig. 6*A*). By immunocytochemistry, Xpress-RD3 mutant protein could

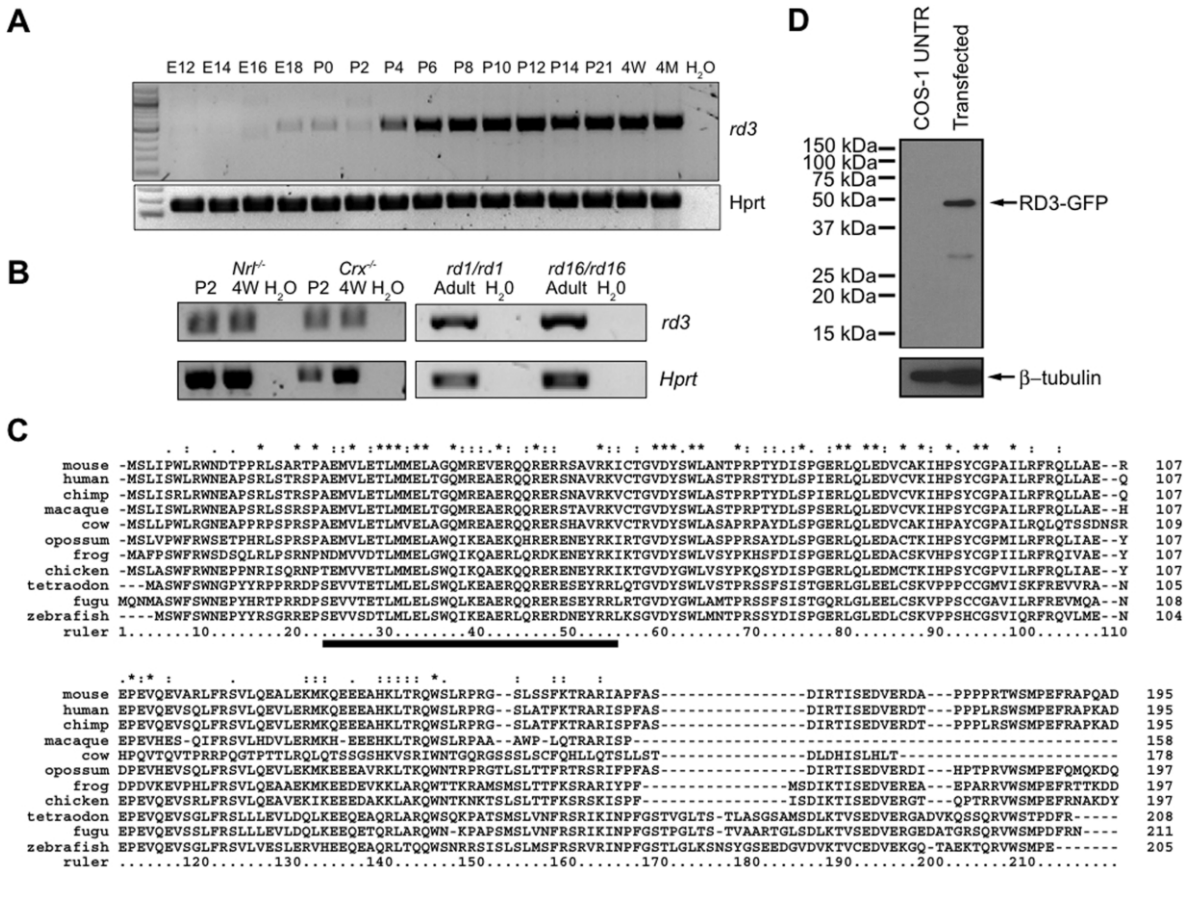

Figure 4. Expression of the *Rd3* gene. *A, Rd3* transcripts in mouse retina (aged E12 to 4 mo), present from at least E18, with a large increase from age P2 to age P6. *Hprt* was used to evaluate RNA quality and to normalize for quantity. *B,* Expression of *Rd3* in $Nrl^{-/-}$, $Crx^{-/-}$, *rd1/rd1,* and *rd16/rd16* mouse retina cDNA from P2, 4W, or adult. *Hprt* was used as a positive control. *C,* Alignment of RD3 protein orthologs. The amino acid sequence of mouse RD3 protein is aligned with those of human, chimpanzee, macaque, cow, opossum, frog, chicken, tetraodon, fugu, and zebrafish. Amino acid residues conserved in all orthologs are indicated by an asterisk (*), and reduced identity is shown using either a colon (:) or a dot (•). The long bar denotes a highly conserved coiled-coiled domain. *D,* Immunoblot expression of RD3-GFP fusion protein. An expression construct containing *Rd3*-GFP cDNA was transfected into COS-1 cells and was examined by immunoblot with use of anti-GFP antibody. The observed band is approximately the size estimated for the fusion protein (~50 kDa). A lower band of 30 kDa may represent a putative degradation product. Beta-tubulin was used to normalize for loading. UNTR = untransfected.

be observed in COS-1 cells, but at much lower levels compared with the WT protein at similar exposure times (fig. 6*B*–6*D*).

Human RD3-*Mutation Screen*

To examine whether mutations in the human *RD3* gene are associated with retinal disease, we performed mutation screening of 461 probands with retinopathy from North America (including at least 30 with cone dystrophy or CRD and 15 probands with LCA), 103 probands of Indian descent who had retinal dystrophy, 302 probands (177 with autosomal dominant RP, 96 with autosomal recessive RP, and 29 with cone dystrophy or CRD) from the United Kingdom, and 15 probands with CRD from Scandinavia. We sequenced all coding exons, including the flanking intron/exon boundaries (fig. 7*A*).

Of particular interest were two siblings from India who had LCA (fig. 7*B*). Both probands have had poor vision since birth: nystagmus and atrophic lesions in the macular area, with pigment migration. Fundus photographs of the affected siblings are shown in figure 7*C*. A homozygous G→A transition in the donor splice site at the end of exon 2 (c.296+1G→A) was observed in both siblings (fig. 7*D*). When the splice site is removed, the 99th codon still encodes arginine and is followed by a stop codon, suggesting that the protein is prematurely truncated. RFLP analysis of other family members demonstrated that the homozygous change was present only in the affected members of the family, with unaffected members heterozygous for the mutation (fig. 7*E*). We examined 121 unrelated ethnically matched controls by RFLP and did not observe this nucleotide substitution. The G→A alteration was not ob-

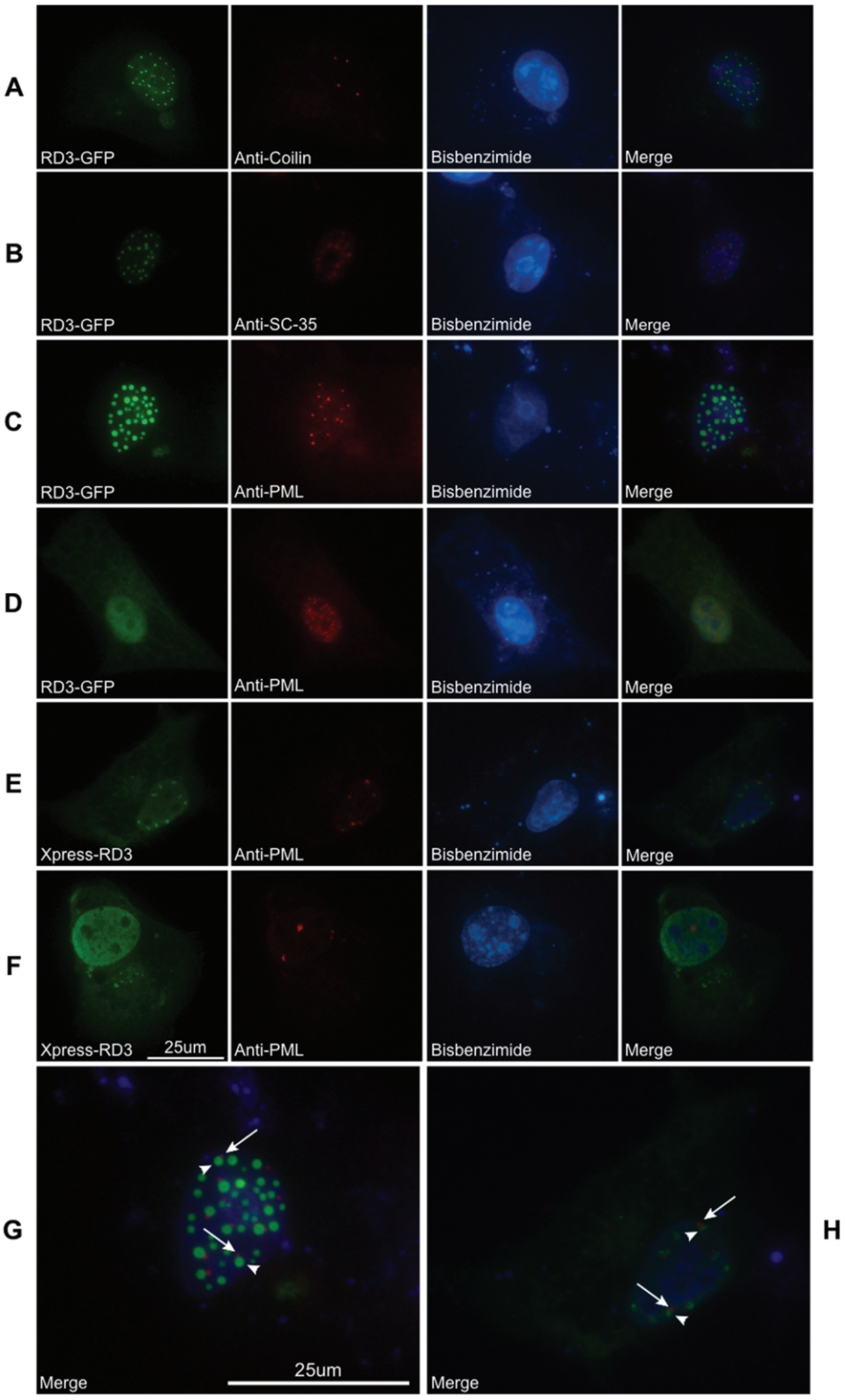

Figure 5. Immunolocalization of the RD3 protein. Mouse *Rd3* cDNA was placed in either the pEGFPN1 or the pcDNA4 vector and was expressed in COS-1 cells. The cells were observed directly via GFP or with use of an anti-Xpress antibody (*green*). Cells were also stained with subnuclear markers (*red*), to test for colocalization. Bisbenzimide was used to stain the nuclei (*blue*). *A,* RD3-GFP and Cajal body marker anti-coilin. *B,* RD3-GFP and nuclear speckle marker anti-SC-35. *C* and *D,* RD3-GFP and PML body marker anti-PML. *E* and F, Xpress-RD3 and anti-PML antibody. *G* and *H,* Higher magnification of the merged images from panels C and E, respectively. Close localization of RD3 and PML bodies are marked with an arrowhead and an arrow, respectively.

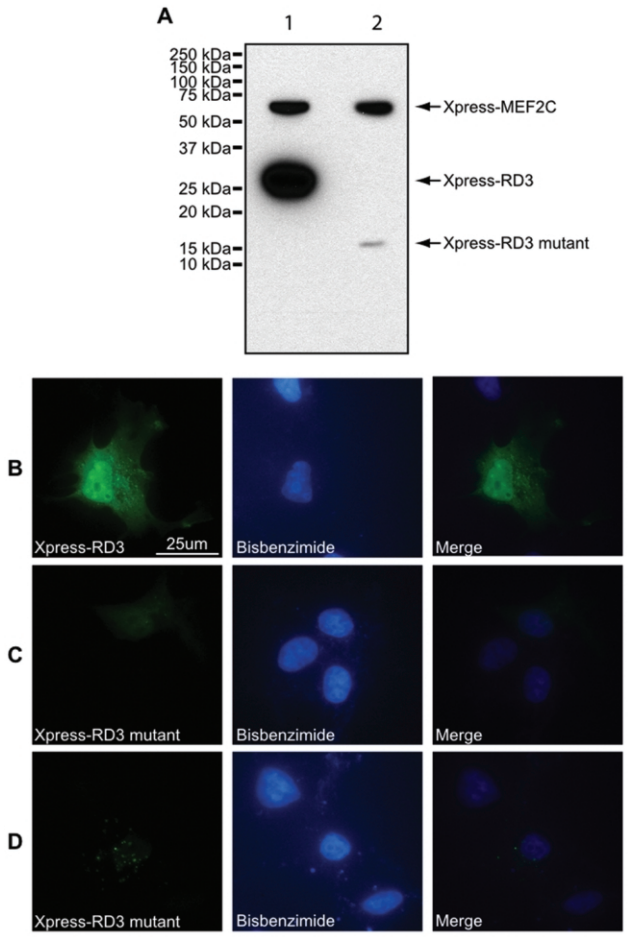

Figure 6. *A,* Examination of the mouse *rd3* mutation in COS-1 cells. Equal amounts of WT (*lane 1*) and mutant (*lane 2*) *Rd3*-pcDNA4 vectors were cotransfected with *Mef2c*-pcDNA4 into COS-1 cells. Cells were examined by immunoblot with use of anti-Xpress antibody. Roughly equal intensity of MEF2C signal shows that equal amounts of protein were loaded on the gel. WT RD3 protein is of expected molecular mass (~26 kDa), whereas the mutant RD3 protein is truncated (~15 kDa) and is expressed at lower levels. *B,* Immunolocalization of the RD3 protein in transfected cells, with use of WT *rd3*-pcDNA4 construct. Bisbenzimide was used to stain the nuclei (*blue*). *C* and *D,* Immunolocalization of the RD3 protein in transfected cells, with use of mutant *rd3*-pcDNA4 plasmid. Cells were examined as in panel B. Image exposures were performed in a consistent manner.

served in any other probands or controls from North America or Europe. To directly examine the impact of this change on RD3 transcript, we performed RT-PCR analysis of RNA from control lymphocytes, but no product could be amplified (data not shown).

Our mutation screening uncovered changes of uncertain significance in three female probands. The first affected individual (from North America) revealed four homozygous alterations (c.16T→C, 69G→C, 84G→A, and 235T→C) leading to two predicted amino acid changes (p.W6R, E23D, T28T, and L79L, respectively). She exhibited an atypical late-onset form of RP. The second proband (also from North America) carried a heterozygous c.389A→T alteration encoding a predicted p.K130M. This girl presented in 1996, then aged 11 years, with a history of poor vision beginning at age 3 years but with no family history of eye problems or blindness. Fundus examination showed round atrophic lesions in both maculae, and there was a cellophane-like sheen and atrophy in the other regions of the posterior poles. By ERG, it was determined that she had a CRD pattern, with cone ERG b-wave amplitudes at about one-third of normal and rod ERG amplitudes at ~80% of normal levels. The third proband (from Scandinavia) had a heterozygous c.170G→T change encoding p.G57V. She had no family history of visual handicap but had visual problems since age 6 years. Her eye disorder was diagnosed by repeated full-field ERG, at ages 9 years and 19 years, as cone-rod degeneration with reduced but still-remaining rod and cone function. At age 19 years, fundus examination revealed macular changes with atrophy and spicular pigment in the midperiphery. Visual acuity was reduced to 20/200, with central scotoma in both eyes.

Several other alterations were observed in the heterozygous form, both in probands and in controls, or did not segregate with the disease in affected families; these include c.103G→A (p.G35R), c.139C→T (p.R47C), c.202C→T (p.R68W), c.500G→A (p.R167K), and c.584A→T (p.D195V). The population group and frequency of each alteration are listed in table 1.

To examine whether missense alterations observed in the human mutation screen affected subcellular localization of the RD3 protein, we generated p.W6R, p.E23D, p.K130M, and p.W6R;E23D mutations in the RD3-GFP–expression construct. These changes were selected because of their absence in normal controls and their presence in individual probands. The GFP-fused mutant RD3 proteins did not appear to have a substantive difference from the control in immunoblot analysis or in COS-1 localization (data not shown). Overall, our data suggest that *RD3* mutations represent a rare cause of retinopathy.

Discussion

RDs are a significant cause of untreatable blindness in the United States. Delineation of precise genetic defects in RDs and of cellular pathways that lead to photoreceptor-cell death are critical for developing knowledge-based design of treatment and therapies. In our continuing effort to identify retinal-disease genes, we have uncovered genetic defects in the *RD3* gene that are responsible for photoreceptor degeneration in the *rd3* mouse and some patients with retinopathies. Notably, RDs can be caused by mutations in photoreceptor-specific (such as rhodopsin, *RP1, CRX,* and *NRL*) or ubiquitously expressed (such as *RPGR, CHM,* and *PRPF31*) genes. The *RD3* gene exhibits an interesting expression profile: whereas it is preferentially (and highly) expressed in the retina and in photorecep-

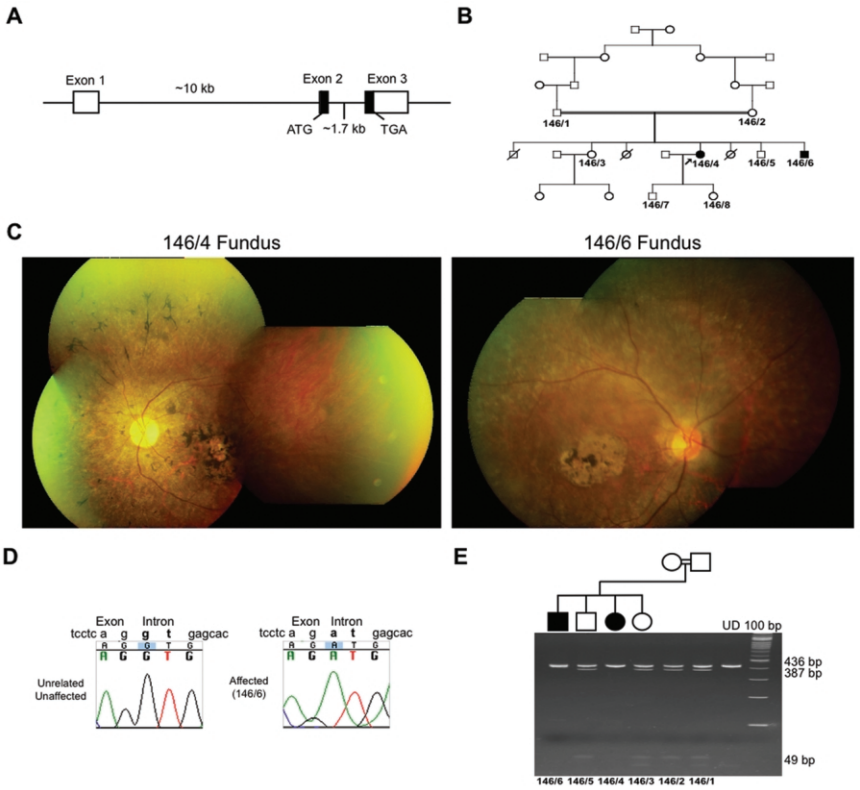

Figure 7. Findings for the LCA-affected family (from India), with a homozygous change in *RD3*. *A,* Genomic structure of the human *RD3* gene. *B,* Pedigree of family 146. Proband 146/4 is marked with an arrow. *C,* Fundus photographs of affected individuals 146/4 and 146/6. *D,* Chromatograms of unrelated unaffected subject and affected proband 146/6 at the exon2/intron2 junction. Individual 146/6 has a homozygous G→A change, which is predicted to remove the donor splice site of exon 2 and result in a stop codon after aa 99. *E,* Pedigree of a portion of family 146 and RFLP analysis of the mutation. Probands 146/4 and 146/6 show only a 436-bp band, whereas all other members show 49-bp and 387-bp bands in addition to the 436-bp band. UD = undigested.

tors, *Rd3* transcripts can be detected in mouse retinas that lack rod and cone photoreceptors.

The RD3 protein has a relatively low molecular mass (22 kDa) and includes a number of conserved sites for protein modification (specifically, phosphorylation and sumoylation). Additionally, the putative coiled-coil domain(s) might serve as protein-interaction site(s). The mutation identified in the *rd3* mouse generates a stop codon in the *Rd3* gene, thereby producing a truncated protein (of 11 kDa) that appears to be less stable, at least in transfected COS-1 cells. Hence, our data strongly implicate partial or complete loss of RD3 protein function as a possible mechanism of retinal degeneration in the *rd3* mouse. Although the *rd3* mutation is in the last exon, nonsense-mediated decay of the mutant transcript cannot be ruled out. In any event, the detection of a truncated RD3 mutant protein in COS-1 cells further validates the causal relationship of this mutation to retinopathy.

Subnuclear structures that commonly exist in cells include PML bodies, Cajal bodies, and nuclear speckles. PML bodies are implicated in diverse biological functions, including DNA repair, antiviral response, apoptosis, proteolysis, gene regulation, and tumor suppression.[33–35] PML is also suggested to be a transcriptional regulator and/or sensor of DNA damage and cellular stress.[33–35] Cajal bodies are associated with snRNPs and snoRNPs (small nuclear and nucleolar RNAs), which are involved in pre-mRNA and rRNA processing, respectively.[36] Nuclear speckles are observed close to genes with highly active transcription, are linked with pre-mRNA splicing, and are suggested to form a compartment for splicing factors and proteins involved in transcription.[37] Interestingly, a number of retinopathy genes are associated with transcription and splicing.[16,38–45] Varied localization of RD3 protein in COS-1 cells suggests its dynamic role in cellular processes and within subnuclear compartment(s). A reduced amount of mutant RD3 protein in transfected cells indicates that the loss of RD3 protein may compromise nuclear function(s). However, the precise role of RD3 in transcription, splicing, or other regulatory processes is subject to further experimentation.

LCA is a cause of early-onset (childhood) blindness, with an estimated prevalence of 1 in 50,000–100,000.[46] Known and putative functions and/or location of proteins encoded by mutant LCA genes are diverse and include pro-

Table 1. Summary of the *RD3* Human Mutation Screen

Change	No. of Subjects with Exon Change					
	United Kingdom/ Scandinavia		India		North America	
	Proband (n = 317)	Control (n = 95)	Proband (n = 103)	Control[a] (n = 121)	Proband (n = 461)	Control (n = 175)
Homozygous c.16T→C, 69G→C, 84G→A, 235T→C (p.W6R, E23D, T28T, L79L)	0	0	0	NA	1	0
c.103G→A (p.G35R)	0	0	1	NA	0	0
c.139C→T (p.R47C)	8	2	2	NA	10	5
c.170G→T (p.G57V)	1	0	0	NA	0	0
c.202C→T (p.R68W)	0	0	1	NA	0	0
c.389A→T (p.K130M)	0	0	0	NA	1	0
c.500G→A (p.R167K)	3	0	0	NA	1	1
c.584A→T (p.D195V)	1	3	0	NA	4	6
c.296+1G→A homozygous	0	0	1[b]	0	0	0

NOTE.—Probands with RP were sequenced for changes in exon 2 and exon 3 of *RD3*.

[a] The c.296+1G→A mutation was examined in 121 Indian controls by RFLP. NA = not applicable.

[b] One proband was found in the initial screen. An affected sibling was subsequently identified during follow-up.

tein trafficking, cell-cycle progression, photoreceptor morphogenesis, transcription, phototransduction, and retinoid cycle.[4,13,18,47] *RD3* is likely responsible for a small subset of LCA, and further examination of this retinopathy might allow us to determine the proportion of *RD3* mutation–based early-onset retinopathy. We have identified two siblings carrying a mutation in the invariant G residue of the exon 2 donor splice site. Splice-site alterations are responsible for at least 15% of human mutations.[48] Mutation of the invariant G at donor splice site +1 is a commonly reported cause of human disease (Human Gene Mutation Database).[49] It is possible that a cryptic splice site within exon 2 or intron 2 is used after the invariant G is changed. Additionally, exon 2 may be skipped entirely,[50] or the mRNA may be subject to nonsense-mediated decay.[51] Within exon 2, there are two potential cryptic splice sites—c.159 and c.169—with scores of 0.50 and 0.43, respectively. After the normal exon 2 splice site, the next putative splice sites are at nucleotides c.296+219 and c.296+432 (respective scores 0.41 and 1.00). The likely splicing site for mutant allele is c.296+432, because of its high score[52] (Berkeley *Drosophila* Genome Project: Splice Site Prediction by Neural Network Web site). The splice-site mutation is predicted to result in a truncated RD3 protein, ending at aa 99. This shortened protein would be similar to the 107-aa protein in the *rd3* mice, thereby raising the possibility that the *rd3* mouse is a useful mouse model for the retinal disease in this family. Notably, the *rd3* mice exhibit a relatively quick degeneration of photoreceptors. For example, ONL loss in RBF/DnJ-*rd3/rd3* mice is complete in ~8 wk.[19] In comparison, the quite severe *Pde6b*^{rd1} and *Rd4* mouse retinas show severe degeneration by age 1 mo and 2 mo, respectively.[53] Several strains of mutant mice reveal much slower photoreceptor loss than do *rd3,* with complete degeneration as late as age 30 mo.[53]

In the one proband carrying four homozygous alterations, W6 and E23 residues are conserved in almost all species. Codon 6 in chimpanzee is arginine (instead of tryptophan), and codon 23 in frog is aspartic acid (instead of glutamic acid). Since W6R and E23D alterations exist individually in chimpanzee and frog, it is difficult to conclude whether these changes cause disease in humans. Additional work would be required to fully characterize the functional effect of these alterations. For c.389A→T (p.K130M)– and c.16T→C;69G→C;84G→A;235T→C (p.W6R; E23D;T28T;L79L)–containing probands, we attempted to collect DNA samples from the respective families but were unsuccessful. Although c.389A→T (p.K130M) and c.170G→T (p.G57V) heterozygous changes are not observed in our cohort of controls, we learned that these subjects are of Chinese and mixed European–Middle Eastern decent, respectively. Screening of ethnically matched controls might be necessary to determine whether these changes are polymorphic in their respective populations. We identified several additional nucleotide changes that do not appear to be associated with disease in heterozygous state; these are c.103G→A (p.G35R), c.139C→T (p.R47C), c.202C→T (p.R68W), c.500G→A (p.R167K). and c.584A→T (p.D195V).

Since the splice–site alteration represents the only likely disease-causing mutation in 881 examined probands, we suggest that *RD3* mutations are a rare cause of retinal disease. *C1orf36* (*RD3*) was tested elsewhere as a candidate retinal-disease gene; however, no significant alterations were observed in this earlier study.[30] Recently, initial screening of coding regions in patients with retinopathy did not reveal any disease-causing mutation in *CEP290/NPHP6,* and only the lymphocyte RNA analysis established it as a major LCA gene.[18] However, unlike *CEP290, RD3* is not detected in lymphocytes.

Recent studies suggest a more dynamic environment in the nucleus than previously expected.[54] Discrete nuclear processes (such as steps in gene transcription and post-transcriptional events) appear to be mediated by association of gene regions, transcribed sequences, and/or proteins in unique subnuclear compartments. PML bodies are

but one component of the nucleus whose role(s) is not completely understood. The discovery of *RD3* and its further characterization might allow us to gain insights into fundamental regulatory events that are necessary for retinal function.

Acknowledgments

We thank Amna Shah, for technical assistance, M. N. Mandal and members of the Swaroop lab, for reagents and critical comments, and S. Ferrara, for administrative support. This work was supported in part by National Institutes of Health grants EY011115, EY007003, and EY007758 and by the Foundation Fighting Blindness, the Elmer and Silvia Sramek Foundation, and Research to Prevent Blindness. J.S.F. is a recipient of a Canadian Institutes of Health Research postdoctoral fellowship.

Web Resources

The URLs for data presented herein are as follows:

Berkeley *Drosophila* Genome Project: Splice Site Prediction by Neural Network, http://www.fruitfly.org/seq_tools/splice.html
Human Gene Mutation Database, http://www.hgmd.org/
NCBI Expression Profile Viewer, http://www.ncbi.nlm.nih.gov/UniGene/ESTProfileViewer.cgi?uglist=Hs.632495 (for Hs.632495)
Online Mendelian Inheritance in Man (OMIM), http://www.ncbi.nlm.nih.gov/Omim/ (for RP and LCA)
RetNet, http://www.sph.uth.tmc.edu/Retnet/

References

1. Rivolta C, Sharon D, DeAngelis MM, Dryja TP (2002) Retinitis pigmentosa and allied diseases: numerous diseases, genes, and inheritance patterns. Hum Mol Genet 11:1219–1227
2. Kennan A, Aherne A, Humphries P (2005) Light in retinitis pigmentosa. Trends Genet 21:103–110
3. Fain GL (2006) Why photoreceptors die (and why they don't). Bioessays 28:344–354
4. Koenekoop RK (2004) An overview of Leber congenital amaurosis: a model to understand human retinal development. Surv Ophthalmol 49:379–398
5. Weleber RG (2005) Inherited and orphan retinal diseases: phenotypes, genotypes, and probable treatment groups. Retina 25:S4–S7
6. Daiger SP (2004) Identifying retinal disease genes: how far have we come, how far do we have to go? Novartis Found Symp 255:17–27
7. Chang B, Hawes NL, Hurd RE, Wang J, Howell D, Davisson MT, Roderick TH, Nusinowitz S, Heckenlively JR (2005) Mouse models of ocular diseases. Vis Neurosci 22:587–593
8. Rakoczy EP, Yu MJ, Nusinowitz S, Chang B, Heckenlively JR (2006) Mouse models of age-related macular degeneration. Exp Eye Res 82:741–752
9. Bowes C, Li T, Danciger M, Baxter LC, Applebury ML, Farber DB (1990) Retinal degeneration in the rd mouse is caused by a defect in the β subunit of rod cGMP-phosphodiesterase. Nature 347:677–680
10. Pittler SJ, Baehr W (1991) Identification of a nonsense mutation in the rod photoreceptor cGMP phosphodiesterase beta-subunit gene of the *rd* mouse. Proc Natl Acad Sci USA 88:8322–8326
11. Travis GH, Brennan MB, Danielson PE, Kozak CA, Sutcliffe JG (1989) Identification of a photoreceptor-specific mRNA encoded by the gene responsible for retinal degeneration slow (*rds*). Nature 338:70–73
12. Akhmedov NB, Piriev NI, Chang B, Rapoport AL, Hawes NL, Nishina PM, Nusinowitz S, Heckenlively JR, Roderick TH, Kozak CA, Danciger M, Davisson MT, Farber DB (2000) A deletion in a photoreceptor-specific nuclear receptor mRNA causes retinal degeneration in the *rd7* mouse. Proc Natl Acad Sci USA 97:5551–5556
13. Chang B, Khanna H, Hawes NL, Jimeno D, He S, Lillo C, Parapuram SK, Cheng H, Scott A, Hurd RE, Sayer JA, Otto EA, Attanasio M, O'Toole JF, Jin G, Shou C, Hildebrandt F, Williams DS, Heckenlively JR, Swaroop A (2006) An in-frame deletion in a novel centrosomal/ciliary protein CEP290/NPHP6 perturbs its interaction with RPGR and results in early-onset retinal degeneration in the *rd16* mouse. Hum Mol Genet 15: 1847–1857
14. Kajiwara K, Hahn LB, Mukai S, Travis GH, Berson EL, Dryja TP (1991) Mutations in the human retinal degeneration slow gene in autosomal dominant retinitis pigmentosa. Nature 354:480–483
15. McLaughlin ME, Sandberg MA, Berson EL, Dryja TP (1993) Recessive mutations in the gene encoding the β-subunit of rod phosphodiesterase in patients with retinitis pigmentosa. Nat Genet 4:130–134
16. Haider NB, Jacobson SG, Cideciyan AV, Swiderski R, Streb LM, Searby C, Beck G, Hockey R, Hanna DB, Gorman S, Duhl D, Carmi R, Bennett J, Weleber RG, Fishman GA, Wright AF, Stone EM, Sheffield VC (2000) Mutation of a nuclear receptor gene, *NR2E3,* causes enhanced S cone syndrome, a disorder of retinal cell fate. Nat Genet 24:127–131
17. Sayer JA, Otto EA, O'Toole JF, Nurnberg G, Kennedy MA, Becker C, Hennies HC, et al (2006) The centrosomal protein nephrocystin-6 is mutated in Joubert syndrome and activates transcription factor ATF4. Nat Genet 38:674–681
18. den Hollander AI, Koenekoop RK, Yzer S, Lopez I, Arends ML, Voesenek KEJ, Zonneveld MN, Strom TM, Meitinger T, Brunner HG, Hoyng CB, van den Born LI, Rohrschneider K, Cremers FPM (2006) Mutations in the *CEP290* (*NPHP6*) gene are a frequent cause of Leber congenital amaurosis. Am J Hum Genet 79:556–561
19. Heckenlively JR, Chang B, Peng C, Hawes NL, Roderick TH (1993) Variable expressivity of rd-3 retinal degeneration dependent on background strain. In: Hollyfield JG, Anderson RE, LaVail MM (eds) Retinal degeneration. Plenum Press, New York, pp 273–280
20. Linberg KA, Fariss RN, Heckenlively JR, Farber DB, Fisher SK (2005) Morphological characterization of the retinal degeneration in three strains of mice carrying the *rd-3* mutation. Vis Neurosci 22:721–734
21. Danciger JS, Danciger M, Nusinowitz S, Rickabaugh T, Farber DB (1999) Genetic and physical maps of the mouse rd3 locus: exclusion of the ortholog of USH2A. Mamm Genome 10:657–661
22. Pieke-Dahl S, Ohlemiller KK, McGee J, Walsh EJ, Kimberling WJ (1997) Hearing loss in the RBF/DnJ mouse, a proposed animal model of Usher syndrome type IIa. Hear Res 112:1–12
23. Pang JJ, Chang B, Hawes NL, Hurd RE, Davisson MT, Li J, Noorwez SM, Malhotra R, McDowell JH, Kaushal S, Hauswirth WW, Nusinowitz S, Thompson DA, Heckenlively JR (2005) Retinal degeneration 12 (*rd12*): a new, spontaneously arising

mouse model for human Leber congenital amaurosis (LCA). Mol Vis 11:152–162
24. Mears AJ, Kondo M, Swain PK, Takada Y, Bush RA, Saunders TL, Sieving PA, Swaroop A (2001) Nrl is required for rod photoreceptor development. Nat Genet 29:447–452
25. Furukawa T, Morrow EM, Li T, Davis FC, Cepko CL (1999) Retinopathy and attenuated circadian entrainment in Crx-deficient mice. Nat Genet 23:466–470
26. Friedman JS, Ducharme R, Raymond V, Walter MA (2000) Isolation of a novel iris-specific and leucine-rich repeat protein (oculoglycan) using differential selection. Invest Ophthalmol Vis Sci 41:2059–2066
27. Friedman JS, Khanna H, Swain PK, Denicola R, Cheng H, Mitton KP, Weber CH, Hicks D, Swaroop A (2004) The minimal transactivation domain of the basic motif-leucine zipper transcription factor NRL interacts with TATA-binding protein. J Biol Chem 279:47233–47241
28. Chang B, Heckenlively JR, Hawes NL, Roderick TH (1993) New mouse primary retinal degeneration (*rd-3*). Genomics 16:45–49
29. Akimoto M, Cheng H, Zhu D, Brzezinski JA, Khanna R, Filippova E, Oh EC, Jing Y, Linares JL, Brooks M, Zareparsi S, Mears AJ, Hero A, Glaser T, Swaroop A (2006) Targeting of GFP to newborn rods by Nrl promoter and temporal expression profiling of flow-sorted photoreceptors. Proc Natl Acad Sci USA 103:3890–3895
30. Lavorgna G, Lestingi M, Ziviello C, Testa F, Simonelli F, Manitto MP, Brancato R, Ferrari M, Rinaldi E, Ciccodicola A, Banfi S (2003) Identification and characterization of *C1orf36,* a transcript highly expressed in photoreceptor cells, and mutation analysis in retinitis pigmentosa. Biochem Biophys Res Commun 308:414–421
31. Blackshaw S, Fraioli RE, Furukawa T, Cepko CL (2001) Comprehensive analysis of photoreceptor gene expression and the identification of candidate retinal disease genes. Cell 107: 579–589
32. Lupas A, Van Dyke M, Stock J (1991) Predicting coiled coils from protein sequences. Science 252:1162–1164
33. Zhong S, Salomoni P, Pandolfi PP (2000) The transcriptional role of PML and the nuclear body. Nat Cell Biol 2:E85–90
34. Strudwick S, Borden KL (2002) Finding a role for PML in APL pathogenesis: a critical assessment of potential PML activities. Leukemia 16:1906–1917
35. Dellaire G, Bazett-Jones DP (2004) PML nuclear bodies: dynamic sensors of DNA damage and cellular stress. Bioessays 26:963–977
36. Cioce M, Lamond AI (2005) Cajal bodies: a long history of discovery. Annu Rev Cell Dev Biol 21:105–131
37. Lamond AI, Spector DL (2003) Nuclear speckles: a model for nuclear organelles. Nat Rev Mol Cell Biol 4:605–612
38. Bessant DA, Payne AM, Mitton KP, Wang QL, Swain PK, Plant C, Bird AC, Zack DJ, Swaroop A, Bhattacharya SS (1999) A mutation in NRL is associated with autosomal dominant retinitis pigmentosa. Nat Genet 21:355–356
39. Sohocki MM, Sullivan LS, Mintz-Hittner HA, Birch D, Heckenlively JR, Freund CL, McInnes RR, Daiger SP (1998) A range of clinical phenotypes associated with mutations in *CRX,* a photoreceptor transcription-factor gene. Am J Hum Genet 63: 1307–1315
40. Banerjee P, Kleyn PW, Knowles JA, Lewis CA, Ross BM, Parano E, Kovats SG, Lee JJ, Penchaszadeh GK, Ott J, Jacobson SG, Gilliam TC (1998) *TULP1* mutation in two extended Dominican kindreds with autosomal recessive retinitis pigmentosa. Nat Genet 18:177–179
41. Boggon TJ, Shan WS, Santagata S, Myers SC, Shapiro L (1999) Implication of tubby proteins as transcription factors by structure-based functional analysis. Science 286:2119–2125
42. McKie AB, McHale JC, Keen TJ, Tarttelin EE, Goliath R, van Lith-Verhoeven JJ, Greenberg J, Ramesar RS, Hoyng CB, Cremers FP, Mackey DA, Bhattacharya SS, Bird AC, Markham AF, Inglehearn CF (2001) Mutations in the pre-mRNA splicing factor gene *PRPC8* in autosomal dominant retinitis pigmentosa (RP13). Hum Mol Genet 10:1555–1562
43. Vithana EN, Abu-Safieh L, Allen MJ, Carey A, Papaioannou M, Chakarova C, Al-Maghtheh M, Ebenezer ND, Willis C, Moore AT, Bird AC, Hunt DM, Bhattacharya SS (2001) A human homolog of yeast pre-mRNA splicing gene, *PRP31*, underlies autosomal dominant retinitis pigmentosa on chromosome 19q13.4 (*RP11*). Mol Cell 8:375–381
44. Chakarova CF, Hims MM, Bolz H, Abu-Safieh L, Patel RJ, Papaioannou MG, Inglehearn CF, Keen TJ, Willis C, Moore AT, Rosenberg T, Webster AR, Bird AC, Gal A, Hunt D, Vithana EN, Bhattacharya SS (2002) Mutations in *HPRP3,* a third member of pre-mRNA splicing factor genes, implicated in autosomal dominant retinitis pigmentosa. Hum Mol Genet 11:87–92
45. Keen TJ, Hims MM, McKie AB, Moore AT, Doran RM, Mackey DA, Mansfield DC, Mueller RF, Bhattacharya SS, Bird AC, Markham AF, Inglehearn CF (2002) Mutations in a protein target of the Pim-1 kinase associated with the RP9 form of autosomal dominant retinitis pigmentosa. Eur J Hum Genet 10:245–249
46. Allikmets R (2004) Leber congenital amaurosis: a genetic paradigm. Ophthalmic Genet 25:67–79
47. Janecke AR, Thompson DA, Utermann G, Becker C, Hubner CA, Schmid E, McHenry CL, Nair AR, Ruschendorf F, Heckenlively J, Wissinger B, Nurnberg P, Gal A (2004) Mutations in *RDH12* encoding a photoreceptor cell retinol dehydrogenase cause childhood-onset severe retinal dystrophy. Nat Genet 36:850–854
48. Krawczak M, Reiss J, Cooper DN (1992) The mutational spectrum of single base-pair substitutions in mRNA splice junctions of human genes: causes and consequences. Hum Genet 90:41–54
49. Stenson PD, Ball EV, Mort M, Phillips AD, Shiel JA, Thomas NS, Abeysinghe S, Krawczak M, Cooper DN (2003) Human Gene Mutation Database (HGMD): 2003 update. Hum Mutat 21:577–581
50. Nakai K, Sakamoto H (1994) Construction of a novel database containing aberrant splicing mutations of mammalian genes. Gene 141:171–177
51. Baker KE, Parker R (2004) Nonsense-mediated mRNA decay: terminating erroneous gene expression. Curr Opin Cell Biol 16:293–299
52. Reese MG, Eeckman FH, Kulp D, Haussler D (1997) Improved splice site detection in Genie. J Comput Biol 4:311–323
53. Chang B, Hawes NL, Hurd RE, Davisson MT, Nusinowitz S, Heckenlively JR (2002) Retinal degeneration mutants in the mouse. Vision Res 42:517–525
54. Akhtar A, Matera AG (2006) In and around the nucleus. Nat Cell Biol 8:3–6

IOVS Papers in Press. Published on April 1, 2009 as Manuscript iovs.09-3479

GENETIC ANALYSIS OF INDIAN FAMILIES WITH AUTOSOMAL RECESSIVE RETINITIS PIGMENTOSA BY HOMOZYGOSITY SCREENING

Hardeep Pal Singh[1], Subhadra Jalali[2], Raja Narayanan[2], Chitra Kannabiran[1*]

[1]Kallam Anji Reddy Molecular Genetics Laboratory, Champalimaud Translational Centre for Eye Research , Hyderabad Eye Research Foundation, L.V. Prasad Eye Institute, Hyderabad, India
[2]Smt. Kannuri Santhamma Retina-Vitreous Service, L.V. Prasad Eye Institute, Hyderabad, India.

Word count: 3483.

Support: Grant RO1 TW06231 from the Fogarty International Center, National Institutes of Health, Bethesda, Maryland, under the Global Health Research Initiative Program (C.K.), Department of Biotechnology, New Delhi, India, and by the Champalimaud Foundation, Portugal.

*Address for correspondence: [1]Kallam Anji Reddy Molecular Genetics Laboratory, L.V. Prasad Eye Institute, L.V. Prasad Marg, Banjara Hills, Hyderabad 500 034, India. E-mail: chitra@lvpei.org

Phone: 91-40-30612345.

Copyright 2009 by The Association for Research in Vision and Ophthalmology, Inc.

Abstract

PURPOSE. To identify the disease-causing genes in families with autosomal recessive RP (ARRP).

METHODS. We screened families for homozygosity at candidate gene loci followed by screening of the selected gene for pathogenic mutations if homozygosity was present at a given locus. A total of 34 families were included of which 24 were consanguineous. Twenty-three genes were selected for screening. The presence of homozygosity was assessed by genotyping flanking microsatellite markers at each locus in affected individuals. Mutations were detected by sequencing of coding regions of genes. Sequence changes were tested for presence in 100 or more unrelated normal controls and for co-segregation in family members.

RESULTS. Homozygosity was detected at one or more loci in affected individuals of 10/34 families. Homozygous disease co-segregating sequence changes (2 frameshift, 2 missense and 1 nonsense; 4 novel) were found in the *TULP1, RLBP1, ABCA4, RPE65* and *RP1* genes in 5 /10 families. These changes were absent in 100 normal controls. In addition, several polymorphisms and novel variants were also found. All of the putative pathogenic changes were associated with severe forms of RP with onset in childhood. Associated macular degeneration was found in three families with mutations in *TULP1*, *ABCA4* and *RP1* genes.

CONCLUSIONS. Novel mutations were found in different ARRP genes. Mutations were detected in about 15% (5/34) of ARRP families tested, suggesting involvement of other genes in the remaining families.

Introduction

Retinal dystrophies are a group of genetically and clinically heterogeneous disorders involving degeneration of the photoreceptors and resulting in partial or complete blindness**.** Retinitis pigmentosa (RP) is the most common clinical expression but this condition represents a clinical manifestation of diverse genetic errors that are inherited as autosomal dominant, recessive, X-linked, digenic or mitochondrial disorders. The manifestation and course of RP can show considerable variation between individuals, and onset of the disease can vary from childhood to adolescence or early adulthood. Initial symptoms include night blindness in the early stages coupled with decreased visual acuity and progressive loss of visual fields. Clinically, changes in the retina include pallor of the optic disc, attenuated vasculature, pigmentary deposits appearing as bony spicules, atrophy of retinal tissue and diminished electroretinographic responses. The prevalence of RP ranges from 1 in 5000 to 1 in 1000 in different parts of the world.[1-3] ARRP appears to be relatively more common than dominant or X-inked forms in patient populations.[4, 5] About 50 genes are known for RP (RetNet-http://www.sph.uth.tmc.edu/Retnet). Mutations in known genes are detectable in only a subset of patients with RP suggesting that more genes are yet to be identified. [6] Functionally RP genes are diverse and encoded proteins are involved in a variety of cellular processes that are retina-specific as well as ubiquitous.

This study was designed to identify genes underlying ARRP in affected families. We screened 34 ARRP families for homozygosity at 23 loci for possible involvement in disease. The 23 loci belong to subset of loci commonly involved in RP and related disorders or were candidates based on expression and function. Screening was done in 2 stages. First, we performed genotyping of

microsatellite markers flanking each of the 23 genes to test for homozygosity at any of these loci among affected individuals. In the second stage, we sequenced coding regions of genes present at homozygous regions for pathogenic mutations.

Methods:

The study protocol was approved by the Institutional Review Board and followed the tenets of the declaration of Helsinki. Probands with a family history suggestive of recessive RP were included in the study and available family members were enrolled. All subjects, both affected and unaffected, were clinically evaluated and informed consent was obtained. A total of 34 families with 2 or more affected individuals were recruited, 24 families were consanguineous and 10 were non-consanguineous.. Essential diagnostic criteria for inclusion included bilateral, diffuse and widespread retinal pigment epithelial degeneration, arterial narrowing, commensurate visual field loss, and reduced amplitudes on electroretinogram (ERG) reduced to less than 25% of the maximal retinal response in normal individuals (normal amplitude of b-wave >350 μV and a-wave >110 μV) with evidence of rod and cone involvement. Other clinical signs that were supportive not essential for diagnosis of RP included pigment migration including bone-corpuscular pigmentation, vitreous opacities and vitreous pigments, associated retinal pigment epithelium atrophic changes in the macular area and diffuse disk pallor. Excluded were patients who had unilateral disease, nystagmus and eye poking behaviour in childhood, exudative retinal detachment, retinal vasculitis, chorioretinitis or any other secondary cause of pigmentary retinal changes. Clinical features of patients were reviewed and confirmed independently by 2 ophthalmologists.

Blood samples were collected from the affected and unaffected members of the families by venipuncture. The DNA was extracted from this blood by phenol-chloroform method.

Twenty-three candidate genes were selected for screening, which included 14 known genes for ARRP (phosphodiesterase 6A (*PDE6A*), phosphodiesterase 6B (*PDE6B*), rhodopsin (*RHO*), cyclic nucleotide gated channel alpha 1(CNGA1), cyclic nucleotide gated channel beta 1 (*CNGB1),* crumbs homolog 1 (*CRB1*), retinitis pigmentosa 1 (*RP1),* neural retina leucine zipper (*NRL*), ATP-binding cassette subfamily A member 4 (*ABCA4*), cellular retinaldehyde binding protein 1(*RLBP1),* retinal pigment epithelium protein 65 KDa (*RPE65),* retinal G-protein coupled receptor (*RGR*), tubby-like protein 1 (*TULP1*), prominin 1 (*PROM1*)); 7 genes for related disorders such as Lebers congenital amaurosis (LCA), cone-rod dystrophy (CRD), dominant/digenic RP (guanylate cyclase 2D, membrane (retina-specific) (*GUCY2D*), guanylate cyclase activator 1A (*GUCA1A*), rod outer segment membrane protein 1 (*ROM1*), retinal degeneration slow (*RDS*), cone-rod homeobox (*CRX),* aryl hydrocarbon receptor interacting protein-like 1 (*AIPL1*), RPGR interacting protein 1 (*RPGRIP1*)); and 2 genes that are candidates for retinal dystrophy but not yet shown to have mutations in humans (phosphodiesterase 6G (*PDE6G*), cellular retinol binding protein 1(*RBP1)*). Each locus was screened for homozygosity by genotyping 2 or more microsatellite markers (total of 57 markers). Microsatellite markers were selected based on reported high heterozygosity values (0.7 or more), and generally located within an interval of ~5-10 megabases of the candidate gene. Information on the primers for amplification of microsatellite markers, marker heterozygosity and location was obtained from the UniSTS (http://www.ncbi.nlm.nih.gov/sites/entrez?db=unists), Human Genome Database and NCBI Mapview, (http://www.ncbi.nlm.nih.gov/mapview/) databases. The detection of homozygosity at a given locus shared only by affected members but not by unaffected family members was investigated further by

typing additional markers at the locus for confirming homozygosity and subsequent screening of the relevant gene for mutations. Uninformative loci in which affected as well as one or more unaffected members were homozygous, were genotyped with additional markers. Genotyping was carried out for 76 affected and 88 unaffected individuals from 34 families. Genotyping was done in multiplex PCR reactions followed by electrophoresis on the ABI310 genetic analyzer. Alleles were determined using GeneScan software (Applied Biosystems Inc, Foster City, California, USA). Screening of coding regions of genes was done by PCR amplification of exons and adjacent intronic regions, followed by direct automated sequencing. Sequence changes observed were checked for co-segregation in the family and for presence/absence in at least 100 healthy control individuals by RFLP or direct sequencing. For RFLP, restriction enzyme-digested products were resolved on 8% or 10% acrylamide gels and visualized after ethidium bromide staining.

Multiple sequence alignment of protein sequences was carried out using ClustalW2 (http://www.ebi.ac.uk/Tools/clustalw2/index.html). Sorting Intolerant from Tolerant (SIFT) analysis (http://blocks.fhcrc.org/sift/) was used to predict the potential impact of a missense substitution on protein function. A SIFT score of below a cutoff of 0.05 for a given substitution is predicted as not tolerated while those with scores above this value are considered as tolerated.

Results:

Based on genotypes obtained at markers flanking the 23 gene loci, homozygosity specific for affected members was detected at 12 loci in 10/34 families (details in Table1). Screening of the relevant

candidate genes in these cases showed putative pathogenic changes in 5 genes (listed in Table 2). Several polymorphisms and other variants of uncertain significance were also detected of which novel polymorphisms are listed in Table 3. A summary of findings in families with mutations is given in the following sections.

RPE65

In family RP205 (pedigree shown in Figure 1), homozygosity was detected at the *RPE65* gene locus. Screening of the *RPE65* gene showed a homozygous single base deletion in exon 10 of *RPE65* (cDNA change c.1060delA). This change co-segregated with the disease in the family. None of 103 control individuals tested by direct sequencing of PCR products of exon 10 showed this change. Both the affected individuals had the initial symptom of night blindness reportedly by 1 year of age (Figure 2A). The fundus showed arterial narrowing and white dots in the periphery due to RPE atrophy. A diagnosis of early onset RP was made for both patients in this family. Clinical features of patients are summarized in Table 4.

RP1

Homozygosity was detected in 2 affected members of family RP170 (Figure 1) at the *RP1* gene locus. Screening of the *RP1* gene showed 4 sequence changes, one novel single base deletion (Table 2) and 3 reported SNPs. The single base deletion, c.2847delT, co-segregated with the disease phenotype in the family and is predicted to result in a frameshift at codon 949 leading to premature termination after 32 amino acid residues (p.Asn949LysfsX32). This change was not observed in any of the 202 control chromosomes screened for this deletion by direct sequencing. In the proband, 3 reported SNPs were

identified in homozygous form (rs444772, rs414352, rs441800 (c.5175A>G); not shown). Affected individuals of this family had symptoms of night blindness beginning in childhood and progressively reduced visual acuity. The fundus showed equatorial RPE degeneration, pale disc, arterial narrowing, vitreous opacities and macular RPE degeneration (Figure 2B). Visual fields showed a central island of vision. This family had a diagnosis of RP with macular degeneration (Table 4).

TULP1

In family RP126 (Figure 1) homozygosity among affected members was detected at 2 gene loci, *TULP1* and *CRB1* and hence both the genes were selected for the mutation screening.

Five homozygous sequence changes were found in the *TULP1* gene in the proband RP126/1, including one novel missense change and 4 reported SNPs. A single base substitution of c.1199G>A was found in exon 12 of the gene, corresponding to a missense change Arg400Gln (Table 2). This change co-segregated with the disease phenotype and was absent in 109 normal control individuals screened using restriction enzyme *Eco57I.* As shown in Figure 3, Arg400 is highly evolutionarily conserved, suggesting that the alteration in this residue would be pathogenic. SIFT analysis of this substitution predicts this change to be possibly damaging to the protein (SIFT score-0.00). Four reported SNPs (rs7764472, rs58984224, rs2064317, rs2064318; data not shown) identified in this gene, were also homozygous in the proband.

Two affected individuals in this family showed initial symptoms of night blindness in childhood, followed by progressively reduced vision. Fundus showed diffuse RPE degeneration, pigment migration, arterial narrowing with prominent macular degeneration and optic disc pallor (Figure 2C, Table 4). The affected individuals had a diagnosis of advanced RP.

RLBP1

In family RP169 (Figure 1), homozygosity was detected at the *RLBP1* gene locus. Screening of the proband RP169/3 for mutations in the *RLBP1* gene showed a novel homozygous substitution in exon 6 (c.451C>T; Table 2), which predicts a missense change Arg151Trp. This change co-segregated with the disease phenotype in RP169. 108 control individuals were tested for the presence of this change by restriction digestion of PCR-amplified product of exon 6 with restriction enzyme *Hpy188III*. None of the control chromosomes were positive for the change. The Arg151 residue is conserved among different species (Figure 4) suggesting that it is essential for protein function. The SIFT score for this change was 0.00 predicting it to be deleterious to the protein.

The affected individuals of this family presented to us at age 16 and 12 years (Table 4). In both the individuals night blindness began in childhood. The fundus showed diffuse RPE degeneration, pigment migration, and arterial narrowing with macular sparing (Figure 2D). These individuals had a visual acuity of 20/50 in both eyes. A diagnosis of RP was made in these individuals.

ABCA4

Genotyping at the 23 candidate gene loci in family RP213 (Figure 1) indicated homozygosity at the *ABCA4* gene locus. Screening of the *ABCA4* gene revealed 7 homozygous sequence changes in the proband. One novel nonsense mutation Tyr665X (c.1995C>A; Table 2) co-segregated with the disease phenotype in family RP213. The Tyr665X change was absent in 101 control individuals (202 chromosomes). This change leads to premature truncation of the ABCA4 protein and is predicted to result in complete loss of 2 ATP binding domains, partial loss of 1st and 2nd transmembrane domains.[7] Among the other variants found in *ABCA4*, one novel missense change Met1419Thr (c.4256T>C) was found (Table 3) that leads to abolition of one of the restriction sites for *NlaIII* in the 229 bp PCR product of exon 29 of ABCA4. 105 normal controls were screened for this change by digestion with *NlaIII*. Five of 105 control individuals (4.8%) were heterozygous for Met1419Thr suggesting that it is a polymorphic variant. Mutiple sequence alignment of ABCA4 proteins showed that this residue is not conserved among different species (not shown). SIFT analysis yielded a score of 0.16 for this substitution interpreting it to be tolerated. Other homozygous sequence changes identified were reported SNPs (rs4847281, rs547806, rs55860151, rs1801359 and rs17110761; data not shown).

Affected individuals of family RP213 showed onset of visual loss at 9 and 11 years of age. The fundus showed equatorial RPE degeneration, pale disc, arterial narrowing and a large patch of macular atrophy (Figure 2E). ERG was extinguished for rods and severely reduced for cones. These patients had a diagnosis of RP with atrophic maculopathy (Table 4).

Changes identified at the remaining loci selected for homozygosity:

Five additional loci listed in Table 1 at which homozygosity was found (*PDE6B*, *CRB1*, *CNCG1*, *RGR* and *NRL*) showed no pathogenic changes upon sequencing. Non-pathogenic variants or changes of unknown significance found in these 5 genes are discussed below.

Affected members of RP126 also showed homozygosity at the *CRB1* locus (Table 1). Screening of the *CRB1* gene in the proband RP126/1 (Figure 1) showed 3 homozygous sequence changes- one novel synonymous change, Arg905Arg (c.2715G>A; Table 3) and 2 reported SNPs (rs58879207, rs3902057; not shown).

The *PDE6B* gene locus showed homozygosity in family RP119 (Table 1). Screening of the *PDE6B* gene in the proband showed 3 homozygous sequence changes and 1 heterozygous change. A novel homozygous sequence change in intron 17, c.2130-15G>A, co-segregated with the disease phenotype and was absent in 108 normal controls. However, the splice site prediction programme (www.fruitfly.org/seq-tools/splice.html) suggests the change to be likely non-pathogenic, as the introduction of the sequence variant changes the accepter site prediction score from 0.90 to 0.89. In addition, no splice site was predicted to be created as a result of the mutation by the splice site prediction tools. Other changes in *PDE6B* were found in the proband including 2 reported SNPs (rs10902758, rs28675771; not shown), both homozygous and a novel heterozygous intronic change, c.1401+31C>A (Table 3).

Screening of the *CNCG1* gene in family RP200 (Table 1) revealed 3 reported SNPs (rs1972883 (homozygous), rs6819506 (homozygous), rs59800634 (heterozygous)). The *CRB1* gene was homozygous in family RP160. 2 known SNPs (rs12042179, rs3902057) were found in homozygous form in the proband. Screening of the the *RGR* gene was carried out in 2 families- RP160, and RP184 (Table 1). Changes detected in the proband from RP160 included the reported SNPs (rs2279227, rs1042454, rs61730895, rs3526) in homozygous form and 1 novel heterozygous synonymous change (c.123C>T, p.Phe41Phe, Table 3). In family RP184 a novel homozygous intronic change (c.760-38C>T, Table 3) was observed in the *RGR* gene, which did not co-segregate with disease in the family. In family RP153, screening of the *NRL* gene showed no detectable sequence changes.

Discussion:

The high degree of genetic heterogeneity in ARRP makes genetic screening and gene identification rather expensive and time-consuming. The use of homozygosity to detect disease gene loci for ARRP enables a relatively rapid screen of a large number of loci and is particularly useful in analysis of consanguineous families in which regions of several centimorgans adjacent to the disease gene are expected to be homozygous by descent.[8] This approach is well suited to screening, consanguineous ARRP families as in this study. Gene identification in families with ARRP has been carried out by homozygosity screening both in screens of pre-existing/candidate gene loci [9, 10] as well as genome-wide screening.[11] A screen of 23 loci in the present study identified putative pathogenic alterations in 5 different genes in 5/34 families (~15%). 2 frameshift, 2 missense, 1 nonsense and 1 intronic sequence changes were detected, of which 5 are not reported previously.

Three of the mutations we identified are of probable severe consequence since they encode prematurely truncated proteins. Two are single base deletions -c.1060delA in the RPE65 gene expected to result in frameshift at codon 356 with premature truncation at codon 371 (p.Asn356MetfsX16) and c.2847delT in the RP1 gene, predicting frameshift at codon 949 and premature termination after 32 amino acids (p.Asn949LysfsX32). Mutations in RP1 known so far to cause ARRP are 1 missense, 2 insertions and 2 deletions reported in 2 different studies involving families of Pakistani origin.[12, 13] The phenotype of patients in the present study is comparable with those reported in the Pakistani families, with typical fundus changes including disc pallor and vascular attenuation and an onset of disease in childhood. We also noted the presence of macular degeneration in family RP170 while Khaliq et al [12] described “macular stippling”. A third mutation encoding premature termination is a

novel nonsense mutation Tyr665X in the ABCA4 gene in family RP213, which is likely to be functionally null or lead to instability of the mRNA or protein due to a premature nonsense codon. The associated phenotype of severe, early-onset disease with early signs of maculopathy is part of the spectrum of phenotypes resulting from 'severe' mutations in ABCA4.[14, 15]

Two missense changes that we identified in 2 families were Arg400Gln (c.1199G>A) in the *TULP1* gene and Arg151Trp (c.451C>T) in the *RLBP1* gene. The high degree of conservation of residues involved in the two cases (Figures 3 & 4), the predicted SIFT scores of 0.00, as well as the nature of the substitutions both of which replace a charged amino acid for a neutral one, argue in favor of their pathogenicity. Codon Arg400 is located in the highly conserved C-terminal 'tubby' domain of the TULP1 protein [16] in which mutations reported so far in *TULP1* are also located. The Arg400 residue is conserved among *TUB, TULP1, TULP3*, Drosophila king tubby and *C. elegans* tub-1. [17] The same residue has been previously described to have the mutation R400W. [18] The phenotype observed in this family (Table 3; Figure 2) is one of severe, early-onset RP with one of the affected siblings having nystagmus. These features are similar to those described earlier for patients with *TULP1* mutations.[19, 20] A notable feature is the presence of maculopathy in the patients in our study as well as those described by Lewis and co-workers. [19] The Arg151Trp mutation in *RLBP1* in our study involves the same residue as a previously reported mutation Arg151Gln [21] shown to have decreased ability to bind 11-*cis* retinal.

The novel intronic change in the *PDE6B* (c.2130-15G>A) gene in family RP119 was absent in at least 100 normal controls and co-segregated with disease in family RP119. Analysis of this sequence change by means of splice site prediction software did not predict any adverse effect of the change.

One possibility that could still be considered is that the G>A change at this site is unfavorable due to creation of the AG dinucleotide in the vicinity of the authentic splice acceptor. It has been suggested that AG dinucleotides are not found to occur within 15 bp upstream of position –4 of the intron,[22] possibly to ensure specificity of spice site selection. . Hence, further investigations are required to confirm the pathogenic/benign nature of this change. Although the *PDE6B* gene locus was selected for further analysis based on homozygosity among affected members of family RP119, the presence of a heterozygous sequence change (c.1401+31C>A) suggests that this locus is unlikely to be homozygous by descent. It is also possible that the heterozygous c.1401+31C>A change arose as a more recent mutation of one of the ancestral alleles.

RP is an important cause of blindness in Southern India with a prevalence of 1 in 1000 in the state of Andhra Pradesh.[23] Few studies on the genetics of RP have been reported in this region.[24-26] Investigation into the genes underlying RP is potentially useful in designing genetic testing and counseling for patients. Our study revealed novel causes of disease in Indian ARRP families, detecting mutations in *RPE65, RP1, TULP1, RLBP1* and *ABCA4* genes, revealing mutations in about 15% (5/34) of ARRP families in the loci tested. Furthermore, this study paves the way to screen larger cohorts of RP patients or families using the same methods in combination with genome-wide screening and/or mapping to identify disease genes in all families.

Acknowledgements

The authors wish to thank patients and family members who participated in this study, staff of the clinical laboratory service of LVPEI for technical assistance and Prof R.J. Biggar for his valuable comments on the manuscript. H.P.S. was supported by senior research fellowship from CSIR India.

REFERENCES

1. Bundey S, Crews SJ. A study of retinitis pigmentosa in the City of Birmingham. I Prevalence. *J Med Genet.* Dec 1984;21(6):417-420.
2. Bunker CH, Berson EL, Bromley WC, Hayes RP, Roderick TH. Prevalence of retinitis pigmentosa in Maine. *Am J Ophthalmol.* Mar 1984;97(3):357-365.
3. Xu L, Hu L, Ma K, Li J, Jonas JB. Prevalence of retinitis pigmentosa in urban and rural adult Chinese: The Beijing Eye Study. *Eur J Ophthalmol.* Nov-Dec 2006;16(6):865-866.
4. Hayakawa M, Matsumura M, Ohba N, et al. A multicenter study of typical retinitis pigmentosa in Japan. *Jpn J Ophthalmol.* 1993;37(2):156-164.
5. Haim M. Prevalence of retinitis pigmentosa and allied disorders in Denmark. III. Hereditary pattern. *Acta Ophthalmol (Copenh).* Oct 1992;70(5):615-624.
6. Kannabiran C. Retinitis pigmentosa: overview of genetics and gene-based approaches to therapy. *Expert Review of Ophthamology* 2008;3(4):417-429.
7. Bungert S, Molday LL, Molday RS. Membrane topology of the ATP binding cassette transporter ABCR and its relationship to ABC1 and related ABCA transporters: identification of N-linked glycosylation sites. *J Biol Chem.* Jun 29 2001;276(26):23539-23546.
8. Lander ES, Botstein D. Homozygosity mapping: a way to map human recessive traits with the DNA of inbred children. *Science.* Jun 19 1987;236(4808):1567-1570.
9. Lalitha K, Jalali S, Kadakia T, Kannabiran C. Screening for homozygosity by descent in families with autosomal recessive retinitis pigmentosa. *J Genet.* Aug 2002;81(2):59-63.
10. Kondo H, Qin M, Mizota A, et al. A homozygosity-based search for mutations in patients with autosomal recessive retinitis pigmentosa, using microsatellite markers. *Invest Ophthalmol Vis Sci.* Dec 2004;45(12):4433-4439.
11. den Hollander AI, Lopez I, Yzer S, et al. Identification of novel mutations in patients with Leber congenital amaurosis and juvenile RP by genome-wide homozygosity mapping with SNP microarrays. *Invest Ophthalmol Vis Sci.* Dec 2007;48(12):5690-5698.
12. Khaliq S, Abid A, Ismail M, et al. Novel association of RP1 gene mutations with autosomal recessive retinitis pigmentosa. *J Med Genet.* May 2005;42(5):436-438.
13. Riazuddin SA, Zulfiqar F, Zhang Q, et al. Autosomal recessive retinitis pigmentosa is associated with mutations in RP1 in three consanguineous Pakistani families. *Invest Ophthalmol Vis Sci.* Jul 2005;46(7):2264-2270.
14. Fukui T, Yamamoto S, Nakano K, et al. ABCA4 gene mutations in Japanese patients with Stargardt disease and retinitis pigmentosa. *Invest Ophthalmol Vis Sci.* Sep 2002;43(9):2819-2824.
15. Singh HP, Jalali S, Hejtmancik JF, Kannabiran C. Homozygous null mutations in the ABCA4 gene in two families with autosomal recessive retinal dystrophy. *Am J Ophthalmol.* May 2006;141(5):906-913.
16. Boggon TJ, Shan WS, Santagata S, Myers SC, Shapiro L. Implication of tubby proteins as transcription factors by structure-based functional analysis. *Science.* Dec 10 1999;286(5447):2119-2125.
17. den Hollander AI, van Lith-Verhoeven JJ, Arends ML, Strom TM, Cremers FP, Hoyng CB. Novel compound heterozygous TULP1 mutations in a family with severe early-onset retinitis pigmentosa. *Arch Ophthalmol.* Jul 2007;125(7):932-935.

18. Hanein S, Perrault I, Gerber S, et al. Leber congenital amaurosis: comprehensive survey of the genetic heterogeneity, refinement of the clinical definition, and genotype-phenotype correlations as a strategy for molecular diagnosis. *Hum Mutat.* Apr 2004;23(4):306-317.

19. Lewis CA, Batlle IR, Batlle KG, et al. Tubby-like protein 1 homozygous splice-site mutation causes early-onset severe retinal degeneration. *Invest Ophthalmol Vis Sci.* Aug 1999;40(9):2106-2114.

20. Paloma E, Hjelmqvist L, Bayes M, et al. Novel mutations in the TULP1 gene causing autosomal recessive retinitis pigmentosa. *Invest Ophthalmol Vis Sci.* Mar 2000;41(3):656-659.

21. Maw MA, Kennedy B, Knight A, et al. Mutation of the gene encoding cellular retinaldehyde-binding protein in autosomal recessive retinitis pigmentosa. *Nat Genet.* Oct 1997;17(2):198-200.

22. Mount SM. A catalogue of splice junction sequences. *Nucleic Acids Res.* Jan 22 1982;10(2):459-472.

23. Dandona L, Dandona R, Srinivas M, et al. Blindness in the Indian state of Andhra Pradesh. *Invest Ophthalmol Vis Sci.* Apr 2001;42(5):908-916.

24. Kumaramanickavel G, Maw M, Denton MJ, et al. Missense rhodopsin mutation in a family with recessive RP. *Nat Genet.* Sep 1994;8(1):10-11.

25. Kumar A, Shetty J, Kumar B, Blanton SH. Confirmation of linkage and refinement of the RP28 locus for autosomal recessive retinitis pigmentosa on chromosome 2p14-p15 in an Indian family. *Mol Vis.* Jun 15 2004;10:399-402.

26. Gandra M, Anandula V, Authiappan V, et al. Retinitis pigmentosa: mutation analysis of RHO, PRPF31, RP1, and IMPDH1 genes in patients from India. *Mol Vis.* 2008;14:1105-1113.

Table 1: Details of families with autosomal recessive RP and loci showing homozygosity.

Chromosomal location	Gene	Family	Informative markers	Distance of the furthest marker from the gene (Mb)
1p31	*RPE65*	RP205	D1S2829, D1S1162	0.6
1q31-q32.1	*CRB1*	RP126, RP160	D1S1726, D1S373, D1S1181, D1S2853, D1S2622	2.8
1p22.1-p21	*ABCA4*	RP213	D1S236, D1S1170, D1S188	1.9
4p16.3	*PDE6B*	RP119	D4S3038, D4S412, D4S432, D4S2936, D4S3023, D4S2285	4.5
4p12-cen	*CNCG1*	RP200	D4S405, D4S174, D4S2996, D4S2971	7.5
6p21.3	*TULP1*	RP126	D6S1568, D6S1629, D6S1583, D6S273	3.7
8q11-q13	*RP1*	RP170	D8S285, D8S1718, D8S1696	8.3
10q23	*RGR*	RP160, RP184	D10S1753, D10S1744, D10S1755, D10S1765	6.3
14q11.1-q11. 2	*NRL*	RP153	D14S1042, D14S990	4.7
15q26	*RLBP1*	RP169	D15S972, D15S1046, D15S111, D15S963, D15S202	3.8

Families and the gene loci are shown with corresponding markers at which homozygosity was identified with the distance of the furthest marker from the gene.

Table 2: Putative pathogenic changes found in autosomal recessive RP.

Family	Gene	Location	Mutation cDNA, protein	Consequence	Reported/ Novel	Restriction site change, if any
RP205	*RPE65*	Exon 10	c.1060delA, p.Asn356fs	Frameshift	Reported (Marlhens et al., 1997)	None
RP170	*RP1*	Exon 4	c.2847delT, p.Asn949fs	Frameshift	Novel	None
RP126	*TULP1*	Exon 12	c.1199G>A, p.Arg400Gln	Missense	Novel	*Eco57I*+
RP169	*RLBP1*	Exon 6	c.451C>T, p.Arg151Trp	Missense	Novel	*Hpy188III* -
RP213	*ABCA4*	Exon 14	c.1995C>A, p.Tyr665X	Nonsense	Novel	None

Pathogenic sequence changes identified. '+' denotes gain of restriction site, ' –' denotes loss of restriction site. Numbering is with respect to first base of ATG. Sequences referred to above have the following Ensembl Transcript Ids: *RPE65*- ENST00000262340, *RP1*- ENST00000220676, *TULP1*- ENST00000229771, *RLBP1*- ENST00000268125, *ABCA4*- ENST00000370225.

Table 3. Novel changes of unknown significance identified in families with autosomal recessive RP.

Family	Gene	Location	Change in cDNA, protein
RP126	*CRB1*	Exon 8	c.2715G>A, p.Arg905Arg
RP213	*ABCA4*	Exon 29	c.4256T>C, p.Met1419Thr
RP119	*PDE6B*	IVS 10	c.1401+31C>A
RP119	*PDE6B*	Intron 17	c.2130-15G>A
RP160	*RGR*	Exon 2	c.123C>T, p.Phe41Phe
RP184	*RGR*	Intron 6	c.760-38C>T

Table 4: Clinical features of affected individuals from families with autosomal recessive RP

Family/ Gene mutation	Patient	Age at presenta-tion	Age of onset	Initial symptoms	Fundus appearance	Visual acuity	ERG	Diagnosis
RP205/ *RPE65*	IV:1	7 yrs	1 yr	Night blindness	Arterial narrowing; widespread white dots in periphery due to RPE atrophy	20/60 OD; 20/50 OS	Extinguished	Early onset RP
	IV:2	5 yrs	1 yr			Teller Acuity: 20/63 OU	ND	
RP170/ *RP1*	II:1	19 yrs	NA, Childhood	Night blindness, reduced vision	Equatorial & macular RPE degeneration, pale disc, arterial narrowing; vitreous opacities	OD 20/60; OS-counting fingers at 1 meter	ND	RP with macular degeneration
	II:2	17 yrs	5 yrs			20/50 OU	ND	
RP126/ *TULP1*	IV:1	22 yrs	NA, Childhood	Night blindness, reduced vision	RPE degeneration, pigment migration, arterial narrowing with prominent macular degeneration; optic disc pallor	20/200 OD; 20/200 OS	Extinguished	Advanced RP
	IV:2	19 yrs	NA, Childhood	Night blindness, reduced vision; Nystagmus		20/400 OD; 20/600 OS	Extinguished	
RP169/ *RLBP1*	IV:3	16 yrs	NA, childhood	Night blindness, progressive loss of vision	RPE degeneration, pigment migration, arterial narrowing with macular sparing; discs normal, peripheral visual field constriction	20/50 OU	ND	Typical RP
	IV:5	12 yrs	NA, childhood			20/50 OU	ND	

RP213/ *ABCA4*	IV:4	19 yrs	11	Progressive visual loss	Equatorial RPE degeneration, pale disc, arterial narrowing; vitreous opacities and large patch of macular atrophy	20/200 OU	Rod-cone pattern	RP with atrophic maculopathy
	IV:3	21 yrs	13			20/200 OU	Rod-cone pattern	

RPE- retinal pigment epithelium; OD-right eye; OS- left eye; OU- both eyes; ERG- electroretinogram; NA- not available; ND- not done.

Figure 1. Pedigrees of families with autosomal recessive retinits pigmentosa in which pathogenic changes were identified.

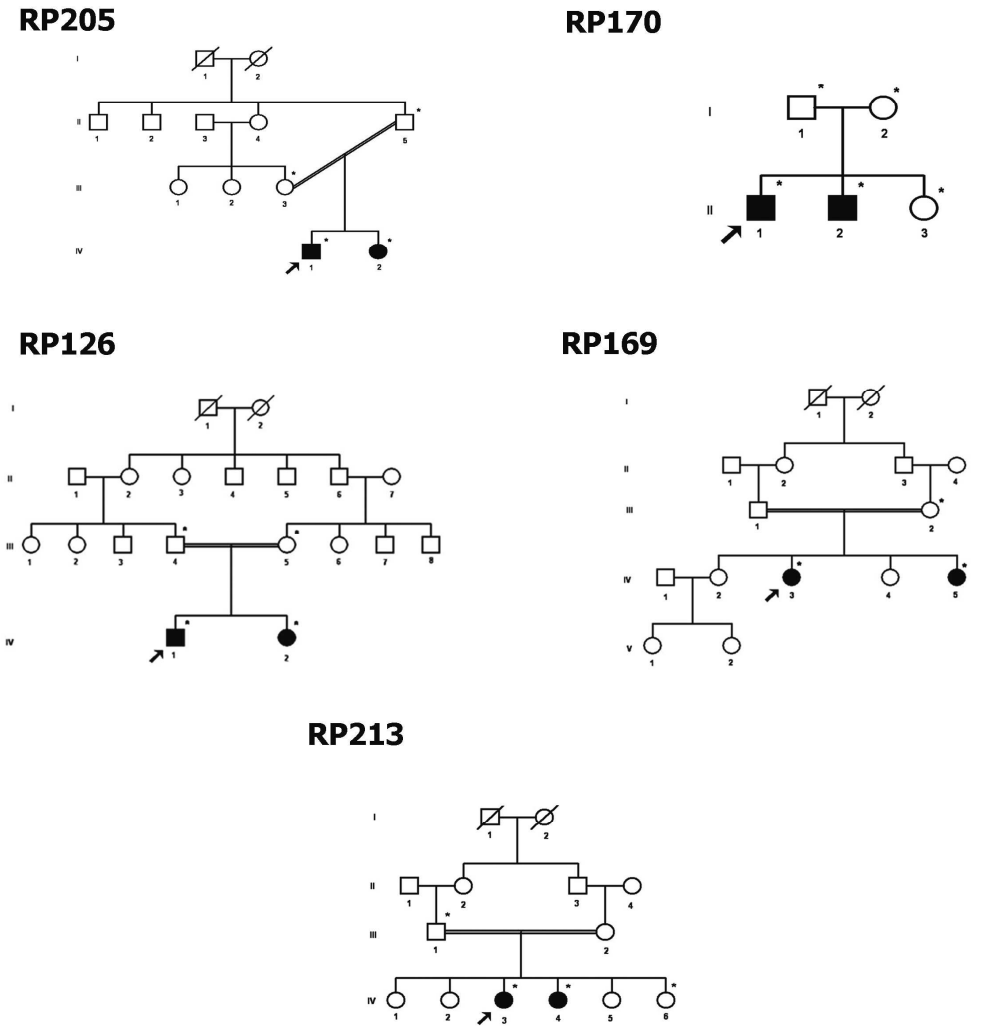

Figure 2. Representative fundus photographs of affected individuals of families with autosomal recessive retinitis pigmentosa. (A) family RP205, (B) family RP170, (C) family 126, (D) family 169, (E) family RP213.

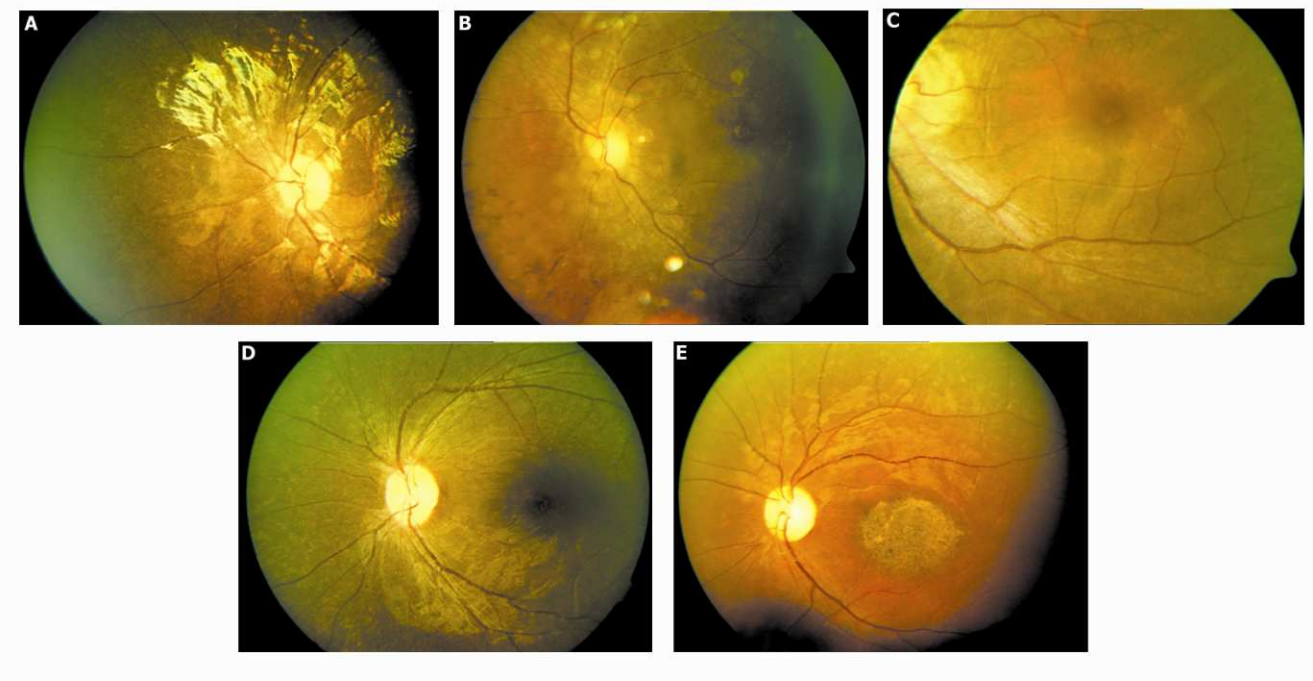

Figure 3. Multiple sequence alignment of TULP1 proteins from different species. Arginine residue at position 400, which is the site of mutation, is boxed.

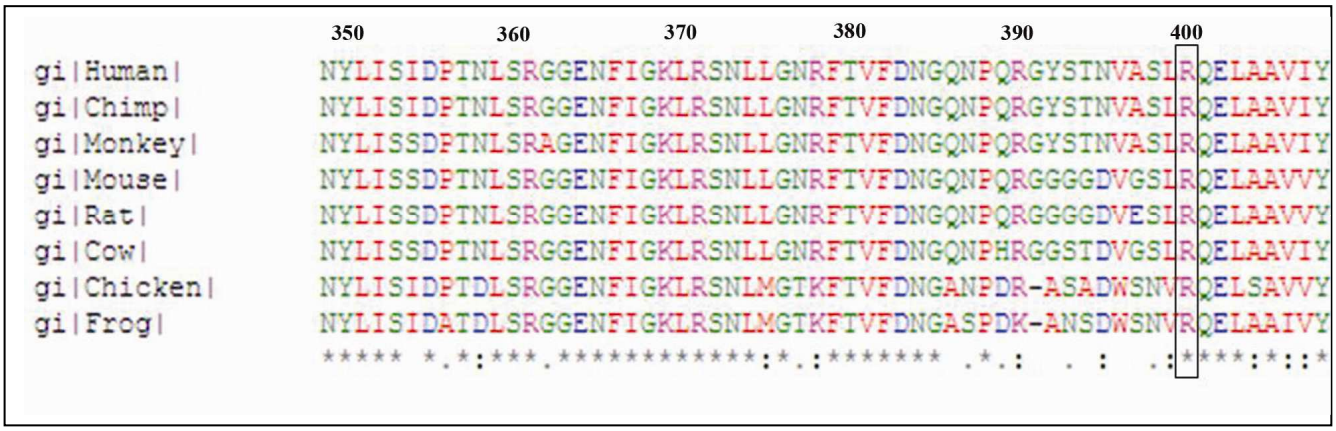

Figure 4. Multiple sequence alignment of the RLBP1 protein sequence in different species. Arginine residue undergoing mutation, at position 151 is boxed.